ULB FACULTÉ DES SCIENCES

UNIVERSITÉ LIBRE DE BRUXELLES

Coastal water management under the mixoplankton paradigm

Thesis submitted by Lisa Kathleen SCHNEIDER
in fulfilment of the requirements of the PhD Degree in agronomics and bioengineering
Academic year 2020-2021

Supervisor: Professor Nathalie GYPENS

Co-supervisor: Dr Willem STOLTE

Thesis jury:

Philippe DUBOIS (Université libre de Bruxelles, Chair)
Nathalie GYPENS (Université libre de Bruxelles, Supervisor, Secretary)
Willem STOLTE (Co-supervisor, Deltares)
Lei CHOU (Université libre de Bruxelles)
Kevin FLYNN (Plymouth Marine Laboratory)
Karline SOETAERT (NIOZ, Universiteit Utrecht)
Tineke A. TROOST (Deltares)
Susanna WILKEN (University of Amsterdam)

ULB ECOLE INTERFACULTAIRE DE BIOINGENIEURS

MIXOTROPH.ORG MIXITIN

Contents

Acknowledgments

Being trained as a physical oceanographer and water resource engineer, this PhD gave me the opportunity to dive into the fascinating discipline of marine plankton and marine ecology. On my journey through that new discipline, I was lucky to have wonderful companions who gave me the freedom to explore, shared their fascination of the discipline and guided me along my way.

First and foremost, I would like to thank my three supervisors Nathalie Gypens, Tineke Troost and Willem Stolte. Nathalie, thank you for always making time for me in your busy schedule, for your great feedback on my work and, most of all, for challenging me to find my own stance. Tineke, your thoughful remarks helped me structure my manuscripts and your optimism helped me laugh my way through any obstacles that came my way. I especially wish to thank Willem. For sharing your extensive knowledge on marine ecology with me, for your playful joy with R coding and, most of all, for having my back. That gave me the freedom to explore and find my own way as a PhD student. I could not have asked for a better supervisor.

Modelling was a big part of my thesis and I would particularly like to thank Kevin J. Flynn, Peter M. J. Herman, Jos van Gils, Michelle Jeuken, Arjen Markus and Lauriane Vilmin for their help in this field. Kevin J. Flynn provided a version of his model equations and helped me improve the model code with his critical, useful questions. Peter M.J. Herman provided helpful feedback on developing equations for aquatic ecosystem models and his calm, thoughtful manner during our discussions greatly helped build my confidence as a young researcher. For that I am especially thankful. Jos van Gils, Michelle Jeuken and Arjen Markus are all DELWAQ experts. They taught me their trade and were always there to help me solve a new DELWAQ puzzle. Last but not least, Lauriane Vilmin not only helped me set up the 3D models, but was always available for a refreshing chat especially during the last months of my PhD.

I would also like to thank Philippe Dubois and Marius Gilbert for reminding me that every thesis needs a clearly formulated hypothesis. Their feedback during our discussions significantly helped form this thesis. Furthermore, I would like to acknowledge Aditee Mitra for getting together such a great team of principle investigators and early stage researchers (ESRs) and I would like to thank my fellow ESRs, especially Maira Maselli and Anna-Adriana Anschütz, for helping me find my way into the beautiful world of plankton.

A PhD can be very lonely work. I would like to thank my department head Paul Saager for always making sure I was part of the team and Gundula Winter for our morning breakfast chats via Teams. Especially during Corona times, my midday walks were a godsend. I would like to thank Teresa, Kathleen, Eva, Valentin and

Nils for hiking across every inch of the Bürgerpark with me and adjusting to my pace as my pregnancy advanced.

This PhD could not have been possible without my parents, siblings and my young family. The warmth and strength I feel when we are together, guide me through life. Mama and Papa, you raised me to speak my mind, be inquisitive and interested in the world around me. These are qualities that I believe greatly helped me during my PhD. I cannot thank you enough for your unwavering support, especially in these last 6 months with Malou. And Mama, thank you for proof-reading my thesis! Christine, Maggie and Karl, thanks to you I am never alone. We go through life together, you can always make me laugh and you are the best aunts and uncle a mother could wish for her daughter.

The biggest thanks of all goes to you Malte. Your good heart, calm manner and firm belief in positive outcomes are my constant companion. My days are simply better when you are around and I cannot wait to continue this next adventure with you. Lastly, Malou. My heart smiles whenever I think of you. You put this whole PhD into perspective and for that I cannot thank you enough.

This project has received funding from the European Union's Horizon 2020 research and innovation programme project "MixITiN" under Marie Skłodowska-Curie grant agreement No 766327.

Abstract

Unicellular, eukaryotic organisms - known as protists - form the base of all aquatic food webs. Frequently, marine protists are divided into either phytoplankton or (proto)zooplankton. Phytoplankton use phototrophy to acquire their energy from light to fix carbon dioxide into organic carbon, while protozooplankton use phagotrophy to directly acquire organic carbon from their prey. Mixoplankton that employ mixotrophy, i.e. the combination of phototrophy and phagotrophy within one cell, are often neglected. However, many marine protists are mixoplankton and they are ubiquitous in the worlds' oceans. In oligotrophic oceans, mixoplankton are the base of food webs and many harmful algal blooms are formed by mixoplankton. Yet, the concept of mixoplankton is slow to mature within coastal water management. This thesis hypothesizes that *the whole protist community, including mixoplankton, needs to be taken into account to understand and predict the effect of anthropogenic pressures on coastal systems.* This thesis is a cumulative summary of three papers that employ data analysis, model developments and modelling scenarios to test this hypothesis. As a study area the Southern North Sea was chosen as it is an exceptionally well sampled coastal sea that is forecast to be heavily modified in the future. In a first step, routine monitoring data from the Southern North Sea were analyzed. The data analysis showed that the relative occurrence of mixoplankton was highest in seasonally stratified, clear, dissolved inorganic nutrient depleted environments. In a second step, a mathematical model, called PROTIST, was developed with the aim to reproduce the trophic composition of protist communities across abiotic gradients. Not only was PROTIST capable of reproducing the trophic composition of protist communities in the Southern North Sea, a sensitivity analysis conducted on the model results also showed that the occurrence of mixoplankton in the Southern North Sea is driven mainly by the availability of dissolved inorganic phosphate and silica and not by the availability of light. In a third step, PROTIST was used in a 3D model scenario of the North Sea to research whether the planned intensification of seaweed aquaculture affects the composition of protist communities. Preliminary 3D model results show that seaweed aquaculture in the Southern North Sea could decrease nutrient concentrations in winter and lead to an increase in mixoplankton biomass. Pooling the information gained from the different approaches, this thesis concludes that coastal zone management should take mixoplankton into account to understand and predict the effect of future anthropogenic pressures on coastal ecosystems.

Résumé

Les protistes planctoniques constituent la base de tous les réseaux trophiques aquatiques. Les protistes marins sont souvent divisés en phytoplancton qui utilise la phototrophie pour acquérir son énergie à partir de la lumière et fixer le dioxyde de carbone en carbone organique et en (proto)zooplancton qui utilise la phagotrophie pour acquérir directement le carbone organique de ses proies. Le mixoplancton qui utilise la mixotrophie, c'est-à-dire la combinaison de la phototrophie et de la phagotrophie dans une même cellule, est souvent négligé. Pourtant, de nombreux protistes marins sont des organismes mixoplanctoniques, présents dans les océans du monde entier et de nombreuses efflorescences algales nuisibles sont formées par le mixoplancton. Malgré cela, le concept de mixoplancton est lent à se développer dans le domaine de la gestion des eaux côtières. Cette thèse émet l'hypothèse que *l'ensemble de la communauté des protistes, y compris le mixoplancton, doit être pris en compte pour comprendre l'effet des pressions anthropiques sur les systèmes côtiers*. Cette thèse est un résumé cumulatif de trois articles qui combinent l'analyse de données, le développement de modèles mathématiques et des scénarios de gestion pour tester cette hypothèse. La Baie Sud de la Mer du Nord a été choisie comme zone d'étude car il s'agit d'une mer côtière exceptionnellement bien échantillonnée et dont on prévoit qu'elle sera fortement modifiée dans le futur. Dans un premier temps, l'analyse des données mesurées dans la Baie Sud de la Mer du Nord a montré que l'occurrence relative du mixoplancton était la plus élevée dans les environnements stratifiés saisonnièrement, clairs et pauvres en nutriments inorganiques dissous. Dans un deuxième temps, le modèle mathématique, PROTIST, a été développé pour reproduire la composition trophique des communautés de protistes à travers des gradients abiotiques. Non seulement PROTIST a été capable de reproduire la composition trophique des communautés de protistes dans la Baie Sud de la Mer du Nord, mais une analyse de sensibilité menée sur les résultats du modèle a également montré que l'occurrence du mixoplancton dans cette zone est principalement déterminée par la disponibilité du phosphate inorganique dissous et de la silice et non par la disponibilité en lumière. Le modèle PROTIST a ensuite été couplé à un modèle 3D de la Mer du Nord afin de déterminer si l'intensification prévue de l'aquaculture des algues marines affecte la composition des communautés de protistes. Les résultats préliminaires du modèle 3D montrent que l'aquaculture d'algues marines dans Baie Sud de la Mer du Nord pourrait réduire les concentrations de nutriments en hiver et entraîner une augmentation de la biomasse du mixoplancton. En mettant en commun les informations obtenues par les différentes approches, cette thèse conclut que la gestion des zones côtières devrait prendre en compte le mixoplancton pour comprendre l'effet des futures pressions anthropiques sur les écosystèmes côtiers.

List of abbreviations

1D-V	1D-vertical
3D	three dimensional
AEM	Aquatic Ecosystem Model
AS	anthropogenically modified systems
Chl-a	chlorophyll-a
CM	constitutive mixoplankton
CS	coastal systems
DCSM-FM	Dutch Continental Shelf Model - Flexible Mesh
Delft3D	open-source modelling suite
Delft3D-WAQ	module to simulate water quality in Delft3D
DIN	Dissolved inorganic nitrogen
DIP	Dissolved inorganic phosphate
DISi	Dissolved inorganic silica
DOC	dissolved organic carbon
ES	estuary systems
ESD	equivalent spherical diameter
eSNCM	endosymbiotic specialist non-constitutive mixoplankton
GNCM	general non-constitutive mixoplankton
HAB	harmful algal bloom
IEM	Index of ecosystem maturity
IMTA	integrated multi-trophic aquaculture
MALG	Delft3D-WAQ module to model primary production of seaweed
NCM	non-constitutive mixoplankton

OS	offshore systems
OWF	offshore wind farm
PCA	principle component analysis
PFT	protist functional type
POC	particulate organic carbon
PON	particulate organic nitrogen
POP	particulate organic phosphate
PROTIST	Delft3D-WAQ module to model primary production of protists
pSNCM	plastidic specialist non-constitutive mixoplankton
RDA	partial redundancy analysis
RWS	Rijkswaterstaat
SNS	Southern North Sea
eSNCM	endosymbiotic specialist non-constitutive mixoplankton
SV	state variable
WoRMS	World Register of Marine Species

List of Figures

List of Tables

Chapter 1

General introduction

1.1 Context

Four billion years ago in the Archean, the earth's atmosphere was anoxic and its surface covered by a global ocean (Canfield, 2005; Johnson and Wing, 2020). Life in the form of microbes evolved in that great primordial ocean (Knoll and Nowak, 2017). Over the course of billions of years, through the evolution of oxygenic photosynthesis and endosymbiotic events (Dyall et al., 2004), those microbes completely changed the face of the earth.

Oxygenic photosynthesis evolved in prokaryotic microbes called cyanobacteria. In the Archean, cyanobacteria evolved the ability to use energy from sunlight to fix inorganic carbon into carbohydrates using water as the source of electrons. They produced oxygen as a byproduct (Hohmann-Marriott and Blankenship, 2011). During most of the Archean, the oxygen consumption through weathering and respiration limited the oxygen accumulation in the atmosphere. However, over the course of 2.5 billion years, the Archean earth lost heat which led to a cooling of the earth's mantle resulting in slower convection rates (Holland, 2002). As a consequence, more organic carbon was buried than released by weathering processes and oxygen was able to accumulate in the atmosphere. This event is now known as the Great Oxidation Event.

The increased oxygen levels in the atmosphere along with two key endosymbiotic events paved the road for the evolution of eukaryotes (Knoll and Nowak, 2017; Keeling, 2010). In a first endosymbiotic event (fig. 1.1), a prokaryotic Archean cell phagothrophically engulfed an α-proteobacterium. This α-proteobacterium was not digested, but underwent a symbiotic relationship with the host cell and ultimately evolved into the mitochondrion (Gray et al., 1999). The ancestor of all eukaryotes had evolved. In another endosymbiotic event, commonly referred to as "primary endosymbiosis" (fig. 1.1), a unicellular, eukaryotic cell phago-

throphically engulfed a phototrophic cyanobacterium (Zimorski et al., 2014). This cyanobacterium was not digested by the host eukaryote, but continued to perform photosynthesis within the eukaryotic cell. Ultimately, the cyanobacterium evolved into the chloroplast (Falcón et al., 2010). The ancestor of all photosynthetic eukaryotes had evolved. Thus, the first photosynthetic eukaryotes combined two different trophic strategies, phago(hetero)trophy and photo(auto)trophy (Keeling, 2010). This combination of autotrophy and heterotrophy within one cell is defined as mixotrophy. Over the course of evolution, secondary and tertiary symbioses as well as specializations led to the diversification of these unicellular eukaryotes (Keeling, 2010).

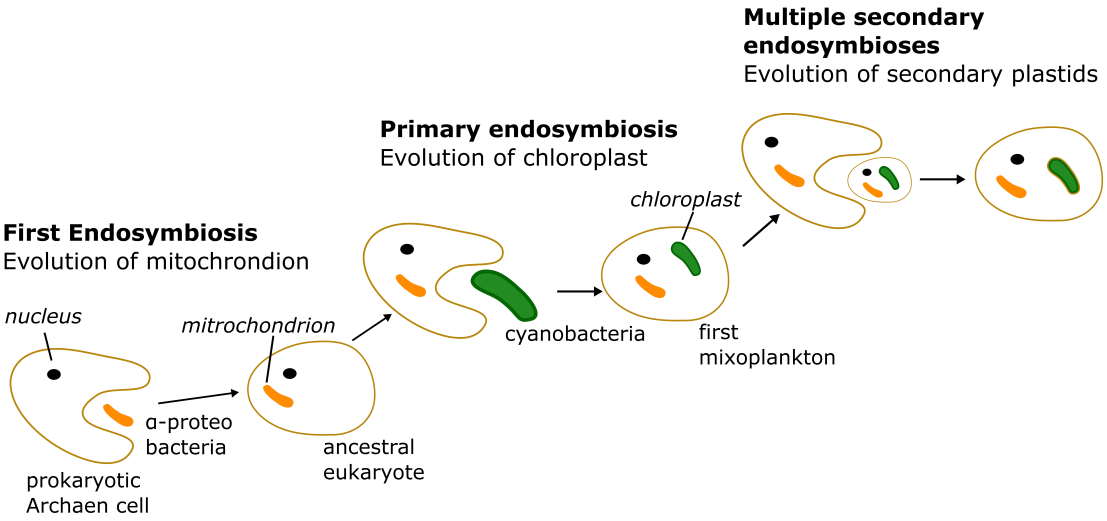

Figure 1.1: Depiction of endosymbiotic events that led to the evolution of mitochondria, chloroplasts and secondary plastids. Adapted and modified from Mansour and Anestis (2021) under CC BY 4.0

Protists, i.e. unicellular eukaryotes, are an incredibly diverse group of organisms that occur in all environments (Foissner and Hawksworth, 2008). Aquatic protist communities consist of phytoplankton (capable of phototrophy), protozooplankton (capable of phagotrophy) and mixoplankton (capable of mixotrophy). Marine protist communities form the base of all marine food webs, produce roughly 50% of the world's oxygen (Falkowski, 1994; Field et al., 1998), play a key role in the global carbon cycle by sequestering carbon to the deep oceans (Bopp et al., 2015; Basu and Mackey, 2018) and are key factors in other global biogeochemical cycles such as nitrogen (Zehr and Kudela, 2011), silica (Tréguer and De La Rocha, 2013) and sulfur (Vallina and Simó, 2007). Thus, protist communities are very important for the functioning of earth's ecosystems.

If we fast forward to the year 2021, most modern-day biology textbooks divide marine protists into either phytoplankton or (proto)zooplankton (Flynn et al., 2013). Phytoplankton use phototrophy to acquire their energy from light to fix carbon dioxide into organic carbon. They employ osmotrophy to acquire inorganic nutrients. Protozooplankton use phagotrophy to directly acquire organic carbon and nutrients from their prey. Within mainstream biological textbooks the ancestral mixotrophy, i.e. the combination of phototrophy and phagotrophy within one cell (Thingstad et al., 1996), is mostly neglected (Mitra et al., 2016).

However, many marine protists can simultaneously employ phototrophy, phagotrophy and osmotrophy. These protists are defined as mixoplankton (Flynn et al., 2019) and they are ubiquitous in the world's oceans (Leles et al., 2017; Leles et al., 2018b; Faure et al., 2019). Mixoplankton are the base of food webs in many oligotrophic open oceans (Hartmann et al., 2012) and their high ingestion rates make them important grazers of the picoplankton and bacterial community (Unrein et al., 2007). Furthermore, many harmful algal blooms are formed by organisms now known as mixoplankton (Smayda, 1997; Burkholder et al., 2008).

While the concept of mixoplankton is slowly gaining recognition among marine phycologists, the concept of mixoplankton is slow to mature within coastal water management. Coastal environments are the most productive areas on earth (Agardy and Alder, 2005; UNEP, 2006) and they face an increasing number of anthropogenic pressures. Global warming (Falkowski, 1994), sea level rise (Muis et al., 2016), offshore energy generation (Burkhard et al., 2011), eutrophication (Rabalais et al., 2009) and aquaculture (Buck and Langan, 2017), to name just a few, impact coastal environments. It is the task of coastal researchers and managers to understand and manage these pressures to secure healthy coastal ecosystems.

An example of such a coastal ecosystem is the North Sea. The North Sea is a marginal sea of the northwestern European continental shelf that is enclosed by Scandinavia in the east, mainland Europe in the south and the UK in the west (fig. 1.2). In the north and via the English Channel in the southwest, the North Sea connects to the North Atlantic. In the southeast, the North Sea exchanges water masses with the Baltic Sea. The rivers of the surrounding land masses discharge high inorganic nutrient loads that lead to a gradient of dissolved inorganic nutrients stretching from the coasts to the central North Sea (Brockmann et al., 1990). The North Sea can roughly be divided into two regions: the deep, seasonally stratified North that is characterized by a low productivity and the shallower, well-mixed, highly productive South (depicted in fig. 1.2).

The proximity to highly populated countries as well as its shallowness makes the Southern North Sea an ideal candidate for offshore wind farms (Wind Europe, 2021). Offshore wind farms are an integral part of the green energy transition of the countries surrounding the North Sea. These offshore wind farms not only

generate energy, but also serve as a platform for seaweed and mussel aquaculture. Along with sea level rise, global warming and eutrophication, it is obvious that the North Sea will undergo drastic changes in the future.

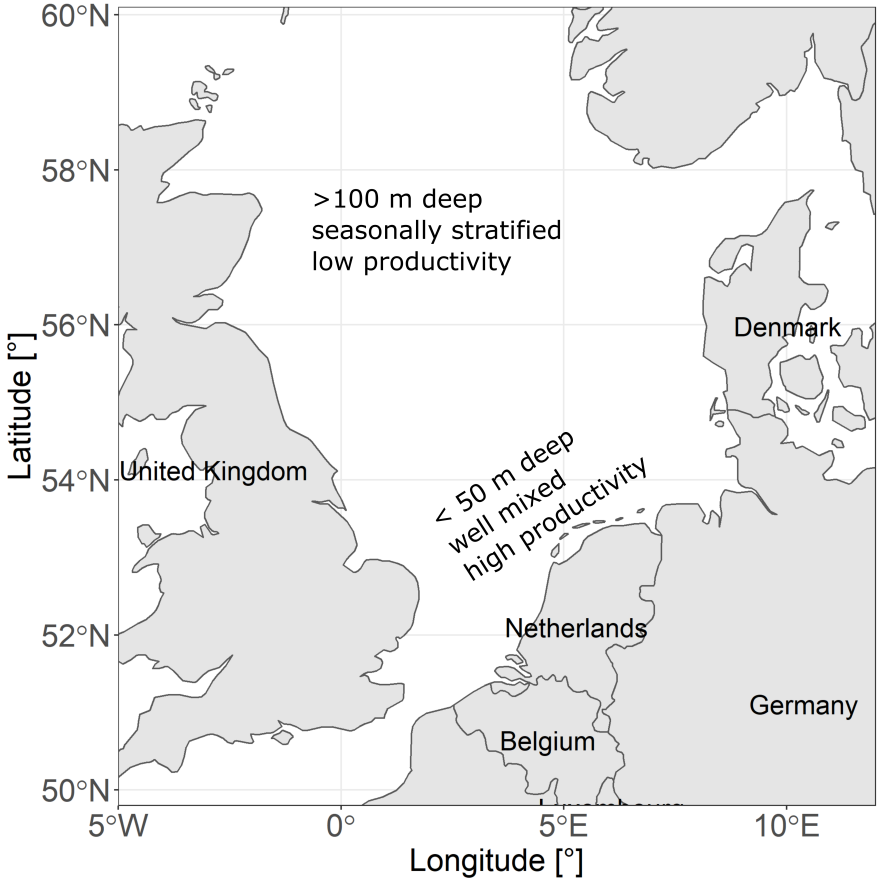

Figure 1.2: Map of the North Sea. The North Sea can be divided into two sections with differing abiotic properties.

As coastal researchers and managers are already dealing with a multitude of issues, it is valid to question whether it is necessary to take the concept of mixoplankton into account. Is it essential for coastal researcher and managers to take mixoplankton into account to understand and predict ecosystem productivity, carrying capacity and bloom forecasts?

1.2 Objectives

Based on the previously posed research question, the **main hypothesis** of this thesis is that **the whole protist community, including mixoplankton, needs to be taken into account to understand and predict the effect of anthropogenic pressures on coastal systems.** The methodology of this thesis combines data analysis, model developments and modelling scenarios to test this hypothesis. The main hypothesis is divided into three subhypotheses which serve as the structure of this thesis.

Firstly, it is important to determine the occurrence of mixoplankton in protist communities of the Southern North Sea. While global analyses of mixoplankton occurrence found mixoplankton to be ubiquitous and abundant across contrasting biogeographies (Leles et al., 2017; Leles et al., 2018b; Faure et al., 2019), the local distribution of mixoplankton in the Southern North Sea has not yet been researched in detail. Thus, **subhypothesis #1** states that **mixoplankton are ubiquitous both spatially and temporally in the Southern North Sea**. To test subhypothesis #1, a 24-year timeseries of abiotic and protist routine monitoring data of the Southern North Sea was analyzed to determine in which environments and seasons mixoplankton occur the most.

Secondly, it is important to research whether there is enough ecological system knowledge available to explain the trophic composition of protist communities across abiotic gradients. This can be tested by formulating system knowledge in mathematical equations and solving them numerically to see whether the results adhere to expectations (Schuwirth et al., 2019). Thus, **subhypothesis #2** states that **a mathematical model is capable of reproducing the trophic composition of protist communities in the Southern North Sea**. To test subhypothesis #2, a new module, called PROTIST, was implemented in the aquatic ecosystem modeling software Delft3D-WAQ. This new module PROTIST is based on a mechanistic model by Flynn (2021). The module PROTIST was applied in 11 column models that mimic the abiotic conditions of the Southern North Sea.

Thirdly, using the module PROTIST, it is possible to test the effect of ecosystem changes, e.g. the construction of multi-use platforms in the Southern North Sea, on the productivity of an ecosystem as well as the trophic composition of protist communities. Thus, **subhypothesis #3** states that **the additional uptake of dissolved inorganic nutrients through aquacultured seaweed affects the annual primary production and/or the trophic composition of protist communities in the Southern North Sea.** To test subhypothesis #3, the module PROTIST was implemented in a 3D model of the North Sea and two scenarios were run with (seaweed scenario) and without (reference scenario) taking the growth of seaweed into account.

1.3 Outline

Chapter 2 provides the necessary background information for this thesis. Chapter 2.1 gives an introduction on metabolic pathways present within marine protist communities. Furthermore, chapter 2.1 elaborates on how these metabolic pathways are combined within the different trophic groups, i.e. phytoplankton, mixoplankton and protozooplankton. Chapters 2.1.1 - 2.1.3 then focus on each of the three trophic groups in more detail. This is followed by chapter 2.2 which gives a description of the North Sea, the study area of this thesis and chapter 2.3 which gives an introduction to aquatic ecosystem models.

Chapter 3 addresses subhypothesis #1 that "mixoplankton are ubiquitous both spatially and temporally in the Southern North Sea". This was approached by analyzing a 24-year timeseries of abiotic and protist routine monitoring data of the Southern North Sea. As it is often difficult to correctly classify marine protists into phyto-, mixo-, or protozooplankton, three different trophic classifications were analyzed. The three trophic classifications focus on A) the traditional phytoplankton-zooplankton dichotomy, B) a mixoplankton-centered paradigm and C) a scenario informed by numerical ecology. The results of chapter 3 show that mixoplankton occur most in the inorganic nutrient-depleted, non-turbid, seasonally stratified environments and that classification C provides a plausible trophic composition of protist communities. Furthermore, the results of chapter 3 link the occurrence of mixoplankton to a newly proposed index of ecosystem maturity, i.e. the ratio of organic to total nitrogen in an environment. However, the analysis was not able to determine what has a larger influence on the occurrence of mixoplankton - the concentration of dissolved inorganic nutrients or suspended sediments.

Chapter 4 provides a description of the dataset on trophic modes of marine protists that was used for the analysis of chapter 3. Long hours of literature research and expert knowledge are needed to correctly assign trophic modes of marine protists. Additionally, the frequent changes of protist taxonomy make it difficult to compare past and present literature references. The dataset presented in chapter 4 was submitted to WoRMS, the World Register of Marine Species, a database that keeps track of taxonomic changes and assigns each organism a unique identifier. By submitting this dataset on trophic modes of marine protists to WoRMS, the trophic modes of marine protists become easily accessible in both a human and machine-readable format.

Chapter 5 focuses on subhypothesis #2 that "a mathematical model is capable of reproducing the trophic composition of protist communities in the Southern North Sea". To this purpose, a new primary production module, called PROTIST, was constructed for the aquatic ecosystem modelling software Delft3D-WAQ. PROTIST can model a protist community consisting of phytoplankton, mixoplankton

and protozooplankton. PROTIST was implemented in 11 1D vertical aquatic ecosystem models that mimic the abiotic gradients present in the Southern North Sea. The model results of chapter 5 display a plausible trophic composition across the abiotic gradients of the Southern North Sea. Lastly, in continuation of the open question that remained from chapter 3, a sensitivity analysis showed that the concentration of dissolved inorganic phosphate and silica have a larger influence on the occurrence of mixoplankton than the concentration of suspended sediments.
Chapter 6 targets the coastal management aspect of this thesis verbalized in subhypothesis #3 "the additional uptake of dissolved inorganic nutrients through aquacultured seaweed affects the annual primary production and/or the trophic composition of the protist community in the Southern North Sea". This was approached by running a 3D model of the North Sea that simulates the growth of the protist community over the whole domain and the growth of seaweed in offshore wind farms. The 3D model results of chapter 6 show that cultivating seaweed could lead to a decrease of dissolved inorganic nutrient concentrations in the areas of the offshore wind farm as well as downstream. The results also show a relative decrease in green algae and protozooplankton biomass and a relative increase of diatom and mixoplankton biomass.
Chapter 7 discusses the results in the context of this thesis' hypothesis. Interlinkages between the chapters were highlighted and the results put into broader scientific context. A focus was placed on how the results advance the field of research. The limitations of this thesis and the possibility of using the index of ecosystem maturity (IEM) as an indicator for mixoplankton were discussed as well. Lastly, an outlook and conclusion on mixoplankton for coastal zone management was presented.

Chapter 2

Background information

2.1 Trophic modes of marine protists

A marine protist community can be analyzed from many different perspectives. One can focus on size, species composition, toxic or harmful organisms, important contributors to nutrient cycles or the trophic composition (Falkowski and Knoll, 2011). Each perspective highlights a different impact of protist communities on ecosystems. This thesis focuses on the trophic composition of protist communities.

The trophic composition of protist communities provides information on how the community as a whole retrieves its nutrition. By studying the trophic composition of protist communities, we gain an understanding of the nutrient acquisition and cycles that take place within protist communities (Worden et al., 2015). Furthermore, we gain information on the trophic transfer efficiency within protist communities and to higher trophic levels (Ward and Follows, 2016). At the heart of every discussion on trophic composition lie the different metabolic pathways present in marine protist communities.

The metabolic pathways differ in terms of their energy, carbon or nutrient source. Energy can be sourced from light or chemical bonds. Phototrophy is the metabolic pathway in which energy is derived from light, while in chemotrophy the energy is derived by breaking chemical bonds. Carbon can be sourced from inorganic or organic forms of carbon. Autotrophy is the metabolic pathway in which inorganic forms of carbon are used, while heterotrophy uses organic forms of carbon. As with carbon, organisms can used inorganic or organic sources of nutrients. Osmotrophy is uptake of dissolved nutrients, while in phagotrophy particulate organic nutrients (and other compounds) are acquired via phagocytosis.

Based on their carbon, energy and nutrient sources protists can be divided into three trophic groups: phytoplankton, mixoplankton and protozooplankton. Phytoplankton employ photo(auto)trophy and osmo(hetero)trophy, while protozooplank-

ton employ only (phago)heterotrophy. The trophic spectrum between phytoplankton and protozooplankton is occupied by mixoplankton, the third major trophic group (Sanders et al., 1990; Flynn et al., 2019).

Mixoplankton can employ photo(auto)trophy, osmo(hetero)trophy as well as (phago)heterotrophy. Mixoplankton can be divided into two broad categories, constitutive mixoplankton (CM) and non-constitutive mixoplankton (NCM). CMs have the innate ability to perform photosynthesis, while NCMs need to acquire their phototrophic capabilities from prey (Mitra et al., 2016). CMs occupy a similar space along the trophic spectrum as phytoplankton. However, in contrast to phytoplankton, CMs have the ability to acquire organic compounds from their prey through phagotrophy (see review by (Stoecker et al., 2017) and references therein, Sanders and Porter (1988), Leles et al. (2018b)). NCMs occupy a similar space along the trophic spectrum as protozooplankton. In contrast to protozooplankton, NCMs can fix inorganic carbon using their acquired chloroplasts (see review by (Johnson, 2011) and references therein, Flynn and Hansen (2013), Leles et al. (2017)).

The metabolic classification of mixoplankton overlaps with that of phyto- and protozooplankton. In general, it is not always straightforward to assign protists to a specific trophic group. The trophic classification of protists is often prone to follow the historical dichotomy of producers (phytoplankton) and consumers (protozooplankton) (Flynn et al., 2013). And even if this bias is addressed, determining the trophic potential of an organism is not straightforward (Flynn et al., 2019).

While it is rather simple to determine the phototrophic potential of an organism using fluorescence signal or microscopy, it is much more difficult to determine whether this organism also has phagotrophic potential (Beisner et al., 2019). Identifying phagotrophy requires precise, labor intensive laboratory experimentation in the correct, yet often unknown environmental conditions that trigger phagotrophy. Similarly, it is also not easily determined whether an organism is purely heterotrophic or whether it just has not been presented with the correct prey from which it can harness the phototrophic machinery (Mansour and Anestis, 2021). Genomic based approaches can aid this research, but the genetic potential of photo- or phagotrophy does not necessarily imply that the organism will also express it (Mansour and Anestis, 2021). Lastly, taxonomic approaches do not necessarily aid this research as phyto-, mixo and protozooplankton cannot be sorted into specific taxonomic lineages (Mansour and Anestis, 2021). Figure 2.1 shows that mixoplankton occur in almost every major taxonomic lineage alongside phyto- and protozooplankton.

The following sections focus on describing the different trophic groups. The aim of the following three sections is not to present a comprehensive overview of all

lineages present in the trophic groups, but to summarize some of the important aspects of each trophic group. As this thesis deals with coastal waters, the focus will be placed on marine taxa.

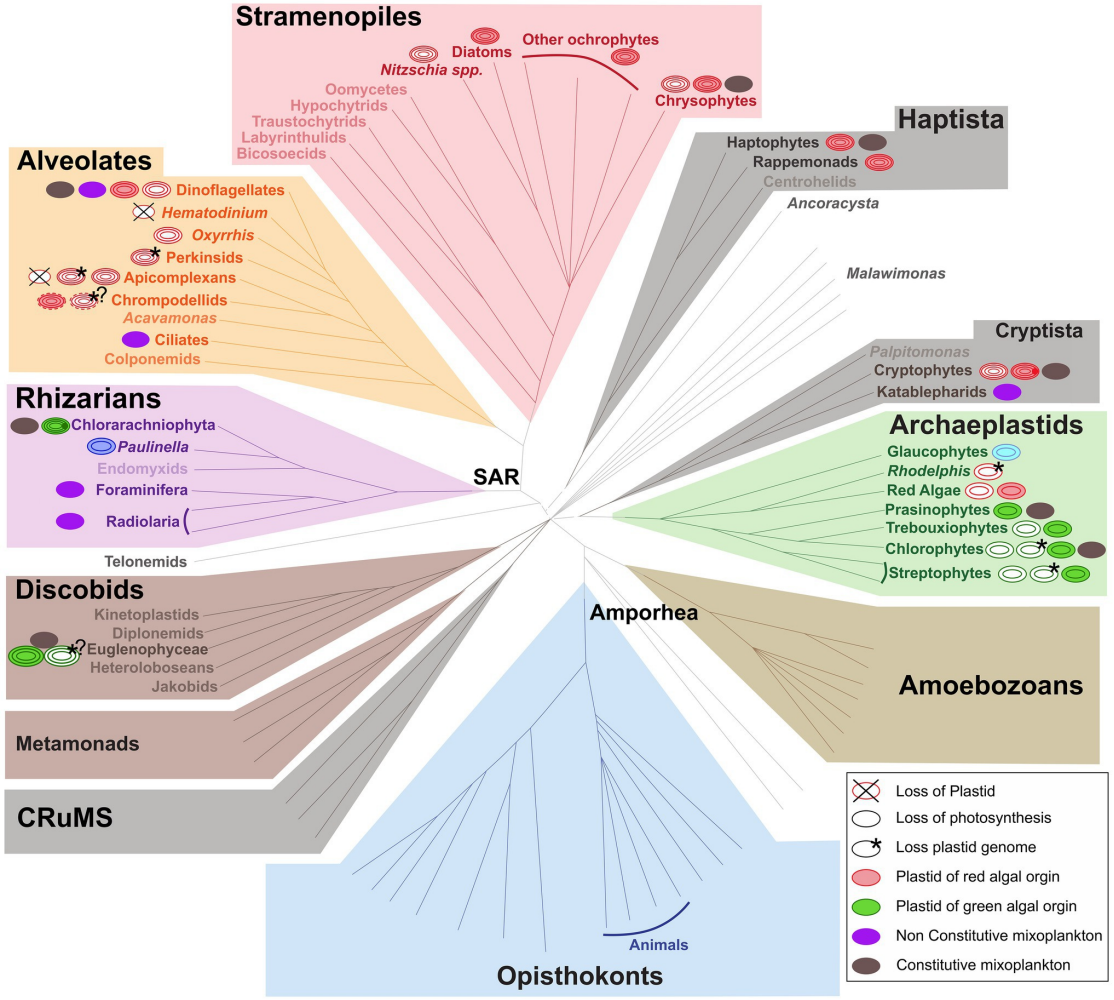

Figure 2.1: Distribution of phytoplankton (red or green plastids), protozooplankton (loss of plastid, photosynthesis or plastid genome) and mixoplankton (constitutive and non-constitutive) in the major taxonomic lineages visualized in the eukaryotic tree of life. The number of ovals visualize the origin of the plastid. Two membranes denote primary plastid, multiple membranes denote secondary/tertiary/quaternary plastids. Reproduced from Mansour and Anestis (2021) under CC BY 4.0

2.1.1 Phytoplankton

Phytoplankton are defined as aquatic plankton that obtain their nourishment via photo(auto)trophy and osmo(hetero)trophy, but are incapable of phagotrophy (Flynn et al., 2019). In terms of abundance and biomass, diatoms, cyanobacteria and coccolithophores are important types of phytoplankton. The top row in figure 2.3 visualizes several phytoplankton taxa.

Diatoms (figures 2.3a and c) range in size from 10 - 200 μm ESD (equivalent spherical diameter) (Pierella Karlusich et al., 2020). Their hallmark characteristic is the incorporation of silica into their cell walls. Diatoms are a major, successful lineage within the phytoplankton and they significantly contribute to global nutrient cycles, food webs and pelagic-benthic coupling. There are three main reasons for the success of diatoms. Firstly, they have a large central vacuole that enables them to store nutrients and also reduces the ratio of structural nutrient to surface area (Stolte and Riegman, 1995). Secondly, they have low trace element requirements, which are important co-factors in biochemical processes. Thirdly, diatoms are very efficient in their CO_2 fixation which could be caused by their use of the C-4 pathway (Kooistra et al., 2007).

Cyanobacteria (figure 2.3d) are prokaryotic, unicellular or filamentous phytoplankton that range in size from 0.5 - 60 μm ESD. They are very common in oligotrophic ocean gyres. Some genera, summed under the term heterocystous cyanobacteria, can fix di-nitrogen gas from the atmosphere. It is estimated that heterocystous cyanobacteria contribute 25-50 % of the atmospheric nitrogen fixation (Canfield et al., 2010). This is especially important in oligotrophic ocean gyres (Sellner, 1997).

Another group of marine phytoplankton are prymnesiophyceae. A notorious prymnesiophyte in eutrophied waters is *Phaeocystis globosa* which can form colonies and cause ecosystem disruptive blooms (O'Kelly, 2007). Coccolithophores (figure 2.3b) are calcifying phytoplankton that range in size from 2 - 75 μm ESD (Pierella Karlusich et al., 2020). Due to their ability to form calcium carbonate into calcareous scales called coccoliths, coccolithophores play an important role in the global carbon cycle. They occur mainly in inorganic nutrient-poor, stratified surface waters (Vargas et al., 2007).

These examples show that phytoplankton range in size from small cyanobacteria to large diatoms and that they are very important contributors to global biochemical cycles. In coastal systems, larger phytoplankton tend to dominate the community, while oligotrophic gyres are populated by smaller pico- and nanoplankton. Because of their high production:biomass ratio (resulting in fast turnover rates), phytoplankton form the basis for higher trophic levels within marine pelagic ecosystems.

2.1.2 Mixoplankton

Mixoplankton are defined as aquatic protists that obtain their nourishment via photo(auto)trophy, osmo(hetero)trophy and phago(hetero)trophy (Flynn et al., 2019). Mixoplankton occur in every microalgal lineage with the exception of diatoms and cyanobacteria (Hansen et al., 2019). As figure 2.2 shows, mixoplankton can be divided into four subcategories based on their ability to perform photosynthesis: the CM, the general non-constitutive mixoplankton (GNCM), the plastid specialist non-constitutive mixoplankton (pSNCM) and the endosymbiotic specialist non-constitutive mixoplankton (eSNCM) (Mitra et al., 2016). The middle row in figure 2.3 visualizes several mixoplankton taxa.

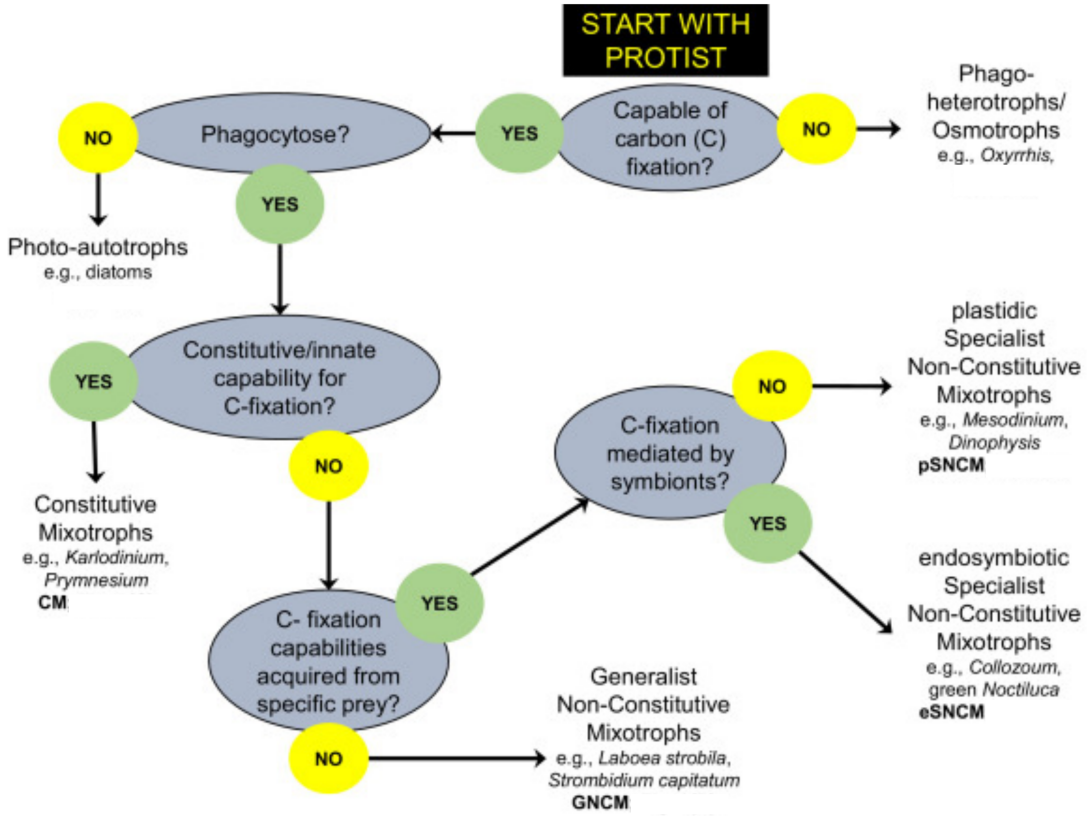

Figure 2.2: Flowchart visualizing the four subcategories of mixoplankton based on their ability to perform photosynthesis. Reproduced from Mitra et al. (2016) under CC BY 4.0

CMs (figure 2.3g) are protists with built-in chloroplasts that are also able to phagotrophically consume prey (Sanders and Porter, 1988). CMs range in size from

1- 190 μm ESD (Pierella Karlusich et al., 2020). Prominent examples of CMs are harmful algae bloom (HAB) species such as the dinoflagellates *Karlodinium* spp. and *Alexandrium* spp. as well as the prymnesiophyte *Chrysochromolina* spp. These species are known to cause fish kills, aquaculture closure and thus damage local economies (Burkholder et al., 2008). Most CM dinoflagellates contain 'peridinin' chloroplasts and use form II rubisco which rapidly fixes CO_2, but at the same time is very sensitive to the presence of oxygen (Delwiche, 2007). Many dinoflagellates are mixoplankton which may be related to their low specific inorganic nutrient uptake and growth rates compared to the phytoplankton (Litchman, 2007).

NCMs (figure 2.3e, f and h) do not have built-in chloroplasts. They need to acquire their chloroplasts from their photosynthetic prey (Stoecker et al., 2009; Flynn and Hansen, 2013). NCMs can be ciliates, heterotrophic dinoflagellates, foraminifera and radiolarians (Hansen et al., 2019). The NCMs can be further divided into the GNCMs, pSNCMs and the eSNCMs.

GNCMs need to acquire chloroplasts on a regular basis as they do not have the ability to maintain the acquired chloroplasts (e.g. Laval-Peuto and Febvre (1986), Stoecker et al. (1988), Schoener and McManus (2012)). GNCMs range in size from 20-60 μm ESD (Pierella Karlusich et al., 2020). The most prominent example of GNCMs are chloroplast-containing oligotrich ciliates, e.g. *Laboea strobila*. Mixotrophic ciliates can make up 30 - 40 % of the ciliate biomass in eutrophic waters (Stoecker et al., 2017) and in the Arctic, mixotrophic ciliates often dominate the ciliate community (Stoecker and Lavrentyev, 2018).

pSNCMs are protists that can only acquire their chloroplasts from specific phototrophic prey (Mitra et al., 2016). pSNCMs range in size from 15-60 μm ESD (Pierella Karlusich et al., 2020). Prominent examples of pSNCMs are the ciliate genus *Mesodinium* and the dinoflagellate genus *Dinophysis*. *Mesodinium* sequesters chloroplasts, nuclei, nucleomorph, mitochondria and some cytoplasm from the red-pigmented cryptophyte prey *Teleaulax* and thus gains some control over the acquired cryptophytes' organelles (Gustafson et al., 2000). The ciliate *Mesodinium* actually serves as prey for the dinoflagellate *Dinophysis*, which acquires its chloroplasts mainly from the ciliate. *Dinophysis* also has a prolonged functioning of the prey chloroplasts and can remain photosynthetically active for several months when starved of prey (Reguera et al., 2012). Both *Mesodinium* and *Dinophysis* are HABs respectively causing red tides and paralytic shellfish poisoning (Burkholder et al., 2008).

eSNCMs are protists that live endosymbiotically with phototrophic protists (Caron et al., 1995). Some of the largest protists are eSNCMs and they range in size from 20- 2000 μm ESD (Pierella Karlusich et al., 2020). Prominent examples of eSNCMs can be found in foraminifera and radiolaria of the supergroup rhizaria as well as the

dinoflagellate green *Noctiluca scintillans*. Within rhizaria, the endosymbionts can be transmitted between host cells (horizontal transmission), but the endosymbionts seem to be digested once the host divides (no vertical transmission) (Decelle et al., 2012). Green *Noctiluca scintillans* harbors the prasinophyte endosymbiont *Pedinomonas noctilucae*. Up until now it has not been possible to cultivate the endosymbiont outside of the green *N. scintillans* cell. However, at the same time, green *N. scintillans* in culture lose their endosymbionts after a couple of weeks (Hansen et al., 2004). Therefore, it has to be concluded that a decisive factor in the physiology of green *N. scintillans* is still not understood (Hansen et al., 2019). In summary, mixoplankton range in size from smaller CMs to large pSNCMs. Mixoplankton cover a wide range of trophic modes from obligate phototrophy, kleptoplastidiy to harboring endosymbionts. While mixoplankton are often associated with mature, oligotrophic ecosystems, they can also be found in coastal, inorganic nutrient-rich waters.

2.1.3 Protozooplankton

Protozooplankton are defined as aquatic protists that obtain their nourishment via phago(hetero)trophy (Flynn et al., 2019). They range in size from 20-200 μm ESD (Calbet and Alcaraz, 2007) and can consume a large fraction of the daily oceanic protist primary production (Calbet and Landry, 2004). Protozooplankton contributors are flagellates, dinoflagellates, ciliates and rhizarians. Many of these contributors also have mixotrophic representatives. Flagellates and ciliates are prominent grazers of the bacterioplankton community (Calbet and Alcaraz, 2007). A famous protozooplankton dinoflagellate is the counterpart to green *Noctiluca scintillans*, the phagotrophic red *Noctiluca scintillans* also responsible for bioluminescence in coastal waters (Harrison et al., 2011). The bottom row in figure 2.3 visualizes two protozooplankton taxa.

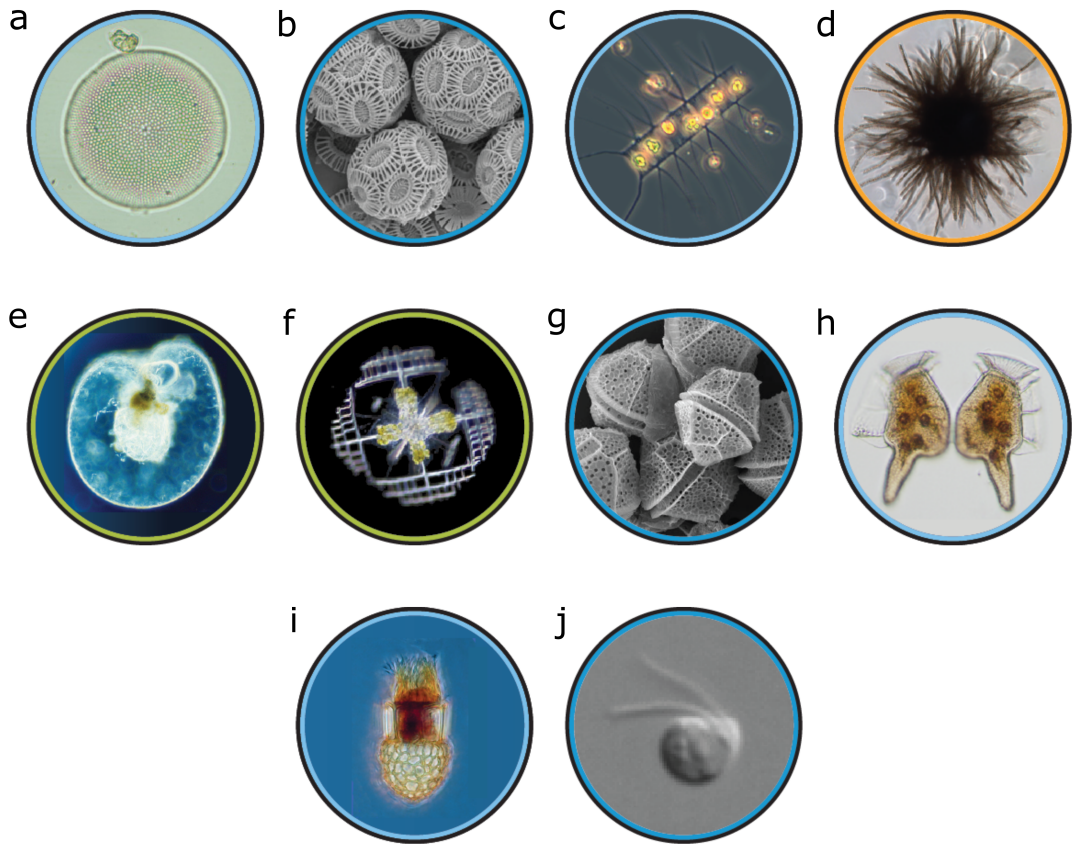

Figure 2.3: Pictures of phytoplankton (a-d), mixoplankton (e-h) and protozooplankton (i-j). a) *Coscinodiscus* sp. (diatom), b) *Emiliania huxleyi* (coccolithophore), c) *Chaetoceros* sp. (diatom), d) *Trichodesmium* sp. (cyanobacteria), e) green *Noctiluca scintillans* (dinoflagellate), f) *Lithoptera* sp. (radiolarian), g) *Alexandrium* sp. (dinoflagellate), h) *Dinophysis* sp. (dinoflagellate), i) *Dictyocysta* sp. (ciliate), j) *Cafeteria roenbergensis*. Assembled from Planktomania (2021) under CC BY 4.0

2.2 Study area: North Sea

The North Sea is a shallow marginal sea of the Atlantic Ocean. It is located on the northwestern European continental shelf. The North Sea is dominated by an anti-clockwise circulation caused by tidal motions (Otto et al., 1990) that flows along the enclosing landmasses with the UK in the West, Scandinavia in the East and mainland Europe in the South (see arrow in figure 2.4b). The North Sea connects to the Baltic Sea in the East and to the Atlantic Ocean via the Norwegian Sea in the North and the English Channel in the South.
The Baltic Sea discharges 470 km^3 of freshwater per year to the North Sea, while the rivers from the surrounding land masses, mainly Rhine and Elbe, discharge up to 354 km^3 of freshwater per year (Kwadijk et al., 2016). As the rivers carry high inorganic nutrient loads, a gradient of dissolved inorganic nutrients establishes from the coasts to the central North Sea (Brockmann et al., 1990). The North Sea is also highly diverse in terms of stratification. In the coastal areas, the tidal currents dominate and so continuous vertical mixing of the water column usually occurs. However, the regions of freshwater influence are (often intermittently) salinity stratified. The deeper waters with less tidal influence show intermittent or seasonal thermal stratification.
A prominent bathymetrical feature of the North Sea is the Doggerbank, which lies in the center of the North Sea basin with an average depth of 18 m (figure 2.4a). The Doggerbank can be used to divide the North Sea into two regions, the Northern and the Southern North Sea (Beusekom and Diel-Christiansen, 2009). The Northern North Sea is on average deeper than 50 m, seasonally stratified, with a low availability of dissolved inorganic nutrients and a low productivity. The Southern North Sea is on average shallower than 50 m, well mixed with intermittently stratified regions due to freshwater influence, high levels of dissolved inorganic nutrients and a high primary productivity (Emeis et al., 2015).
This thesis focuses mainly on the Dutch economic zone in the Southern North Sea (51 - 55 °N) (see grey polygon in figure 2.4b). The Southern North Sea is a well-monitored shelf sea in which abiotic and biotic parameters are routinely measured by the Rijkswaterstaat monitoring program (Dutch Directorate-General for Public Works and Water Management). Figure 2.4c visualizes the location of the sampling stations. The sampling frequency for the different stations varies from bi-weekly to once every 4 months. At each station, water samples are taken for environmental parameters such as dissolved inorganic nutrients, suspended sediments, oxygen and chlorophyll-a. Furthermore, the water samples are fixed in Lugol in order to determine the biomass and abundance of protist taxa. As this has been done since the late 1980s, a long timeseries of abiotic and protist data is available for analysis and model validation.

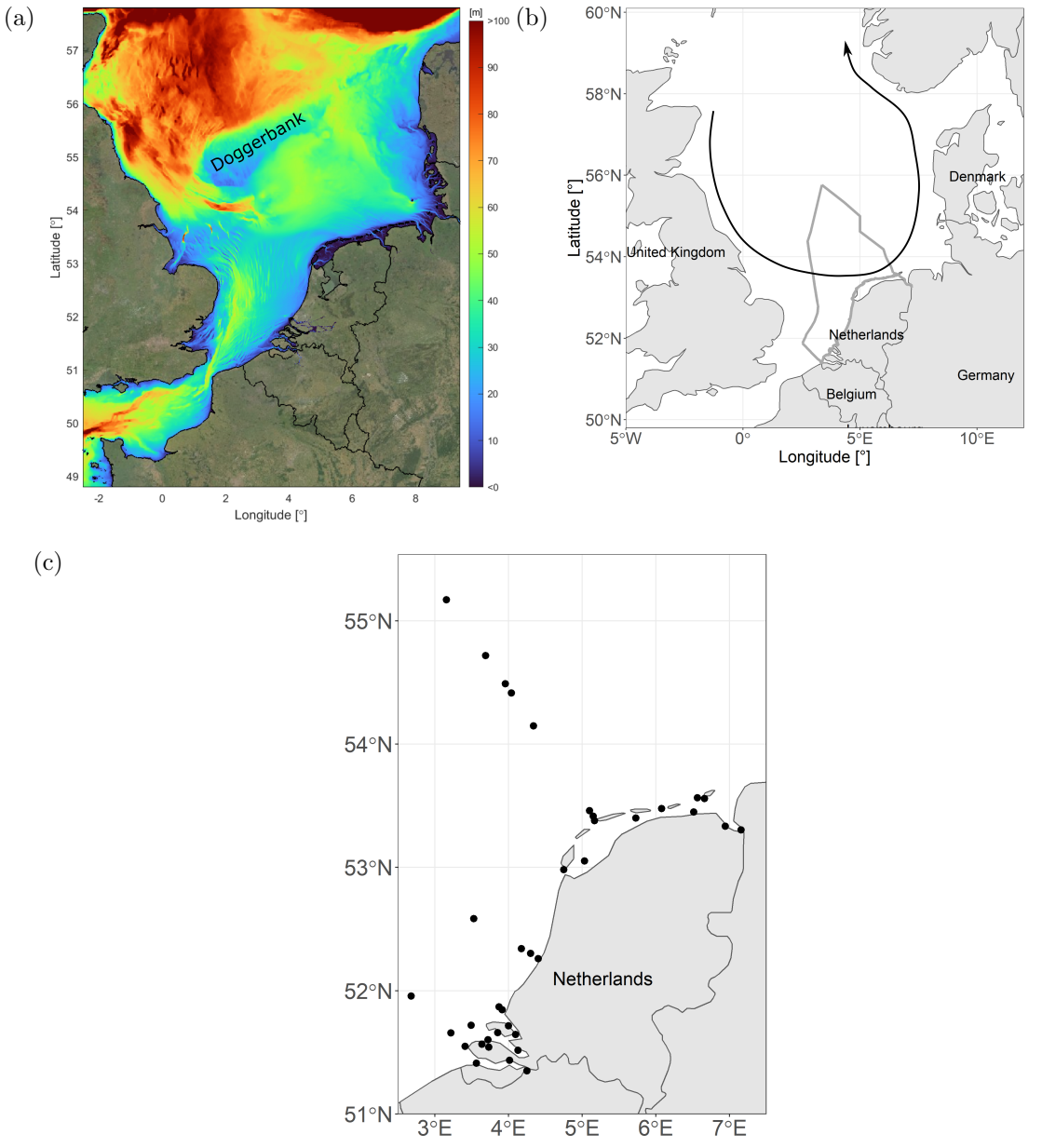

Figure 2.4: a) Visualization of the bathymetry of the North Sea (Courtesy of Stendert Laan, Deltares). The Doggerbank can be used separate the North from the South of the North Sea. b) Visualization of the dominant anti-clockwise circulation of the North Sea (arrow) as well as the Dutch economic zone (grey polygon - Flanders Marine Institute (2019)). c) Locations of the sampling stations of the Rijkswaterstaat monitoring program.

2.3 Aquatic ecosystem models

A model is a simplified representation of reality. Thus, a model does not contain all characteristics of the reality, but only those that are relevant for the purpose of the model (Soetaert and Herman, 2009). Models can be employed for a variety of reasons. They can be used to quantify process rates that are hard to measure in the field or as an analysis tool to determine the effect of certain changes or measures on, e.g., an ecosystem (Schuwirth et al., 2019). By formulating processes in mathematical equations, models can also be used to test our system knowledge or to investigate different scenarios (Soetaert and Herman, 2009).

There are many approaches to classify models. An often used classification approach is to classify models into three broad categories: physical, conceptual and mathematical models. A physical model is a simplified and miniaturize version of the original, such as a downscaled spillway. Thus, a physical model looks and works like the object it represents (given that the processes scale proportionally to the original). A conceptual model is a set of concepts or processes that help to understand and structure the subject that the model represents. Food web models are examples of conceptual models (e.g., Stoecker (1998)). Mathematical models build upon conceptual models by formulating the processes using mathematical concepts. Examples of mathematical models are statistical or mechanistic models. A statistical model is based on observations and a set of statistical assumptions, while a mechanistic model formulates the knowledge of certain mechanisms in mathematical equations (Janssen et al., 2015).

Aquatic ecosystem models (AEM) are often expressed as mathematical models that estimate the impact of external or internal forcings on aquatic ecosystem dynamics (Janssen et al., 2015). Models that describe the primary production of an aquatic ecosystem are usually an integral part of AEMs. Primary production models cover a wide variety of model descriptions. Some focus on large functional compartments (e.g., Fasham et al. (1990)), others focus on specific organisms (e.g., Flynn and Martin-Jézéquel (2000), Lancelot et al. (2005)) or simulate the growth of entire plankton communities (e.g., Litchman et al. (2006), Los (2009)), while others focus on certain size classes (e.g., Yoshiyama and Klausmeier (2008), Edwards et al. (2011)).

While many stand-along primary production models have have been developed that include mixoplankton (e.g., Hammer and Pitchford (2005), Flynn and Mitra (2009), Stickney et al. (2000), Mitra et al. (2014a), Ward and Follows (2016), Anschütz and Flynn (2020)), up until now, there are only a few primary production models for AEMs that represent mixoplankton activity as a functional trait. Ghyoot et al. (2017b) and Ghyoot et al. (2017b) implemented CMs and GNCMs into the MIRO model. Leles et al. (2018c) and Leles et al. (2021) implemented CM,

GNCM and SNCMs into the European Regional Seas Ecosystem Model (ERSEM). Those studies showed that including mixoplankton in AEMs changes the overall allocation of nutrients and energy resources within the trophic base of marine ecosystems. Thus, addressing the effect of mixoplankton in AEMs is essential to understand matter and energy fluxes in marine pelagic ecosystems and the ecosystems response to environmental changes such as climate change or other human impacts.

Chapter 3

Exploring the trophic spectrum: placing mixoplankton into marine protist communities of the Southern North Sea

Published article: Schneider, L.K., Flynn, K.J., Herman, P.M.J., Troost, T.A. and Stolte, W. (2020). Exploring the trophic spectrum: placing mixoplankton into marine protist communities of the Southern North Sea. *Frontiers in Marine Science*. 7

Abstract

While traditional microplankton community assessments focus primarily on phytoplankton and protozooplankton, the last decade has witnessed a growing recognition of photo-phago mixotrophy (performed by mixoplankton) as an important nutritional route among plankton. However, the trophic classification of plankton and subsequent analysis of the trophic composition of plankton communities is often subjected to the historical dichotomy. We circumvented this historical dichotomy by employing a 24 year-long time series on abiotic and protist data to explore the trophic composition of protist communities in the Southern North Sea. In total, we studied three different classifications. Classification A employed our current knowledge by labeling only taxa documented to be mixoplankton as such. In a first trophic proposal (classification B), documented mixoplankton and all phototrophic taxa (except for diatoms, cyanobacteria and colonial *Phaeocystis*) were classified as mixoplankton. In a second trophic proposal (classification C), documented mixoplankton as well as motile, phototrophic taxa associated in a principle component analysis with documented mixoplankton were classified as mixoplankton. In all three classifications, mixoplankton occurred most in the inorganic nutrient-depleted, seasonally stratified environments. While classification A was still subjected to the traditional dichotomy and underestimated the amount of mixoplankton, our results indicate that classification B overestimated the amount of mixoplankton. Classification C combined knowledge gained from the other two classifications and resulted in a plausible trophic composition of the protist community. Using results of classification C, our study provides a list of potential unrecognized mixoplankton in the Southern North Sea. Furthermore, our study suggests that low turbidity and the maturity of an ecosystem, quantified using a newly proposed index of ecosystem maturity (ratio of organic to total nitrogen), provide an indication on the relevance of mixoplankton in marine protist communities.

3.1 Introduction

Plankton communities form the base of all open-water ecosystems. Traditionally, organisms of these communities have been primarily classified into either phototrophs or heterotrophs. However, the dichotomous plankton classification has been increasingly questioned, and now the photo-phago mixotrophic potential (i.e., the combination of photo- and phagotrophy in one cell) of many phytoplankton and protozooplankton species is being recognised (Flynn et al., 2013; Glibert, 2016; Mitra et al., 2016; Stoecker et al., 2017). Flynn et al. (2019) proposed to use the term mixoplankton for these organisms and the terms phyto- or protozooplankton, respectively, for organisms incapable of phagotrophy or phototrophy.

Mixoplankton have the potential to access more resources than are available to pure phyto- and protozooplankton (Barton et al., 2013; Stoecker et al., 2017). By employing both photo- and phagotrophy, mixoplankton can overcome the limitations of low inorganic nutrient environments that restrict the growth of phytoplankton or prey limitations that restrict the growth of protozooplankton. Mitra et al. (2016) provided a functional classification separating mixoplankton into different groups. Constitutive Mixoplankton (CM) have the innate ability to perform photosynthesis while Non-Constitutive Mixoplankton (NCM) need to acquire photosynthetic capabilities from their prey. As a result, the different types of mixoplankton have varying abiotic and biotic requirements (Anschütz and Flynn, 2020).

Mixoplankton can potentially increase the trophic transfer efficiency (Stoecker et al., 2017). Including mixoplankton in aquatic ecosystem models is necessary to capture this change in system dynamics (Mitra et al., 2014a; Ghyoot et al., 2017b; Flynn et al., 2018). Furthermore, mixoplankton are important for the management of marine environments, as many harmful algal bloom species are known mixoplankton (e.g., *Dinophysis*) (Burkholder et al., 2008; Reguera et al., 2012). For modelling and management discussions, it is important to research the trophic composition of plankton communities and link the trophic composition to abiotic environments.

The link between marine phytoplankton communities and abiotic environments has long been researched. The Southern North Sea microplankton community has also been well studied; Baretta-Bekker et al. (2009) and Prins et al. (2012) did so using data from the same monitoring program employed in this study. Most of these studies did not include the role of mixoplankton. However, there have been various local (e.g., Stoecker et al. (1989), Löder et al. (2012) and Duhamel et al. (2019)) and even specific global (Harrison et al., 2011) studies of certain mixoplankton groups. More recently, Leles et al. (2017), Leles et al. (2018b) and Faure et al. (2019) presented the first comprehensive analyses on the global biogeography of mixoplankton. While Hansson et al. (2019) recently published a study on abiotic

drivers of mixoplankton in boreal lakes, our work is, to the best of our knowledge, the first study that addresses the relation between marine plankton community assessments in different abiotic environments and the identification of potential mixoplankton in these marine communities.

However, even when a consensus to include mixoplankton in ecosystem studies is reached, a high uncertainty remains when assigning a trophic mode to taxa. Many chlorophyll-containing flagellates are classified as phototrophs by default while most are actually potentially mixotrophic (Selosse et al., 2017). The difficulty of observing marine mixoplankton feeding in the wild or in the laboratory adds to this uncertainty (Worden et al., 2015; Anderson et al., 2017; Stoecker et al., 2017).

Currently, there are two contrasting views on the trophic mode of marine plankton communities present in literature. On the one hand, photo- or phagotrophy are assumed to be the default trophic modes of all planktonic protists. If photo-phago-mixotrophy is considered at all, only taxa proven to be capable of such are classified as mixoplankton. On the other hand, if photo-phago-mixotrophy is assumed to be the default trophic mode in all protists, then only taxa proven to be incapable of photo-phago-mixotrophy are classified as phyto- or protozooplankton (Flynn et al., 2013; Mitra et al., 2014a; Leles et al., 2017; Leles et al., 2018b).

The aim of this study is to explore the uncertainty of these two trophic views and their implications for plankton community assessments using quantitative, long term data. To do this, we exploited a 24 year-long time series on abiotic and protist data in the Southern North Sea along with literature on mixoplankton. While most routine monitoring data on protists fail to count small and fragile protists (Haraguchi et al., 2018; Flynn et al., 2019), routine monitoring data such as the ones employed in this study are still useful as they cover a long time frame and a wide range of abiotic gradients. This makes the dataset ideal for researching the trophic composition of protist communities in varying abiotic environments.

Using this dataset, we studied three trophic classifications to take the trophic uncertainty of marine protist communities into account. In classification A (the 'documented mixoplankton' classification), only documented mixoplankton were labelled as such. In classification B (the 'presumed mixoplankton' classification), only diatoms, cyanobacteria and colonial *Phaeocystis* were labelled as phytoplankton. The other motile, phototrophic taxa and documented mixoplankton were labeled as mixoplankton. Then, using a principle component analysis (PCA), we constructed a third numerical classification (classification C - the 'environmentally-defined mixoplankton' classification) in which documented mixoplankton and motile, phototrophic taxa associated with documented mixoplankton were labeled as mixoplankton. Due to the trophic uncertainty, we were not able to verify the results of the different classifications against other existing datasets. Thus, we proceeded to use literature and a partial redundancy analysis (RDA) to determine which

classification seemed the most likely.
More specifically, the steps taken in this study were 1) to determine the spatial and temporal variations of the abiotic parameters and the protist communities, 2) to establish where mixoplankton occur in the Southern North Sea, 3) to determine which abiotic factors favour mixoplankton and 4) to explore the implications of the three trophic classifications.

3.2 Material and methods

3.2.1 Study site

The North Sea is a shallow marginal sea of the Atlantic Ocean located on the European continental shelf. The North Sea is roughly divided into two regions, the Northern and the Southern North Sea. This study focuses on the Dutch continental shelf in the Southern North Sea (51 - 55 °N) (see fig. 3.1).
In terms of inorganic nutrients, the Southern North Sea ranges from nutrient-rich estuaries to offshore regions that seasonally become relatively nutrient-poor (Beusekom and Diel-Christiansen, 2009). The Southern North Sea is also highly diverse in terms of stratification and seasonality. Where tidal currents dominate, continuous vertical mixing of the water column occurs. Regions of freshwater influence are (often intermittently) salinity stratified, while deeper waters with less tidal influence show intermittent or seasonal thermal stratification (Große et al., 2016). Apart from nutrient and stratification gradients, the Southern North Sea is also impacted by gradients of suspended sediments, dissolved oxygen, pH and salinity (Emeis et al., 2015).
The Southern North Sea is an umbrella term for regions commonly referred to as the Southern Bight, the Wadden Sea and the Doggerbank (Beets and Spek, 2000). The depth of the Southern Bight and the Wadden Sea increases from the coast towards the central North Sea. The central North Sea can reach down to 40 m depth. However, the Doggerbank, which is located in the central North Sea, is only 18 m deep (Nielsen et al., 1993). Based on these hydrographic environments and geographic locations, we grouped 37 stations into 11 location classes (see fig. 3.1).
The Westerschelde, the Wadden Sea and the Oosterschelde are geographically distinct environments. The location class Voordelta groups coastal sampling stations northwest of the Rhine estuary. The location class Holland Coast groups sampling stations northeast of the Rhine estuary that lie in the region of freshwater influence (Simpson et al., 1993). The sampling stations north of the Wadden Sea barrier islands were grouped into the location class Coastal Wadden Sea. The Veerse Meer was separated from the North Sea and the Oosterschelde in 1961

and reopened towards the Oosterschelde in 2004. Thus, the Veerse Meer has a unique hydrographic environment (Bakker, 1972). Grevelingen is a closed-off arm of the Rhine-Meuse estuary with a sluice maintaining the saline character of the system. The location class Offshore Mixed had no records of summer stratification over the 24 year period and was thus separated from the Offshore location class. Doggerbank was placed into a separate location class due to its shallow depth.

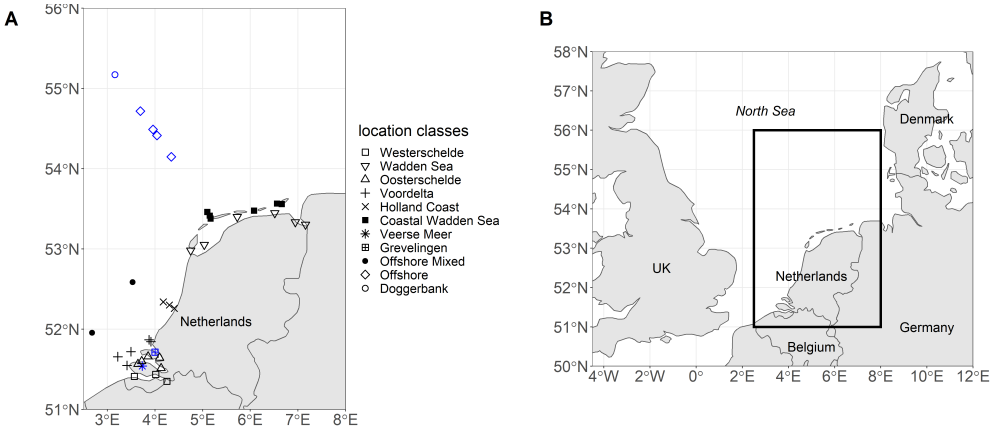

Figure 3.1: **A** The map displays the locations of the 37 sampling stations in the Southern North Sea labelled according to their location class. Black indicates that only surface samples were taken. Blue indicates that summer stratification occurred and three depths were sampled (surface, pycnocline and bottom). **B** The map places the sampling region within the context of the North Sea.

3.2.2 Datasets

In our study, we used abiotic and protist data from 1990 to 2014 that were sampled by the Rijkswaterstaat monitoring program (RWS - Dutch Directorate-General for Public Works and Water Management). On average, the 37 stations were monitored every four weeks from October - February and every two weeks from March - September. The abiotic and protist samples were usually taken at the same time. However, after 2010, the sampling frequency of plankton data decreased and from 2010 onward, for all stations (with the exception of Doggerbank), protist samples were taken quarterly during the growth season (March - September). Doggerbank was sampled once in each of the months January, April, June and August. The samples were taken at the surface (typically at 1 m depth). When stations showed (seasonal) stratification, they were sampled near the bottom and pycnocline as well. In this study, we focused on the routine sampling data for surface-waters; in

doing so it should be noted that seasonal mixing of the water column affects how well such sampling reflects the whole protist community. To determine the yearly vs. spatial variation in the datasets, we conducted an estimation of variance components analysis (VCA) using the R-package VCA (Schuetzenmeister and Dufey, 2019) (see supplementary material for more details).

3.2.2.1 Abiotic data

The abiotic data were retrieved from a Deltares database (Waterbase Deltares, 2019). Nutrients, i.e., NO_3^-, NH_4^+, NO_2, dissolved inorganic phosphate (DIP) measured as soluble reactive phosphate, dissolved inorganic silica (DISi), total nitrogen (TN; the sum of dissolved inorganic, dissolved organic and particulate organic nitrogen), as well as suspended sediment and salinity were extracted. Dissolved inorganic nitrogen (DIN) was calculated from its separate components (DIN $= NO_3^- + NH_4^+ + NO_2$). The data were grouped according to the previously described location classes. For DIP, outliers (values over the 98$^{\text{th}}$ percentile) were removed.
In addition, the relative availability of DIN was determined using the ratio of organically bound nitrogen (orgN) to total nitrogen $\left(\frac{\text{orgN}}{\text{TN}} = \frac{\text{TN}-\text{DIN}}{\text{TN}}\right)$. Margalef (1963) defined maturity in terms of energy flow. Applying this line of thought, we termed this ratio the index of ecosystem maturity (IEM) as it describes the shift from abundant inorganic to mostly organism-bound nitrogen typical for ecosystem maturation. Thus, the IEM enables a comparison between environmental systems that differ from each other in terms of absolute nitrogen concentrations. The IEM is given as a value between 1 (mature) and 0 (immature).

3.2.2.2 Protist data

The protist data were retrieved from the RWS data servicedesk (RWS, 2019). The dataset contains information on taxa, location, cell counts, biovolumes, biomass as well as trophic mode. During monitoring, 1 L plankton bottle samples were collected and preserved with 4 mL acid Lugol's iodine. The samples were then identified and counted using inverted microscopy to determine the number of cells per taxon. As the sampling technique was not optimized towards sampling ciliates, ciliates (with the exception of *Mesodinium rubrum*) were not identified. Whenever possible, the cells were identified down to their species level, otherwise the cells were identified to their genus or higher taxonomic levels. Cell counts were transformed into carbon biomass using biovolume coefficients (Baretta-Bekker et al., 2009). The sampling methodologies can be reviewed in more detail in Baretta-Bekker et al. (2009) and Prins et al. (2012). The taxa were matched against the World Register of Marine Species (WoRMS Editorial Board, 2020) and the accep-

ted scientific name was used for the subsequent analysis to harmonize taxonomic names over the 24 year time period.

A partial PCA as well as a partial RDA was completed using the vegan package in R (Stevens et al., 2019). We used the partial PCA to determine the environmental envelope of proven mixoplankton. We define an environmental envelope as the polygon that encloses all taxa of a certain group, in this case the proven mixoplankton. We used the partial RDA to associate the different trophic groups with the abiotic factors. Due to changes in the identification and counting protocol in 2000 and the change of sampling frequencies after 2010, an observer effect was applied as a condition within the partial PCA and RDA which ensures that the resulting axes are linearly unrelated to the observer effect.

For each classification, the fraction of each trophic mode of the total biomass per month, year and location class was calculated. The trophic mode was processed in three different ways to study the three trophic analysis scenarios.

Classification A: documented mixoplankton Literature by Jeong et al. (2010), Löder et al. (2012), Leles et al. (2017) and Leles et al. (2018b) was used to identify taxa with a documented ability to perform photo-phago mixotrophy. These taxa were binned as "mixoplankton" and the type of mixotrophy as per Mitra et al. (2016) was allocated. The other taxa were binned as "phytoplankton" or "protozooplankton". When a taxon was only identified down to genus level and species belonging to that genus were also present in the dataset, the entire genus was assigned the trophic mode that was most abundant (in terms of biomass) among the species belonging to that genus. Five taxa (class *Dinophyceae*, family *Gymnodiniaceae*, family *Peridiniaceae*, order *Peridiniales*, class *Raphidophyceae*) were labelled as "unknown trophy" as it was not possible to assign a trophic mode to those taxonomic ranks with confidence.

Classification B: presumed mixoplankton According to the functional classification argued by Flynn et al. (2013) and Mitra et al. (2016), all organisms capable of phototrophy were labelled as "mixoplankton" except for those that are proven to be incapable of phagocytosis. Thus, only diatoms, cyanobacteria and colonial *Phaeocystis* were labelled as "phytoplankton". The "protozooplankton" remained the same as in classification A.

Classification C: environmentally-defined mixoplankton Proven mixoplankton and motile, phototrophic taxa associated with the environmental envelope of proven mixoplankton were binned as "mixoplankton". Phototrophic taxa not associated with the environmental envelope of proven mixoplankton as well as diatoms, cyanobacteria and colonial *Phaeocystis* were labelled as "phytoplankton". The "protozooplankton" remained the same as in the other two classifications.

3.3 Results

3.3.1 Abiotic data

Figures 3.2 and 3.3 visualise the nutrient concentrations (DIN, DIP and DISi) and the IEM as well as suspended sediment, salinity and stratification for each location class. In all figures, abiotic gradients from the estuaries to the offshore are evident. Based on these abiotic parameters, the location classes can be grouped into four systems.
1) Unstratified estuary systems (ES): Westerschelde and Wadden Sea. Both location classes were characterised by salinity values around 20 and high suspended sediment values (long term average of 50 mg/L). The Westerschelde had a low IEM and high DIN, DIP and DISi concentrations throughout the time period with the exception of DISi that showed a slight decrease during summer. During summer, the Waddensea had a high IEM and medium DIN, DIP and DISi concentrations during the summers.
2) Unstratified coastal systems (CS): Oosterschelde, Voordelta, Holland Coast and Coastal Wadden Sea. These location classes could be clearly separated from the other location classes by their salinity (around 30) and their suspended sediment values (between 20-45 mg/L). Compared to the estuary systems, the coastal systems had lower nutrient concentrations during summer. After 2010, the DISi concentration decreased. All four location classes showed seasonality in the IEM (high during summer).
3) Seasonally stratified, anthropogenically modified systems (AS): Veerse Meer and Grevelingen. Both location classes were characterised by low salinity and suspended sediment values. Both location classes had low DIN concentrations and had a high IEM during summer. While Grevelingen displayed decreased DIP and DISi concentrations during spring, Veerse Meer had high nutrient concentrations throughout this time period. The opening of the Veerse Meer to the Oosterschelde in 2004 was reflected in the salinity and suspended sediment values.
4) Offshore systems (OS): Offshore Mixed (unstratified), Offshore (stratified) and Doggerbank (stratified). These location classes were characterised by high salinity (35) and very low suspended sediment values. The offshore systems had very low nutrient concentrations during summer and had high IEM. Compared to the coastal systems (category 2), the period nutrient concentration decrease was longer in the offshore systems. The DIN concentrations decreased from 2000 - 2006, while the DISi concentrations decreased after 2007.
Year-to-year variations were visible for all location classes, especially for Veerse Meer. However, the VCA showed that the location classes contributed over 80 % of the variation while the yearly changes contributed less than 4 %.

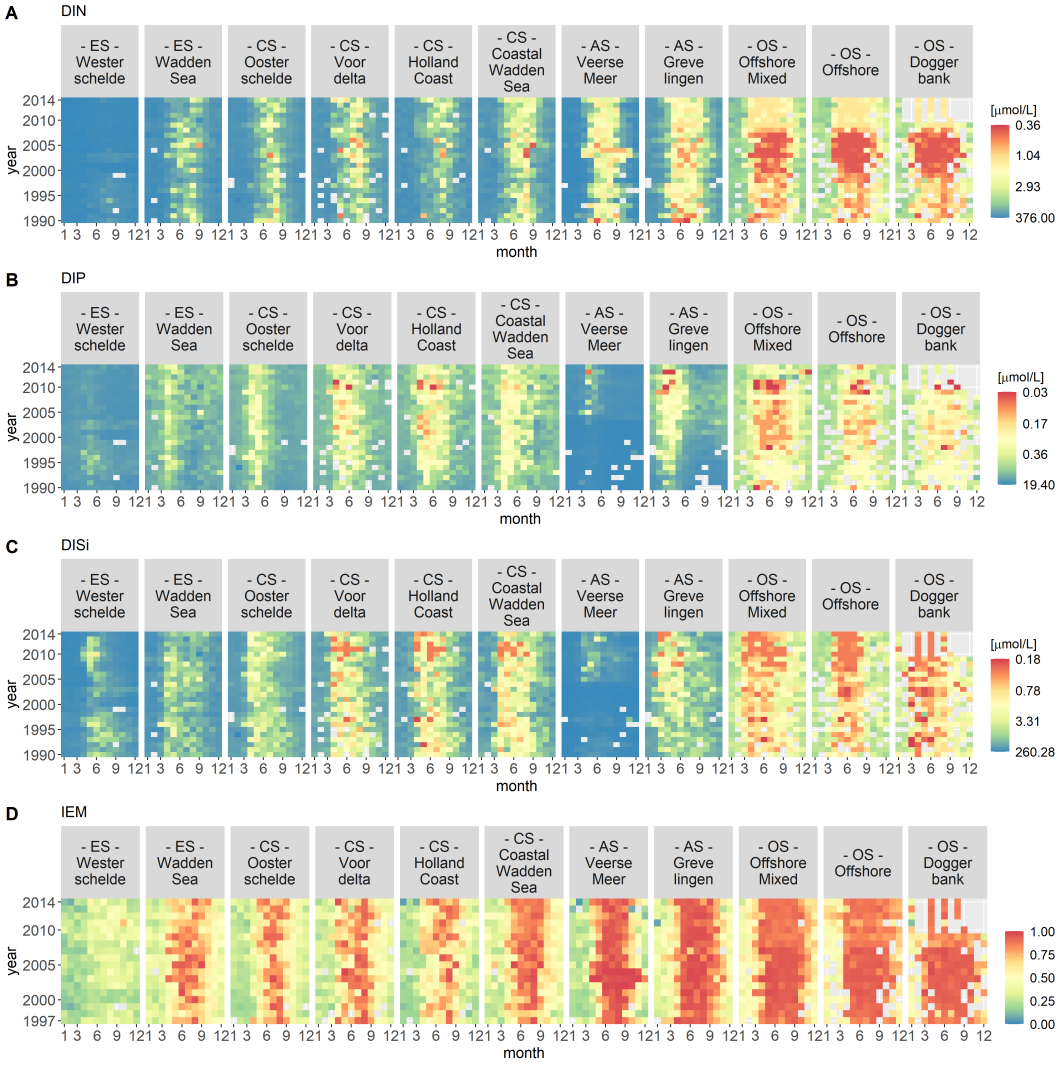

Figure 3.2: Monthly median of nutrient concentrations for DIN (**A**), DIP (**B**) and DISi (**C**) as well as the IEM (index of ecosystem maturity - **D**) for each location class per year. The nutrient concentrations were hyperbolically transformed. The location classes are grouped into estuary (ES), coastal (CS), anthropogenically modified (AS) and offshore systems (OS). The figures display gradients (left to right) from the estuary systems (ES) to the offshore systems (OS).

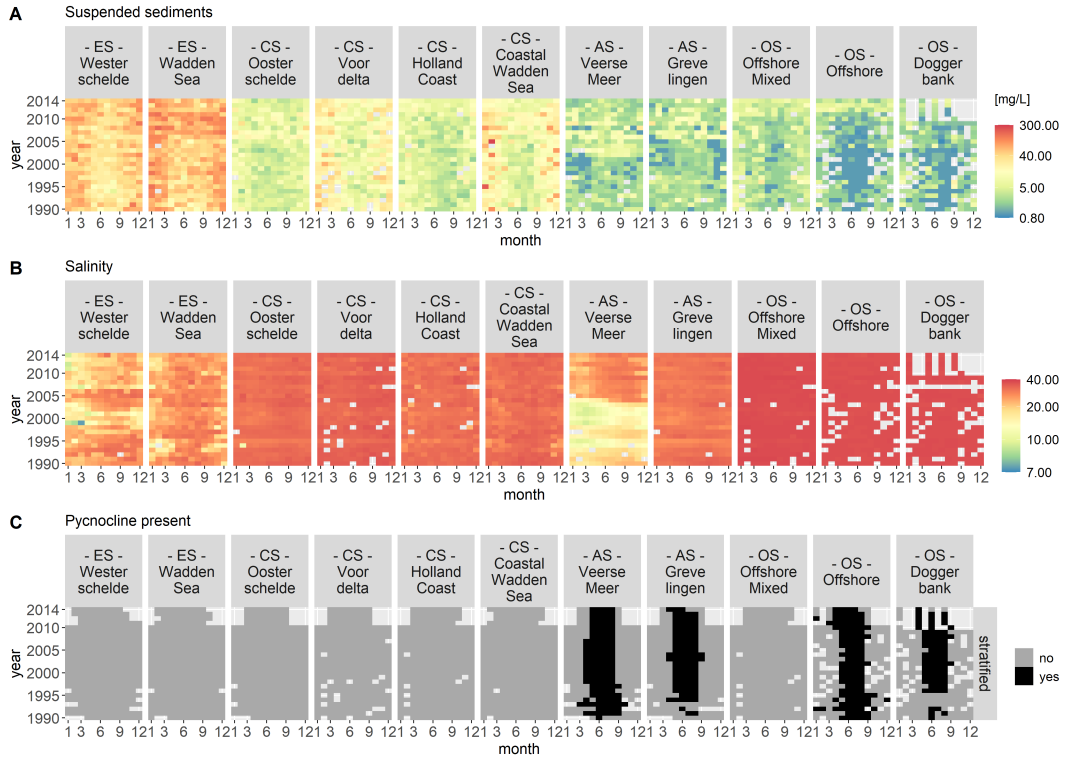

Figure 3.3: Monthly median of suspended sediments (**A**), salinity (**B**) and stratification (**C**) for each location class per year. Suspended sediment and salinity use a logarithmic colour scale. The location classes are grouped into estuary (ES), coastal (CS), anthropogenically modified (AS) and offshore systems (OS). The figures display gradients (left to right) from the estuary systems (ES) to the offshore systems (OS). In **C**, the colour black indicates that a pycnocline was detected at the location classes Veerse Meer, Grevelingen, Offshore and Doggerbank.

3.3.2 Protist data

The protist data set contained 621 unique taxa in a size range from 1 to 800 μm. It should be noted that small nanoflagellates might be poorly represented (see figure S1 in the supplementary material). Table 3.1 summarizes the number of taxa per trophic mode for each classification and table 3.2 summarizes the trophic modes of the five most abundant taxonomic classes.
Figures 3.4 visualizes the site ordination plots from the partial PCA of the protist data. The ordination plot is dominated by two gradients. In figure 3.4A, the estuaries compose a group in the upper right quadrant, the coastal systems are grouped around the origin while the anthropogenically modified and offshore

Table 3.1: The table presents the number of taxa per trophic mode and trophic classification.

	Classification		
	A	B	C
phytoplankton	466	308	390
mixoplankton	49	212	130
protozooplankton	101	101	101
microplankton of unknown trophy	5	0	0

Table 3.2: The table presents the types of trophic mode for the five most important taxonomic classes for each trophic classification. The five taxonomic classes presented here make up over 90 % of the plankton biomass.

		phyto-plankton	mixo-plankton	protozoo-plankton	unknown trophy
Dinophyceae	A	48	37	91	4
	B	-	89	91	-
	C	14	75	91	-
Bacillariophyceae	A	289	-	-	-
	B	289	-	-	-
	C	289	-	-	-
Chlorophyceae	A	31	-	-	-
	B	-	31	-	-
	C	23	8	-	-
Prymnesiophyceae	A	9	2	-	-
	B	-	11	-	-
	C	3	8	-	-
Cryptophyceae	A	4	-	-	-
	B	-	4	-	-
	C	2	2	-	-

systems are grouped towards the lower left quadrant. Thus, the location class gradient divides the ordination plot into two triangles with a top right triangle depicting the estuaries and a bottom left triangle depicting the offshore systems. No distinguishable trend from year to year can be seen in figure 3.4B. Figure 3.4C shows a clear seasonal pattern with the seasons gradient dividing the ordination plot into two triangles - a top left triangle depicting the fall/winter months and a bottom right triangle depicting the spring/summer months.

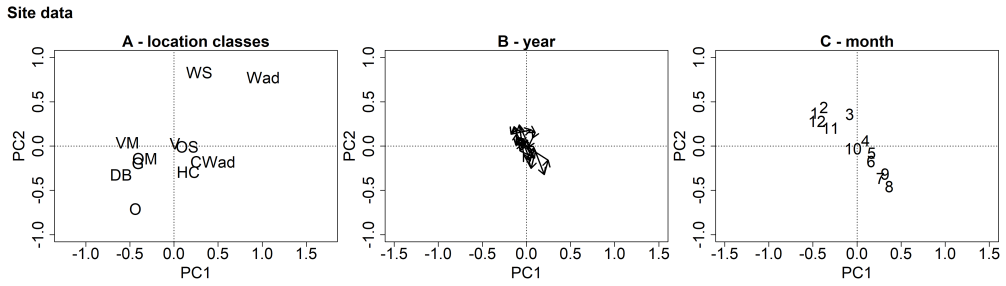

Figure 3.4: PCA ordination plots for the site data. **A** displays the ordination centers for the location classes (WS - Westerschelde, Wad - Wadden Sea, OS - Oosterschelde, VD - Voordelta, HC - Holland Coast, CWad - Coastal Wadden Sea, VM - Veerse Meer, G - Grevelingen, OM - Offshore Mixed, O - Offshore, D - Doggerbank), **B** the ordination centers for the years and **C** the ordination centers for the months. The plots are dominated by two opposite, diagonally oriented gradients representing the location classes and months.

Figures 3.5 display the species scores from the partial PCA for all three trophic classifications and they highlight the differences in the mixoplankton between the three different trophic classifications. All protists are located in the spring/summer months triangle which corresponds to the protists growth period.
For classification A, the protozooplankton, mixoplankton and microplankton of unknown trophy occupy the lower right quadrant (corresponding to the summer months and non-estuary systems), while the phytoplankton extend over both right quadrants (corresponding to the summer months and all location classes). For classification B, mixoplankton form two groups one in the lower right quadrant (corresponding to the summer months and non-estuary systems) and one in the upper right quadrant (corresponding to the summer months and the estuary system). The orientation of phytoplankton and protozooplankton is the same as in trophic classification A. For classification C, only those motile, phototrophic taxa of analysis scenario B that were located within the environmental envelope of proven mixoplankton were retained in the mixoplankton category and so the orientation of mixoplankton for classification C corresponds to that of classification

A. Table S2 in the supplementary data provides a list of motile, phototrophic taxa associated with the environmental envelope of proven mixoplankton.

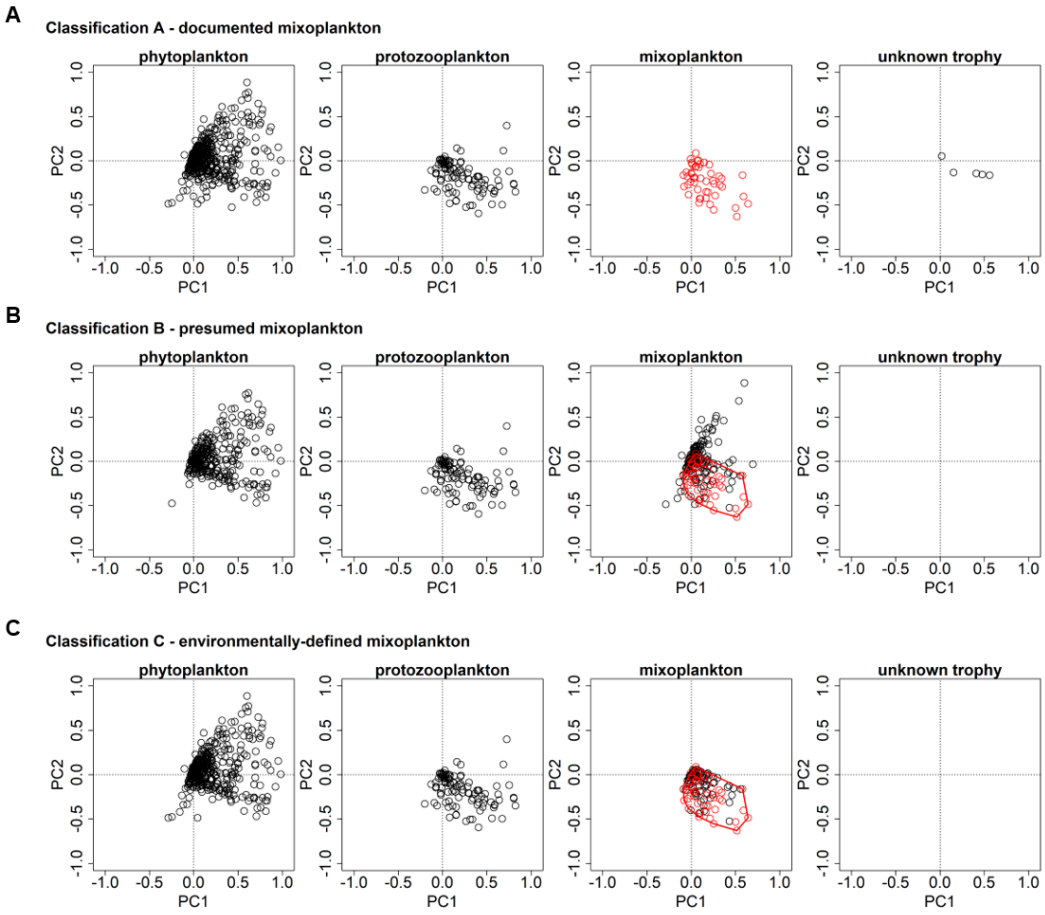

Figure 3.5: PCA ordination plots for the species data of the three trophic classifications. **A**) The documented mixoplankton (in red) are oriented towards the bottom right quadrant. **B**) The presumed mixoplankton are oriented towards both right quadrants. The documented mixoplankton of **A** are displayed in red and the red polygon highlights the environmental envelope of the documented mixoplankton. **C**) The documented mixoplankton are displayed in red and the additional environmentally-defined mixoplankton are displayed in black. The additional environmentally-defined mixoplankton were chosen as they lie within the environmental envelope of documented mixoplankton of **A** (displayed by the red polygon).

3.3.2.1 Trophic classification A (documented mixoplankton)

Trophic classification A visualises the trophic composition of the protist community in which only proven mixoplankton were classified as such. Figure 3.6A displays the biomass per month, year and location class for each trophic mode. The fraction of mixoplankton displayed a clear spatial gradient and was highest in the offshore location classes. Figure 3.6B shows that the mixoplankton consisted almost entirely of CMs.

In the estuary systems (Westerschelde and Wadden Sea), phytoplankton constituted the largest part of the plankton community in April/May as well as in August/September. Protozooplankton constituted the largest group in June or July, depending on the year. In the estuaries, mixoplankton and microplankton of unknown trophy did not contribute notably to the overall plankton composition.

In the coastal systems (Oosterschelde, Voordelta, Holland Coast and Coastal Wadden Sea), phytoplankton were the largest group in April/May as well as in August/September, whereas protozooplankton were the largest group in June/July. In the Coastal Wadden Sea, protozooplankton constituted the largest group into early autumn. In the four coastal systems, microplankton of unknown trophy contributed around 25% to the protist community during August and September. For all coastal systems, mixoplankton contributed only slightly to the trophic plankton composition during the late summer/fall period. However, after 2009 in the Oosterschelde, mixoplankton contributed around 25% to the protist community during summer and fall.

The anthropogenically modified systems (Veerse Meer and Grevelingen) differed from the estuary and coastal systems through their lack of a consistent protozooplankton bloom in the summers. For both location classes, mixoplankton peaked during a few months over the 24 year time period to over 50% of the community biomass. In Veerse Meer, phytoplankton were the largest group throughout the whole period. However, in Grevelingen, phytoplankton did not dominate to the same extent. Microplankton of unknown trophy contributed notably to Grevelingen, which was not the case for Veerse Meer.

The offshore systems (Offshore Mixed, Offshore and Doggerbank) displayed a diverse trophic composition. For these location classes, phytoplankton constituted the largest group in spring. The rest of the year, microplankton of unknown trophy made up around 50% and mixoplankton 25% of the plankton community. There was no consistent fraction of protozooplankton during the summer months.

The temporal variations in the plankton data were more pronounced compared to the abiotic data. However, the VCA showed that the spatial components contributed more to the variation (over 25 %) than the temporal components (less than 10 %). The temporal variations visible in the abiotic data for the anthropogenically modified systems were not visible in the plankton data.

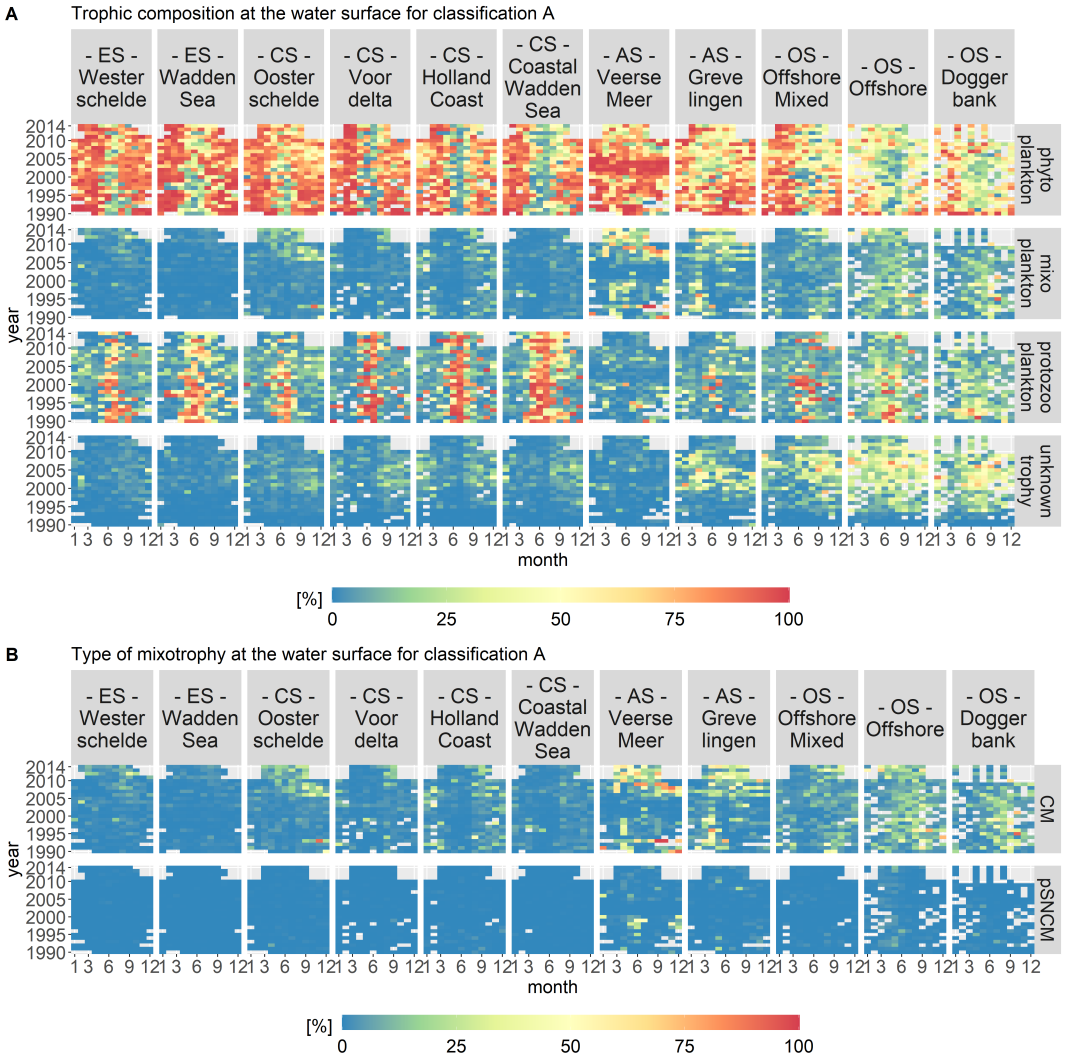

Figure 3.6: Monthly fractions of the total biomass per trophic mode (**A**) and per type of mixotrophy (**B**) for trophic classification A. The location classes are grouped into estuary (ES), coastal (CS), anthropogenically modified (AS) and offshore systems (OS). CM stands for Constitutive Mixoplankton and pSNCM for plastid Specialist Non-Constitutive Mixoplankton, which are a subcategory of NCMs. The occurrence of constitutive mixoplankton displays a clear spatial gradient.

3.3.2.2 Trophic classification B (presumed mixoplankton)

Figure 3.7 displays the biomass per month, year and location class for each trophic mode for trophic classification B. In contrast to classification A, classification B assumed all motile, phototrophic taxa to be mixoplankton. Only diatoms, cy-

anobacteria and colonial *Phaeocystis* are classified as phytoplankton. The protozooplankton remained the same as in classification A. The fraction of mixoplankton was highest in the offshore location classes and mixoplankton seasonally occurred in the early summer and fall at all location classes.

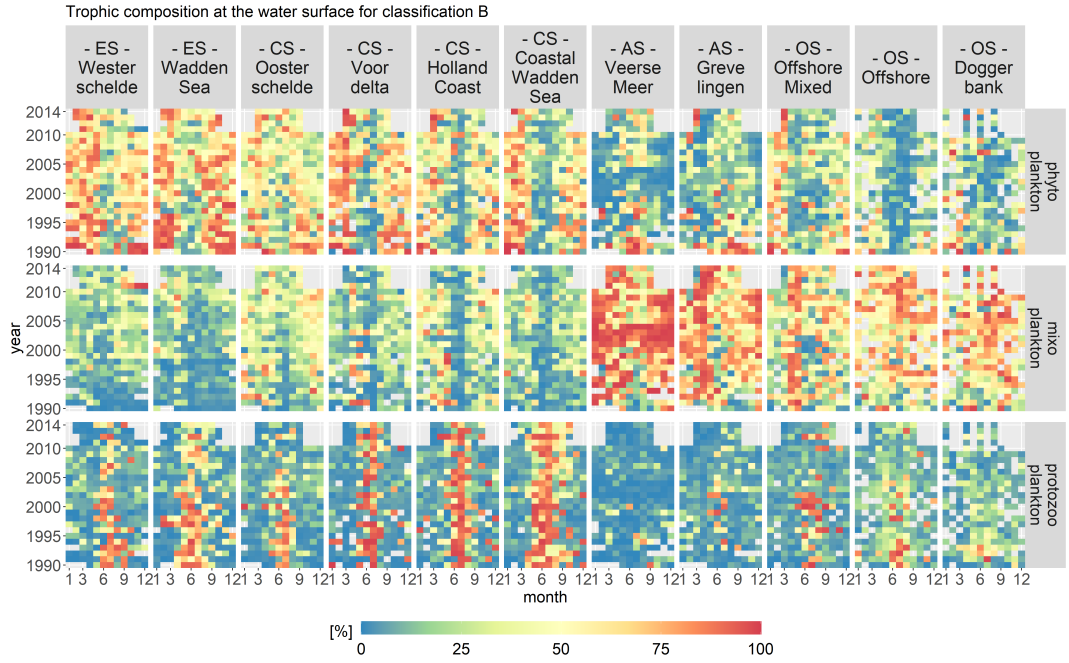

Figure 3.7: Monthly fractions of the total biomass per trophic mode for trophic classification B. The location classes are grouped into estuary (ES), coastal (CS), anthropogenically modified (AS) and offshore systems (OS). The fraction of mixoplankton is highest in the offshore location class. All location classes display a seasonal occurrence of mixoplankton in the early summer and fall.

The spatial distribution for classification B remained in principle the same as for classification A. The highest fraction of mixoplankton still occurred in the offshore and anthropologically modified location classes. However, the seasonal succession of trophic modes changed as compared to trophic classification A. The mixoplankton fraction increased at all location classes in the early summer and fall compared to analysis scenario A. The anthropogenically modified systems displayed interesting anomalies. From 2002 - 2004 in Veerse Meer, mixoplankton (taxa *Chlorophyceae*) contributed around 100% to the protist community. During the summer months after 2006, phytoplankton and mixoplankton both contributed equally (both 50%) to the plankton community. Overall, Grevelingen had a high fraction of mixoplankton in the early spring season.

The temporal variations in classification B were more pronounced as compared to classification A. Nonetheless, the VCA showed that the spatial components contributed more to the variation (over 50%) than the temporal components (10 %). The temporal variations visible in the abiotic data for the anthropogenically modified systems were reflected in classification B.

3.3.2.3 Trophic classification C (environmentally-defined mixoplankton)

Figure 3.8 displays the biomass per month, year and location class for each trophic mode for trophic classification C. Classification C categorized mixoplankton using the partial PCA results. For classification C only documented mixoplankton and motile, phototrophic taxa associated with the environmental envelope of documented mixoplankton were labeled as mixoplankton. In contrast to the other two trophic classifications, the seasonal distribution of mixoplankton for all location classes was oriented more towards the late summer/autumn season.

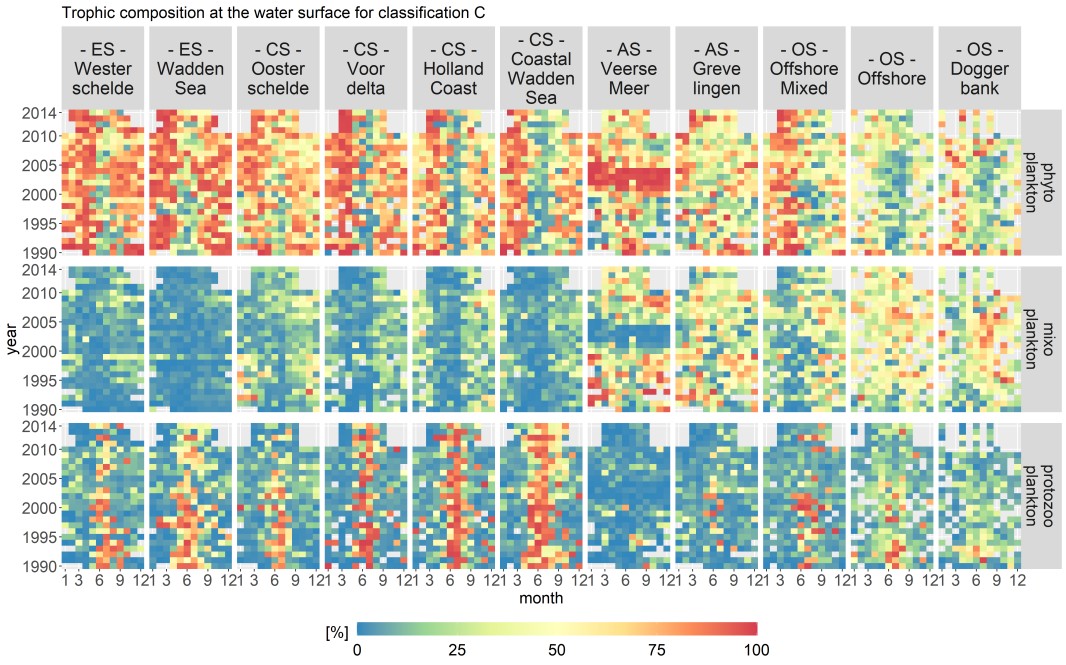

Figure 3.8: Monthly fractions of the total biomass per trophic mode for trophic classification C. The location classes are grouped into estuary (ES), coastal (CS), anthropogenically modified (AS) and offshore systems (OS). The mixoplankton fraction displays a clear spatial and seasonal gradient.

The mixoplankton fraction displayed a clear spatial and seasonal gradient. Spa-

tially, the mixoplankton fraction was highest in the offshore location classes. Seasonally, mixoplankton occurred more during the late summer months. Especially in the estuary and coastal location classes, a seasonal succession of trophic modes was visible from phyto- (spring) to protozoo- (summer) to mixoplankton (fall). Veerse Meer and Grevelingen were exceptions. In Grevelingen, mixoplankton contributed 50% to the plankton community during the whole year. Veerse Meer displayed a stark shift from 2002 - 2004 in which phytoplankton completely dominated the plankton community (taxa *Chlorophyceae*). This shift coincided well with the opening of Veerse Meer to the Oosterschelde.
Of all three trophic classifications, the temporal variations in classification C were the most pronounced, which was especially visible in the trophic composition of Veerse Meer. However, the temporal contribution to variance was still small (around 10 %) compared to the spatial contribution (over 40 %).

3.3.3 Abiotic drivers of mixoplankton distribution

Figure 3.9 displays the partial RDA ordination plots for phytoplankton and mixoplankton for the three trophic classifications. For all three trophic classifications of figure 3.9A, phytoplankton are oriented towards the suspended sediment gradient. In figure 3.9B, documented and environmentally-defined mixoplankton (trophic classifications A and C) are oriented towards the IEM and nutrient concentration gradients and away from the suspended sediment gradient. The assumption that all motile, phototrophic protist are mixoplankton (as in trophic classification B) places some mixoplankton along the suspended sediment gradient, which is clearly associated with phytoplankton (see fig. 3.9A).

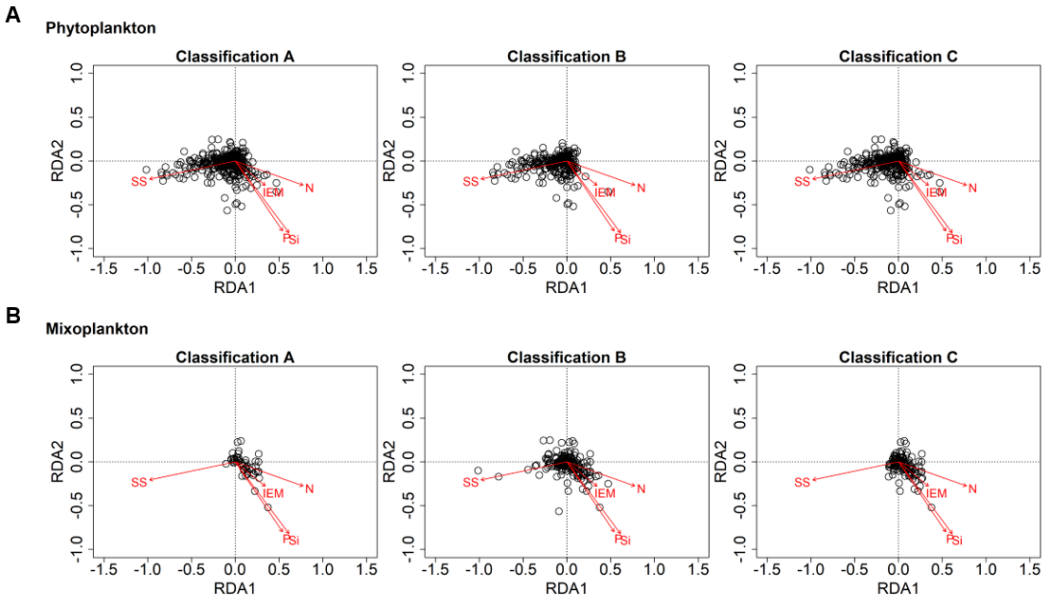

Figure 3.9: RDA ordination plots for phytoplankton (**A**) and mixoplankton (**B**) (SS - suspended sediment, IEM - index of ecosystem maturity, N/P/Si - nitrogen, phosphorus, silica concentration). **A**) Phytoplankton are oriented along the suspended sediment gradient. **B**) Documented and likely mixoplankton are oriented towards the IEM and nutrient concentration gradients.

3.4 Discussion

By exploring three trophic classifications, this study helps close a gap between plankton community assessments within varying abiotic environments and our developing knowledge of mixoplankton. It makes use of a dataset that covers a wide range of taxa, a long time period and strong abiotic gradients. We did not discover any basin-wide yearly trends in the trophic composition of the protist community. This is consistent with the absence of basin-wide yearly trends in abiotic parameters as the North Sea system is mainly driven through large scale hydrodynamics and terrestrial runoff (Emeis et al., 2015).
Peperzak (2010) showed an observed effect linked to changes in the identification and counting protocols in 2000. As the sampling frequency after 2010 changed as well, we took both changes into account by employing a partial PCA and RDA. However, we did not take these observer effects into account in the trophic aggregation for the heatmaps. Apart from an apparent increase of mixoplankton in Oosterschelde after 2009, the trophic classifications do not display other changes that can be linked to the observer effects. The reason for this lies in the aggreg-

ation of the protist data at the trophic level. The trophic level is directly related to the abiotic system though inorganic nutrients, light and food availability. The apparent increase of mixoplankton in Oosterschelde was caused by the identification of the mixoplankton *Micromonas sp*, which before 2009 was grouped into the phytoplankton classes *Chlorophyceae* or *Prasinophyceae* (Brochard et al., 2013). We conclude that by aggregating on a trophic level, the timeseries becomes independent of the observer effects and is thus suitable for analyzing the trophic composition of protist communities.

Furthermore, in the offshore environments, the sampling frequency declined after 2010. While Hinder et al. (2012) found a marked increase in the ratio of diatoms to dinoflagellates after 2006 using data from the continuous plankton recorder, we could not determine such a marked increase in our dataset. The dataset used in our study is decidedly different from continuous plankton recorder datasets and more suited to the analysis of mixoplankton because of the observed size range (Flynn et al., 2019). However, especially for Doggerbank, the bloom succession becomes indistinguishable due to the low sampling intervals.

In order to determine the contribution of mixoplankton to the trophic composition of plankton communities, we studied three trophic classifications. We determined that in inorganic nutrient-depleted, seasonally stratified, predominantly offshore environments, mixoplankton periodically constitute up to 25% (classification A - documented mixoplankton), over 75% (classification B - presumed mixoplankton) or around 50% (classification C - environmentally-defined mixoplankton) of the protist community. An oligotrophic environment is clearly associated with mixoplankton (Troost et al., 2005; Hartmann et al., 2012; Stoecker and Lavrentyev, 2018; Duhamel et al., 2019; Livanou et al., 2019). However, comparing the determined percentages with current literature is more difficult. Mixoplankton contribution to a certain community is often either sampled within a certain size fraction (Safi and Hall, 1999; Sato et al., 2017; Anderson et al., 2017), within certain taxa (Li et al., 2000b; Millette et al., 2017; Haraguchi et al., 2018) or with a certain grazing focus (Unrein et al., 2007).

In general, the sampled size range coincides well with the size range in which mixoplankton occur (Flynn et al., 2019). However, nanoflagellates were most likely undersampled and ciliates other than *Mesodinium rubrum* were not identified. This is in general an issue for most (routine) monitoring programs (Haraguchi et al., 2018). Many nanoflagellates can be mixotrophic (Safi and Hall, 1999) and some ciliates are NCMs as they can retain kleptochloroplastids (Haraguchi et al., 2018). Stelfox-Widdicombe et al. (2004) showed that in offshore environments ciliates constitute 50 % of the microzooplankton community and of those ciliates 50 % are mixotrophic. In nearshore environments, heterotrophic dinoflagellates dominate the microzooplankton community and oligotrich ciliates contribute

around 20 % to the microzooplankton community. Thus, it can be said that the trophic composition of the studied community in reality includes more protozoo- and mixoplankton. While CMs are known to belong to the most abundant types of mixoplankton (Faure et al., 2019), the lack of ciliates and the low abundance of *Dinophysis* (NCMs) is also the reason for the dominance of CMs in the Southern North Sea.

While all trophic classifications clearly associate mixoplankton with certain location classes, the trophic classifications differ in terms of mixoplankton seasonality and succession. Classifications A and C display a clear seasonal succession of trophic modes as described in Mitra et al. (2014a). In classification B, which presumes all phototrophic organisms to be capable of mixotrophy unless they have been explicitly proven incapable, mixoplankton additionally occur in the estuaries during winter/early spring, in which there is low light, high turbidity and an ample amount of inorganic nutrients. While Millette et al. (2017) showed that in the Choptank river (U.S.A.) *Heterocapsa rotundata* employs mixotrophy to overcome light limitation in winter, the nutrient concentrations in that study were much lower as compared to the nutrient concentrations of the Westerschelde and the Wadden Sea. There is little evidence of mixoplankton in turbid, eutrophic, temperate systems (such as the Southern North Sea estuaries).

We conclude that classifications A (documented mixoplankton) and B (presumed mixoplankton) display the two extremes of the trophic spectrum. While classification A is still highly subjected to the traditional dichotomy, classification B places mixoplankton into improbable environments. Clearly, the actual trophic composition of protist communities in the Southern North Sea lies in between trophic classifications A and B. Classification C (environmentally-defined mixoplankton) provides an indication of what the actual trophic composition could possibly look like. Classification C classifies mixoplankton according to environmental conditions associated with proven mixoplankton. Furthermore, classification C does not pre-define mixoplankton to certain broad functional groups as trophic classification B does. Using the partial PCA scores, we can provide a list of likely unrecognized mixoplankton in the Southern North Sea (see table S2 in the electronic supplements). Many of these taxa belong to the class Dinophyceae as well as the phyla Haptophyta and Chlorophyta which are associated with mixoplankton (Stoecker and Lavrentyev, 2018).

The offshore environments of the Southern North Sea in which we predominantly found mixoplankton are generally characterised by a low total biomass and thus mixoplankton do not necessarily contribute notably to the absolute biomass of the Southern North Sea. However, as certain cryptic mixoplankton are often associated with noxious or harmful events (Davidson et al., 2014), properly accounting for changes in trophic plankton composition is nonetheless important. Further-

more, Bouvier et al. (1997) found that even though mixoplankton biomass is often significantly lower than those of other trophic modes, their high specific ingestion rates let mixoplankton contribute significantly to the grazing of bacteria and nanoplankton, indicating a local importance.

In inorganic nutrient depleted, seasonally stratified, low biomass environments, mixoplankton have a clear advantage over phyto- and protozooplankton as they can use their mixotrophic capabilities to obtain nutrients and energy from multiple sources. In inorganic nutrient replete, turbid environments such as the estuary systems, phytoplankton are at an advantage due to their superior light-harvesting capabilities (Geider et al., 1997). This explains the strong orientation of phytoplankton along the suspended sediment gradient in the RDA (see figure 3.9). In environments with abundant prey, protozooplankton are at an advantage due to their superior prey ingestion capabilities in the dark (Skovgaard, 1996; Li et al., 1999; Adolf et al., 2006; Anderson et al., 2018).

The environments in which mixoplankton occur are often called mature (Mitra et al., 2014a; Haraguchi et al., 2018; Flynn et al., 2018). In many studies, maturity is often associated with geographic location and/or season. This study proposes the IEM (index of ecosystem maturity) as a functional definition of energy flow based on measured environmental parameters. It describes the shift from abundant inorganic to mostly organism-bound nitrogen typical for ecosystem maturation. Consequently, the IEM provides information on the availability of inorganic nutrients without being pre-defined to occur at a particular location or season. We conclude from the partial RDA results that our proposed IEM along with low turbidity provides an indication on the relevance of mixoplankton in plankton communities.

In the coming years, with advancements of laboratory and field methods along with the new understanding of mixoplankton, the trophic composition of plankton communities can be refined. This study demonstrates that numerical ecology methods can assist experimental methods in the attempt to determine mixoplankton in plankton communities. Yet, it remains difficult to determine the cause and effect between abiotic and plankton systems using only field data. Modelling provides a tool (Flynn and Mitra, 2009) to test hypotheses on the causal relationship between abiotic environments and the trophic composition of plankton communities. Until now, mixotrophy as a functional trait is still poorly represented in aquatic ecosystem models (Ghyoot et al., 2017b). Including mixotrophy into aquatic ecosystem models changes the overall allocation of nutrient and energy resources within the base of marine ecosystems. Furthermore, by including mixotrophy into aquatic ecosystem models, hypotheses on the trophic spectrum could be tested.

Plankton communities are the base of our marine ecosystems. With climate change (Hays et al., 2005) and offshore wind farms (Heath et al., 2017) changing the marine coastal environment, we need to better understand the trophic composition of

plankton communities within their abiotic environment (Caron, 2016). This study provides a first quantitative delineation of the possible boundaries of the trophic spectrum within marine protist communities and provides a list of potential unrecognized mixoplankton in the Southern North Sea. It can serve as a benchmark for subsequent efforts to include mixotrophy into ecosystem models as well as placing mixoplankton into marine plankton community assessments.

Chapter 4

A dataset on trophic modes of aquatic protists

Published article: Schneider, L.K., Anestis, K., Mansour, J., Anschütz, A.A., Gypens, N., Hansen, P.J., John, U., Klemm, K., Lapeya Martin, J., Medic, N., Not, F. and Stolte, W. (2020). A dataset on trophic modes of aquatic protists. *Biodiversity Data Journal*, 8.

Abstract

An important functional trait of organisms is their trophic mode. It determines their position within food webs, as well as their function within an ecosystem. For the better part of the 20th century, aquatic protist communities were thought to consist mainly of producers (phytoplankton) and consumers (protozooplankton). Phytoplankton cover their energy requirements through photosynthesis (phototrophy), while protozooplankton graze on prey and organic particles (phagotrophy). However, over the past decades, it was shown that another trophic group (mixoplankton) comprise a notable part of aquatic protist communities. Mixoplankton employ a third trophic mode by combining phototrophy and phagotrophy (mixotrophy). Due to the historical dichotomy, it is not straightforward to gain adequate and correct information on the trophic mode of aquatic protists. Long hours of literature research or expert knowledge are needed to correctly assign trophic modes. Additionally, aquatic protists also have a long history of undergoing taxonomic changes which make it difficult to compare past and present literature. While WoRMS, the World Register of Marine Species, keeps track of the taxonomic changes and assigns each species a unique AphiaID that can be linked to its various historic and present taxonomic hierarchy, there is currently no machine-readable database to query aquatic protists for their trophic modes. This paper describes a dataset that was submitted to WoRMS and links aquatic protist taxa, with a focus on marine taxa, to their AphiaID and their trophic mode. The bulk of the data used for this dataset stems from (routine) monitoring stations in the North Sea and the Baltic Sea. The data were augmented and checked against state-of-the-art knowledge on mixoplankton taxa by consulting literature and experts. Thus, this dataset provides a first attempt to make the trophic mode of aquatic protists easily accessible in both a human- and machine-readable format.

4.1 Introduction

Protists (i.e. unicellular eukaryotes) form the base of aquatic ecosystems by providing food for higher trophic levels. Even though protist communities are so important for the trophic functioning of aquatic ecosystems, the trophic diversity within those protist communities is not always clear. For the better part of the 20th century, aquatic protist communities were divided into producers, the phytoplankton and grazers, the (proto)zooplankton (Flynn et al., 2013). Over the past decade, there has been an effort to reshape the traditional dichotomy of aquatic protist communities by taking mixotrophic protists into account (Mitra et al., 2016). Mixotrophic protists can function both as producers and grazers and, recently, the term mixoplankton has been suggested to describe this group (Flynn et al., 2019). However, taking the correct trophic mode into account is still a challenge. Due to the historical bias, most aquatic protists are still by default categorised as either phytoplankton or protozooplankton. Intensive experimental work is required to determine mixotrophy in protists. While, in the past years, quite a few papers were published that contained lists of currently-proven marine mixoplankton (Faure et al., 2019; Leles et al., 2017; Leles et al., 2018a), there is no database available which allows the trophic mode of aquatic protists to be queried. This makes it very time-consuming to take the trophic mode into account for large data-driven approaches on aquatic protist communities. A further complication is added through the frequent taxonomic changes within the protist community which make it difficult to compare literature references.

This dataset provides information on the trophic mode of aquatic protists and links them to the WoRMS database that keeps track of taxonomic name changes by using a unique species identifier, the AphiaID. By combining information on trophic modes with an already existing and widely-used database such as WoRMS, the authors hope to make data on trophic modes of aquatic protists more accessible in a machine-readable fashion. Thus, the dataset can help facilitate a better understanding of trophic dynamics and the functional role of protist groups within aquatic ecosystems. The trophic mode of the taxa included in this dataset can be accessed via the attributes of the WoRMS taxa search tool (see, for example, `http://www.marinespecies.org/aphia.php?p=taxdetails&id=232772#attributes`).

However, this dataset is only a start. The authors hope that, as more information on mixoplankton becomes available, this dataset will actively be expanded through community effort. New data can easily be submitted to WoRMS using the instructions available on `https://www.marinespecies.org/contribute.php`.

4.2 General description

Purpose: The purpose of this project was to establish a dataset on trophic modes of aquatic protists. As correct classification of trophic modes is especially important within the context of analysing routine monitoring data, the idea arose to make this work more accessible to the broad aquatic science and management community. This dataset was assembled in the scope of the H2020 Marie-Curie ITN "MixITiN".

4.3 Project description

Title: A dataset on trophic modes of aquatic protists

Personnel: Lisa K. Schneider (management, data collection, literature research, tidy data implementation, data concatenation, manuscript preparation), Konstantinos Anestis (data collection, literature research, manuscript contribution), Joost Mansour (literature research, manuscript contribution), Anna A. Anschütz (literature research, manuscript revision), Nathalie Gypens (data collection, expert knowledge, manuscript revision), Per J. Hansen (data collection, expert knowledge, manuscript revision), Uwe John (data collection, expert knowledge, manuscript revision), Kerstin Klemm (data collection, manuscript revision), Jon Lapeya Martin (data collection, manuscript revision), Nikola Medic (literature research, manuscript revision), Fabrice Not (expert knowledge, manuscript revision), Willem Stolte (management, concept development, expert knowledge, manuscript preparation).

Design description: To gather, analyse and disseminate the trophic mode of aquatic protists, a dataset was submitted to the World Register of Marine Species, WoRMS at `http://www.marinespecies.org`. WoRMS provides "an authoritative and comprehensive list of names of marine organisms, including information on synonymy" (WoRMS Editorial Board, 2020) and this list of marine organisms can be augmented with metadata, such as traits, for example, trophic modes. Each organism is labelled with a unique AphiaID with which it is possible to keep track of taxonomic name changes (Vandepitte et al., 2015). This approach of keeping track of taxonomic name changes allows the database to be accessed and used in different ways, for example, by searching for single organisms or matching a list of taxa.
Furthermore, for each mixoplankton, the type of mixotrophy is assigned as a trait. In the dataset, the type of mixotrophy is defined by assigning CM, GNCM, pSNCM

or eSNCM to the mixoplankton, according to the types identified in Mitra et al. (2016). Constitutive Mixoplankton (CM) have the innate ability to perform photosynthesis, while Non-Constitutive Mixoplankton need to acquire chloroplasts from their prey. These Non-Constitutive Mixoplankton are divided into the General Non-Constitutive Mixoplankton (GNCM), the plastid Specialists Non-Constitutive Mixoplankton (pSNCM) and the endosymbiotic Specialist Non-Constitutive Mixoplankton (eSNCM). The GNCMs can use chloroplasts from multiple phototrophic prey, while the pSNCMs and eSNCMs only use chloroplasts from specific preys or endosymbionts.

Funding: This project has received funding from the European Union's Horizon 2020 research and innovation programme under the Marie Skłodowska-Curie grant agreement No 766327 and EMODnet Biology (EC Service contract – EASME /EMFF/2016/1.3.1.2/Lot 5/SI2.750022).

4.4 Sampling methods

Study extent: This dataset focuses on the trophic modes of aquatic protists. It combines data from five different sources: routine monitoring (HELCOM, 2019; RWS, 2019), scientific cruises (John, 2020; Martin, 2020), scientific papers (primary literature), review papers and a book chapter (secondary literature). Sampling for routine monitoring and on scientific cruises was performed using Niskin bottles, followed by inspection of the samples using light microscopy. In the case of the scientific cruises, metabarcoding was employed for further validation of the microscopic data. Suppl. material 1 lists all sources and their complete references.

Sampling description: This dataset (Suppl. material 2) covers 1296 taxa. Fig. 4.1 shows that the bulk of the taxa stem from routine monitoring (72 %) and are mainly labelled as phytoplankton (89 %). Secondary literature (reviews and book chapter) contributes 10 % and 1.9 % of the total taxa, respectively, which are all labelled as mixoplankton. Primary literature (scientific papers) contributes 11 % of the total taxa and are divided evenly between protozooplankton and mixoplankton. Recent scientific cruises in the North Sea contribute 3 % of the total taxa and display the most even distribution of trophic modes.
In total, 21 % of the taxa are classified as mixoplankton, 66 % as phytoplankton and 13 % as protozooplankton (Fig. 4.2). However, as 72 % of the taxa originate from routine monitoring, the percentage of mixoplankton is most likely under-represented. Most routine monitoring undersample mixoplankton due to the employed sampling techniques (Flynn et al., 2019). An example is the routine monitoring data of the Dutch Southern North Sea in which ciliates, as well as

nanoflagellates, are often not identified and counted. Both of these groups are known to contain mixoplankton (Haraguchi et al., 2018; Stoecker and Lavrentyev, 2018). Furthermore, mixotrophy must be proven in phyto- and protozooplankton by observing either feeding or utilisation of chloroplasts from prey or symbionts. It must be assumed that taxa remain labelled according to the historical dichotomy until proven otherwise. This remains an issue also for this dataset, of which the user should be aware. It can only be remedied by continually updating the dataset as new mixoplankton taxa are empirically determined.

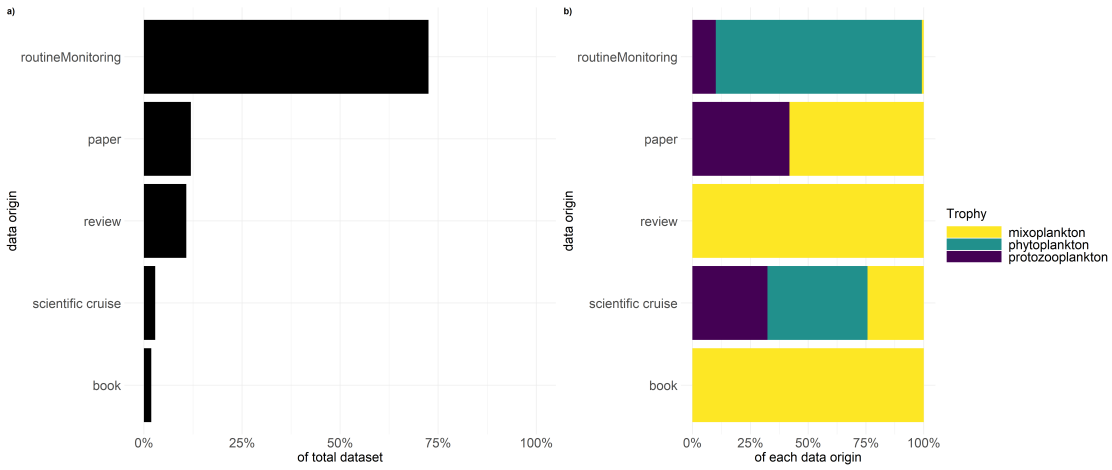

Figure 4.1: Depiction of a) percentage of the data origin to the complete dataset and b) percentage of trophic mode per data origin.

Quality control: In order to ensure consistent taxonomy over the various data sources, each data source was matched against the WoRMS taxonomic database using the WoRMS "Match taxa" tool. This ensured that each taxon was given the currently-accepted scientific name and referenced with an AphiaID. Data sources were tidied (Wickham, 2014) and joined into one dataset. If the various sources disagreed with each other on the trophic mode of the taxon, two decision pathways were possible. Firstly, mixoplankton data sources were always given precedence over other sources. Secondly, if the data sources disagreed on non-mixoplankton, then expert knowledge and literature was used to assign the trophic mode of that organism. Lastly, the list was checked by expert witnesses to ensure correct trophic classifications. This described workflow is visualised in Fig. 4.3.

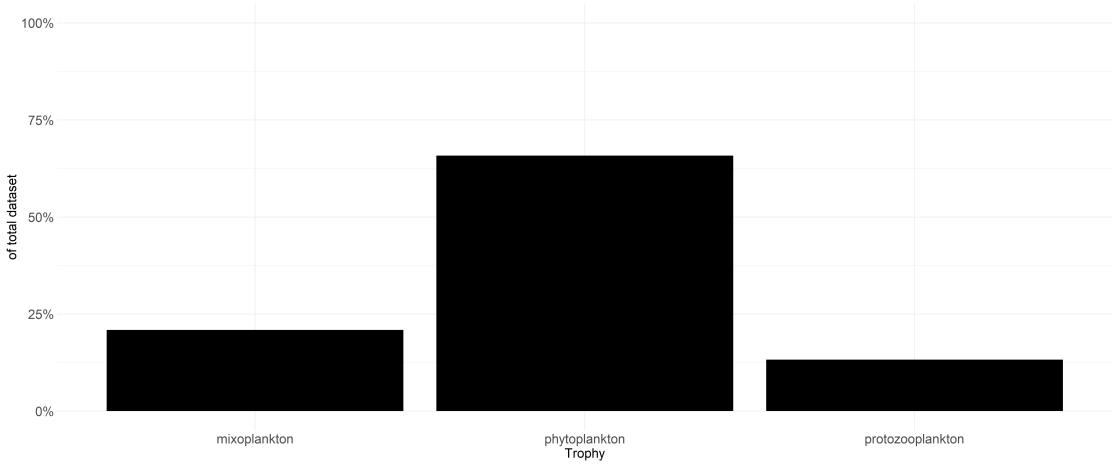

Figure 4.2: Contribution of trophic modes to total dataset.

4.5 Geographic coverage

Description: As this consortium is based in the EU, data stemming from routine monitoring is biased towards European waters. Data derived from literature extends beyond the EU. We hope that this dataset will be built upon with data contributions from other scientists, to establish a more encompassing collaborative resource that will promote research on trophic modes. New data can easily be submitted to WoRMS using the instructions available on `https://www.marinespecies.org/contribute.php`.

4.6 Taxonomic coverage

Description: Fig. 4.4 visualises the contribution of each class to the total dataset (Fig. 4a), as well as the contribution of trophic modes across those classes (Fig. 4b). It should be noted that only those classes are displayed that make up 90 % of the total dataset. The largest class, represented in the dataset, is Bacillariophyceae, followed by Dinophyceae and Cyanophyceae. In terms of trophy, the classes which contain the most phytoplankton are Bacillariophyceae, Cyanophyceae, Chlorophyceae and Trebouxiophyceae. The classes which contain the most mixoplankton are Dinophyceae, Polycystina, Oligotrichea, Globothalamea, Prymnesiophyceae, Acantharia and Cryptophyceae. Protozooplankton are represented in the classes Dinophyceae, Polycystina, Oligotrichea, Globothalamea and Acantharia, in which they contribute between 5 % and 30 %.

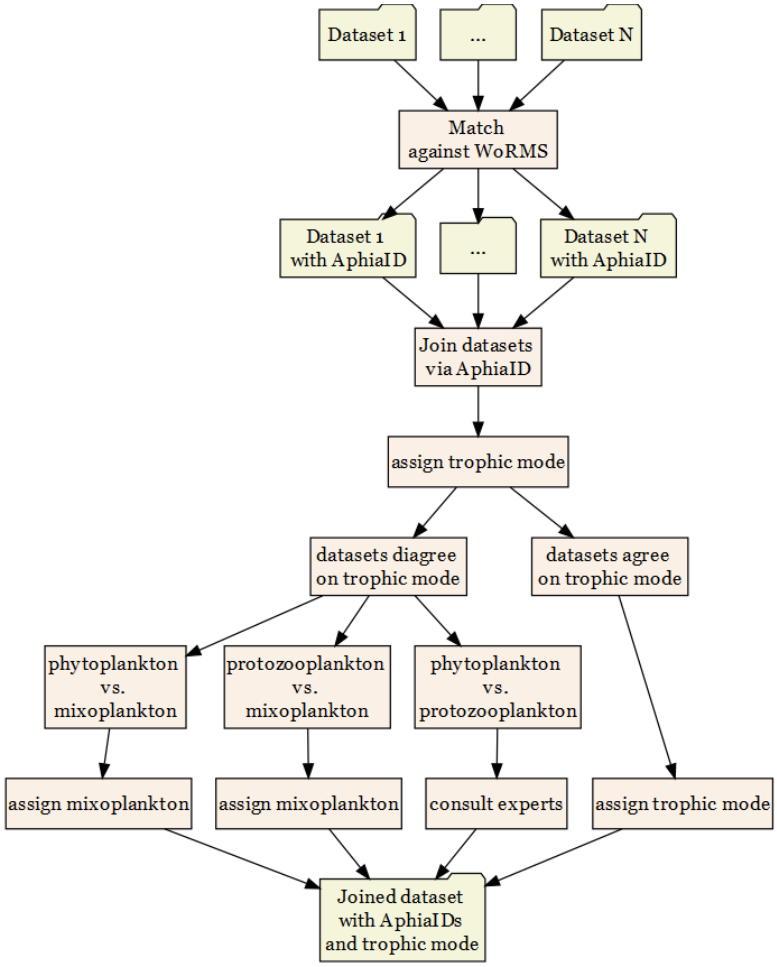

Figure 4.3: Workflow depiction beginning with single data sources and ending with the complete dataset.

4.7 Traits coverage

This dataset focuses on the trophic mode of aquatic protists. As mentioned, aquatic protists can be divided into phytoplankton, protozooplankton and mixoplankton. This next section will give more detail on these different functional groups and their impact on aquatic ecosystems.
Phytoplankton are defined as those protists that perform photosynthesis and are incapable of phagotrophy. The most prominent examples of phytoplankton groups are cyanobacteria, diatoms and green algae. Attributing to their need of light for photosynthesis, phytoplankton are found in the euphotic zone, where light is available. It is estimated that aquatic photosynthesis by phytoplankton totals

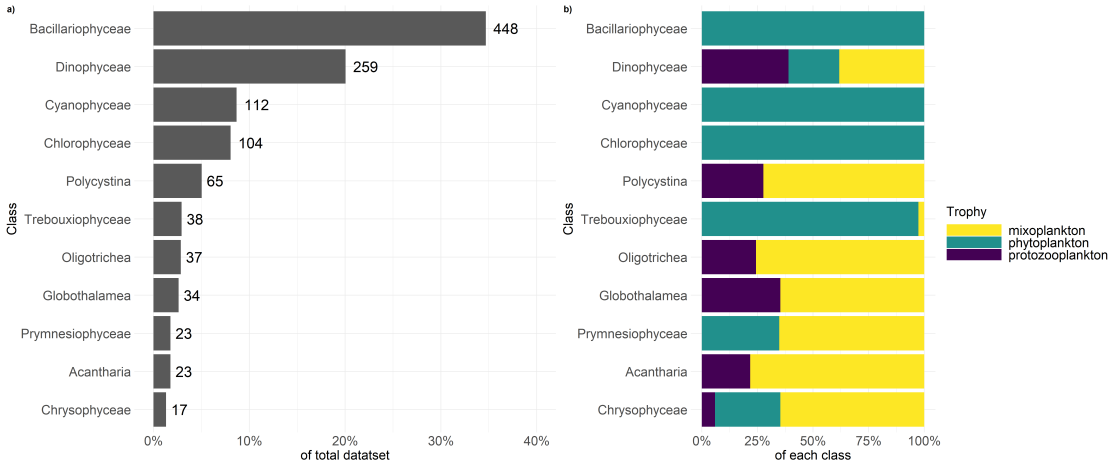

Figure 4.4: Depiction of a) percentage of each class to the complete dataset and b) percentage of trophic mode per class.

about half of the total primary production on Earth (Falkowski, 1994; Field et al., 1998). Phytoplankton in marine ecosystems play an important role in major biogeochemical cycles. For example, cyanobacteria species are known for their capacity to fix atmospheric nitrogen (25-50 % of global natural fixation), a unique feature for this phytoplankton group (Canfield et al., 2010) (Canfield et al. 2010). Furthermore, diatoms contribute considerably to the global carbon cycling as they are responsible for 30-40 % of global primary productivity (Sarthou et al., 2005). The diatom cell wall is composed of silica and thereby diatoms are considered the world's largest contributors to the silica cycle (Tréguer and De La Rocha, 2013). Moreover, sinking of phytoplankton contributes to the carbon export to the deep oceans (Falkowski, 1994).

Protozooplankton are defined as those protists that gain their nutrition through capture and ingestion of prey (or organic particles). Protozooplankton do not have the capability for photosynthesis, nor other means of producing their own organic carbon. Examples of protozooplankton are heterotrophic ciliates, heterotrophic dinoflagellates and heterotrophic (nano)flagellates. The grazing of heterotrophic protists on phytoplankton plays an important role in controlling the growth and population of phytoplankton taxa. Heterotrophic protists are the connecting link for energy transfer towards higher trophic levels and, in some cases, can be responsible for the removal of the largest part of primary production (Calbet and Landry, 2004; Lawrence and Menden-Deuer, 2012). Apart from the consumption of phytoplankton, heterotrophic protists also ingest prokaryotes indicating their further involvement in planktic food web energy transfer (Cho et al., 2000; Pernice et al., 2015; Šimek et al., 2019).

Mixoplankton are defined as those protists that can combine phototrophy and phagotrophy (sensu Flynn et al. (2019)). Mixoplankton are often associated with mature ecosystems (Mitra et al., 2014a; Moorthi et al., 2017) and many harmful algal bloom species are known to be mixotrophic. Due to their ability to combine phototrophy and phagotrophy, they can simultaneously fulfil many of the functions (Selosse et al., 2017) described for both phytoplankton and protozooplankton. Mixoplankton can thus also contribute significantly to primary productivity and functionality of ecosystems (Ghyoot et al., 2017b). The additional energy acquired by the consumption of prey can increase the gross growth efficiency of mixoplankton (Schoener and McManus, 2012) and subsequently, have major effects on trophic transfer in the food web (Ward and Follows, 2016). CMs (e.g. *Prymnesium parvum*, *Karlodinium veneficum*) that have the innate ability to perform photosynthesis, can express bacterivory (Unrein et al., 2007) or ingest other protists to supplement their nutritional needs (Stoecker et al., 2017). NCMs, such as the kleptoplastidic ciliate *Strombidium basimorphum*, can be voracious grazers, achieving grazing rates comparable with pure heterotrophic species (Maselli et al., 2020). Furthermore, NCMs also contribute significantly to primary production through either their ability to use prey chloroplasts after ingestion (Nielsen et al., 2012) or others (eSNCMs, like many Acantharia and Foraminafera) through chloroplast containing endosymbionts (Caron et al., 1995).

Chapter 5

Modeling mixoplankton along the biogeochemical gradient of the Southern North Sea

Accepted article: Schneider, L.K., Gypens, N., Troost, T.A. and Stolte, W. (2021). Modeling mixoplankton along the biogeochemical gradient of the Southern North Sea. *Ecological Modelling, 459*

Abstract

The ecological importance of mixoplankton within marine protist communities is slowly being recognized. However, most aquatic ecosystem models do not include formulations to model a complete protist community consisting of phytoplankton, protozooplankton and mixoplankton. We introduce PROTIST, a new module for the aquatic ecosystem modelling software Delft3D-WAQ that can model a protist community consisting of two types of phytoplankton (diatoms and green algae), two types of mixoplankton (constitutive mixoplankton and non-constitutive mixoplankton) and protozooplankton. We employed PROTIST to further explore the hypothesis that the biogeochemical gradient of inorganic nutrient and suspended sediment concentrations drives the observed occurrence of constitutive mixoplankton in the Dutch Southern North Sea. To explore this hypothesis, we used 11 1D-vertical aquatic ecosystem models that mimic the abiotic conditions of 11 routine monitoring locations in the Dutch Southern North Sea. Our models result in plausible trophic compositions across the biogeochemical gradient as compared to in-situ data. A sensitivity analysis showed that the dissolved inorganic phosphate and silica concentrations drive the occurrence of constitutive mixoplankton in the Dutch Southern North Sea.

5.1 Introduction

The trophic mode of marine protists is an important functional trait with which to characterize protists (Mitra et al., 2016). Flynn et al. (2019) classified marine protists into three categories based on their trophic mode: phytoplankton, protozooplankton and mixoplankton. Phytoplankton, such as diatoms and green algae (phototrophic non-diatoms), are defined as protists that can only utilize the photo-osmotrophic pathways. They cover their energy requirements through the photosynthetic fixation of inorganic carbon and their nutrient requirements through the uptake of dissolved inorganic nutrients. Protozooplankton are defined as protists that can only utilize the phagotrophic pathways. They cover their energy and nutrient requirements through the assimilation of prey.

In contrast to phytoplankton and protozooplankton, mixoplankton can utilize the photo-, osmo- and phagotrophic pathways simultaneously (Flynn et al., 2019). They can be divided into constitutive mixoplankton (CM) and non-constitutive mixoplankton (NCM) (Mitra et al., 2016). CMs have the constitutive ability to perform photosynthesis and they can uptake dissolved inorganic nutrients as well as assimilate prey. NCMs need to acquire the photosynthetic machinery from their prey. They cover their nutrient requirements mainly through the assimilation of prey (Stoecker et al., 2017).

The composition and productivity of protist communities is an interplay between external resource availability (such as nutrients, light and prey) and the protists' physiologies. While the importance of phytoplankton (as the base of marine ecosystems) and protozooplankton (as trophic transfers) has long been recognized, the ecological relevance of mixoplankton has long been ignored (Flynn et al., 2013). However, mixoplankton contribute notably to marine protist communities worldwide (Leles et al., 2017; Leles et al., 2018b; Faure et al., 2019), change the inorganic nutrient and predation dynamics (Hansen et al., 2019) and have a non-negligible impact on the carbon cycle (Worden et al., 2015). Furthermore, mixoplankton are an important connector between microbial, protist and mesozooplankton food webs (Stoecker et al., 2017) and they play an important role in ecosystems governed by strong light and nutrient gradients (Selosse et al., 2017).

In a recent analysis of routine monitoring data on the protist community of the Dutch Southern North Sea (from here on referred to as the Southern North Sea - SNS), Schneider et al. (2020b) showed that CMs occur mostly in inorganic nutrient depleted, highly transparent, stratified environments. Eutrophied, turbid, mixed environments were devoid of CMs. Schneider et al. (2020b) hypothesized that the environmental factors which exhibit a biogeochemical gradient drive the trophic composition of protist communities in the SNS. However, Schneider et al. (2020b) were not able to elucidate which environmental factor - the dissolved inorganic

nutrient or the suspended sediment gradient - governed the occurrence of CMs.
While routine monitoring data allows us to gain insight on protist communities in different environments, it is difficult to test causalities between separate abiotic factors and the community composition using field data. Aquatic ecosystem models (AEM) provide a tool to estimate the impact of external or internal forcing on aquatic ecosystem dynamics (i.e. Janssen et al. (2015)). AEMs are able to depict various aquatic processes such as primary production, secondary grazing, remineralization or denitrification. However, most AEMs still do not include adequate formulations for mixoplankton (Flynn et al., 2019).
To help close this gap, we implemented a new module that includes formulations to model a protist community consisting of diatoms, green algae, protozooplankton, CMs and NCMs in the open-source AEM Delft3D-WAQ. This new module is called PROTIST and can be used to model the primary production of as well as the competition and grazing within the protist community.
We validated PROTIST using 11 1D-vertical (1D-V) models that mimic 11 routine monitoring location classes located in the estuaries, coasts and offshore regions of the Dutch SNS (Schneider et al., 2020b). The 11 1D-V models were forced with timeseries of inorganic nutrients and suspended sediments sampled at the 11 location classes. Thus, we were able to quantitatively and qualitatively validate PROTIST across the biogeochemical gradient of the SNS using timeseries comparisons, target diagrams and heatmaps.
Using the 11 1D-V models, we were also able to further explore the hypothesis put forward by Schneider et al. (2020b) that the biogeochemical gradient drives the trophic composition of protist communities. We conducted a sensitivity analysis to determine whether the inorganic nutrients or the suspended sediment concentration has more effect on the occurrence of CMs. Especially against the background of climate change (Wilken et al., 2013) and anthropogenic changes to marine environments (Burkhard et al., 2011), it is important to acquire more knowledge about the abiotic drivers of protist community compositions.
In summary, the objectives of this study are 1) to introduce the module PROTIST, 2) to quantitatively and qualitatively validate PROTIST against routine monitoring data and 3) to further explore the hypothesis that the biogeochemical gradient drives the trophic composition of protist communities.

5.2 Material and methods

5.2.1 The module PROTIST

The module PROTIST simulates the growth and mortality of the protist community while taking the trophic modes of protists into account. PROTIST can thus be used to simulate primary production in marine ecosystems. The module PROTIST combines model equations from Flynn (2001), Flynn and Mitra (2009) and Flynn (2021). These equations are based on first principles that were implemented unchanged in PROTIST. Firstly, the growth of protists is not only determined by the external availability of resources such as light, nutrients and prey, but also by the protists' internal stoichiometry. The internal nutrient quotas of the protists regulate the protists' affinity to uptake nutrients (Grover, 1991), synthesize chlorophyll-a (Davey et al., 2008) and assimilate prey (Mitra and Flynn, 2005). Secondly, the trophic modes of protists determine the interactions within protist communities (Flynn et al., 2019). However, some changes were needed for the equations to run stably and efficiently as a Delft3D-WAQ module:

- the nutrient uptake equations were described using continuous functions (instead of coupled conditional statements as in Flynn (2021)).

- the uptake of dissolved amino acids was not implemented, as Delft3D-WAQ does not simulate dissolved amino acids explicitly due to the lack of validation data.

- the assimilation of dissolved organic carbon was not implemented, as all protist functional types (PFT) can assimilate dissolved organic carbon (DOC) (Stoecker et al., 2017), so it is not a distinguishing pathway between the PFTs.

- PROTIST enables multiple PFTs to interact with, compete against and graze on each other.

PROTIST consists of five different PFTs and each PFT consists of state variables (SV) that describe carbon (C), nitrogen (N) and phosphorus (P) biomass. Chlorophyll-a (Chl) is an additional SV for phototrophic protists. Diatoms contain an additional SV to describe the silica (Si) content. This makes PROTIST fully stoichiometrically variable. The PFTs require either light and/or prey and/or nutrients. Figure 5.1 visualizes the SVs required for PROTIST and the interactions between the different SVs.

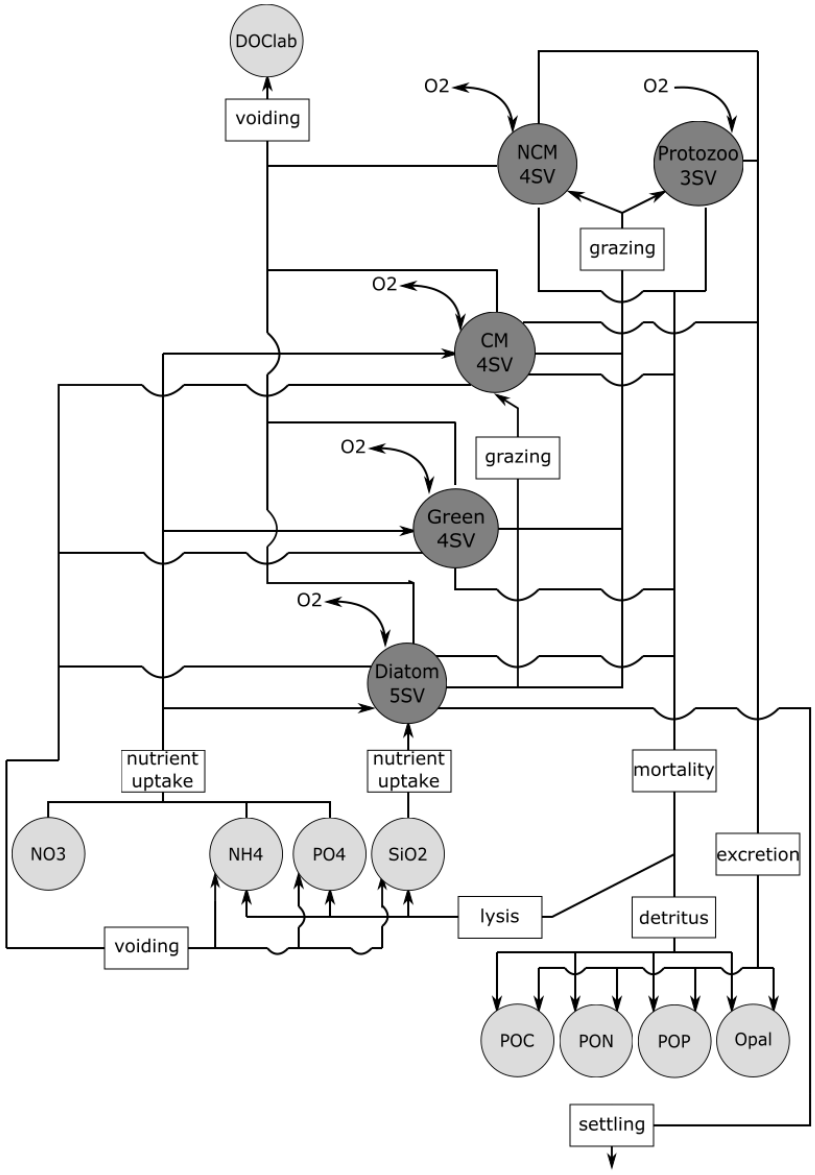

Figure 5.1: Conceptual visualization of the module PROTIST. The lightgrey circles are abiotic state variables (SV) and the darkgrey circles the protist functional types (PFT). Each PFT consists of multiple SVs. The arrows and the labels depict the interaction between the PFTs as well as the interactions between the abiotic SVs and the PFTs. DOClab stands for labile dissolved organic carbon.

5.2.2 Functional types in PROTIST

5.2.2.1 Diatoms

The PFT diatoms are defined as phytoplankton that can utilize silica. Diatoms are described with five SVs: $Diat_C$, $Diat_N$, $Diat_P$, $Diat_{Si}$ and $Diat_{Chl}$. Table B.7 provides the conservation equations for the diatom SVs. The diatom SVs increase over time through the uptake of nutrients (up_{NH4}, up_{NO3}, up_{PO4}, up_{Si}), the fixation of carbon ($Cfix$) and the synthesis of chlorophyll-a ($synChl$). The diatom SVs decrease over time through predation ($Pred$), mortality (mrt), the leakage of photosynthate ($Cleak$), the voiding of excess nutrients or carbon ($Nout$, $Pout$, $Cvoid$), the degradation of chlorophyll-a ($degChl$) and respiration ($totR$).

5.2.2.2 Green algae

The PFT green algae are defined as phytoplankton that cannot utilize silica. Green algae are described with four SVs: $Green_C$, $Green_N$, $Green_P$ and $Green_{Chl}$. Table B.8 provides the conservation equations for the green algae SVs. The green algae SVs increase over time through the uptake of nutrients (up_{NH4}, up_{NO3}, up_{PO4}), the fixation of carbon ($Cfix$) and the synthesis of chlorophyll-a ($synChl$). The green algae SVs decrease over time through predation ($Pred$), mortality (mrt), the leakage of photosynthate ($Cleak$), the voiding of excess nutrients or carbon ($Nout$, $Pout$, $Cvoid$), the degradation of chlorophyll-a ($degChl$) and respiration ($totR$).

5.2.2.3 Protozooplankton

The PFT protozooplankton are defined as protists that are only capable of phagotrophy. Protozooplankton are described using three SVs: Zoo_C, Zoo_N and Zoo_P. Table B.9 provides the conservation equations for the protozooplankton SVs. The protozooplankton SVs increase over time through the assimilation of prey ($assC$, $assN$, $assP$). The protozooplankton SVs decrease over time through mortality (mrt - includes implicit grazing by higher trophic levels through use of a quadratic closure function), the voiding of unassimilated prey ($POCout$, $PONout$, $POPout$) and respiration ($totR$).

5.2.2.4 Constitutive Mixoplankton

The PFT CM are defined as mixoplankton that are primarily phototrophic, but are also capable of phagotrophy. CMs require four SVs: CM_C, CM_N, CM_P and CM_{Chl}. Table B.10 provides the conservation equations for the CM SVs. The CM SVs increase over time through the uptake of nutrients (up_{NH4}, up_{NO3},

up_{PO4}), the fixation of carbon ($Cfix$), the synthesis of chlorophyll-a ($synChl$) and the assimilation of prey ($assC$, $assN$, $assP$). The CM SVs decrease over time through predation ($Pred$), mortality (mrt), the leakage of photosynthate ($Cleak$), the voiding of excess nutrients or carbon ($Nout$, $Pout$, $Cvoid$), the voiding of unassimilated prey ($POCout$, $PONout$, $POPout$), the degradation of chlorophyll-a ($degChl$) and respiration ($totR$).

5.2.2.5 Non-Constitutive Mixoplankton

The PFT NCM are defined as mixoplankton that are primarily phagotrophic, but are also capable of enslaving the photosynthetic machinery of their phototrophic prey. NCMs require 4 SVs: NCM_C, NCM_N, NCM_P and NCM_{Chl}. Table B.11 provides the conservation equations for the NCM SVs. While NCMs have been shown to also uptake inorganic nutrients, the percentage of uptake is negligible compared to the acquisition of nutrients from prey (Schoener and McManus, 2017). The NCM SVs increase over time through the assimilation of prey ($assC$, $assN$, $assP$), the uptake of chloroplasts ($upChl$) and the fixation of carbon ($Cfix$). The NCM SVs decrease over time through predation ($Pred$), mortality (mrt), the leakage of photosynthate ($Cleak$), the voiding of unassimilated prey ($POCout$, $PONout$, $POPout$), the loss of chlorophyll-a ($lossChl$) and respiration ($totR$).

5.2.3 Physiological processes in PROTIST

The following sections describe the mathematical formulations needed to compute the physiological processes of the different PFTs. The equations are listed in B.2.6.

5.2.3.1 Cellular status

For each PFT the cellular quota, the maximum growth rate, the mortality rate, the basal respiration rate, the total respiration rate, the carbon-specific growth rate as well as the cellular nutrient status of nitrogen, phosphate and silica needs to be calculated. Table B.13 summarizes the description of the auxiliaries and B.2.6.2 provides the detailed mathematical equations.
The cellular quotas (NC, PC, SC) describe the ratio of the respective protist nutrient SVs to the protist carbon SVs according to Droop (1974). The maximum growth rate (UmT) as well as the mortality rate (mrt) are calculated using the Q10 approach (Van't Hoff, 1884). The basal respiration rate (BR) is defined as a fraction of maximum growth rate (Geider and Osborne, 1989). The total respiration is the sum of the metabolic cost ($redco$) of nitrate reduction ($upNO3$) (Flynn and Flynn, 1998), the anabolic cost (AR) of nitrogen utilization ($upNH4$,

$assN$) (Wirtz and Pahlow, 2010), the foraging costs for prey (SDA, $assC$) (Pahlow and Prowe, 2010) and the basal respiration (BR) (Geider and Osborne, 1989).

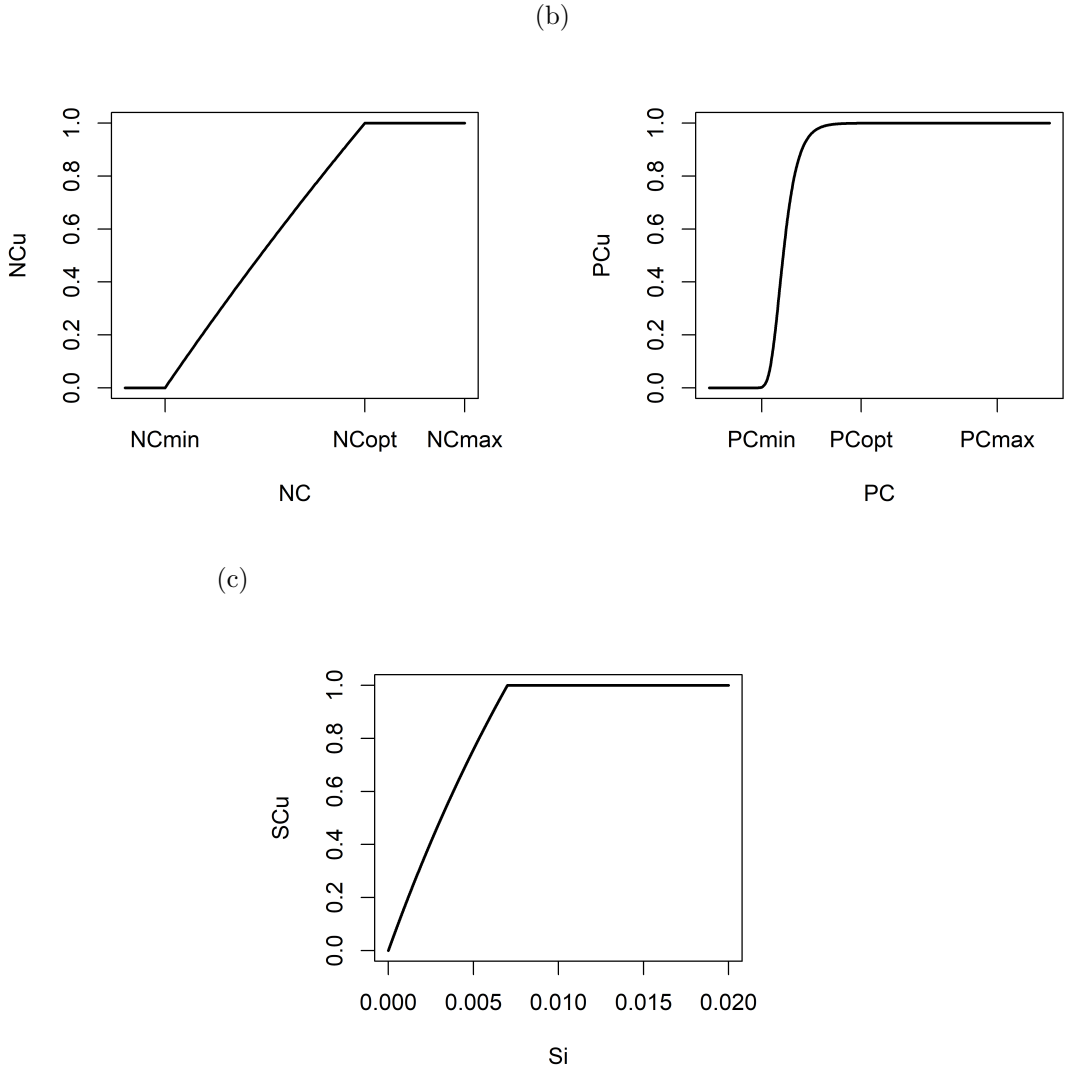

Figure 5.2: Visualization of the internal nutrient status for a) nitrogen NCu [dl], b) phosphate PCu [dl] and c) silica SCu [dl] (modified from Flynn (2021)). A value of 1 denotes that the internal nutrient stores are optimal, a value of 0 that the internal nutrient stores are completely depleted. The figures display that while NCu decreases linearly as soon as the optimal quota is not reached, PCu does not. These functions mathematically describe that nitrogen cannot be stored within the cell, while phosphate as polyphosphate can.

Furthermore, the nutrient status for nitrogen (NCu), phosphate (PCu) and silica (SCu - only for diatoms) is calculated. The nutrient status returns values between 0 (severely deprived of the respective nutrient) and 1 (at the optimal nutrient quota). The form of the functions depends on the protist's physiology to store the respective nutrient (see fig. 5.2). As protist cells store nitrogen in a form that is not physiologically active (Andersen et al., 1991), the nutrient status for nitrogen (NCu - see fig. 5.2a) is a linear function between the minimum and maximum quota. The nutrient status for phosphate (PCu - see fig. 5.2b) is calculated using a sigmoidal function to mimic the storage of phosphate as polyphosphate within the cell (Lin et al., 2016). The cellular status of silica (SCu - see fig. 5.2c) is a function of the external silica availability, as incorporated silica is not accessible by the cells anymore (Martin-Jézéquel et al., 2003). Applying Liebig's law of minimum (Liebig, 1840), the limiting nutrient ($NPCu$ or $NPSiCu$ - for diatoms) is determined by the minimum nutrient status within the cell.
To ensure that the nitrogen:carbon and phosphate:carbon quotas do not exceed the maximum nutrient quota between time steps, cellular nitrogen and phosphate is voided as soon as the cellular nutrient quota exceeds the maximum nutrient quota ($Nout$ and $Pout$). This does not occur for silica, as incorporated silica cannot be dispelled from the cell walls of diatoms (Martin-Jézéquel et al., 2003). If the nitrogen:carbon quota falls below the minimum nitrogen:carbon quota, then carbon is voided ($Cvoid$).

5.2.3.2 Uptake

In general, the uptake of dissolved inorganic nutrients ($upNH4$, $upNO3$, upP, $upSi$) is a combination of the external availability of the nutrients and the acquisition capability, which depends on the internal nutrient status (Grover, 1991; Moreno and Martiny, 2018). This is achieved by enhancing or repressing the optimal nutrient uptake via sigmoidal functions (see fig. 5.3). Table B.14 summarizes the description of the auxiliaries and B.2.6.3 provides the detailed mathematical equations.
The nutrient uptake at the optimal nutrient quota is regulated via the Michaelis-Menten function and scaled to the maximum growth rate and the optimal nutrient:carbon quota. For the uptake of NH_4^+ and NO_3^-, the optimum nutrient uptake is also scaled to the relative growth feasible with the respective nutrient. If the cellular nutrient quota is below the optimum nutrient quota (i.e. nutrient stressed), the nutrient uptake is enhanced until the maximum nutrient uptake is reached (Goldman and Glibert, 1982; Perry, 1976). If the cellular nutrient quota is above the optimum nutrient quota, the nutrient uptake for NH_4^+ and PO_4^{3-} are repressed (Wirtz and Pahlow, 2010), while the nutrient uptake for NO_3^- (Dugdale et al., 2007; Domingues et al., 2011) and silica are stopped all together. Furthermore,

the uptake of nitrogen is a function of the cellular phosphate:carbon quota resulting in a decrease of the cellular nitrogen:carbon quota during phosphate stress (Pahlow and Oschlies, 2009).

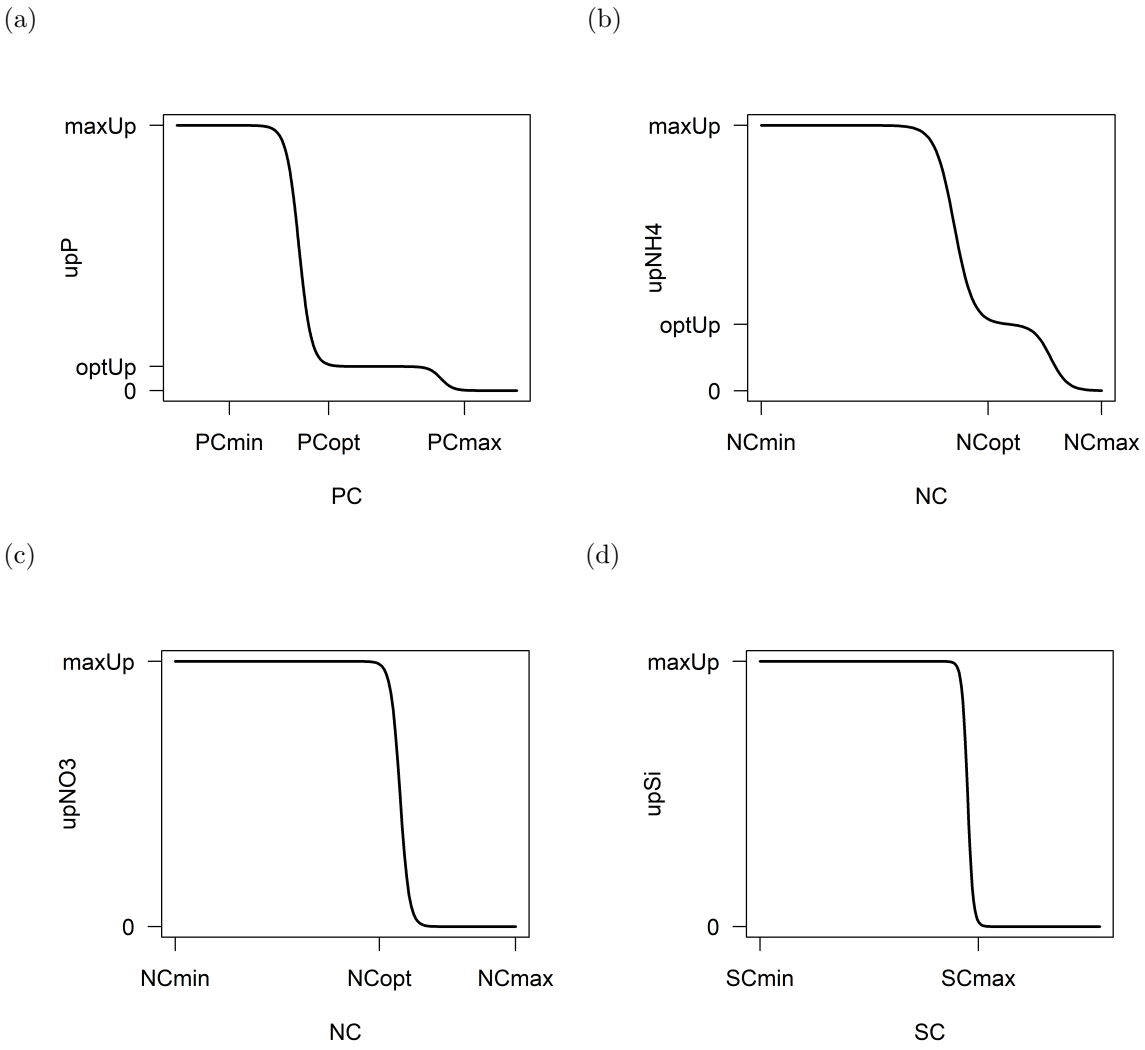

Figure 5.3: Visualization of the nutrient uptake for a) phosphate (upP [gP gC^{-1} d^{-1}]), b) ammonium ($upNH4$ [gN gC^{-1} d^{-1}]), c) nitrate ($upNO3$ [gN gC^{-1} d^{-1}]) and d) silica ($upSi$ [gSi gC^{-1} d^{-1}]) (modified from Flynn (2021)). The figures display that the uptake of phosphate and ammonium is repressed once the optimum cellular status is reached, while the uptake of nitrate and silica is stopped all together after the optimum quota is passed.

5.2.3.3 Phototrophy

The photosynthesis equations are based on the photosynthesis-irradiance curve that requires three input parameters: the maximum photosynthetic rate ($PSqm$), the chlorophyll-a specific initial slope (α^{Chl}) and photon flux density (PFD) (Jassby and Platt, 1976). Table B.15 summarizes the description of the auxiliaries and B.2.6.4 provides the detailed mathematical equations.

The maximum rate of photosynthesis covers the basal respiration (BR), the maximum growth rate (UmT), the leakage of photosynthate as DOC ($PSDOC$) (Thornton, 2014) and the costs of reducing nitrate ($redco$ and AR) (Dugdale et al., 2007) which (with the exception of basal respiration) are all influenced by the nitrogen quota of the cell (NCu) (Droop, 1974; Thornton, 2014; Flynn and Flynn, 1998). Furthermore, the maximum rate of photosynthesis depends on the organism's physiology, i.e. their capability to overcompensate the photosynthetic rate ($relPS$) (Geider, 1993). The maximum photosynthetic rate along with the initial slope (α^{Chl}) and the photon flux density (PFD) are used to calculate gross photosynthesis ($Cfix$) using the Smith equation (Smith, 1936). The net photosynthesis rate ($netPS$) is determined by subtracting the loss through leakage ($Cleak$).

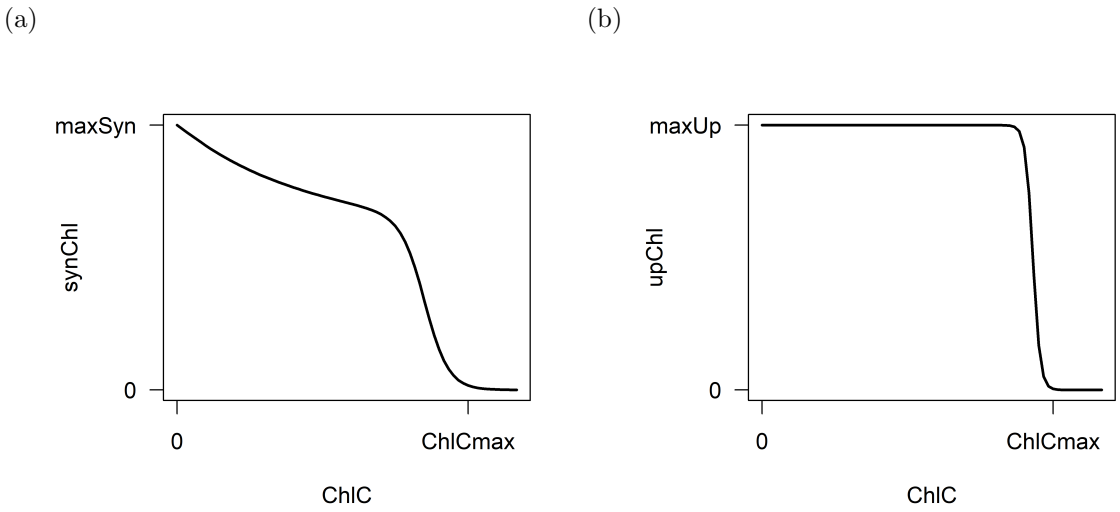

Figure 5.4: Visualization of the a) synthesis of chlorophyll-a for diatoms, green algae and CMs (synChl)and b) the uptake of chloroplasts by NCMs from their prey (upChl). The figures display that the synthesis of chlorophyll-a is repressed depending on the amount of carbon fixed and that NCMs can uptake chloroplasts until a maximum chlorophyll-a:carbon is reached.

Primarily phototrophic organisms such as diatoms, green algae and CMs can regulate their chlorophyll-a synthesis (*synChl* - see fig. 5.4a) (Geider and Piatt, 1986). If the cell is nutrient limited or the cell fixed too much carbon, the synthesis of chlorophyll-a is repressed (Moreno and Martiny, 2018). Under low light, the synthesis of chlorophyll-a is enhanced (Sukenik et al., 1987). Chlorophyll-a is also decomposed with a linear relationship to the nitrogen status (*degChl*) (Wirtz and Pahlow, 2010). Primarily phagotrophic organisms such as NCMs cannot produce their own chloroplasts, so they acquire them from prey (*upChl*). This acquisition is limited by a maximum chlorophyll-a:carbon quota via a sigmoidal function (see fig. 5.4b). Those acquired chloroplasts are subsequently lost at a fixed linear rate (*lossChl*) (Ghyoot et al., 2017a).

5.2.3.4 Phagotrophy

The phagotrophic functions can be divided into four subsections: determining the prey capture, determining the prey quality, determining the predator ingestion rate and determining the predator assimilation rate. Table B.16 summarizes the description of the auxiliaries and B.2.6.5 provides the detailed mathematical equations.

The prey capture depends on the motility of predator and prey as well as the density of the prey. The motility (*mot*) is derived from a linear regression by Flynn and Mitra (2016) that uses the organisms' equivalent spherical diameter as an input. The density of the prey (*nrPrey*) is calculated from the cellular carbon content (*Ccell*) and the current carbon protist state variable (*protC*). The motility of predator and prey as well as the density of prey are input parameters to determine the encounter rate (*enc*) according to the empirical Rothschild equation (Rothschild and Osborn, 1988). This encounter rate multiplied with the optimum capture rate (*optCR*) of the predator and the predator specific prey handling index (*PR*) determines the amount of specific prey the predator can capture. This is summed over all prey items (*sumCP*). As mixoplankton do not have the same capacity to ingest prey in the dark as in light (Skovgaard, 1996; Anderson et al., 2018), a light-dependent inhibition curve (*inhLight* - sigmoidal curve) is multiplied with the encounter rate and limits the capture of prey depending on the light availability. The light-dependent inhibition curve takes the photon flux density as well as the parameter *relPhag* (fraction of prey that can be ingested in the dark) as input.

The prey quality determines the assimilation efficiency (*opAE*) of the predator. A decrease in prey quality leads to a decrease in assimilation efficiency (Elser et al., 2000). The nutrient quota of the captured prey is compared against the nutrient quota of the predator. This returns a value between minimum (*AEo*) and the maximum assimilation efficiency (*AEm* see solid, black line in figure 5.5).

The predator ingestion rate ($ingC$ - see figure 5.5) at very low prey densities is limited by the amount of prey ($sumCP$) that can be captured and at very high prey densities by the predator's satiation ($ingSat$) (Flynn and Mitra, 2016). This satiation ingestion rate is calculated using a Holling type II curve (Holling, 1959) scaled to its maximum ingestion rate ($maxIng$). The maximum ingestion covers the maximum growth rate and basal respiration rate taking the quality of the captured prey into account. The ingestion of the other prey nutrients ($ingN$, $ingP$) is referenced to the carbon ingestion and the prey nutrient quota.

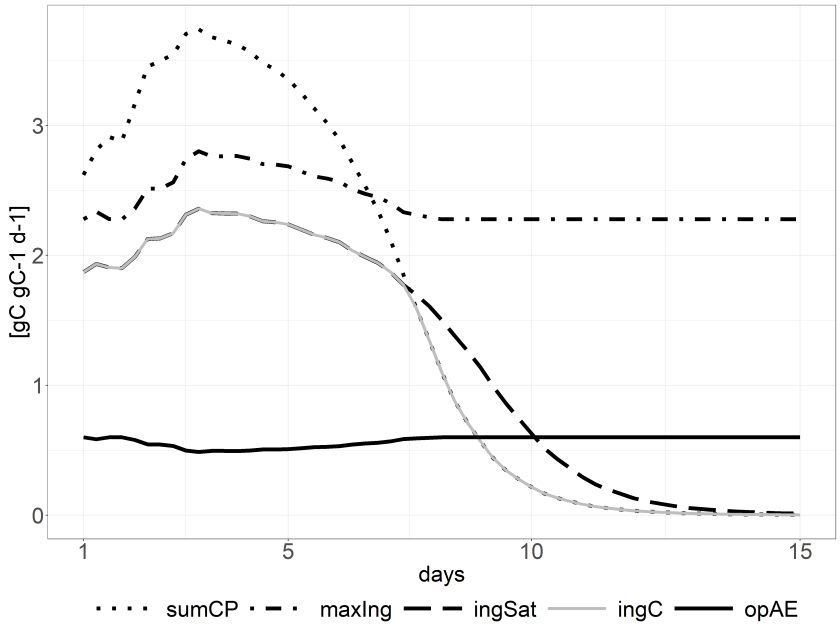

Figure 5.5: Visualization of the ingestion rate. The ingestion increases with decreasing prey quality ($opAE$ - solid, black line), while the actual ingestion ($ingC$ - solid, grey line) is limited either by the satiation rate ($ingSat$ - dashed, black line) or by the amount of captured prey ($sumCP$ - dotted, black line).

The predator assimilation rate ($assC$) is determined by taking the carbon specific ingestion rate and limiting it to the assimilation efficiency. The assimilation of the other prey nutrients ($assN$, $assP$) is referenced to the carbon assimilation and the optimum predator nutrient quota. Non-assimilated prey is voided as particulate organics, i.e. $POCout$, $PONout$ and $POPout$.

5.2.4 AEM application

The module PROTIST was implemented in the software Delft3D-WAQ. Delft3D-WAQ solves the advection-diffusion reaction equation on a predefined grid and is part of the open-source modelling suite Delft-3D maintained by Deltares (Deltares, 2020).
The AEM of this study employs established Delft3D-WAQ modules to simulate nutrients (NH_4^+, NO_3^-, PO_4^{3-} and Si), organic matter i.e particulate organic nitrogen (PON), phosphate (POP) and carbon (POC) as well as opal, dissolved oxygen, solar radiation and suspended sediment. The modules compute the settling of organic matter, the decomposition of organic matter, the dissolution of silica, nitrification and denitrification, the extinction of light as well as the reaeration of the water column. For more information on those modules, the authors refer to Blauw et al. (2009).
To simulate primary production, this AEM employs PROTIST. Although the aim was to run the AEM with all five PFTs, it was difficult to parameterize NCMs for this AEM application using literature and data-based knowledge. Unfortunately, NCMs are not sampled in the routine monitoring program of the SNS (Schneider et al., 2020b), so there is a lack of knowledge about the distribution of NCMs in the SNS. Furthermore, there is still a lack of physiological understanding of NCMs (Hansen et al., 2019). So, for this AEM, we were only able to simulate four PFTs: diatom, green, protozooplankton and CM.
However, using a steady-state box model, we successfully demonstrated growth and competition between the five PFTs in a simplified, idealized environment. For more details on this technical test, the authors refer to B.5.

5.2.4.1 Model domain

The SNS was chosen as a model domain as it is a well-monitored shelf sea that covers strong abiotic gradients. Abiotic and biotic parameters are routinely monitored at 11 location classes by the Rijkswaterstaat monitoring program (Dutch Directorate-General for Public Works and Water Management). Schneider et al. (2020b) showed that these 11 location classes can be grouped into four environmental systems based on dissolved inorganic nutrient concentrations, suspended sediment concentrations and water column stratification. These four environmental systems are a) the unstratified estuary systems (ES) with high dissolved inorganic nutrient and high suspended sediment concentrations, b) the unstratified coastal systems (CS) with lower dissolved inorganic nutrient and suspended sediment concentrations compared to the estuary systems, c) the anthropogenically modified systems (AS) that are characterized by high dissolved inorganic nutrient but low suspended sediment concentrations and d) the offshore systems (OS) that

have low dissolved inorganic nutrient and low suspended sediment concentrations throughout the year. Figure 5.6 shows the geographic location of these routine monitoring location classes.

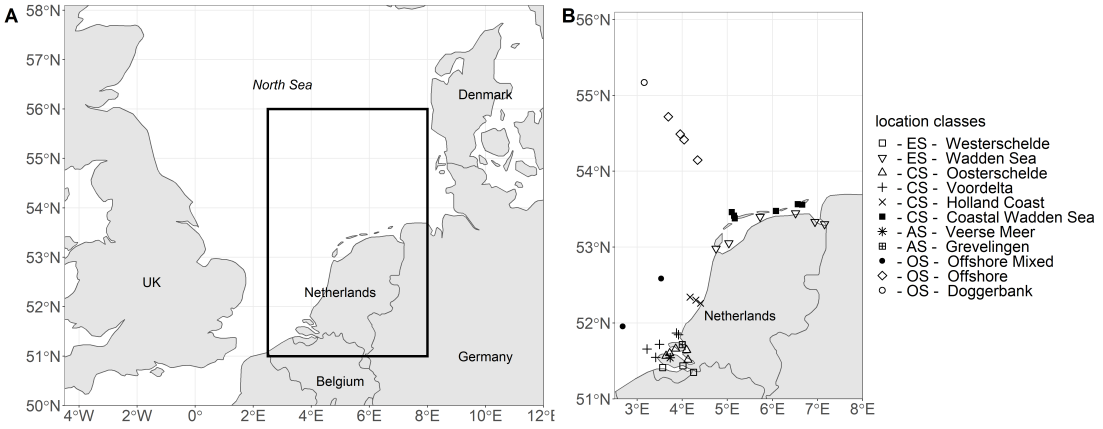

Figure 5.6: Geographic location of the location classes (A - overview and B - detailed) that are simulated with the 1D-V models.

5.2.4.2 Model schematization

11 1D-V models, consisting of two model cells each, were constructed to mimic these 11 location classes of the SNS. The 11 1D-V models differ from each other in dissolved inorganic nutrient and suspended sediment concentration boundary conditions as well as depth and stratification. Salinity was not considered. The dissolved inorganic nutrient and suspended sediment concentrations forced at the boundaries were derived from monthly averaged data (see fig. B.1 - B.5 in B.3). Total nitrogen was distributed in a ratio of 5:1 to the NO_3^- and NH_4^+ timeseries. Total phosphate and silica were used as an input for PO_4^{3-} and SiO_2, respectively. The depth was determined from the average depth at the location classes. Stratification was applied to the location classes Veerse Meer, Grevelingen, Offshore and Doggerbank during the summer months by decreasing the diffusion parameter in the model set-up. Figure 5.7 visualizes the physical attributes of the 11 1D-V models.

The same temperature and radiation timeseries were applied to all 1D-V models (see fig. B.6 and B.7 in B.4), as the geographical extent of the SNS is small enough to allow this simplification. Furthermore, the transport through the 1D-V models was determined in such a way that the water residence time for all 1D-V models was equal (30 days). A very low biomass concentration of each PFT was applied

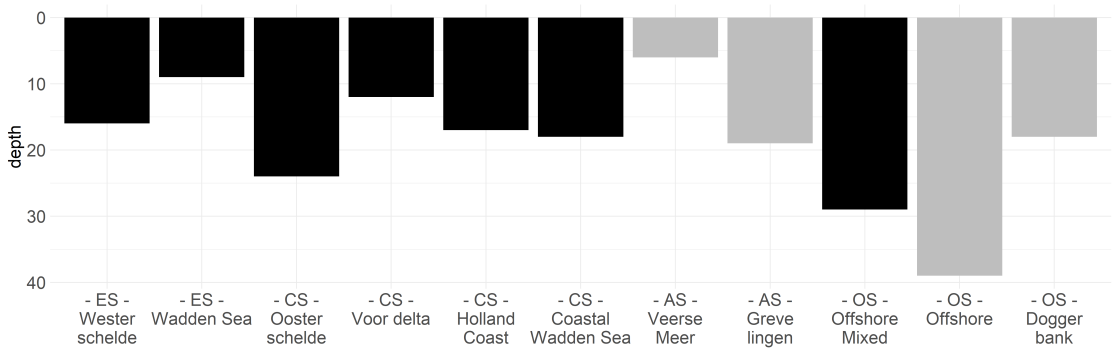

Figure 5.7: Depth of the 1D-V models. The grey color highlights that stratification was applied to those 1D-V models.

to the boundaries at all 11 1D-V models to ensure that there is always seeding biomass available for each PFT. Lastly, the 1D-V models were run with a timestep of 3 min from 2000 to 2010 and an output timestep of 2h. The first year was used as a spin-up.

5.2.4.3 Model parameterization

For the PFTs capable of nutrient uptake, the minimum, optimum and maximum nutrient quotas (e.g. $NCmin$, $NCopt$, $NCmax$) for the different PFTs were derived from Leonardos and Geider (2004). The minimum and optimum nitrogen:carbon quotas ($PCminNCmin$ and $PCminNCmax$) during phosphate limitation were calibrated using the quotas from Leonardos and Geider (2004). The optimum and maximum nitrogen:carbon quotas for the uptake of nitrate ($NO3Copt$ and $NO3Cmax$) were set to be slightly lower than the optimum and maximum nitrogen:carbon quotas for the uptake of ammonium ($NCopt$ and $NCmax$). The minimum, optimum and maximum nutrient quotas (e.g. $NCmin$, $NCopt$, $NCmax$) for protozooplankton were set according to Flynn (2021).
The maximum chlorophyll-a:carbon quota ($ChlCmax$) as well as the initial slope α^{Chl} for the different PFTs were set according to averages per class taken from Geider et al. (1997). Phototrophic organisms have an overcapacity for photosynthesis in order to cover their loss rates (Geider et al., 1998), so the dimensionless parameter $relPS$ (the ratio of photosynthesis rate to maximum growth rate) was set to 2 for the primarily phototrophic organisms.
Previous studies (Skovgaard, 1996; Li et al., 1999; Adolf et al., 2006; Anderson et al., 2018) showed that CMs ingest very little prey in the dark, so ingestion of prey by CMs is light dependent via the dimensionless parameter $relPhag$. Jeong

et al. (2010) showed that CMs cannot capture prey larger than themselves. This was implemented by setting the prey handling index (PR) for each predator accordingly. The sedimentation of diatoms (sed) was set according to Stokes law. A variable density in diatoms due to vacuole was not implemented. Lastly, the size of each PFT was derived from the median size per PFT from the protist dataset used in Schneider et al. (2020b) that covers the same study area.
All 1D-V models were initialized with the same biomass values and the same reference maximum growth rate for each PFT (UmRT = 0.81 d^{-1}). Thus, no initial advantage was given to any PFT. A linear mortality function with a reference mortality of 0.07 d^{-1} (Blauw et al., 2009) was applied to the modelled diatom, green algae and CM. A quadratic mortality function with a reference mortality of 0.007 d^{-1} was applied as a closure function to the modelled protozooplankton. Table B.3 summarizes PFT specific parameters established through literature.

5.2.4.4 Model validation

Routine monitoring data on the SNS provided the in-situ comparison data for the 1D-V model runs (Schneider et al., 2020b). A quantitative comparison of the SVs was done in a target diagram. A target diagram compactly visualizes standard deviations, bias and correlations between model results and field observations (Joliff et al., 2009). On target diagrams, the unity circle provides a marker for the quantification of the fit between model results and observations. SVs that lie within the unity circle are positively correlated and perform well compared to observations. SVs that lie outside of the unity circle have a significant bias and difference in variance between model results and observations. Furthermore, modelled phytoplankton biomass as well as chlorophyll-a timeseries were compared visually against field data timeseries. Nutrients were not compared as they are forced with the transport (see figures B.1 - B.5 in B.3). The modelled trophic composition was compared qualitatively to the in-situ trophic composition provided in Schneider et al. (2020b). The trophic compositions were calculated as fractions per PFT of the total protist biomass.

5.2.4.5 Sensitivity analysis

A sensitivity analysis was completed to determine the influence of different abiotic factors on the biomass concentration of CMs. To verify that the abiotic factors had variations in the same order of magnitude, the normalized standard deviation was calculated ($\overline{sd_x} = sd_x/mean_x$). In separate model runs, the inorganic nutrient concentrations and the suspended sediment concentration were modified by 10 % and the resulting CM biomass analysed.

5.3 Results

5.3.1 PFT timeseries

Figure 5.8 displays results of the eleven 1D-V models for the years 2001 to 2010. It shows the carbon biomass of each PFT within each 1D-V model over the whole timeframe. The 1D-V model results can be grouped into four categories that align with the environmental systems previously described (see figures 5.6 and 5.7).
This figure highlights five important aspects. Firstly, the 1D-V models were unable to capture the dynamics of estuary systems (ES) with protist biomass near zero along the 10-year simulation in both the Westerschelde and Waddensea location classes. Through tidal mixing these systems import protist biomass produced in neighbouring coastal waters where conditions are more favourable. Since this transport of PFTs is not included in these simple 1D-V models, it can be expected that the model underestimates PFT values within the 1D-V estuary models and, thus, the model results of the ES must be neglected. Secondly, the biomass order of magnitude varies between the 1D-V models with the coastal systems (CS) (Oosterschelde to Coastal Waddensea) displaying the highest peaks in biomass and the offshore systems (OS) the lowest (Offshore Mixed to Doggerbank). Thirdly, in each 1D-V model, the effect of the year-to-year variations of the nutrient and suspended sediment boundary conditions (see figures B.1 - B.5 in B.3) are visible in the spring bloom strength, timing and composition. Fourthly, the onset of the spring bloom is the earliest in the 1D-V models that are stratified (Veerse Meer, Grevelingen, Offshore and Doggerbank). Lastly, the 1D-V models of the OS display protists throughout the whole year, while the 1D-V models of the CS display stark peaks at the beginning of spring.

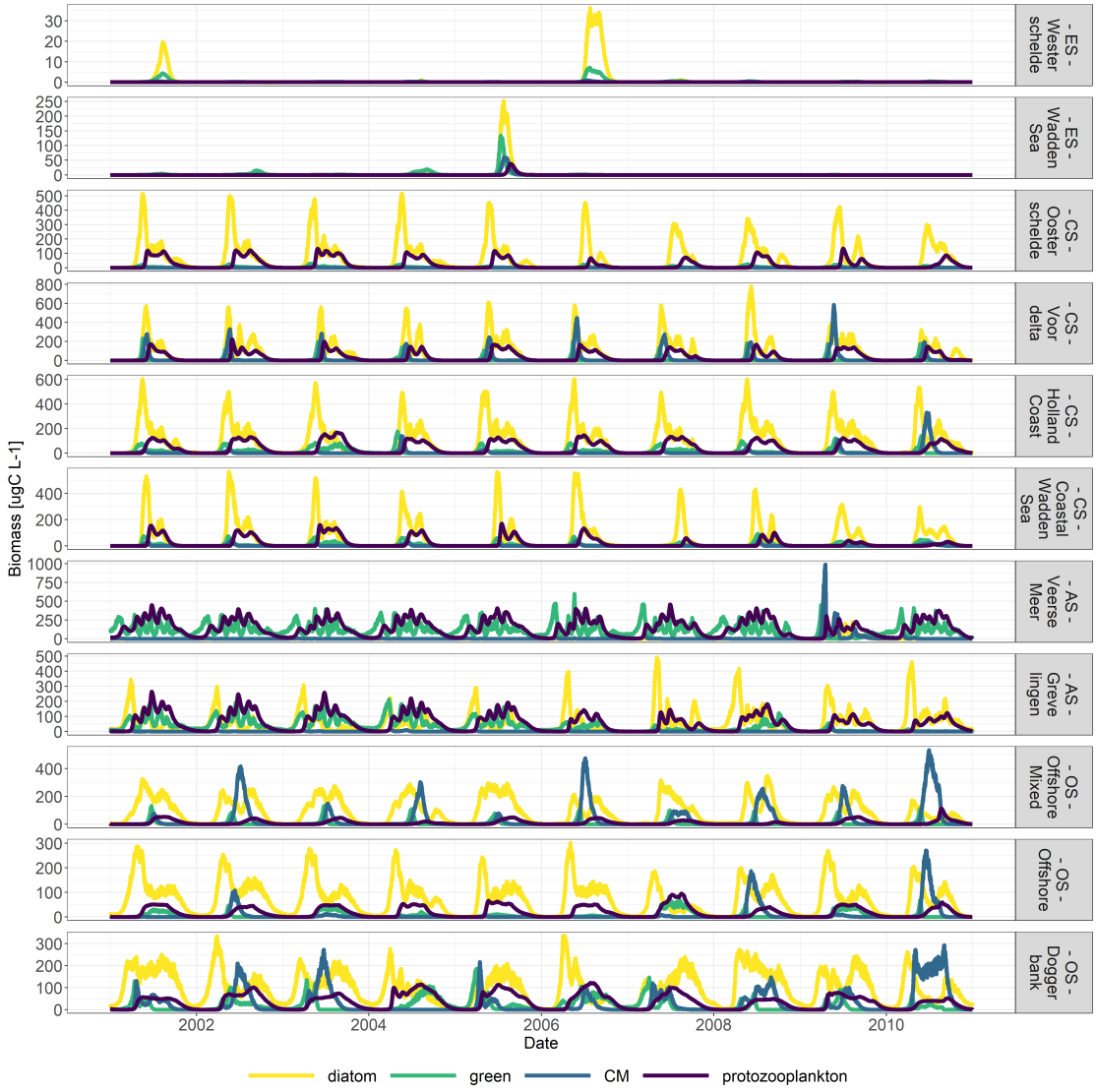

Figure 5.8: Timeseries of protist carbon SVs for the four different PFTs. The color yellow depicts diatoms, the color green the green algae, light blue the CMs and dark blue the protozooplankton. The timeseries clearly show different orders of magnitude from CS to OS as well as year-to-year variations. Please note the differences in the y-axes.

5.3.2 Quantitative validation

Figures 5.9 and 5.10 show the comparison between the model and data for chlorophyll-a and phytoplankton biomass. These two variables were chosen as they have the most reliable and complete data source. The figures show that the model manages to capture the most relevant dynamics. Especially in the CS, the model results for chlorophyll-a and phytoplankton biomass compare well against observations. In the OS, both the chlorophyll-a and phytoplankton biomass tend to be overestimated by the model in the late summer months. The figures also show that the model did not manage to capture the dynamics of Veerse Meer.
Figure 5.11 displays model-data comparisons for inorganic nutrients, carbon biomass of the different PFTs and chlorophyll-a in a target diagram. It should be noted that the ES Westerschelde and Waddensea were not taken into account as the dynamics of those location classes could not be captured by the 1D-V models. Furthermore, to determine whether the 1D-V models manage to capture the difference in order of magnitude between the location classes, the maximum values for the protist and chlorophyll-a state variables per year and location class were extracted. Therefore, this target diagram evaluates the ability of the models to capture the variation over the whole biogeochemical gradient.
Three important aspects can be highlighted in figure 5.11. Firstly, all nutrients, except for ammonium, lie within the unity circle and thus compare well to the sampled data. This is not unexpected as the nutrient timeseries are transported into the column models via the boundary. Secondly, phytoplankton, CM and chlorophyll-a lie on the boundary of the unity circle and thus also compare well to the observations. Lastly, ammonium and protozooplankton lie outside the unity circle and thus show significant bias and difference in variance between the model results and the in-situ data.

Figure 5.9: Comparison of model chlorophyll-a (line) and data chlorophyll-a (points).

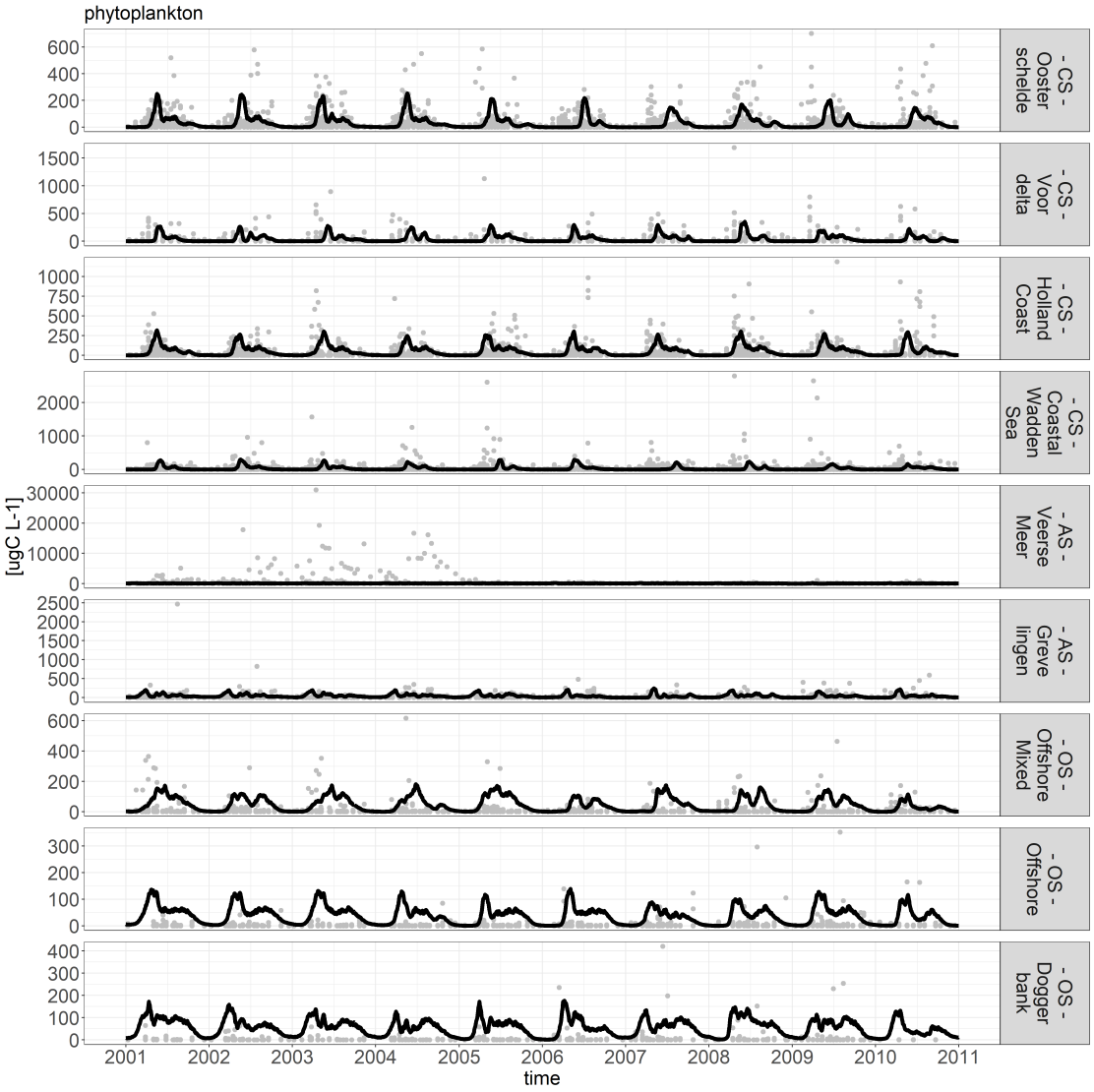

Figure 5.10: Comparison of model phytoplankton (line) and data phytoplankton (points).

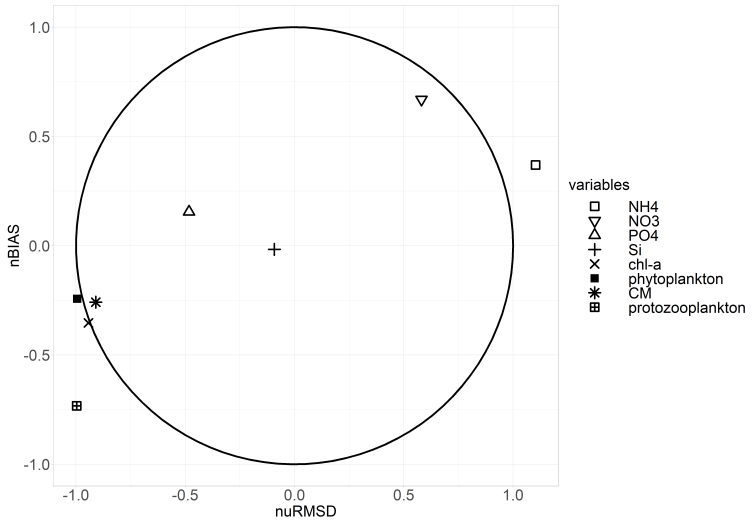

Figure 5.11: Target diagram visualizing the model-sample data comparison (nuRMSD - normalized root-mean square difference; nuBIAS - normalized bias). Silica, nitrate, phosphate, chlorophyll-a and phytoplankton lie within the unity circle which shows that the model performs well compared to the in-situ data. Ammonium, CM and protozooplankton display a significant bias and difference in variance between the model results and the in-situ data.

5.3.3 Qualitative validation of the trophic composition

Figure 5.12 displays the protist community composition of the 1D-V models (fig. 5.12a) and the monitoring data (fig. 5.12b) over the whole timeframe for environmental systems except the ES. The ES were removed because the 1D-V schematization was not able to capture the dynamics of those systems. The colors depict the percentage of each PFT. Figure 5.12 can once again be divided according to the environmental systems and both figures display a increasing gradient of CMs from the CS to the OS.

It must be noted that there are severe shortcomings in the protozooplankton identification of the monitoring program, as it is geared towards identifying phytoplankton. Mainly easily recognizable protozooplankton such as *Noctiluca scintillans* were identified and, thus, the protozooplankton of the routine monitoring data in figure 5.12b are only indicative for protozooplankton occurrence in the 1D-V models.

The CS of the 1D-V model runs are mainly dominated by diatoms, but also green algae and CMs until June and are succeeded by the occurrence of protozooplankton (figure 5.12a). In the data analysis (figure 5.12b), the CS are also dominated by a spring phytoplankton bloom, followed by a very distinct bloom of protozo-

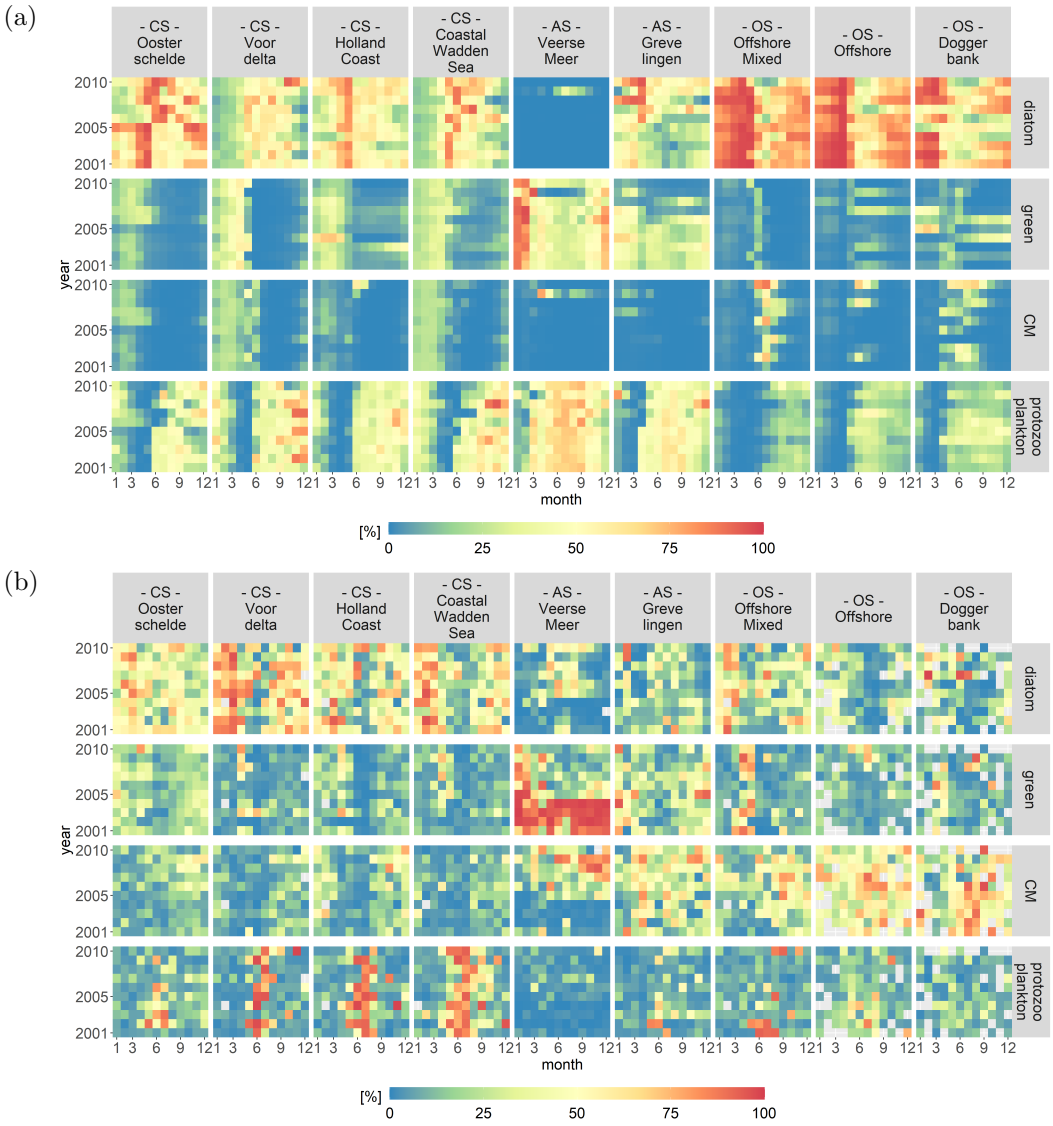

Figure 5.12: Heatmaps displaying the monthly fractions of the total biomass per PFT from a) the 1D-V models mimicking the SNS and b) the routine monitoring data (modified from Schneider et al. (2020b)).

oplankton.
The 1D-V model run of the anthropogenically modified system (AS) Veerse Meer (figure 5.12a) is characterized by a lack of diatoms and CMs compared to the measured concentrations (figure 5.12b). The biomass is almost evenly divided among green algae and protozooplankton. During the first part of the simulation period (until 2007), the biomass of the 1D-V model run of the AS Grevelingen is divided fairly even between green algae, protozooplankton and diatoms. After 2007, the fraction of diatoms increases in the simulated results (figure 5.12a). In the data analysis (figure 5.12b), the AS are characterized by a lack of protozooplankton. Apart from an obvious dominance of green algae in Veerse Meer before 2004, the measured biomass is fairly evenly divided among diatoms, green algae and CMs.
The OS of the 1D-V model runs are characterized by a dominant diatom bloom in spring, succeeded by a bloom of CMs. Protozooplankton also occur to a lesser extent in the offshore 1D-V models compared with the other systems. Compared to the measured concentrations, the Offshore Mixed and Doggerbank model runs perform well as they display a dominance of diatoms at the beginning of the year followed by CMs. However, the modelled CM occurrence ends earlier in the year compared to the measured concentrations.

5.3.4 Sensitivity analysis to test CM occurrence hypothesis

The normalized standard deviations of the abiotic factors verified that the variations for the abiotic factors are in the same order of magnitude (see table B.17 in B.6). Thus, the sensitivity analyses of the different abiotic factors are comparable. The sensitivity analysis results show that the CM biomass changes anti-propor tionally to the dissolved inorganic nutrient concentrations (see figure 5.13). A decrease of dissolved inorganic nutrient concentrations leads to an increase of CM biomass and vice versa. The sensitivity analyses in which each dissolved inorganic nutrient was modified independently show that a decrease of phosphate and of silica result in an increase of CM biomass, while an increase of phosphate and silica result in a decrease of CM biomass. However, increasing or decreasing the suspended sediment, ammonium or nitrate concentration by 10% does not result in similar changes of the CM biomass. Thus, changes in phosphate and silica concentrations have a larger relative effect on the CM biomass.

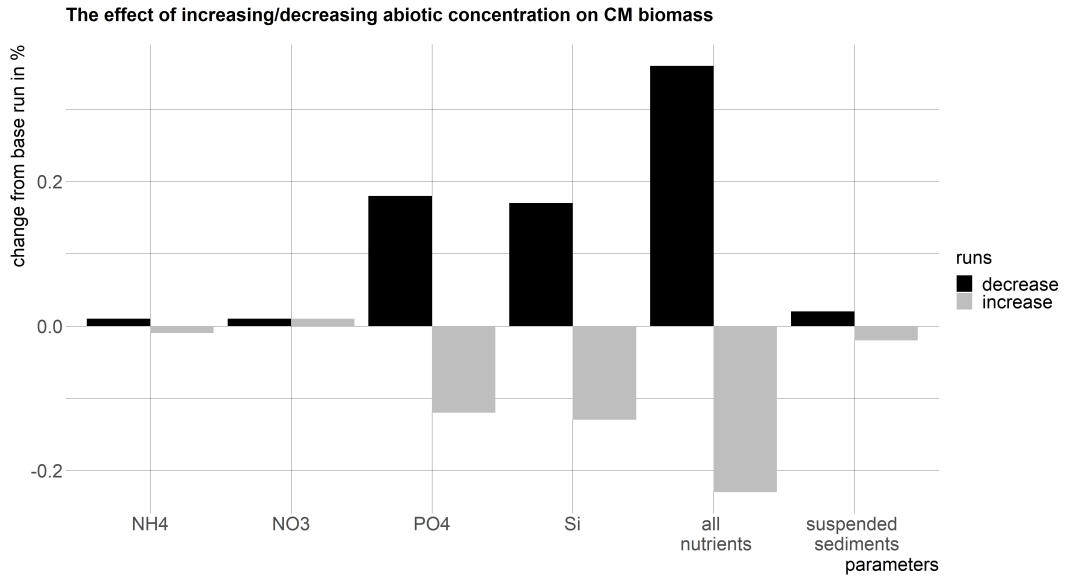

Figure 5.13: The sensitivity analysis shows that changing the nutrient concentration, specifically phosphate and silica concentrations, has the largest effect on the CM biomass. The values display the changes from the base run in %.

5.4 Discussion

In this study, we introduced PROTIST, a module that calculates the primary production of and competition within protist communities. The aim of this study was to estimate the ability of the module PROTIST to simulate the growth and mortality of a protist community and to further explore the hypothesis put forward by Schneider et al. (2020b) that the biogeochemical gradient drives the trophic composition of protist communities in the SNS. By applying the module PROTIST to a group of 1D-V models that mimic the biogeochemical gradient of the SNS, we were able to show that it responds to different biogeochemical forcings and results in different, plausible trophic compositions that are in line with observed data (see fig. 5.12).

CMs have often been shown to occur in oligotrophic environments (Stoecker and Lavrentyev, 2018; Duhamel et al., 2019). Using state-of-the art knowledge on protist physiology, trophic pathways and protist parameters, this modelling study shows that CMs are likely to occur in environments and during months with low dissolved inorganic nutrient supply. The sensitivity analysis showed that the avail-

ability of dissolved inorganic phosphate and silica strongly influenced the occurrence of mixoplankton. However, the availability of dissolved inorganic nitrogen had little effect on the occurrence of mixoplankton, which is most likely due to the fact that dissolved inorganic nitrogen concentrations are rarely limiting in the North Sea coastal zone (Philippart et al., 2007). The suspended sediment gradient (which affects light availability) had very little impact on the occurrence of mixoplankton. Using experimental data, Li et al. (2000a) and Smalley et al. (2012) found that nutrient limitation induces phagotrophy in mixoplankton. So, based on the model results, we can conclude that in the SNS the biogeochemical gradient drives the trophic composition of the protist community primarily through the availability of dissolved inorganic nutrients such as phosphate and silica.

The chosen schematization and set-up of the 1D-V models proved useful as a first approach, but also shows some caveats. While the 1D-V models of the CS and OS perform well compared to the observations, the 1D-V models of the ES and AS perform poorly. The poor performance in the ES is due to three reasons. Firstly, the lack of transport of biotic SVs from coastal waters into the estuary environments and secondly, the lack of tidal dynamics. Most of the organic carbon stems from allochthonous sources (Soetaert and Herman, 1995) and tides dominate the estuaries (Heip, 1988). Thirdly (in concert with the tidal dynamics), the depth distribution of the location classes is not captured in the 1D-V models. There are very shallow places where growth can occur, but as we used the average depth over all sampling locations per location class this is not represented in the current schematization. A 3D grid with hydrodynamics that include transport and stratification could improve simulations also with regard to the timing and duration of blooms.

The 1D-V models of the AS perform poorly as the anthropogenic impact on the hydrodynamics of those systems was not considered. This is clearly visible in the lack of modelled CMs (see fig. 5.12). In general, it is difficult to capture the dynamics of those AS with the limited hydrodynamics of the generic 1D-V models. In 2004, Veerse Meer was re-opened to the Oosterschelde thus allowing exchange of water masses between the Oosterschelde and Veerse Meer (Wijnhoven et al., 2010) turning the freshwater lake into a marine fjord-like water body. During the transition period (2002-2004), a period of high phytoplankton biomass was observed likely due to the absence of benthic grazers (RIKZ, 2007). This could not be captured by the 1D-V models. Grevelingen was also hydrodynamically altered during the 10-year time period (Hoeksema, 2002).

Furthermore, the occurrence of green algae was low in all 1D-V models with the exception of the AS Veerse Meer and Grevelingen. The main reason for this lies in the lack of modelling a defining trait of *Phaeocystis*, a phytoplankton which commonly occurs in the Dutch SNS. *Phaeocystis* avoids predation by forming

colonies (Lancelot et al., 2005), a trait currently not included in PROTIST.
Lastly, the organisms' size determines competition between the organisms (Finkel, 2007). To have a point of reference, the size of the PFTs was derived from routine monitoring data by taking the median size per PFT. However, protist sizes within a community are often not normally distributed, but rather bi- or multimodal. As there is only one size per PFT and the handling rate of the prey depends mainly on the relation between predator and prey size, the chosen size of the organisms impacts the model results. Applying multiple species per PFT may give better results, but will also increase calculation times. At the same time, with only one species per PFT, the model results look realistic. We conclude that while these 1D-V models have caveats, the model results are realistic and the caveats correspond to the chosen model schematization.
An interesting outcome of this study was the coupling of the trophic pathways for CMs within PROTIST. Even though the model equations used in PROTIST for the different trophic pathways are quite detailed in their physiological descriptions, the trade-off between the phototrophic and phagotrophic pathways for CMs is not. Both the phototrophic and phagotrophic pathways are accessible to CMs. The efficiency of each trophic pathway per PFT is set using measured physiological parameters derived from literature. CMs have a lower affinity to light (lower α^{Chl}) and a lower chlorophyll-a:carbon quota compared to diatoms and green algae (Geider et al., 1997). Additionally, CMs have very low ingestion rates during night (Skovgaard, 1996; Li et al., 1999; Adolf et al., 2006; Anderson et al., 2018) compared to protozooplankton. So, it can be hypothesized that CMs employ their mixotrophic genes to remain competitive (Litchman, 2007).
Consequently, CMs do well in environments and seasons in which there is an advantage of combining both trophic modes (Hartmann et al., 2012). Such environments or seasons have a low supply of dissolved inorganic nutrients and/or prey (Mitra et al., 2014a). The great ocean gyres can be classified as such environments and so it is not surprising that recent research has found mixoplankton to occur notably in the world's oceans (Faure et al., 2019). Global warming and the construction of offshore windfarms may change the pelagic environment towards stronger stratification and longer nutrient limitation (Falkowski, 1994; Richardson and Schoeman, 2003; Falkowski and Oliver, 2007). This could allow CMs to become successful due to their mixotrophic genes. As many harmful algal blooms are caused by CMs (Burkholder et al., 2008), it is important for managers to have access to adequate monitoring and modelling techniques with which to assess the probability of potentially harmful CMs occurring (Peperzak, 2003).

5.5 Conclusion

This study has shown that the newly developed module PROTIST for Delft3D-WAQ is capable of modelling different PFTs that interact with, compete against and graze on each other. The module PROTIST responds to biogeochemical gradients and results in different trophic compositions for the protist communities very similar to in-situ observations in those simulations where comparison is useful. Furthermore, this study used modelling results to provide a layer of evidence that the availability of dissolved inorganic phosphate and silica drives the occurrence of CMs in a system with strong gradients of dissolved inorganic nutrients and suspended sediments.
This study demonstrates that PROTIST can be applied in an AEM setting. AEMs provide an important tool to help understand and predict the consequence of changing pressures on the productivity of an ecosystem (Schuwirth et al., 2019). Especially against the background of future anthropogenic changes in coastal environments, it is important that AEMs, such as the one presented here, can model the main trophic pathways within the protist community under dynamic conditions.

Chapter 6

Modelling the impact of seaweed cultivation on the protist community

Article in preparation: Lisa K. Schneider, Nathalie Gypens, Tineke A. Troost, Luca van Duren, Lauriane Vilmin, Willem Stolte (in prep). Modelling the impact of seaweed cultivation on the protist community.

Abstract

There are growing efforts to increase seaweed cultivation in the North Sea. While seaweed aquaculture does not compete with other commercially viable forms of aquaculture, this study hypothesizes that the additional uptake of dissolved inorganic nutrients through seaweed could affect the trophic composition of the protist community and/or the annual primary production. To test this hypothesis, the 3D Dutch Continental Shelf Model - Flexible Mesh of the North Sea was modified to be able to simulate diatoms, phototrophic non-diatoms, constitutive mixoplankton, protozooplankton and seaweed. Two scenarios were run with (seaweed scenario) and without (reference scenario) taking the growth of seaweed into account. The seaweed scenario displays a relative decrease of dissolved inorganic nitrogen and phosphate concentrations, a relative decrease of green algae and protozooplankton biomass, but a relative increase of diatoms and constitutive mixoplankton biomass compared to the reference scenario. The annual planktonic primary production did not change notably in the seaweed scenario. The decreased availability of dissolved inorganic nutrients seems to favour mixoplankton as they do not rely solely on dissolved inorganic nutrients as their only source of nutrients.

6.1 Introduction

To mitigate global warming, there is a growing requirement for renewable energy (Bruckner et al., 2008) as well as alternative food and fuel sources (Bindoff et al., 2019). Multi-use platforms in coastal or open marine waters are an upcoming innovation that could potentially satisfy these needs. Multi-use platforms, such as integrative multi-trophic aquaculture (IMTA) combine electrical energy generation with food production and are seen as a promising step forward (Buck and Langan, 2017).

In the Dutch North Sea, 0.8 % of the area is currently comprised of existing, licensed or under-construction offshore wind farms (OWF) (Ministry of Infrastructure and the Environment, 2014). By 2050, 15-20 % of the Dutch economic area could be taken up by offshore wind farms (Wind Europe, 2021). Multi-use platforms could potentially decrease the cost per MWh by as much as 40% through the sharing of operation and maintenance costs (Bartelings et al., 2014). As finfish aquaculture is challenging in the Dutch North Sea due to technical and biological constraints (Burg et al., 2013), the focus lies on intensifying extractive species aquaculture such as shellfish and seaweed.

Seaweed cultivation has several positive aspects. Seaweeds are dissolved inorganic nutrient absorbers that can be used for inorganic nutrient biomitigation in waters affected by eutrophication and fish fed aquaculture (Roleda and Hurd, 2019). Through photosynthesis seaweed cultivation can also help combat coastal hypoxia and by harvesting the seaweed the cultivation can indirectly contribute to carbon sequestration (Buck and Langan, 2017). Seaweed is harvested for food and animal feed production as well as many further applications such as hydrocolloids, chemicals or biofuels (Burg et al., 2013).

Shellfish aquaculture is already a well-established sector in the Netherlands that will be expanded in the future (Burg et al., 2017). Shellfish filter the water column for protists as well as particulate organic matter. Especially diatoms have a high nutritional value for shellfish (Brown et al., 1997). Shellfish regenerate nutrients quickly, so a co-culture of seaweed and shellfish is advantageous through the exchange of oxygen and regenerated inorganic nutrients (Burg et al., 2013).

While seaweed and shellfish aquaculture do not compete with each other nor with any other commercially viable form of aquaculture (Burg et al., 2013), there could possibly be a competition between seaweed and naturally occurring protists for inorganic nutrients. Photosynthetic protists form the base of our aquatic ecosystems and are responsible for more than 45 % of the global net primary production (Falkowski et al., 2004). In the North Sea, the annual primary production is determined by the dissolved winter inorganic nutrient concentration (Beusekom and Diel-Christiansen, 1993). Dissolved Inorganic nutrient concentrations and protist

biomass display strong gradients from the coast to the offshore (Baretta-Bekker et al., 2009; Schneider et al., 2020b). Nearshore the spring bloom is dominated by diatoms and Phaeocystis, offshore dinoflagellates occur more often.

The competition between seaweeds and planktonic primary producers is based on the fact that seaweed is a winter crop that consumes inorganic nutrients during winter when protists are not competitive (Broch and Slagstad, 2012). In consequence, the uptake of dissolved inorganic nutrients by seaweed during winter could decrease the amount of dissolved inorganic winter nutrients available for the protist bloom in spring.

This study hypothesizes that the uptake of dissolved inorganic nutrients through seaweed could affect the trophic composition of the protist community and/or the annual primary production. While the bulk of the marine primary production is carried out by phytoplankton, recent research has shown that mixoplankton, i.e. protists that can utilize both phototrophy and phagotrophy, contribute notably to marine protist communities (Mitra et al., 2016). Mixoplankton often perform well in oligotrophic stratified environments where the supply of dissolved inorganic nutrients or prey is low (Hansen et al., 2019; Schneider et al., 2021). The decreased availability of dissolved inorganic nutrients could favor mixoplankton as they do not rely solely on dissolved inorganic nutrients as their only source of nutrients.

This shift in trophic composition of the protist community could potentially affect the food quality available for shellfish by decreasing the competitiveness of diatoms that are a major component in the diet of shellfish (Beninger and Decottignies, 2005). A shift towards more mixoplankton could lead to more nutrients being retained in the upper water layers (Stoecker et al., 2017), more carbon exported to the deep ocean (Ward and Follows, 2016) and more harmful algal blooms (Burkholder et al., 2008).

As seaweed cultivation in the North Sea is still in its infancy there is not enough suitable in-situ data available to test this hypothesis. Aquatic ecosystem models (AEM) are a useful tool as they can be used to test the impact of changes on the aquatic environment. To determine not only the local effect of seaweed cultivation, but also the effect on downstream areas it is important to use 3D models. To test the impact of seaweed on the trophic composition of the protist community such a 3D AEM must be able to simulate the growth of seaweed and the protist community.

In a 3D modelling study using Delft3D-WAQ, Vilmin and Duren (2021) employed the module MALG to explore the effect of seaweed cultivation on the inorganic nutrient concentrations and primary production of the Southern North Sea (SNS). Those model results showed a relative decrease in dissolved inorganic nutrient concentrations and primary production. The primary production module employed in Vilmin and Duren (2021) simulates only the growth of phytoplankton.

In order to also simulate the effect on the trophic composition, this study employed the primary production module PROTIST. PROTIST is a rather newly implemented primary production module for Delft3D-WAQ that is capable of simulated the growth and mortality of a protist community consisting of phytoplankton, mixoplankton and protozooplankton (Schneider et al., 2021). Using 1D-vertical column models, Schneider et al. (2021) showed that PROTIST is capable of reproducing the trophic composition of the protist community along a coastal-offshore transect of the SNS.
This study tested the impact of seaweed cultivation on the trophic composition of the protist community in a 3D model application. For this, we modified the 3D Dutch Continental Shelf Model - Flexible Mesh (3D DCSM-FM) of the North Sea (Zijl et al., 2018; Vilmin and Duren, 2021) to include diatoms, phototrophic non-diatoms (greens), constitutive mixoplankton (CM), protozooplankton and seaweed. The protist community is modelled using the module PROTIST described in Schneider et al. (2021). Seaweed is modelled using the module MALG (Schueder and Van Duren, 2019) in the areas of the current and designated OWFs. In every OWF, 25 % of the area was seeded with seaweed which is in accordance with current estimations for seaweed aquaculture upscaling in the North Sea (Vilmin and Duren, 2021).
The first objective of this study is to validate the performance of PROTIST in this 3D model application against in-situ observations. Towards this goal, a reference scenario without taking the growth of seaweed into account was run. The reference scenario was quantitatively validated against in-situ timeseries of inorganic nutrient and chlorophyll-a concentrations as well as protist biomass for 6 stations along two routine monitoring transects of the SNS. The second objective of this study is to test the impact of seaweed cultivation on the trophic composition of the protist community and on the annual primary production. Towards this goal, a second scenario (seaweed scenario) was run in which the growth of seaweed was simulated. The two scenarios were compared to each other in terms of inorganic nutrient concentrations, the trophic composition of the protist communities and the annual planktonic primary production.

6.2 Material and methods

6.2.1 Study area

The North Sea is a marginal sea located on the northwestern European continental shelf (see black rectangle in fig. 6.1a). It is enclosed by the UK in the West, Scandinavia in the East and mainland Europe in the South. The North Sea is dominated by an anti-clockwise circulation (see arrow in fig. 6.1b) caused by tidal

motions (Otto et al., 1990). A prominent bathymetrical feature of the North Sea is the Doggerbank which lies in the center of the North Sea basin with an average depth of 18 m (see figure 6.1b). The Doggerbank divides the North Sea into two distinct systems (Beusekom and Diel-Christiansen, 2009). The North Sea north of Doggerbank is seasonally stratified and has a low productivity. The North Sea south of Doggerbank is well mixed with intermittently stratified regions due to freshwater influence and high primary productivity (Emeis et al., 2015).

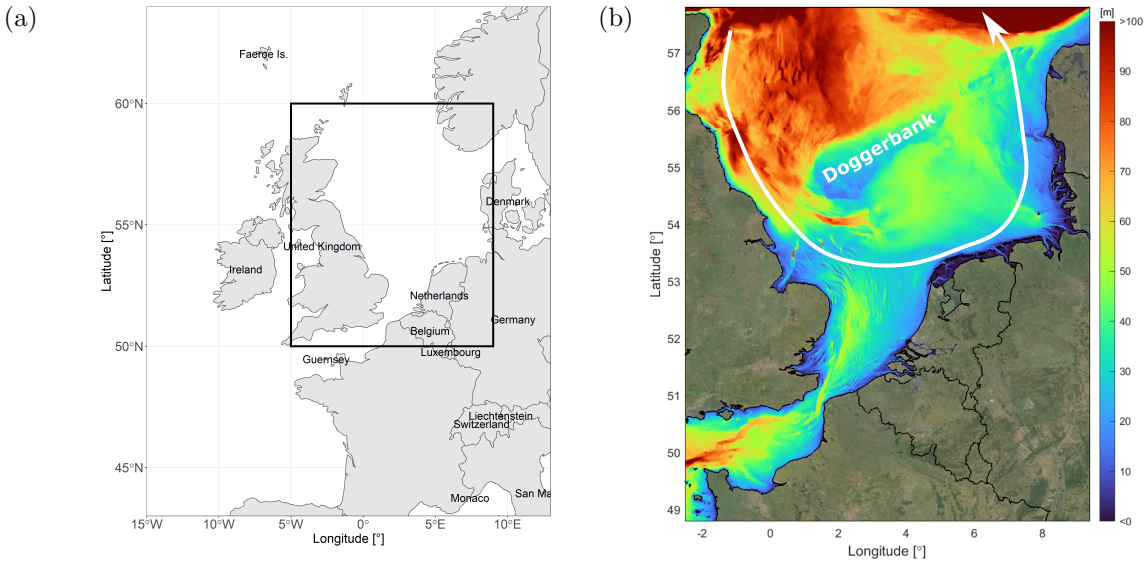

Figure 6.1: a) Visualization of the Northwestern European continental shelf. This corresponds to the 3D DCSM-FM model domain. The black rectangle highlights the geographic extent of the North Sea. b) Bathymetry of the North Sea (courtesy of Stendert Laan, Deltares). North of Doggerbank the North Sea is seasonally stratified and has a low productivity. South of Doggerbank the North Sea is well mixed and has a high productivity. The white arrow denotes the anti-clockwise circulation that dominates the North Sea.

The North Sea connects to the Atlantic Ocean via the Norwegian Sea in the North and the English Channel in the South. In the East, the North Sea connects to the Baltic Sea, its largest freshwater source (470 km^3 per year) (Kwadijk et al., 2016). The surrounding land masses contribute up to 354 km^3 of freshwater per year of which the rivers Elbe and Rhine provide the most discharge (Kwadijk et al., 2016). The rivers also discharge high inorganic nutrient loads from land that lead to a gradient of dissolved inorganic nutrients stretching from the coasts to the central North Sea (Brockmann et al., 1990). The dissolved inorganic nutrient

gradient impacts the composition of the protist community with the coastal areas being dominated by phytoplankton and protozooplankton and the central North Sea by a mixed protist community consisting of phytoplankton, protozooplankton and mixoplankton (Schneider et al., 2020b).

6.2.2 Model specification

To test the impact of seaweed aquaculture on the primary production and trophic composition of the protist community, scenarios were run using a three-dimensional model of the Northwestern European continental shelf. The model 3D DCSM-FM was developed in D-HYDRO to simulate the North Sea along with its adjacent estuaries Western Scheldt and Wadden Sea. The model 3D DCSM-FM simulates physical and ecological processes of the North Sea. The physical model simulates horizontal and vertical flow velocities, volume transport, water levels, ambient water temperature, solar radiation at the water surface, salinity and bottom shear stress (Zijl et al., 2018). The ecological model simulates nitrification and denitrification, primary production, reaeration, settling and light extinction in the water column (Vilmin and Duren, 2021). The most important aspects of 3D DCSM-FM will be highlighted in the following sections. For more detailed information on the 3D DCSM-FM setup and validation, the authors refer to Zijl et al. (2018) and Vilmin and Duren (2021).

6.2.2.1 Domain and grid

The model grid of 3D DCSM-FM covers the northwestern European continental shelf between 15 °W to 13 °E and 43 °N to 64 °N (see figure 6.1A). The model area is delineated by an unstructured grid of varying resolution. The resolution decreases with increasing depth (largest cell 4 x 4 nautical miles - smallest cell 1 x 1 nautical miles). The area of the SNS was assigned the highest resolution to ensure a correct depiction of the highly variable bathymetry. The bathymetry was derived from the bathymetric dataset from the European Marine Observation and Data Network (EMODnet, 2020).

6.2.2.2 Boundary conditions and forcings

At the open ocean boundaries, water levels, tidal water levels and wind surge were defined. Temperature and salinity values were derived from the World Ocean Atlas 2013 (Boyer et al., 2013). The open ocean inorganic nutrient boundary conditions were derived from CMEMS (Copernicus Program, 2020). Due to the significant distance from the open ocean boundaries to the Dutch SNS (the area of interest

in this study), the biotic boundary conditions for protists were neglected and set to very low default values.
At the river boundaries, the freshwater discharge was derived from climatological means of EHYPE data from 1989-2013 (Donnelly et al., 2020). Salinity was set to a constant value of 0.001. The inorganic nutrient inflow from the German and Dutch rivers was derived from Paetsch and Lenhart (2004). For the other river discharges, the EHYPE model was used to create the inorganic nutrient inflow (Donnelly et al., 2020). It can safely be assumed that freshwater protists die as they enter more saline water, so the biotic river boundary conditions for protists were set to very low default values.
The atmospheric deposition of NH_4^+ and NO_3^- was derived from EMEP data (MET Norway, 2020) and forced over the whole model grid. For this study, the suspended sediment was forced using input from the MER model of the Dutch SNS (Deltares, 2017). As the MER model had a smaller grid, the suspended sediment fields were extrapolated beyond the Dutch SNS.

6.2.2.3 Ecological processes

The ecological model applied in this study simulates the interaction between dissolved inorganic nutrients (NH_4^+, NO_3^-, PO_4^{3-} and SiO_2), organic matter (PON, POP, Opal and POC), dissolved oxygen (DO), primary production by protists and seaweed as well as consumption by mixoplankton and phagotrophic protists. Figure 6.2 visualizes the conceptual ecological model employed in this study. Established Delft3D-WAQ modules were employed to simulate the decomposition and settling of organic matter, the dissolution of silica, nitrification and denitrification, the extinction of light and the reaeration of the water column. For more information on these modules, the authors refer to Blauw et al. (2009). Two newly developed modules, the PROTIST and the MALG module, were employed to simulate the growth and mortality of the protists and seaweed, respectively.
The module PROTIST was configured to simulate the primary production of and competition within a protist community consisting of diatoms, green algae, CMs and protozooplankton. PROTIST is fully stoichiometrically variable and simulates the different trophic pathways within the protist community (phototrophy, phagotrophy and mixotrophy). For more information on the module PROTIST, the authors refer to Schneider et al. (2021).
The module MALG was employed to simulate the nutrient uptake, primary production and structural growth of seaweed, more specifically the seaweed *Saccharina latissima*. The MALG module employs model equations formulated in Broch and Slagstad (2012) to simulate the seaweed growth dynamics and the uptake of carbon and nitrogen. The uptake and assimilation of phosphate was added by Vilmin and Duren (2021) using similar equations as for nitrogen. Thus, the MALG model con-

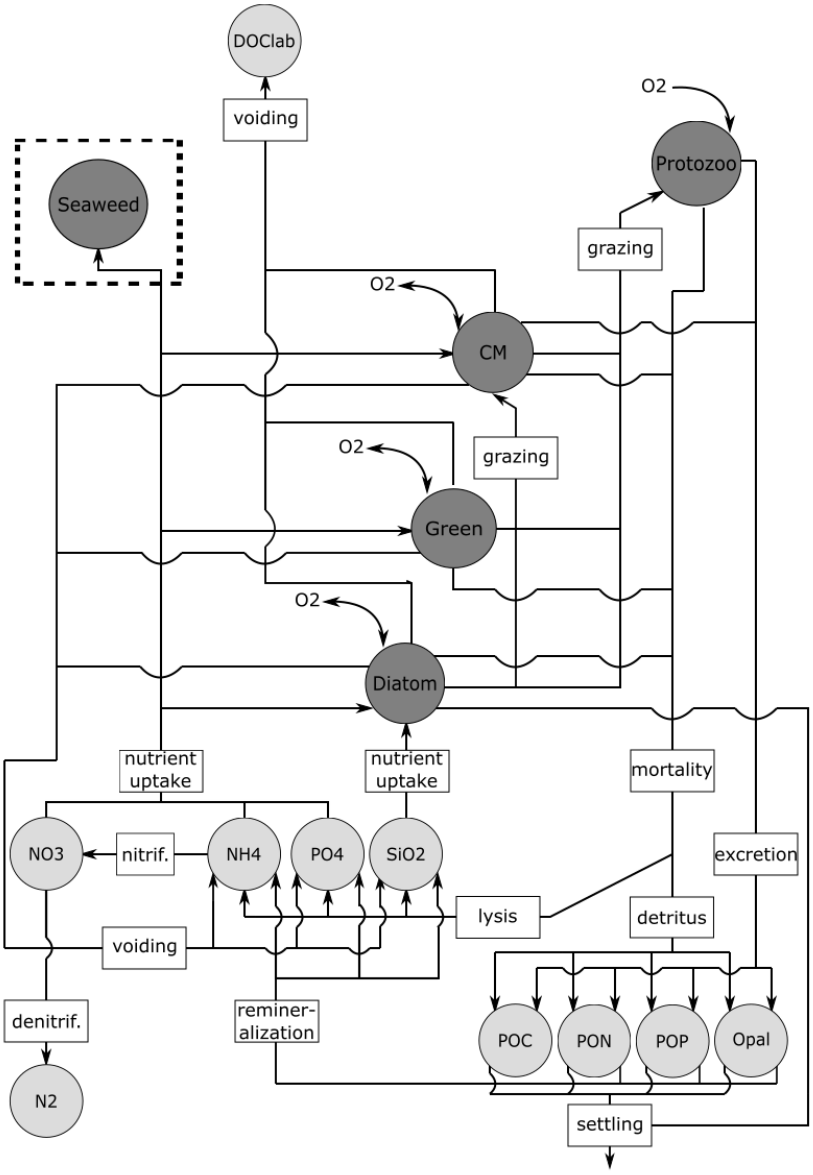

Figure 6.2: Conceptual ecological model. The light grey circles are abiotic state variables (SV), the dark grey circles the protist functional types (PFT) and seaweed. The arrows and the labels depict the interaction between the different SVs. For the reference run, the seaweed state variables (in dashed box) are deactivated.

sists of four state variables: the structural mass (MALS) and the internal carbon, nitrogen and phosphate storage pools (MALC, MALN, MALP). Figure 6.3 describes the relationship and flows between the seaweed state variables and abiotic state variables.

MALS describes the frond of the seaweed that grows in length and area by using the internal reserves MALC, MALN and MALP. While MALS has a fixed C:N:P composition, the ratio of stored to structural mass can vary as well as the ratios of the internal reserves to each other (Broch and Slagstad, 2012). The state variable MALC increases through photosynthesis, but decreases through exudation, respiration and structural growth. The state variables MALN and MALP increase through uptake of dissolved inorganic nitrogen and phosphate, respectively and decrease through growth of structural biomass. The state variable MALS increases through growth and decreases through decay and erosion. While seaweed naturally grow on the seafloor, seaweed is generally cultivated near the water surface using floating buoy systems in environments such as the North Sea. Thus, in the present scenarios, seaweed grows downward in OWFs through multiple vertical water layers as implemented by Schueder and Van Duren (2019). For more information on the module MALG, the authors refer to Vilmin and Duren (2021) and Schueder and Van Duren (2019).

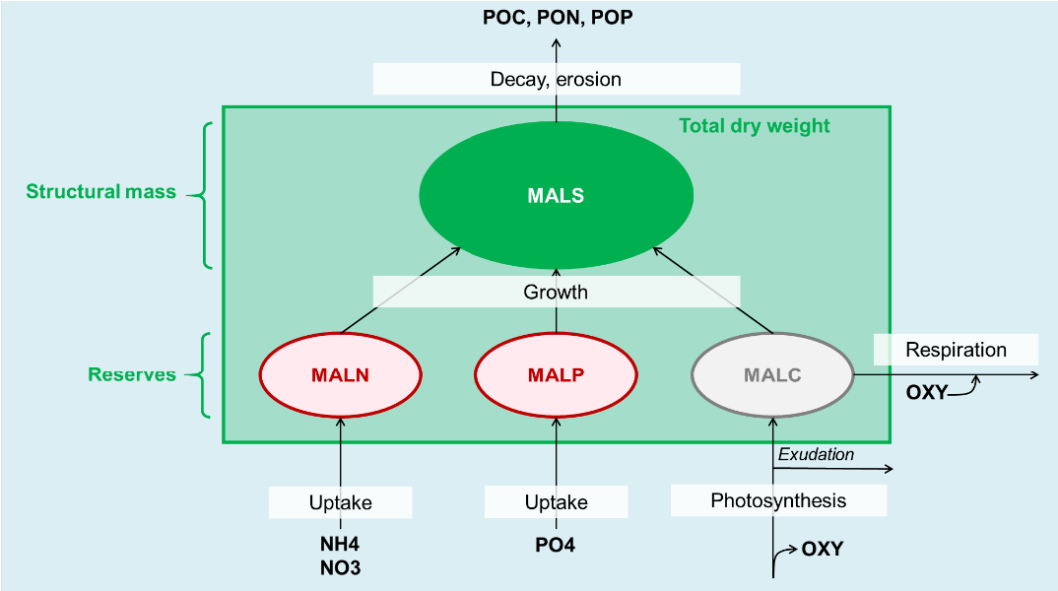

Figure 6.3: Visualization of the MALG state variables and processes. Reprinted with permission from Lauriane Vilmin.

6.2.3 Model application, validation and analysis

Two model set-ups were simulated, a reference simulation and a seaweed simulation. In the reference scenario, state variables for inorganic nutrients, particulate organic matter and protists were simulated. In the seaweed scenario, in addition to the state variables present in the reference run, state variables for seaweed were simulated as well. The seaweed run includes the seaweed state variables and interaction visualized in fig. 6.2 within the dashed black box. Those pathways are excluded in the reference run.

The simulations were run over one production cycle of seaweed from September 2016 to September 2017. The reference simulation was run twice, so that the first run could be used as a spin-up for the reference and seaweed simulation. Both model simulations were calculated with a 10 min timestep and had an output interval of 12 h. The protist functional types (PFTs) were parameterized according to Schneider et al. (2021). Seaweed was parameterized and seeded in the areas for the OWF according to Vilmin and Duren (2021). Figure 6.4 visualizes the location of the OWFs and with the monitoring stations used for model validation.

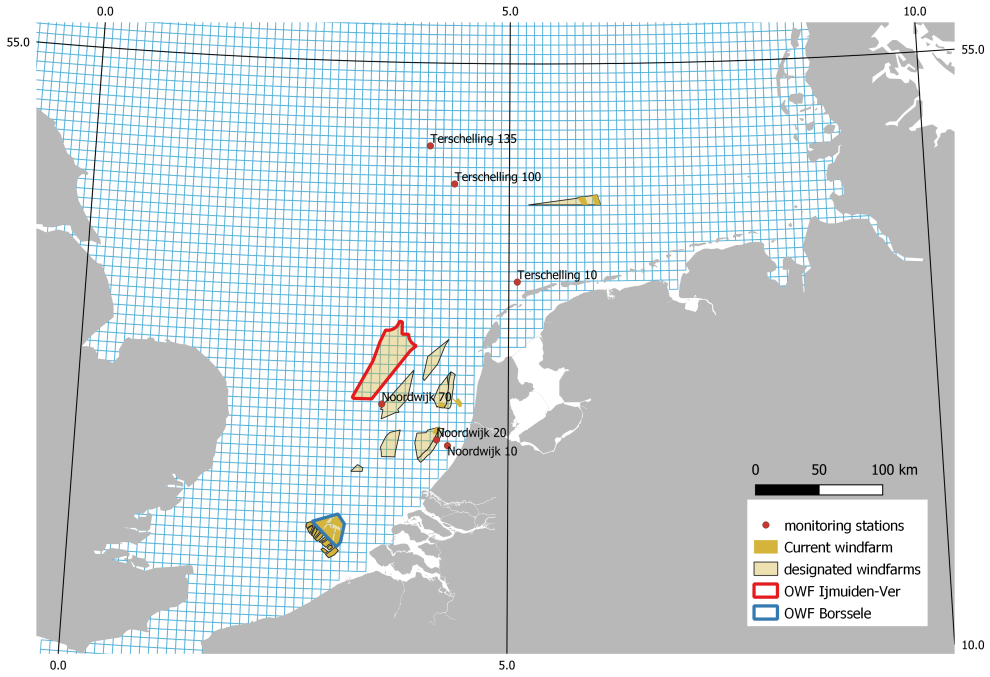

Figure 6.4: Location of the OWFs (yellow polygons), the MWTL sampling stations (red dots) and the mass balances areas of the OWFs Borssele and Ijmuiden-Ver (blue and red polygons).

To validate the model, the reference scenario was compared to observations for dissolved inorganic nutrients, chlorophyll and protist biomass. To analyze whether seaweed cultivation impacts the trophic composition of protist communities, comparison maps were created. The maps display the mean difference between the reference and the seaweed scenario for the dissolved inorganic nutrients and the PFTs during the summer months (June - August 2017). The impact of seaweed cultivation on the annual planktonic primary production was estimated for two OWFs Borssele and Ijmuiden-Ver (blue and red polygons in figure 6.4).

6.3 Results

6.3.1 Reference scenario validation

6.3.1.1 Dissolved inorganic nutrients

Figures 6.5 and 6.6 visually compare the nitrate and phosphate concentrations of the model against in-situ data along two routine measurement transects, Terschelling and Noordwijk, for 3 stations each.
At all stations, the in-situ nitrate concentrations (fig. 6.5) increase as of November 2016 and display clear peaks around March 2017 that decline to minimum values around May 2017. The stations Noordwijk 10 and Noordwijk 20 display the highest in-situ peak concentrations of nitrate with values between 0.5 - 0.7 mgN/L (fig. 6.5b and 6.5d). The stations Noordwijk 70, Terschelling 10 and Terschelling 100 (fig. 6.5f, 6.5a, and 6.5c) have in-situ peak nitrate concentrations ranging between 0.15 and 0.3 mgN/L. The station Terschelling 135 (fig. 6.5e) displays the lowest in-situ peak nitrate concentration of around 0.05 mgN/L. The timing of the modelled nitrate concentration peaks coincides well with the in-situ concentration peaks. For the stations Terschelling 10 and 100 as well as Noordwijk 70 (fig. 6.5a, 6.5c and 6.5f), the magnitude of the modelled concentration peaks compares well the in-situ observations. For Terschelling 135 (fig. 6.5e), the magnitude of the modelled concentration peak is overestimated compared to the in-situ observations. For stations Noordwijk 10 and 20 (fig. 6.5b and 6.5d), the magnitude of the modelled concentration peak is underestimated compared to the in-situ observations.
At all stations, the in-situ phosphate concentrations (fig. 6.6) display peak concentrations around March 2017. The stations Noordwijk 10 and Noordwijk 20 display the highest in-situ peak concentrations of phosphate with values around 0.02 mgP/L (fig. 6.6b and 6.6d). The stations Noordwijk 70, Terschelling 100 and Terschelling 135 (fig. 6.6f, 6.6c, and 6.6e) have in-situ peak concentrations ranging between 0.016 and 0.0175 mgP/L. The station Terschelling 10 (fig. 6.6a) displays the lowest in-situ peak concentration of phosphate (around 0.013 mgP/L).

For all stations, the timing and strength of the modelled phosphate concentrations compare well to the in-situ observations.

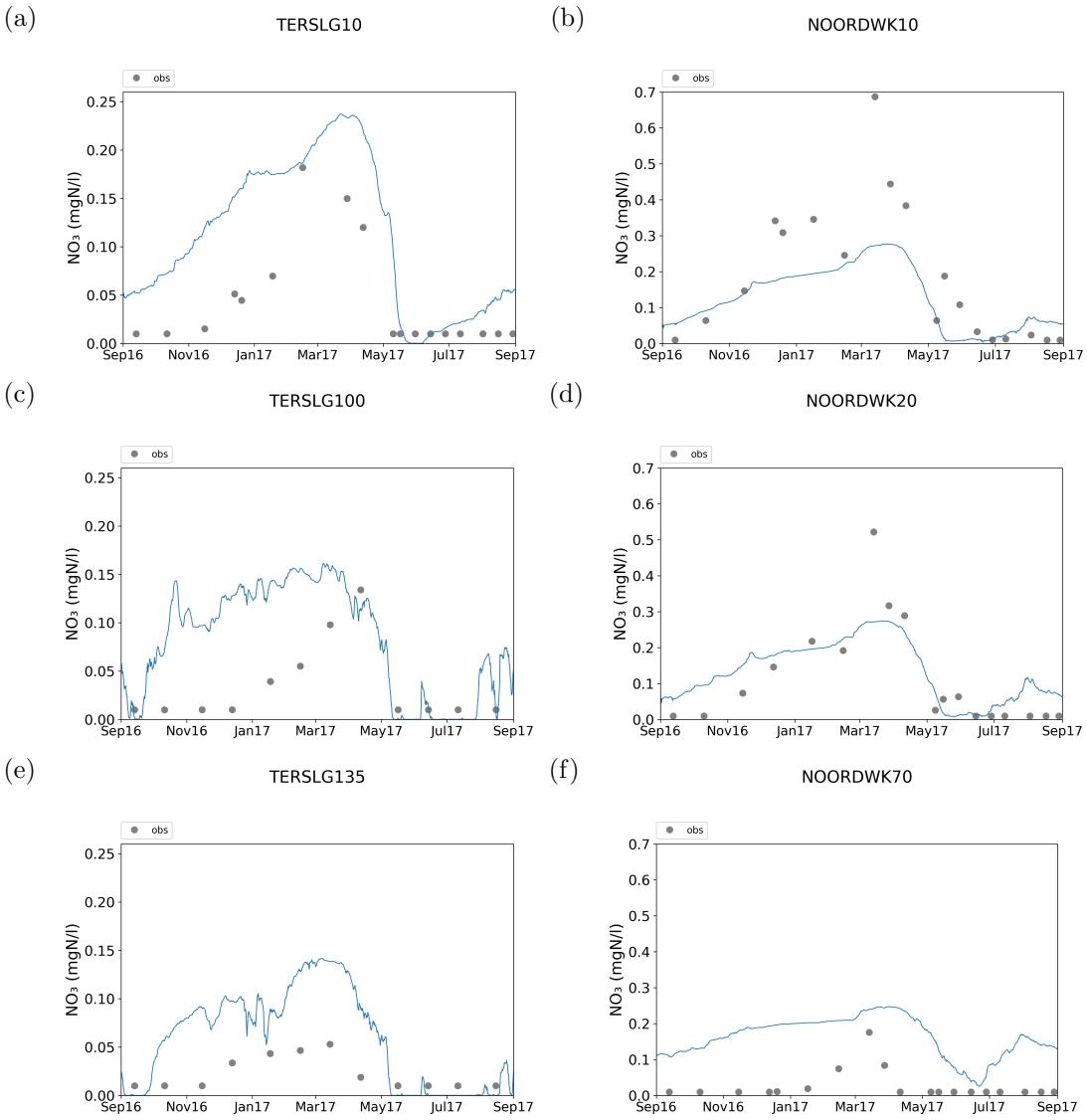

Figure 6.5: Comparison of nitrate concentrations between modelled (blue line) and in-situ (grey dots) timeseries for the Terschelling (left column) and Noordwijk (right column) transects. The timing of the modelled peak concentrations compare well to the in-situ observations.

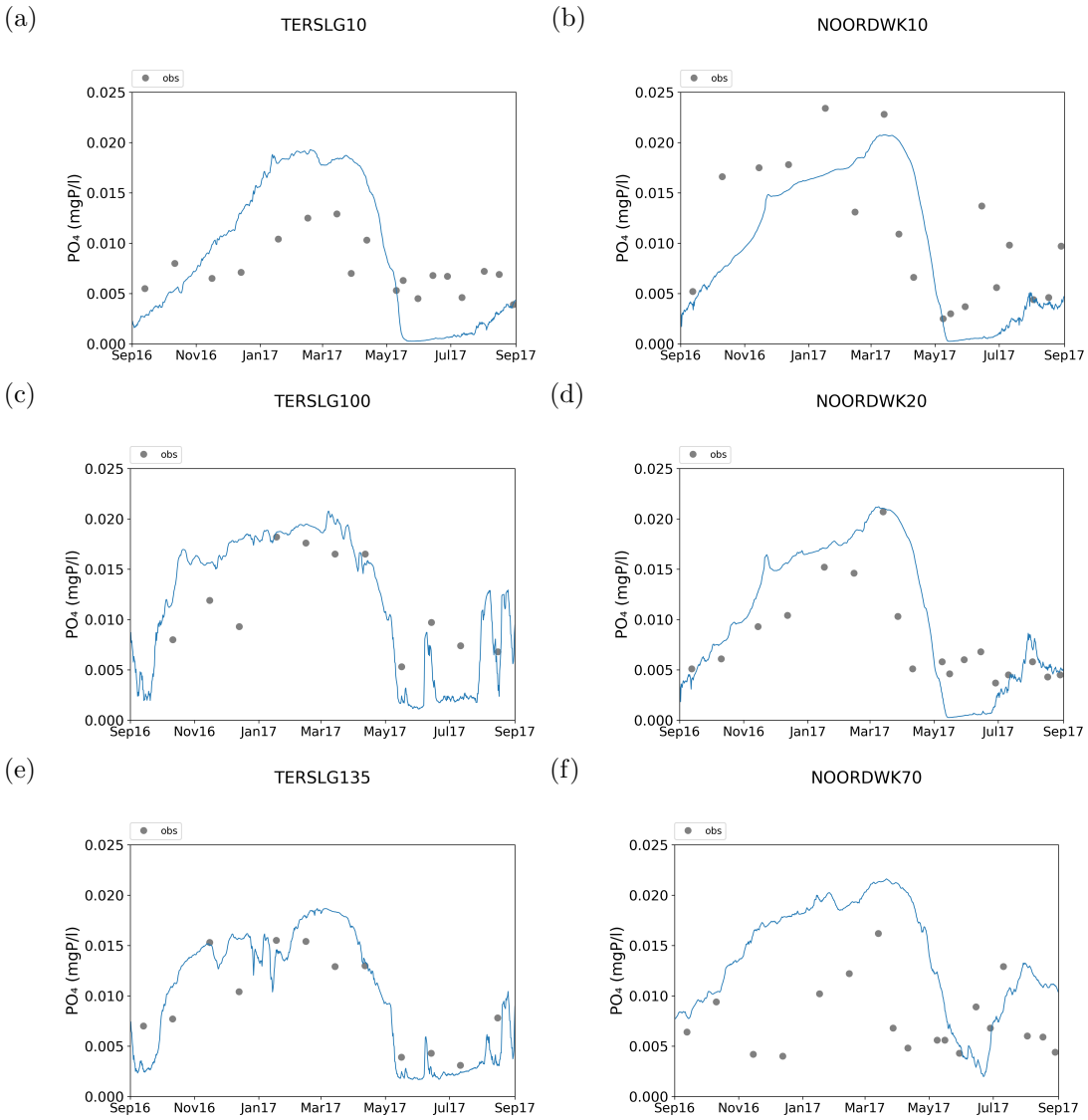

Figure 6.6: Comparison of phosphate concentrations between modelled (blue line) and in-situ (grey dots) timeseries for the Terschelling (left column) and Noordwijk (right column) transects. The modelled data compare well to the in-situ observations.

6.3.1.2 Chlorophyll-a

Figure 6.7 visually compares the chlorophyll-a concentration of the model against in-situ data along two routine measurement transects, Terschelling and Noordwijk, for 3 stations each. For all stations, the spring peak of chlorophyll-a is captured by the model.

At all stations, the modelled chlorophyll-a concentrations display the highest values during May 2017. For the Noordwijk transect and the station Terschelling 10 (fig. 6.7b, 6.7d, 6.7f and 6.7a), the peak modelled chlorophyll-a concentrations display values of between 30 - 40 μg/L, while the stations Terschelling 100 and 135 (fig. 6.7c and 6.7e) display modelled peak values around 20 μg/L. The magnitude of the modelled chlorophyll-a spring peaks is much larger compared to the in-situ observations. However, the timing of the modelled spring peak aligns well the in-situ observations.

6.3.1.3 Carbon biomass

Figure 6.8 visually compares the phytoplankton (diatom and green algae), CM and protozooplankton carbon biomass of the model against 10 years of monthly averages of in-situ data (2004 - 2014) along two routine measurement transects, Terschelling and Noordwijk, for 3 stations each. In general, the modelled phytoplankton and protozooplankton carbon biomass are overestimated and the modelled mixoplankton carbon biomass are underestimated compared to the observations.

The modelled phytoplankton carbon biomass (fig. 6.8a and 6.8b) display seasonal variations that can also be seen in the in-situ data. For the stations Terschelling 10, Noordwijk 10 and Noordwijk 20, the modelled phytoplankton carbon biomass is at the upper limit of the in-situ data. For the stations Terschelling 100, Terschelling 135 and Noordwijk 70, the modelled phytoplankton carbon biomass is higher than the in-situ data.

For Terschelling 10 and 100 as well as all Noordwijk stations (top two rows in fig. 6.8c as well as fig. 6.8d), the modelled mixoplankton carbon biomass shows biomass peaks from May to July 2017. For those stations, the modelled mixoplankton carbon biomass is also at the lower limit of the in-situ data. At Terschelling 135 (bottom row in fig. 6.8c), the modelled mixoplankton carbon biomass displays a seasonal succession similar to the modelled phytoplankton carbon biomass.

At all stations, the modelled protozooplankton carbon biomass (fig. 6.8e and 6.8f) is higher than the in-situ data. Also, the seasonal variability in the modelled protozooplankton carbon biomass is not very pronounced. However, it must be noted that this cannot be clearly observed in the in-situ data either.

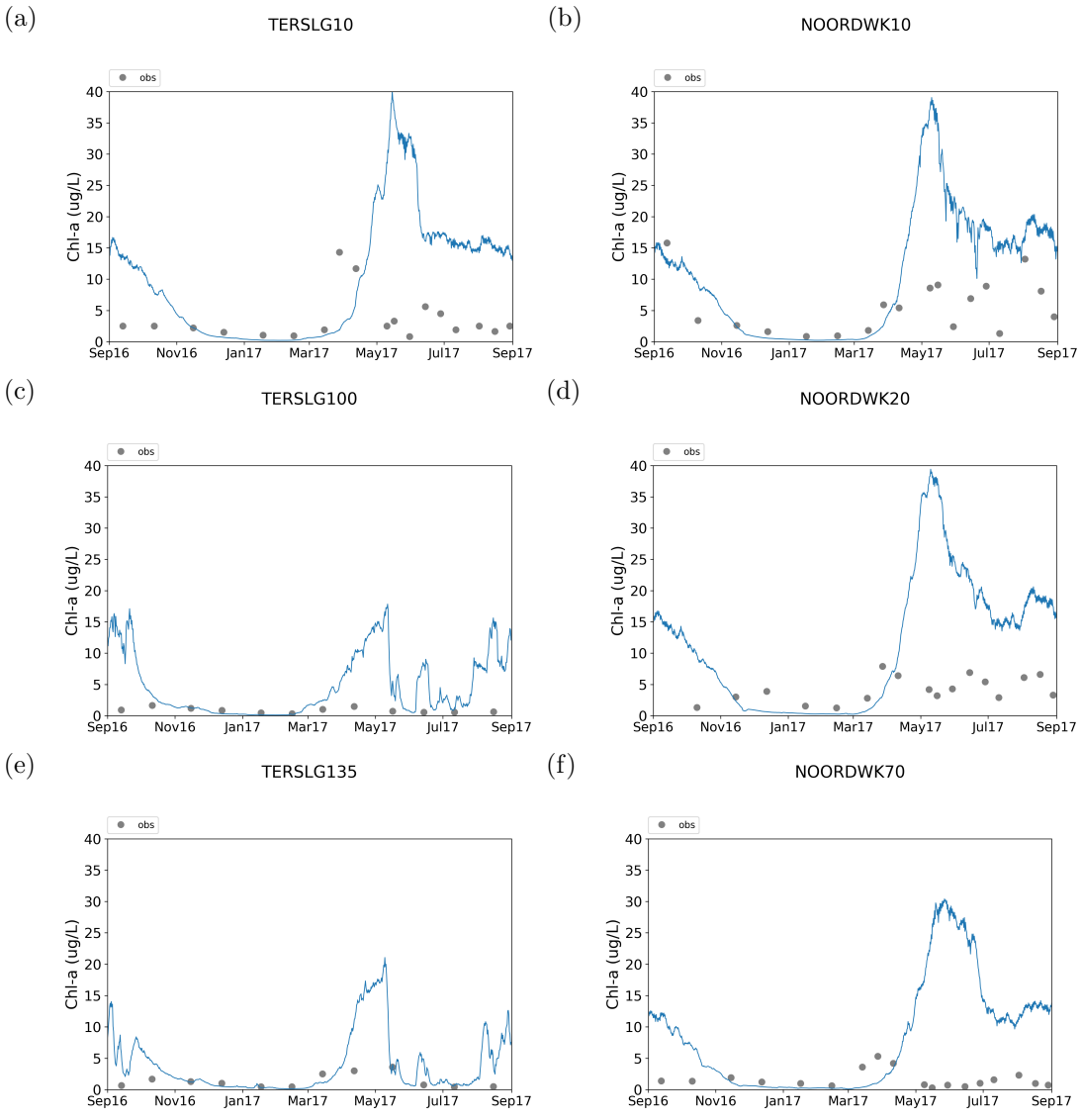

Figure 6.7: Comparison of chlorophyll-a concentrations between modelled (blue line) and in-situ (grey dots) timeseries for the Terschelling (left column) and Noordwijk (right column) transects. While the timing of the modelled spring peaks of chlorophyll-a compare well to the in-situ observations, the modelled spring peak magnitudes are much higher.

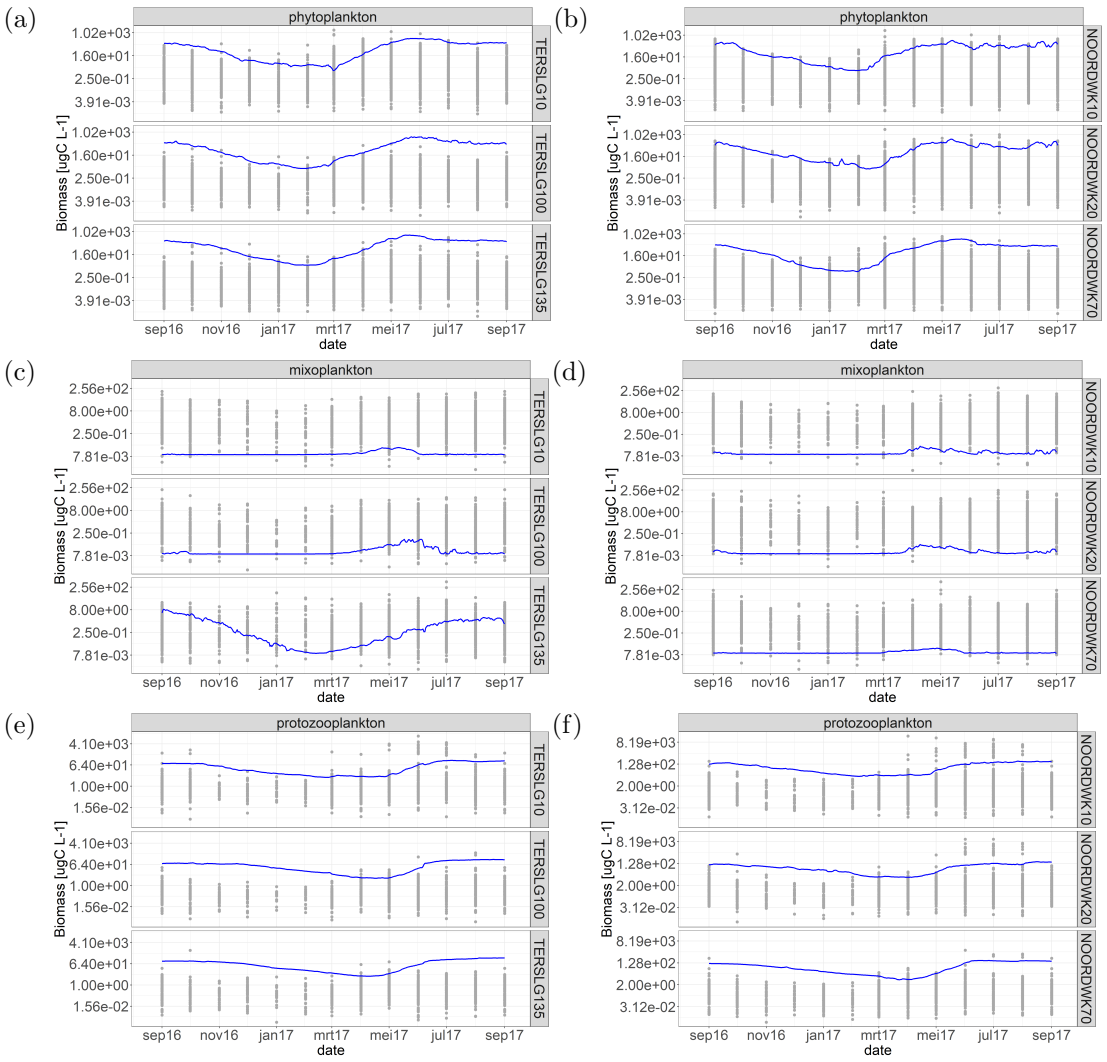

Figure 6.8: Comparison of phytoplankton (top), mixoplankton (middle) and protozooplankton (bottom) carbon biomass between modelled (blue line) and in-situ (grey dots) timeseries for the Terschelling (left) and Noordwijk (right) transects. One model year is compared against 10 years of monthly in-situ averages. The modelled phytoplankton and protozooplankton timeseries are too high and the modelled mixoplankton too low compared to the in-situ observations.

6.3.2 Growth of seaweed

Figure 6.9a maps the growth of seaweed in the OWFs of the SNS for June 2017, while figure 6.9b plots a timeseries of seaweed growth for the sampling station Noordwijk 20. Figure 6.9a shows that seaweed growth is restricted to the areas of the OWFs. There is no obvious spatial gradient visible between the different OWFs in the structural mass of seaweed. Figure 6.9b shows that the simulated seaweed increases as of January 2017 and reaches its peak dry weight in June 2017. The total weight and carbon reserve then decline, while the nitrogen and phosphate reserve continue to increase until the carbon reserve is completely depleted.

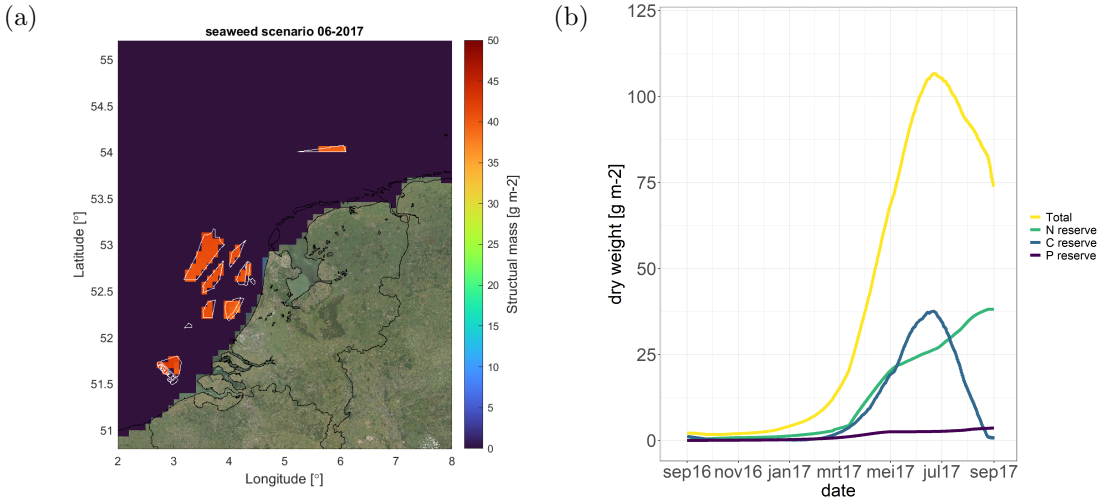

Figure 6.9: a) Seaweed extent in the OWFs of the SNS during June 2017. b) Total structural mass and reserves in dry weight at Noordwijk 20. Seaweed reaches a peak mass during June.

6.3.3 Scenario comparisons

6.3.3.1 Annual primary production

In both OWFs Borssele and IJmuiden-Ver, the integrated annual planktonic primary production does not change notable between the reference and the seaweed scenario. In the OWF Borssele (close to the coast), the integrated annual planktonic primary production did not change between the two scenarios (216 gC m^{-2} $year^{-1}$ in both scenarios). In the OWF IJmuiden-Ver (further away from the coast), the integrated annual planktonic primary production did not change either in the seaweed scenario (253 gC m^{-2} $year^{-1}$ for both scenarios).

6.3.3.2 Relative difference maps

Figures 6.10, 6.11 and 6.12 map the mean values of the summer months June, July and August 2017 for dissolved inorganic nitrogen and phosphate concentrations as well as for diatom, CM, green algae and protozooplankton carbon biomass over the North Sea. Each left map displays the absolute values of the reference scenario and each right map the relative difference between the reference and seaweed scenario. The summer months were chosen as they show the most distinct differences. Plots comparing the two scenarios for the winter and spring months can be viewed in the appendix C.
The left maps in figure 6.10 shows that the highest concentration for dissolved inorganic nitrogen (> 1.5 mgN/L) and phosphate (> 0.05 mgP/L) are located in the estuaries of the rivers Rhine and Weser. The North Sea basin has concentrations of around 0.5 mgN/L of dissolved inorganic nitrogen and of around 0.02 mgP/L of dissolved inorganic phosphate. In the seaweed scenario (right maps in fig. 6.10), both dissolved inorganic nitrogen and phosphate decrease by 40 % in the area of the OWFs and along the Dutch coast towards Germany following the direction of the anti-clockwise circulation.
The left maps in figures 6.11 and 6.12 display absolute biomass distribution of the North Sea for diatom (fig. 6.11a), CM (fig. 6.11b), green algae (fig. 6.12a) and protozooplankton (fig. 6.12b). The diatom biomass in the central North Sea displays values ranging between 0.3 - 0.6 mgC/L. Compared to the diatom biomass, the CM biomass is very low. The highest CM biomass (0.05 mgC/L) can be found along the coast of Denmark. The central North Sea displays value around 0.01 mgC/L. The highest green algae biomass (0.05 mgC/L) can be found off the coast of South England and Northern Germany, while the central North Sea displays values around 0.01 mgC/L. The highest protozooplankton biomass (0.35 mgC/L) can be found off the coast of South England, while the central North Sea displays values around 0.1 mgC/L.
The right maps in figures 6.11 and 6.12 display the relative difference between the reference and seaweed scenario for diatom (fig. 6.11a), CM (fig. 6.11b), green algae (fig. 6.12a) and protozooplankton (fig. 6.12b). The diatom and CM biomass increase by 10% and 50 %, respectively, in the area of the OWFs and along the Dutch coast towards Germany following the direction of the anti-clockwise circulation. Over a similar geographic extent, the green algae and protozooplankton biomass decrease by 10% and 30 %, respectively.

(a)

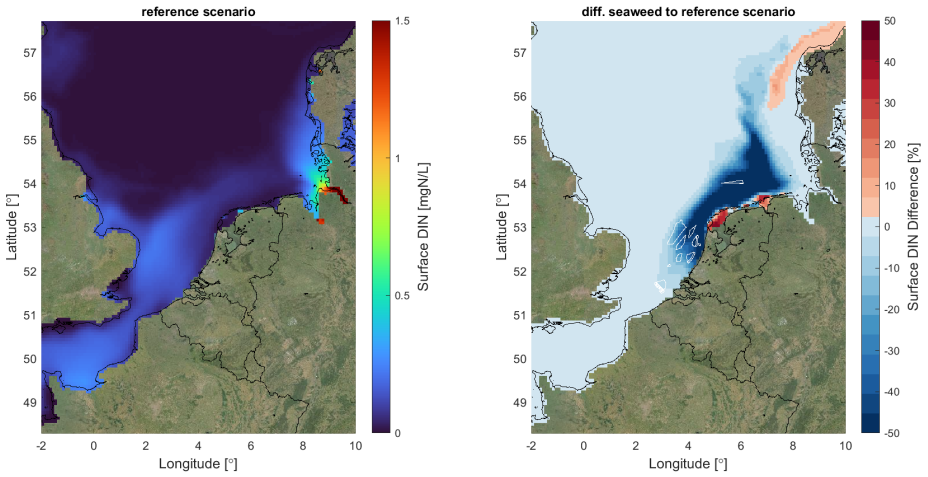

(b)

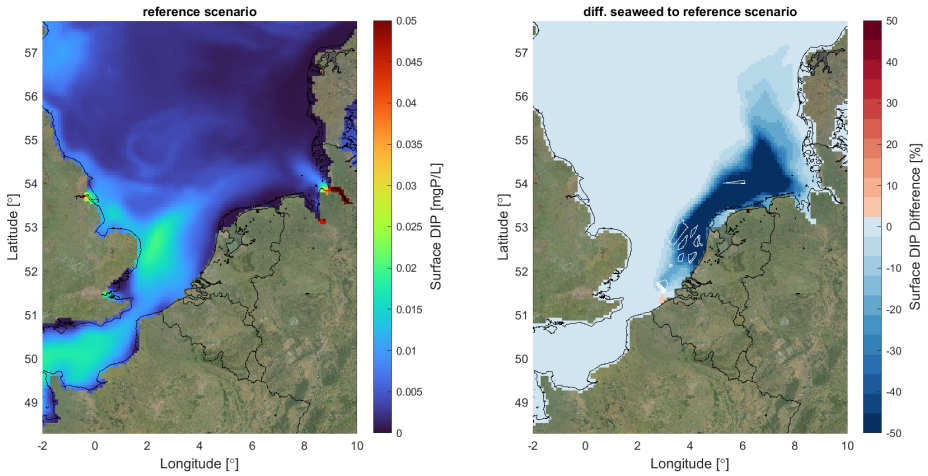

Figure 6.10: Visualization of averaged dissolved inorganic nitrogen (a) and phosphate (b) concentrations for the months June, July and August 2017. The left maps visualizes the absolute values for the reference scenario and the right maps the relative difference between the reference and seaweed scenario. The seaweed scenario results display an average decrease of dissolved inorganic nutrients of 40 % in the vicinity of the OWFs (right maps).

(a)

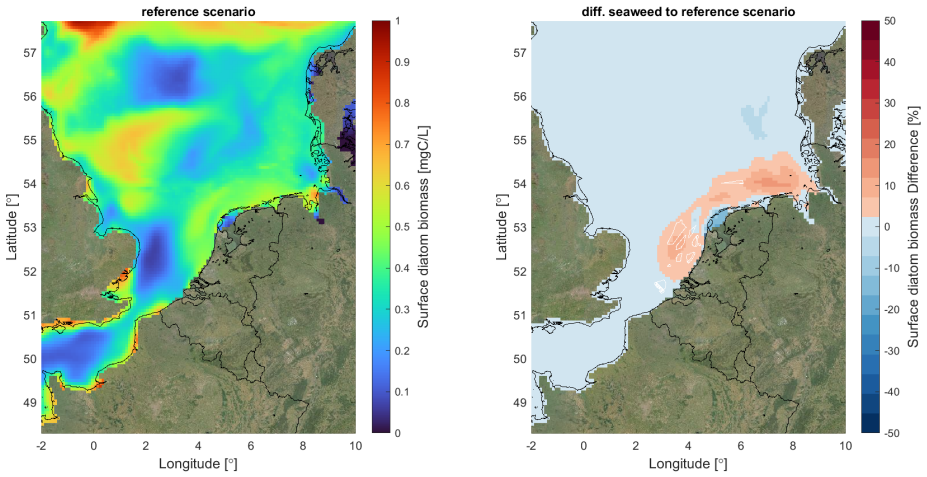

(b)

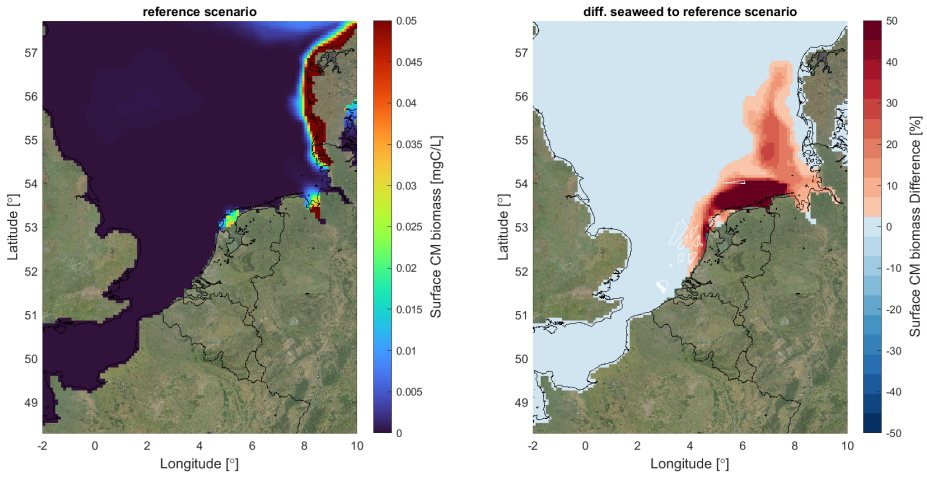

Figure 6.11: Visualization of averaged diatom (a) and constitutive mixoplankton (b) biomass for the months June, July and August 2017. The left maps visualizes the absolute values for the reference scenario and the right maps the relative difference between the reference and seaweed scenario. The seaweed scenario results in an average increase of diatoms by 10 % and an increase of CM by 50 % in the vicinity of the OWFs (right maps).

(a)

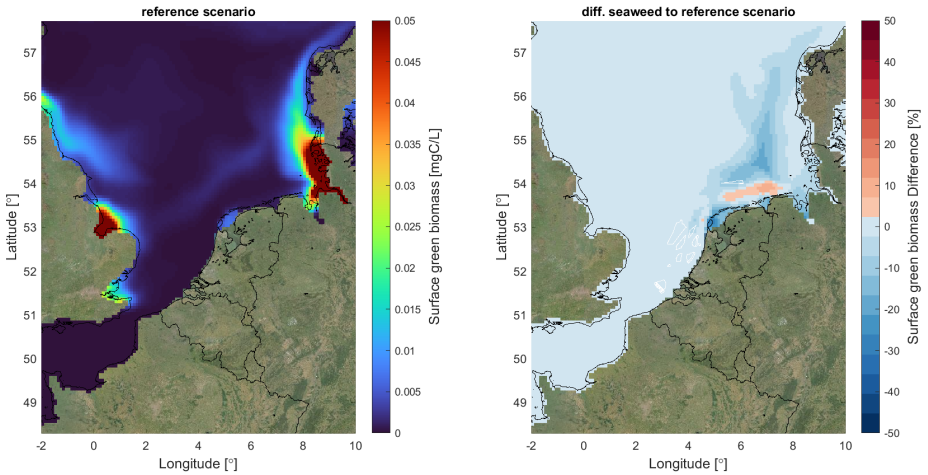

(b)

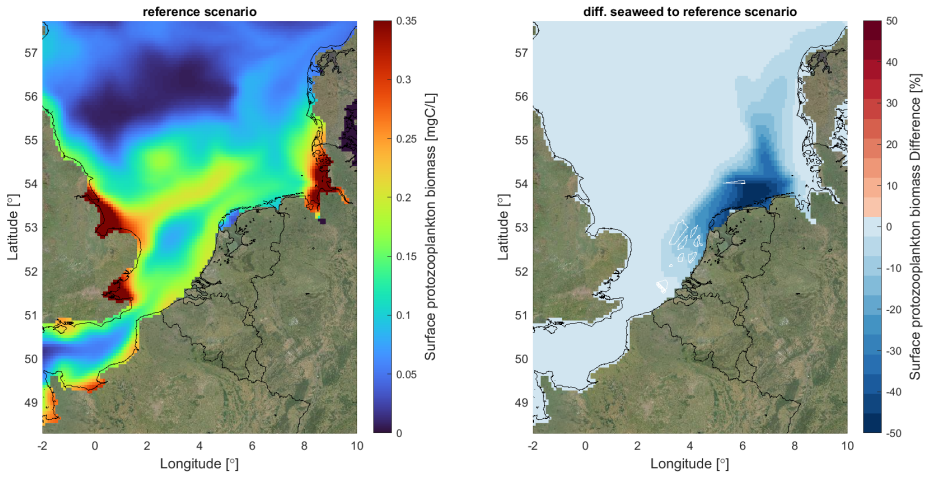

Figure 6.12: Visualization of averaged green algae (a) and protozooplankton (b) biomass for the months June, July and August 2017. The left maps visualizes the absolute values for the reference scenario and the right maps the relative difference between the reference and seaweed scenario. The seaweed scenario results in an average decrease of green algae and protozooplankton by 10 % in the vicinity of the OWFs (right maps).

6.4 Discussion

The objectives of this modelling study were 1) to validate the performance of PROTIST within a 3D model application and 2) to test the impact of seaweed cultivation on the trophic composition of the protist community and the annual primary production. Towards this goal, we implemented PROTIST, a primary production module capable of modelling different protist functional types, in the 3D DCSM-FM model of the North Sea and ran two model scenarios. In the reference scenario, only the growth of the protist community was simulated, while the seaweed scenario additionally simulated the growth of seaweed in the OWFs.

In the first step, we validated the model results by comparing them to in-situ observations. We were able to show that the model captures the important dynamics of the ecosystem such as the timing of the spring bloom as well as the increase and magnitude of dissolved inorganic nutrient concentrations during winter. However, all stations overestimate the chlorophyll-a concentrations in the fall of 2016. In terms of biomass, the modelled phytoplankton and protozooplankton biomass lie within the upper limits of the observation data while the modelled mixoplankton biomass are underestimated.

The model could be further improved by calibrating the mortality and extinction rates of the protist community. Adding an explicit grazer module could also delay the turnover rates and decrease the biomass, however would also add another layer of complexity to the model. Currently the model is run on the coarse grid, but running it on the fine grid would improve the sediment models that in turn could improve the primary production modelling by improving the light regime simulations. It would also be useful to examine the situations in which, e.g., the chlorophyll peaks are too high to see if there are underlying hydrodynamic processes, e.g. micro-stratification, which the deviations can be linked to.

The growth of seaweed cannot be directly compared to in-situ observations in the SNS as there are none available. The timing and decrease of the peak correspond well to observations and data of Broch et al. (2013). However, the start of the growth period is earlier compared to Broch et al. (2013). This discrepancy is most likely related to the fact that Broch et al. (2013) investigated seaweed in Norwegian fjords with colder temperatures compared to the SNS. We conclude that the results of the protist and seaweed growth compare reasonably well to in-situ observations and allow for a comparison between the two scenarios.

In the second step, we assessed the impact of commercial seaweed cultivation on the natural protist community by comparing the two scenarios with each other. In this comparison, we were able to highlight three key points. Firstly, the seaweed scenario displays a relative decrease of dissolved inorganic nitrogen and phosphate concentrations. Secondly, the trophic composition of the protist community

changes in the seaweed scenario with a relative decrease of green algae and protozooplankton biomass and a relative increase in diatom and CM biomass. Thirdly, the annual primary production in two OWFs does not change notably between the reference and the seaweed scenario.

The relative decrease of DIN and DIP in the summer months is a result of the uptake of DIN and DIP through seaweed in the OWFs during the winter months. Seaweed extracts a certain fraction of DIN and DIP during winter from the ambient environment (see figure C.1 in the appendix) and this fraction is not returned to the ambient environment over the course of spring and summer. As the absolute DIN and DIP concentrations decrease in the summer months, the relative difference of DIN and DIP concentrations between the reference and seaweed scenario is most pronounced during the summer months. This absolute and relative decrease of DIN and DIP in the ambient environment in the seaweed scenario is in line with model results by Vilmin and Duren (2021) and Broch et al. (2013).

The decrease in the availability of DIN and DIP results in a shift of the trophic composition of the protist community. On the one hand, there is a relative decrease of green algae and protozooplankton biomass, on the other hand, a relative increase of diatom and CM biomass. The relative increase of CM biomass is notably more pronounced than the relative increase of diatoms. Diatoms and green algae as phytoplankton rely solely on dissolved inorganic nutrients to cover their nutrient needs (Flynn et al., 2019). CM as mixoplankton can cover their nutrient demands through phagotrophy as well as osmotrophy and can thus cope better with the decreased availability of dissolved inorganic nutrients (Stoecker et al., 2017). This response of the CM to decreased inorganic nutrient concentrations is in line with literature references. Multiple studies have shown that feeding can be a mean of obtaining nutrients (see e.g. Smalley et al. (2012) and review by Stoecker et al. (2017)) and a modelling studies showed that mixoplankton occurrence increases when dissolved inorganic nutrients decrease (Leles et al., 2018c; Schneider et al., 2021).

Locally in the areas of the OWFs, the integrated annual planktonic primary production did change notably between the two scenarios. There is a slight increase in planktonic primary production that is a result of the relative increase of CM and diatoms. While calculated primary production of the reference scenario corresponds to literature references (Lancelot and Billen, 1984; Skogen et al., 1995), the calculated primary production of the seaweed scenario differs from model findings of Vilmin and Duren (2021). For both Borssele and Ijmuiden-Ver, Vilmin and Duren (2021) showed a decrease in annual integrated planktonic primary production. It must be noted that the seaweed growth of this study differs from the seaweed growth modelled by Vilmin and Duren (2021). In Vilmin and Duren (2021), the seaweed mass does not decline after May but remains at a constant

levels. Thus, in Vilmin and Duren (2021), the seaweed does not release nutrients into the water as it does not die.
This issue could be resolved by implementing a forcing function that simulates the harvest of seaweed. In seaweed aquaculture, the seaweed is harvested at the peak of their growth during the early summer (Burg et al., 2013) and the biomass and accumulated nutrients within the seaweed are removed from the water column. So, the ambient inorganic nutrient concentration decrease with each subsequent year of seaweed cultivation. However, as seaweed is not harvested in the seaweed scenario, nutrients are released into the ambient environment when the seaweed dies. As this is currently not implemented in this study, the competition between seaweed and the protist community for inorganic nutrients decreases as of June 2017. This is most likely also the reason why the integrated annual planktonic primary production did change notably between the two scenarios.
Even though this study shows a relative increase in CMs, the biomass values of CMs are quite low compared to the biomass values of diatoms. As diatoms also display an increase, a potential co-cultivation of shellfish and seaweed would not be affected by this shift in trophic composition. However, future anthropogenic pressures could have cumulative effects on the trophic composition. Global warming may lead to mixotrophic organisms becoming more heterotrophic (Wilken et al., 2013), increased stratification could lead to a longer period of inorganic nutrient limitation in the upper layers (Falkowski and Oliver, 2007) and multi-use platforms will not only potentially change the local hydrodynamics (Carpenter et al., 2016), they will also introduce consumers into water layers in which they naturally would not be present (Burg et al., 2017).
The model results show that the additional uptake of dissolved inorganic nutrients through seaweed causes a shift in the trophic composition of the protists community towards mixoplankton and diatoms. In the future, anthropogenic pressure will change the abiotic environments of coastal ecosystems which could affect the trophic composition of the protists community. So, it is important to have modelling tools with which the effect of the changes can be explored.

Chapter 7

Discussion

This thesis explored the hypothesis whether the whole protist community, including mixoplankton, needs to be taken into account to understand and predict the effect of anthropogenic pressures on coastal systems such as the Southern North Sea. This hypothesis was subdivided into three subhypotheses which were investigated by combining three different methodologies: time-series analysis, model development and model scenario analysis.
Figure 7.1 visualizes how the different methodologies presented in this thesis build upon and interlink with each other. In chapter 3, a timeseries analysis of routine monitoring data was conducted to determine the trophic composition of protist communities in the Southern North Sea. In chapter 5, a primary production module (PROTIST) was implemented that simulates the growth of a protist community consisting of phytoplankton, mixoplankton and protozooplankton in large ecosystem models. This module was used to examine the environmental factors driving the occurrence of mixoplankton. In chapter 6, two 3D model scenarios of the North Sea were analyzed to research the impact of seaweed cultivation, a likely anthropogenic pressure of the future, on the protist community.
This chapter discusses the results in the context of this thesis' hypothesis. Towards this goal, sections 7.1 to 7.3 place the results into broader scientific context by discussing the trophic composition of protist communities (section 7.1), the environmental drivers of mixoplankton (section 7.2) and the impact of anthropogenic changes on the trophic structure of protist communities (section 7.3). Section 7.4 then focuses on how this thesis advances the field of research. Section 7.5 focuses on the limitations of this thesis, while section 7.6 looks at the possibility of using the index of ecosystem maturity (IEM) as an indicator for mixoplankton. Lastly, section 7.7 presents an outlook and the overall conclusion.

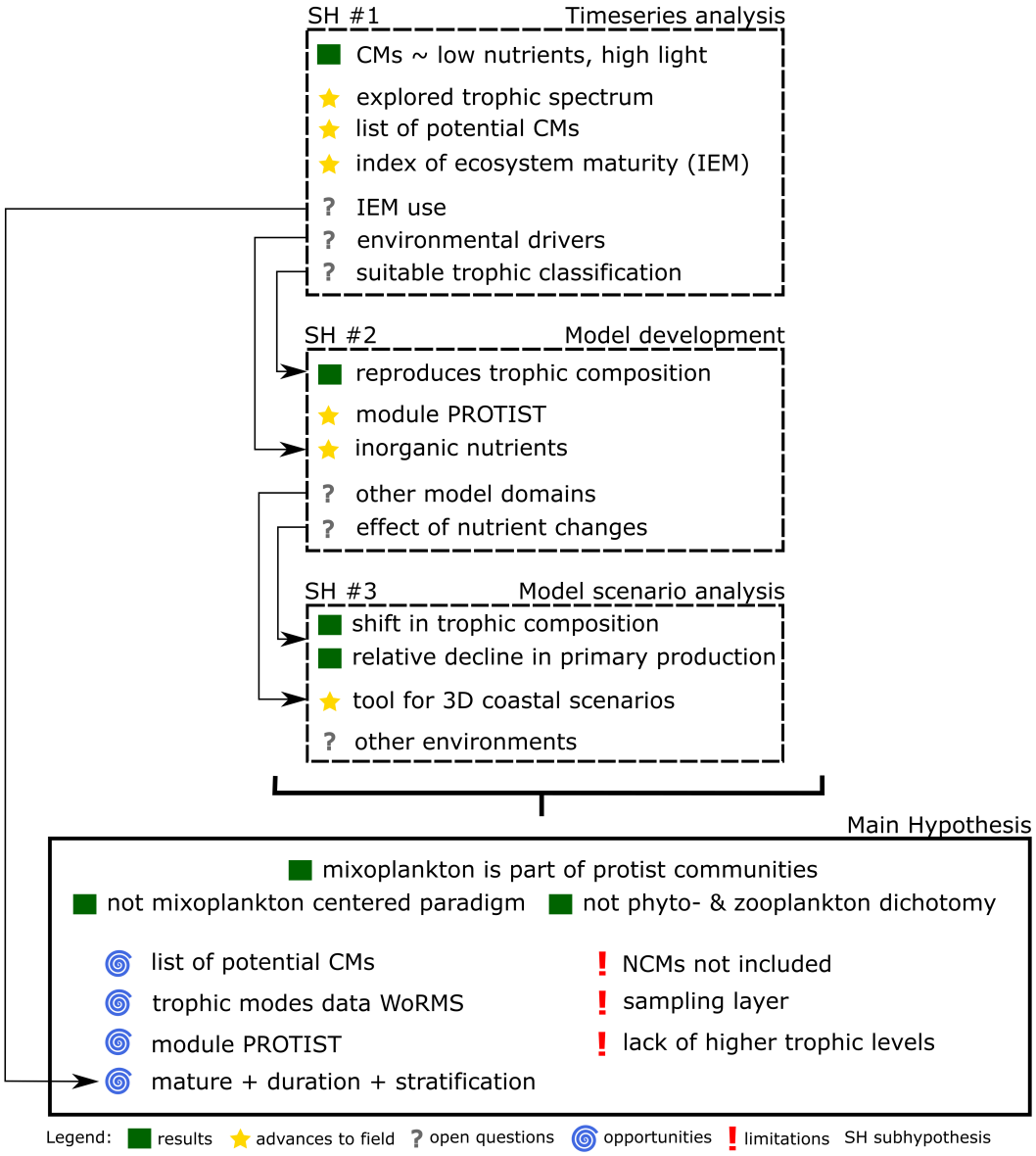

Figure 7.1: Graphical summary of the global discussion. Each dashed black rectangle contains the key results (green square), advances to field (yellow star) and open questions (grey question mark) of each subhypothesis. The arrows visualize how the different subhypotheses interlink with each other. The solid black rectangle summarizes the results of the main hypothesis as well as the opportunities (blue spiral) and limitations (red exclamation mark) of this thesis.

7.1 Trophic composition of protist communities in the Southern North Sea

The analysis of the routine monitoring timeseries (chapter 3) showed that the fraction of mixoplankton to the total sampled plankton community was highest in the offshore environments of the Southern North Sea, whereas the estuary and coastal environments were dominated by phytoplankton. With the routine monitoring data, the two contrasting views on trophic modes of marine protist communities were explored: Classification A in which mixoplankton are an exception (traditional view of the planktonic food web) and classification B in which mixoplankton are the base of most planktonic food webs (mixoplankton-centered paradigm (Mitra et al., 2014a)). The analysis showed that these two contrasting classifications respectively, under- and overestimate the contribution of mixoplankton to the trophic composition of protist communities in the Southern North Sea. The actual trophic composition must lie between these two contrasting views. Using methods from numerical ecology, an environmentally-defined mixoplankton classification (classification C in chapter 3) was calculated that presents a visualization of what the trophic composition might look like.

The column models and the module PROTIST (chapter 5) can be used to investigate which of the trophic classifications explored in chapter 3 develops in a model setting that is not constrained by historical dichotomies. The 11 1D-vertical column models were set up to mimic the 11 specific environmental systems of the Southern North Sea that were determined during the data analysis. The protist functional types were parameterized using literature studies and information from the routine monitoring data. Thus, the column models were designed to simulate the growth of protist communities found in the abiotic conditions of the Southern North Sea. A visual comparison of the model results (see figure 5.12a) with the trophic classification proposed by the mixoplankton paradigm (classification B in chapter 3 - figure 3.7) shows that the trophic composition in the idealized model setting does not mimic classification B. This suggests that the trophic classification proposed by the mixoplankton paradigm (classification B in chapter 3) is unlikely in coastal environments such as the Southern North Sea.

The results of both the data analysis and the column models display a trophic classification of protist communities in which CMs occur mainly in the offshore environments of the Southern North Sea which are inorganic-nutrient limited, clear and stratified. This validates subhypothesis #2 that the module PROTIST is capable of reproducing the trophic composition of protist communities in the Southern North Sea. However, mixoplankton are not ubiquitous in the Southern North Sea which conflicts with subhypothesis #1.

The results of this thesis correspond to other data analyses by Baretta-Bekker

et al. (2009), Stelfox-Widdicombe et al. (2004) and Löder et al. (2012) in which mixoplankton occur in high percentages mainly in offshore environments and not over the whole Southern North Sea. This also corresponds to modelling studies in which mixoplankton are linked to inorganic nutrient-limited environments (Troost et al., 2005; Leles et al., 2018c). Especially clear, i.e. high light availability, and inorganic-nutrient limited environments have been linked to high occurrences of mixoplankton (Hartmann et al., 2012; Duhamel et al., 2019; Edwards, 2019).

7.2 Environmental drivers of mixoplankton

As stated above, this thesis links mixoplankton to inorganic-nutrient depleted, clear environments. While these environmental factors correspond well with other in-situ observations (e.g., Stelfox-Widdicombe et al. (2004), Hartmann et al. (2012) and Duhamel et al. (2019)), it is not possible to derive which environmental factor specifically drives the occurrence of mixoplankton. Using the column models, it was also possible to research that open question: does the inorganic nutrient, the suspended sediment concentration or the combination of both have a larger effect on the occurrence of CMs?
A sensitivity analysis was conducted to explore that question. The sensitivity analysis showed that decreasing the inorganic nutrient concentrations, specifically phosphate and silica, led to an increase in CM biomass. Changing the suspended sediment concentrations had very little effect on the CM biomass. Thus, modeled CMs respond to inorganic nutrient limitations. This corresponds to experimental and model finding by Li et al. (2000b), Smalley et al. (2012) and Leles et al. (2018c).
Based on the column model results, the availability of dissolved inorganic nutrients drives the trophic composition of protist communities. This in turn poses the question of what happens to the trophic composition of protist communities when external pressures change the dissolved inorganic nutrient concentrations in the Southern North Sea.

7.3 Impact of anthropogenic pressures on protist communities

The 3D modelling scenarios (chapter 6) showed that seaweed cultivation leads to a decrease in dissolved inorganic nutrient concentrations. This results in a shift in the trophic composition of the protist community with a relative decrease in green algae and protozooplankton biomass and a relative increase in diatom and CM biomass. This is in line with findings from chapter 5 that inorganic nutrient

limitation favors CM occurrence. However, this shift in trophic composition did not notably change the annual planktonic primary production. Thus, the results of this thesis partly validate subhypothesis #3 as the cultivation of seaweed affects the trophic composition of protist communities, but not the annual planktonic primary production.

The decrease of dissolved inorganic nutrients as a cause of seaweed cultivation is well documented in literature (Fei, 2004; Broch et al., 2013; Duarte et al., 2017; Chung et al., 2017; Zheng et al., 2019). In areas with excess inorganic nutrients such as coastal, eutrophied water or in the vicinity of finfish aquaculture, seaweed aquaculture is a key tool to mitigate negative effects of excess inorganic nutrients. Xiao et al. (2017) projected that by 2026 close to 100 % of the phosphorus runoff from land could be removed from coastal water using seaweed aquaculture. In integrated multi-trophic aquaculture (IMTA), seaweeds recover excess inorganic nutrients released from finfish cultivation, ideally resulting in a closed-loop-system (Buck and Langan, 2017; Kim et al., 2017; Stévant et al., 2017). In offshore areas without external input of inorganic nutrients, extensive seaweed cultivation would consume large quantities of inorganic nutrients, which is most likely not sustainable (Fernand et al., 2017).

The shift in the species composition of the protist community as a result of changing inorganic nutrient concentrations is also well-documented in the literature (e.g. Baretta-Bekker et al. (2009), Beusekom et al. (2009) and Prins et al. (2012)). As shown in chapter 5, CMs apparently can better cope with a decrease in inorganic nutrient availability than phytoplankton. Even though the diatom biomass still exceeded the mixoplankton biomass by far, the shift in trophic composition of the protist community towards a larger proportion of CMs should not be neglected. Especially against the background of global warming, this relative increase of mixoplankton is important. In an experimental study, Peperzak (2003) showed that mixoplankton HAB species (CMs) could increase in the abiotic conditions projected for the Southern North Sea under climate change. Thus, the two factors, decrease of dissolved inorganic nutrients through seaweed aquaculture and global warming, seem to benefit the occurrence of CMs. However, those are not the only factors that will affect the trophic structure of protist communities in the future.

Beardall et al. (2014) illustrated the impact climate change will have on abiotic parameters and marine primary production. Figure 7.2 is a modified version of a Beardall et al. (2014) illustration. Figure 7.2 visualizes how anthropogenic climate change will impact the trophic structure of marine protist communities by changing key abiotic parameters. Temperature, inorganic nutrient concentrations and light are the key abiotic parameters that will impact the trophic composition of marine protist communities.

Elevated CO_2 levels in the atmosphere warm the planet leading to a rise in global

atmospheric and oceanic temperatures (IPCC, 2014). This rise in temperature has direct effects on the physiology of marine protists. The growth rates of phototrophic organisms increase according to the Q_{10} for growth (Eppley, 1972). Species respond differently to temperature changes, which could result in a geographic shift of thermophilic species Beardall et al. (2009a). For the North Sea, Peperzak (2003) showed that higher temperatures could lead to an increase in harmful dinoflagellate blooms some of which are CMs. Increasing temperatures could also favor heterotrophy as temperature exerts a stronger influence on the heterotrophic than the autotrophic metabolism (Rose and Caron, 2007). Wilken et al. (2013) showed that with increasing temperatures, mixoplankton rely more on their heterotrophic metabolism. Thus, increasing temperatures could potentially favor organisms that have heterotrophic pathways.

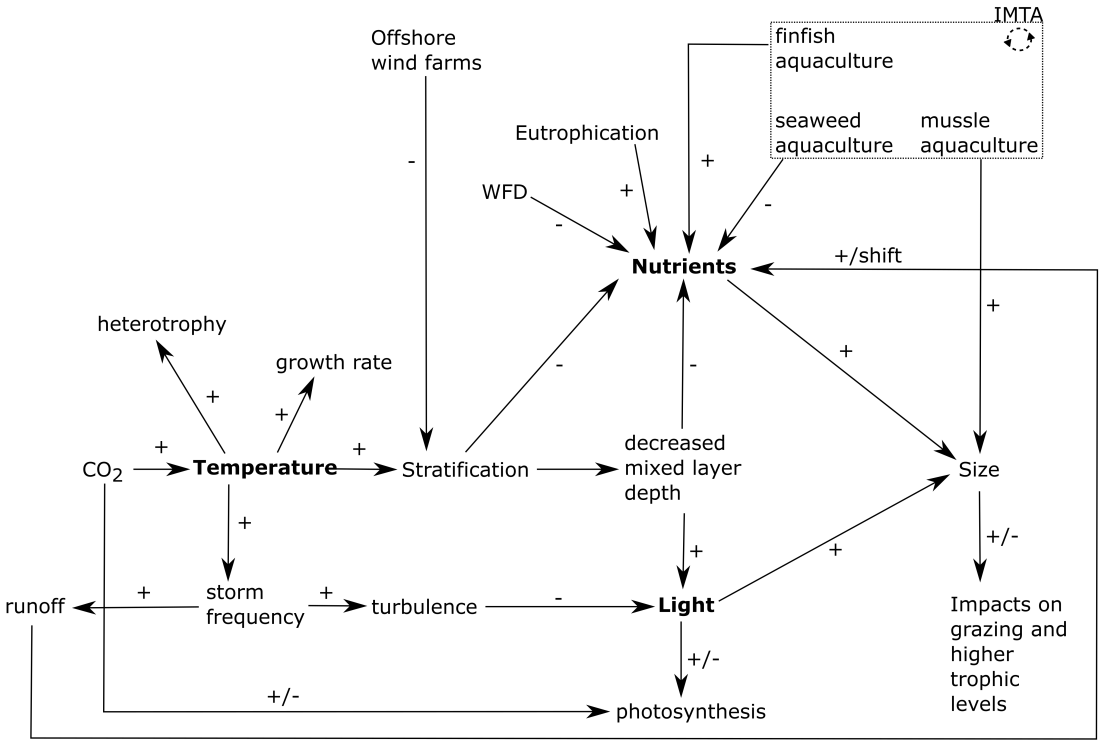

Figure 7.2: Schematic visualizing the effect that anthropogenic climate change could have on key abiotic parameters (bold text) that govern the trophic structure of marine protist communities. Modified from Beardall et al. (2014) under CC BY 4.0.

The rise in temperature also has indirect effects on abiotic factors all of which ultimately affect the inorganic nutrient concentration in marine waters. Seasonal stratification could increase while the mixed layer depth decreases (Polovina et al.,

2008). The construction of offshore wind farms could locally decrease stratification as well, however only when extensive areas are occupied by offshore wind farms (Carpenter et al., 2016). Increased stratification could lead to a decreased input of dissolved inorganic nutrients to the surface layer especially in the sub-tropics (Behrenfeld et al., 2006) . At higher latitudes, increased storm frequency could lead to a higher and/or shifting runoff which in turn could change the inorganic nutrient concentration in coastal systems (Beardall et al., 2014; Tamarin-Brodsky and Kaspi, 2017).

Inorganic nutrient concentrations will be affected by other aspects as well. Eutrophication leads to an increase of inorganic nutrients within coastal areas (Doney et al., 2012). At the same time, to meet targets of, e.g., the Water Framework Directive, land-based measures are being implemented that will decrease nutrient concentrations in coastal water (PBL, 2008). Finfish aquaculture could increase eutrophication, while seaweed/mussel aquaculture uptake dissolved/particulate nutrients from the ambient environment, thus, decreasing the nutrient concentrations (Price et al., 2014). It should be noted that within idealized IMTA settings, finfish, seaweed and mussel aquaculture theoretically form a closed loop in which seaweed and mussels utilize excess nutrients and particulates from finfish cultivation (Price et al., 2014). Thus, different factors of anthropogenic climate change affect the nutrient concentrations, which could lead to nutrient limitations or shifts in nutrient ratios both of which could favor or hamper mixoplankton (Wilken et al., 2019).

Light availability will also be affected. Decreased mixed layer depths will lead to an increase in light availability of marine protist in the surface mixed layer. On the one hand, this could boost photosynthetic rates (possibly leading to more rapid nutrient depletion), while on the other hand, it could lead to an increase of photodamage (Behrenfeld et al., 2016). The photosynthetic rates will be affected by rising CO_2 levels as well, however the direction of the change will differ between species (Beardall et al., 2009b). In coastal areas, increased storm frequency could lead to higher turbulence, decreasing the light availability (Beardall et al., 2014). So, anthropogenic pressures affect light availability, which will impact the trophic structure of the protist community.

This change in light and nutrient availability could also affect the size structure of a protist community. Light and nutrient limitation generally favors smaller protists, while larger protists perform better in high-light, nutrient replete environments (Finkel et al., 2010). This change in size structure influences the trophic composition of protist communities as size affects the predators' capture and handling rates. In conclusion, climate change affects temperature, nutrient concentrations and light availability, the basic abiotic parameters that influence the trophic composition of the marine protist community. As the marine protist community is the base of our marine pelagic ecosystems, it is important that tools assessing the

impact of pressures upon them take the whole protist community into account.

7.4 Advances to the field of research

This thesis presents five aspects that have the potential to advance the fields of research on the trophic structure of protist communities.

1. This thesis established a data-driven baseline for the trophic composition of protist communities in the Southern North Sea which can be used as a reference for future modelling studies or in-situ research.

2. The classification of marine protists into the different protist functional types is by no means at an end. Meticulous experimental work to identify the mixotrophic potential of organisms is needed (Mansour and Anestis, 2021) as well as accessible, machine-readable datasets on the trophic modes of marine protists. This thesis provides

   (a) A list of potentially unrecognized mixoplankton, published in the electronic supplementary information of Schneider et al. (2020b), which could provide a starting point for experimental work.

   (b) The trophic data extracted from the routine monitoring dataset was augmented with data from literature and published as Schneider et al. (2020a) (chapter 4) in the World Register of Marine Species (WoRMS) database. Thus, a dataset on trophic modes of marine protists is now easily accessible in both human and machine-readable format.

3. Chapter 3 introduced the index of ecosystem maturity (IEM), an index that describes the availability of dissolved inorganic nitrogen in an environment. The data analysis showed that high fractions of mixoplankton predominantly occur in environments with high IEM. Thus, the IEM could potentially be used as an indicator for mixoplankton. This idea is further explored in section 7.6.

4. The module PROTIST presented and applied in chapters 5 and 6 advances the field of research by

   (a) providing a module for aquatic ecosystem models that simulates the growth of phytoplankton, mixoplankton and protozooplankton

   (b) providing a tool for water managers to explore the effect of future anthropogenic pressures, such as seaweed cultivation, bioremediation or eutrophication, on protist communities of coastal systems

5. The scenario analyses presented in chapter 6 focused on the potential impact of offshore wind farms/IMTA on the protist community. Up until now, it is one of the few studies to do so (Carpenter et al., 2016).

7.5 Limitations

7.5.1 Focus on CMs

The main limitation of this thesis is the mixoplankton focus on CMs. This focus is a result of the available routine monitoring data and knowledge available from literature. It was not the original focus of the thesis.
The routine monitoring data used in this study provided a huge advantage. The taxa were identified by microscopy and (when possible) identified to their species level (Brochard et al., 2013). If, e.g., only chlorophyll or only certain taxa had been sampled, then the routine monitoring data could not have been used to research the spatial and temporal trophic composition of protist communities. However, the routine monitoring data samples were skewed towards non-fragile, high abundance organisms such as diatoms, cyanobacteria or Noctiluca, which became visible during the data analysis. Fragile organisms such as ciliates were most likely destroyed during sampling, species that occur only sporadically such as Dinophysis were most likely not regularly caught and very small nanoflagellates were not in the filtrate for the microscopy sample. As a consequence, NCMs and many small protozooplankton are not well-represented in the routine monitoring data.
Stelfox-Widdicombe et al. (2004) presented data on NCMs and protozooplankton in the Southern North Sea. Stelfox-Widdicombe et al. (2004) showed that while the nearshore sites were characterized by a community consisting of phytoplankton and large heterotrophic dinoflagellates, the offshore sites were dominated by ciliates, especially NCMs. Löder et al. (2012) presented similar data at Helgoland Roads, North Sea where ciliates and heterotrophic dinoflagellates dominated during the summer. While mixoplanktonic dinoflagellates generally played a secondary role, they were capable of forming an intense bloom during late summer. While those studies do not offer the same spatial and temporal extent as the routine monitoring data, they give an idea of how the results of this thesis would change if data on ciliates and NCMs had been available.
This lack of NCMs in the routine monitoring data also influenced the modeling of NCMs. The module PROTIST contains the processes to simulate the growth and mortality of GNCMs. The growth of GNCMs within a box model (comparable to a batch culture) fits well to expectations as can be seen in appendix B.5 (supplementary material of chapter 5). However, it proved to be too difficult to

parameterize the GNCM for the ecosystem models used in chapters 5 and 6 for two reasons. Firstly, there was not enough data available on the spatial and temporal distribution of GNCMs in the Southern North Sea that could be used to compare the model to observations. Secondly, there still is a lack of knowledge on the physiology of NCMs (Hansen et al., 2019) which made it difficult to separate the GNCM PFT from the other PFTs. Thus, for chapters 5 and 6, it was decided to place a focus on CMs as well.
The module PROTIST is theoretically capable of simulating the growth of pSNCMs. This can be achieved by modifying NCM parameters so that the PFT NCM handles only specific types of prey, uses prey chloroplasts for longer (i.e. slower degradation of captured chloroplasts) and performs photosynthesis more efficiently with the captured chloroplasts. However, the performance of PROTIST with a pSNCM has not been tested within a modelling environment up until now.
The module PROTIST does not simulate the growth of eSNCMs such as green *Noctiluca scintillans*, radiolarians or acantharians. Green *Noctiluca scintillans* do not occur in the North Sea (Harrison et al., 2011). A quick check of the Emodnet biology database showed that acantharians, radiolarians and foraminiferas were neither sampled nor occurred in the North Sea (see EMODnet Biology (2021)). As eSNCMs do not seem to play an active role within the North Sea, the study area of this thesis, the active decision was taken to not include eSNCMs as a PFT in the module PROTIST.

7.5.2 Surface layer

Potential HAB species often aggregate around pycnocline layers (e.g., Olli (1999), Fux et al. (2010), Dundas et al. (2013)). As many HAB species are known to be mixotrophic (Burkholder et al., 2008; Glibert and Burkholder, 2018), the focus on the surface layer could be another limitation of this study. The routine monitoring data was usually sampled at 1 m depth. When (seasonal) stratification was detected, water samples were taken from the bottom and pycnocline as well. The data analysis of chapter 3 focused only on the surface layer. Appendix A.3 shows that the trophic composition of the protist community sampled at the pycnocline and the bottom follow the same pattern as the trophic composition at the water surface. For the data analysis, the chosen focus on the surface layer does not seem to have missed a change in trophic composition in the deeper layers.
The results of the 1D-V column models in chapter 5 were aggregated over the whole vertical model domain. This was done as stratification was only implicitly implemented in the column models via the nutrient and suspended sediment timeseries that were imported into the column models via the boundaries. While the data analysis of chapter 3 did not show a difference in trophic composition between the surface, pycnocline and the bottom, this could not be tested with the column

models.
The 3D model presented in chapter 6 has an accurate representation of the hydrodynamics. So, the 3D model results could be used to analyze the trophic composition of protist communities at the pycnocline. However, only results for the surface layer were extracted for chapter 6. Deeper layers, e.g. the deep chlorophyll maximum, should be extracted and analyzed in a future study.
So while the focus on the surface layer does not seem to have been a limitation for the data analysis, this could not be tested for the modelling results. For future modelling studies, deeper layers should analyzed as well. Especially taking into account the possibility that stronger stratification and nutrient limitations through climate change (Falkowski and Oliver, 2007) could lead to stronger HAB blooms (Hallegraeff, 2010).

7.5.3 Lack of other modules and data

The modelling work of this thesis mainly focused on parameterizing, calibrating and applying the newly developed module PROTIST for the aquatic ecosystem modelling software Delft3D. In the work undertaken in this thesis, PROTIST state variables were linked to abiotic state variables. Further work will include linking PROTIST to grazing by zooplankton and/or shellfish filter feeders.
Thus, it is currently not possible to simulate the grazing of zooplankton and/or shellfish on a protist community that is simulated with the module PROTIST. This lack of higher grazers has two main limitations that must be taken into account. Firstly, zooplankton grazing can exert a high grazing pressure on planktonic protist community in the water column (Mitra et al., 2014b). Secondly, in the shallow nearshore regions shellfish can exert a high grazing pressure on the planktonic protist community (Maar et al., 2007). Furthermore, in OWFs shellfish will be cultivated or grow naturally on the pillars of the wind turbines (Jansen et al., 2016) and exert a grazing pressure on planktonic protists in the water column as well. Both zooplankton and shellfish structure protist communities through their size, prey, and quality preferences.
Seaweed and protists do not exert direct effects on each other via grazing. Seaweed and those protist capable of nutrient uptake compete for the same nutrients pools and thus interact with each other. Thus, the PROTIST state variable and the seaweed state variables did not have to be explicitly linked with each other (as needs to be the case for the above mentioned grazers). Consequently, it was possible for this thesis to simulate the growth of protist community and seaweed simultaneously. However, there is no in-situ data available to compare the growth of modelled seaweed in the Southern North Sea to (Vilmin and Duren, 2021). So, the performance of seaweed could only be qualitatively assessed. As soon as data on the growth of seaweed in the Southern North Sea becomes available, the

modelling of the interaction between seaweed and the protist community can be improved.

7.5.4 1D and 3D model limitations

7.5.4.1 Chosen model parameters

In the column models of chapter 5, the minimum nitrogen:carbon quotas were unintentionally chosen unrealistically high as were the reference growth rates. To judge the effect these parameters could have on the model results, the column models were run again with different parameters. Figure 7.3 shows the column model results for which the minimum nitrogen:carbon quota was set to 0.05 [gN gC^{-1}] for all phototrophic PFTs (default value taken from Flynn (2021)). The minimum nitrogen:carbon quota for the protozooplankton was not changed as the model results showed that the internal nitogen:carbon quota of the protozooplankton did not make use of the complete range offered by the set minimum and maximum nitrogen:carbon parameters. Thus, the internal protozooplankton nitrogen:carbon quota is restricted by processes not by the set parameters. Figure 7.4 shows the column model results in which additionally $UmRT$ was set to 0.69 [d^{-1}] for all PFTs. While there were slight local changes in the timeseries, the relative biomass heatmaps and the target diagrams do not show any obvious differences compared in figures 5.12a and 5.11, respectively. Thus, the change in parameter values had only a small effect on the column model outcomes concerning the relative biomass distribution of the different PFTs and so changing the parameters had no effect on the general conclusions derived from chapter 5.

7.5.4.2 3D model results

However, changing the above mentioned model parameters may have a positive effect on the results of the 3D models of chapter 6. In the current 3D model results especially the ambient nitrate concentrations are too high during the winter months compared to the in-situ data. This could be because the organisms do not take up enough nitrate during the growth period. In the future, it should also be researched whether changed those parameters ($NCmin$ and $UmRT$) would have an effect on the 3D model results displayed in chapter 6.
Generally, the results of the 3D model run should be improved. The ambient nitrate concentrations are too high in winter, the chlorophyll concentrations too high in spring, the phytoplankton biomass too high and the mixoplankton biomass too low over the whole year. This needs to be improved in subsequent model runs by e.g. calibrating model parameters, adding grazer components, implementing a minimum protist biomass seeding threshold or improving the light regime. As the

3D model runs are computationally and time intensive to run, the ideal 3D model result could not be achieved within the time frame of this thesis and is still work in progress.

(a)

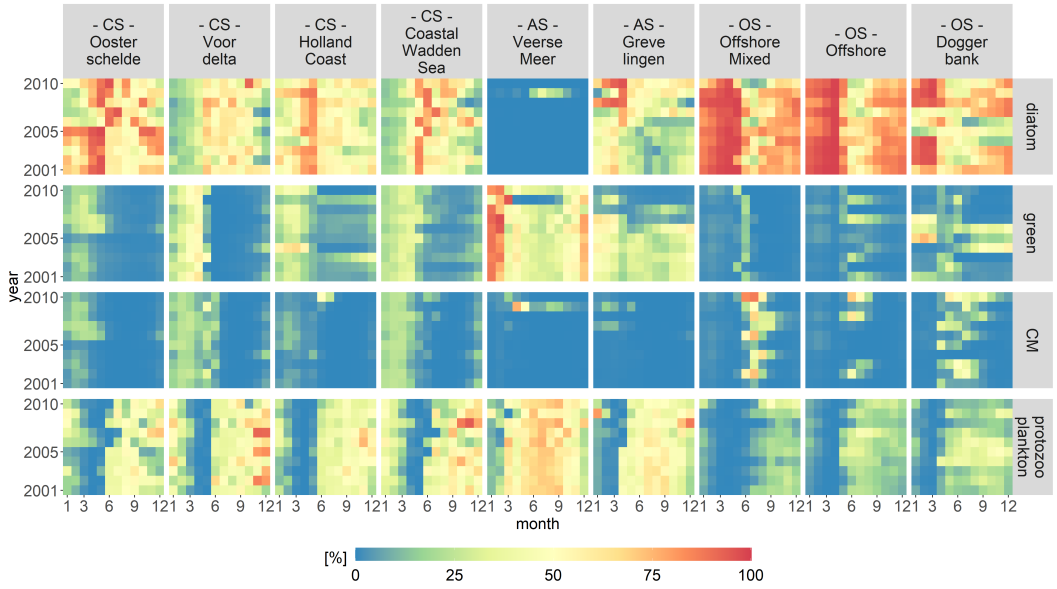

(b)

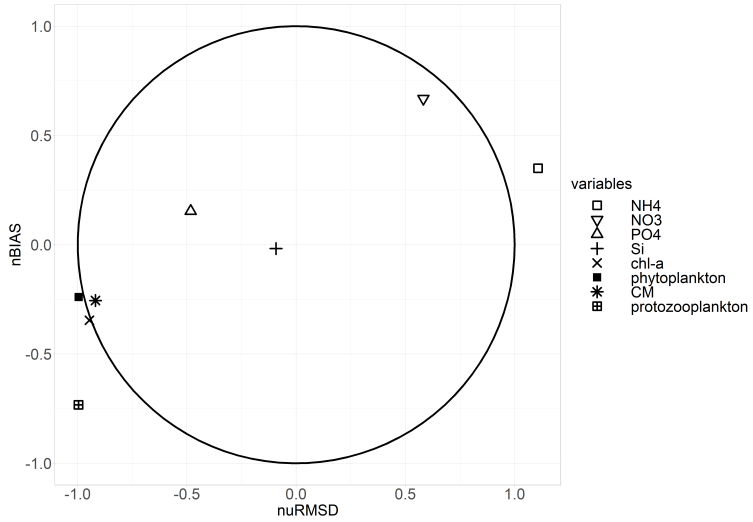

Figure 7.3: a) Trophic heatmaps and b) target diagram using $NCmin$ of 0.05 [gN gC^{-1}] for all PFTs. The changed parameters do not change the overall conclusion of column model results of chapter 5.

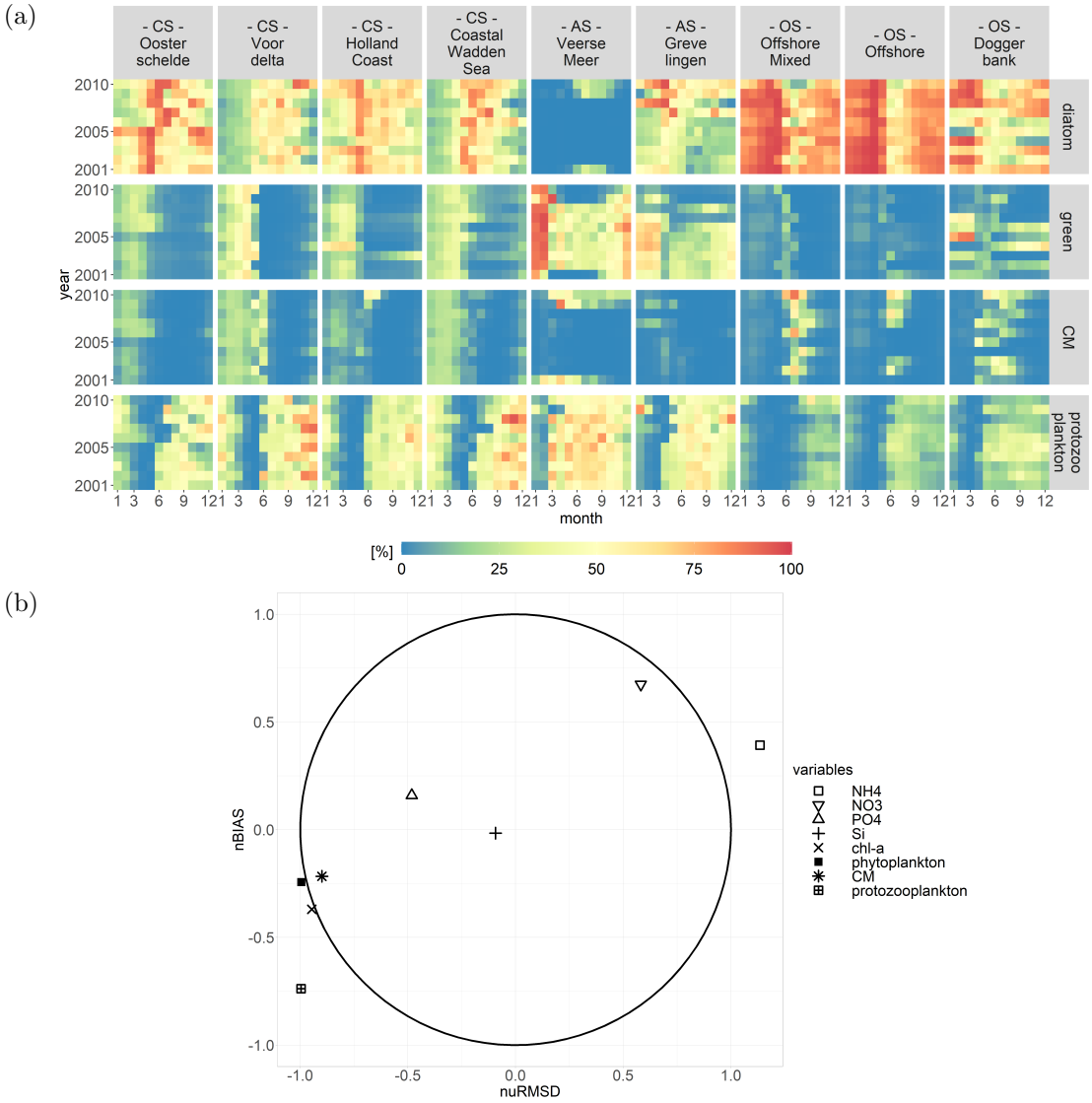

Figure 7.4: a) Trophic heatmaps and b) target diagram using $NCmin$ of 0.05 [gN gC^{-1}] and $UmRT$ of 0.69 [d^{-1}] for all PFTs. The changed parameters do not change the overall conclusion of column model results of chapter 5.

7.6 The IEM - an indicator for mixoplankton?

The IEM presented in chapter 3 could be used as an indicator for environments in which mixoplankton are more likely to occur. Data on NH_4^+, NO_3^- and total nitrogen are needed to calculate the IEM. These parameters are easy to sample and so the IEM is easy to calculate from in-situ data. The IEM returns a value of close to 0 when all the nitrogen is available in its dissolved inorganic form. Such an environment can be described as immature because there is a high potential for opportunistic algal species to grow using the inorganic forms of nitrogen. The IEM returns a value of 1 when all the nitrogen is bound organically. Such an environment can be described as mature because there is no ready-to-use inorganic nitrogen. Primary producer growth must be based on regeneration or consumption of organic nitrogen. The heatmaps presented in chapter 3 visualize that the offshore location classes are mature for longer periods (i.e. have a high IEM value). Those offshore location classes also display high fractions of mixoplankton.
However, the level of maturity alone is not enough to link the IEM to the occurrence of mixoplankton. This is clearly visualized by figure 7.5a that shows that high fractions of mixoplankton cannot be linked to high IEM values alone. Figure 7.5b and 7.5c show that the level of the maturity index along with its duration provide an indicator for the occurrence of mixoplankton. The location classes Grevelingen, Offshore Mixed, Offshore and Doggerbank have high IEM values for the better part of the year with yearly averaged IEM values over 0.75. With the exception of Offshore Mixed, these location classes also have the highest yearly averaged fractions of mixoplankton compared to the other location classes. In contrast to the location classes Grevelingen, Offshore and Doggerbank, the location class Offshore Mixed is not stratified. Thus, the combination of IEM values, IEM duration and stratification could provide an indication for higher fractions of mixoplankton.
Figure 7.6 visualizes the sum of 12 months of averaged IEM values for the whole North Sea. The longer an area is mature, the higher the value. Figure 7.6 displays that there are certain areas in the North Sea, e.g., Doggerbank, that are mature during 6 months of the year, i.e., most of the nitrogen is bound organically. The IEM map along with a map depicting stratified areas in the North Sea could be used to produce static potential habitat maps for mixoplankton. Such static maps could also be useful for coastal managers to gain a first impression of the regions that are likely to produce HABs caused by mixoplankton.

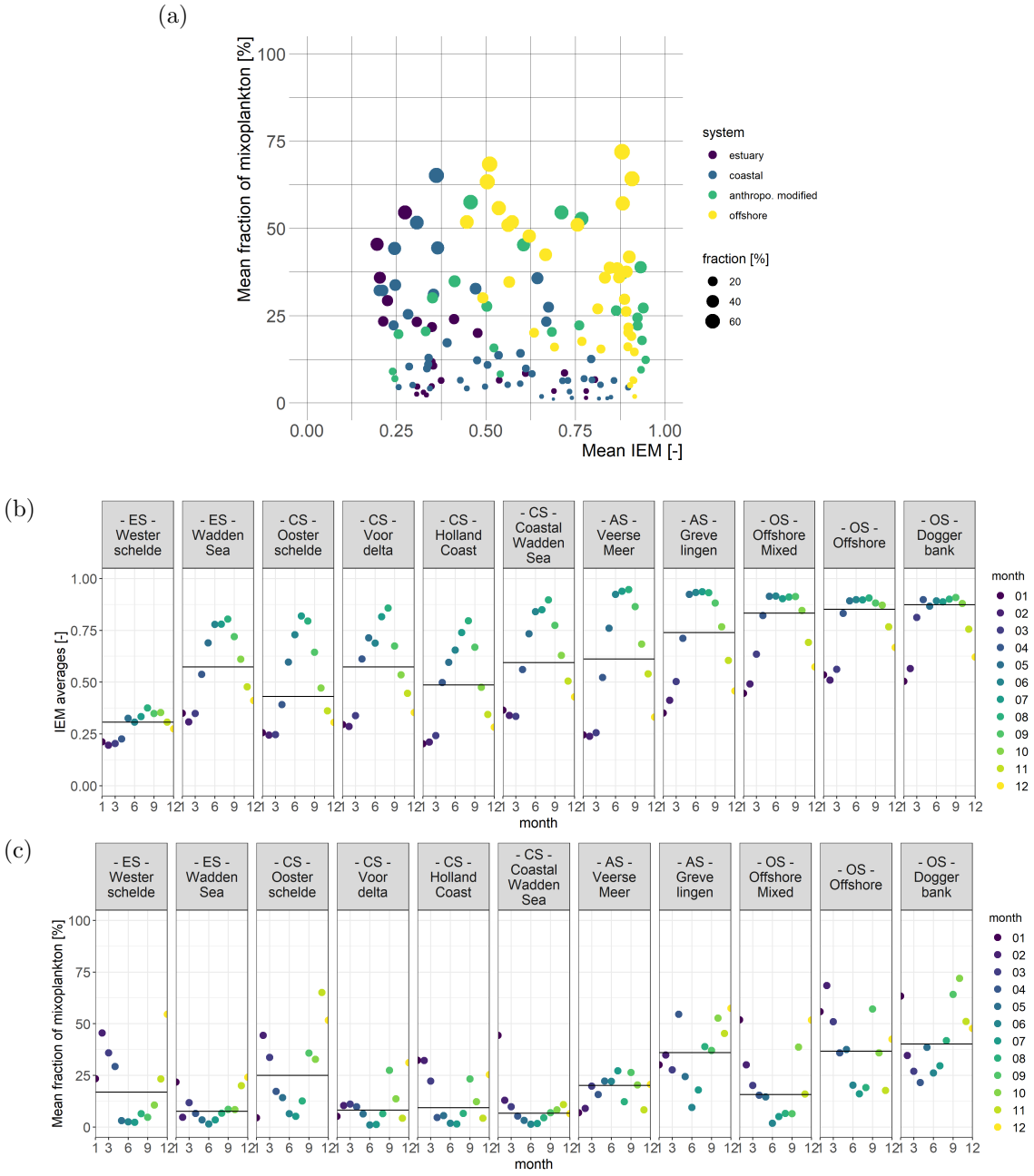

Figure 7.5: a) Distribution of mean mixoplankton fractions along mean values of IEM. Visualization of the mean monthly b) IEM and c) mixoplankton fraction for the 11 location classes. The colors correspond to the different months. The black line depicts the yearly average.

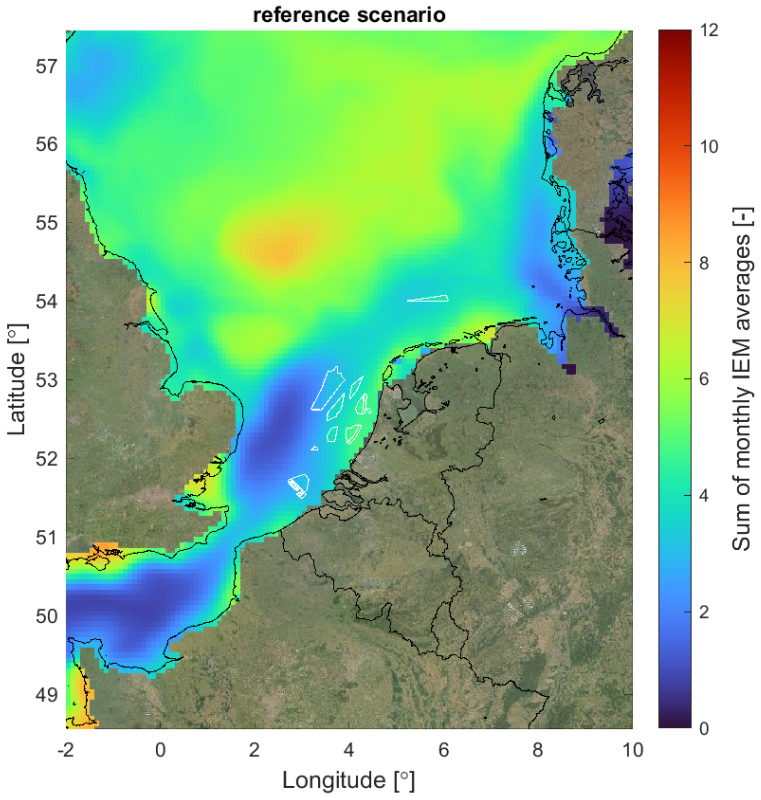

Figure 7.6: Sum of monthly mean IEM values for the North Sea. The colors red/blue respectively highlight regions that are mature/immature the whole year.

7.7 Outlook and conclusions

Anthropogenic pressures will continue to change our coastal ecosystems in the future. The pressures will have complex and non-linear interactions with each other and the biotic environment that will often be difficult to predict. This thesis showed that mixoplankton must be taken into account to understand and predict the effects of anthropogenic pressures on coastal systems. It also showed that protist communities should neither be viewed using the mixoplankton-centered paradigm nor the traditional dichotomy. Mixoplankton are simply and definitely a part of marine protist communities as a functional type with characteristics that are separate from phyto-and protozooplankton. Especially as future anthropogenic pressures will interact and influence each other, it is important to understand the effect those pressures can have on the different functional types present in marine

protist communities.
This thesis hopes to provide a basis for coastal water management on the contribution of mixoplankton to coastal ecosystems and why the knowledge on mixoplankton can be important for coastal zone management. Using this thesis as a starting point, certain tasks can be envisioned for the future.
Data forms the basis for system knowledge. The routine monitoring data used in this thesis already forms a good basis to gain system understanding. However, at the moment, the routine monitoring data is biased towards high-abundance, non-fragile organisms. A high-frequent, high-resolution sampling campaign during the spring and summer months that would provide abiotic and protist data would be highly beneficial for coastal water managers. This proposed sampling campaign would provide information on which taxa are missing from the routine monitoring. Future analysis of the routine monitoring data could take that information into account. Ideally, the proposed sampling campaign would be conducted at regular intervals so that the routine monitoring data can be regularly augmented with high-resolution sampling data.
New system knowledge can be tested and explored with models. The aquatic ecosystem model using PROTIST forms a good basis for future improvements. The extra data from the proposed sampling campaign could be used to parameterize the GNCMs and improve the parameterization of CMs. An aquatic ecosystem model using PROTIST could be improved by linking PROTIST to modules that simulate the growth and mortality of zooplankton and shellfish. Such modules are already available in the Delft3D modelling suite. This would not only provide a better description of the food web, but could also be used to simulate the effect that anthropogenic changes have on higher trophic levels via the protist community. Also the module PROTIST could be validated in different areas. For example, the Swan River in Western Australia is known for its strong Karlodinium blooms (CM) in mid-summer that often result in fish kills (Hallegraeff et al., 2010).
Models and data could also be combined to gain information on certain harmful algal bloom taxa such as *Dinophysis*, a dinoflagellate that causes diarrhetic shellfish poisoning. For example, it could be interesting to research whether model output from PROTIST, e.g. occurrence of CMs - potential prey for pSNCMs such as *Dinophysis*, along with abiotic factors such as stratification could be used to produce risk maps for the occurrence of *Dinophysis* in the North Sea.
Lastly, managing coastal ecosystems in the future will not be an easy task. Limited resources and time will always force coastal water managers to decide what needs to be focused on and what not. This decision should always be an informed one, guided by state-of-the-art knowledge and a sense of proportion. Mixoplankton are an essential part of protist communities and should be seen as such.

Bibliography

Adolf, J. E., D. K. Stoecker and L. W. Harding (2006). 'The balance of autotrophy and heterotrophy during mixotrophic growth of Karlodinium micrum (Dinophyceae)'. In: *Journal of Plankton Research* 28.8, pp. 737–751. ISSN: 01427873. DOI: 10.1093/plankt/fbl007.

Agardy, T. and J. Alder (2005). *Coastal Systems*. Island Press, pp. 559–586. DOI: 10.1017/cbo9781139019507.023.

Andersen, T., A. K. Schartau and E. Paasche (1991). 'Quantifying external and internal nitrogen and phosphorus pools, as well as nitrogen and phosphorus supplied through remineralization, in coastal marine plankton by means of a dilution technique'. In: *Marine Ecology Progress Series* 69.1-2, pp. 67–80. ISSN: 01718630. DOI: 10.3354/meps069067.

Anderson, R., S. Charvet and P. J. Hansen (2018). 'Mixotrophy in Chlorophytes and Haptophytes—Effect of Irradiance, Macronutrient, Micronutrient and Vitamin Limitation'. In: *Frontiers in Microbiology* 9. DOI: 10.3389/fmicb.2018.01704.

Anderson, R., K. Jürgens and P. J. Hansen (2017). 'Mixotrophic phytoflagellate bacterivory field measurements strongly biased by standard approaches: A case study'. In: *Frontiers in Microbiology* 8. ISSN: 1664302X. DOI: 10.3389/fmicb.2017.01398.

Anschütz, A. and K. Flynn (2020). 'Niche separation between different functional types of mixoplankton: results from NPZ-style N-based model simulations.' In: *Marine Biology* 167. DOI: https://doi.org/10.1007/s00227-019-3612-3.

Bakker, C. (1972). 'Milieu en plankton van het Veerse Meer, een tien jaar oud brakwatermeer in Zuidwest-Nederland'. In: *Hydrobiologische Vereniging: Mededelingen van de Hydrobiologische Vereniging* 6.

Baretta-Bekker, J. G., J. W. Baretta, M. J. Latuhihin, X. Desmit and T. C. Prins (2009). 'Description of the long-term (1991-2005) temporal and spatial d1istribution of phytoplankton carbon biomass in the Dutch North Sea'. In: *Journal of Sea Research* 61, pp. 50–59. ISSN: 13851101. DOI: 10.1016/j.seares.2008.10.007.

Bartelings, H., S. van den Burg, R. Jak et al. (2014). *Combining offshore wind energy and large-scale mussel farming: background and technical, ecological and economic considerations*. Tech. rep. August. IMARES Wageningen UR.

Barton, A. D., A. J. Pershing, E. Litchman et al. (2013). 'The biogeography of marine plankton traits'. In: *Ecology Letters* 16, pp. 522–534. ISSN: 1461023X. DOI: 10.1111/ele.12063.

Basu, S. and K. R. Mackey (2018). 'Phytoplankton as key mediators of the biological carbon pump: Their responses to a changing climate'. In: *Sustainability* 10. ISSN: 20711050. DOI: 10.3390/su10030869.

Beardall, J., D. Allen, J. Bragg et al. (2009a). 'Allometry and stoichiometry of unicellular, colonial and multicellular phytoplankton.' In: *The New phytologist* 181, pp. 295–309. ISSN: 1469-8137. DOI: 10.1111/j.1469-8137.2008.02660.x.

Beardall, J., S. Stojkovic and K. Gao (2014). 'Interactive effects of nutrient supply and other environmental factors on the sensitivity of marine primary producers to ultraviolet radiation: Implications for the impacts of global change'. In: *Aquatic Biology* 22, pp. 5–23. ISSN: 18647790. DOI: 10.3354/ab00582.

Beardall, J., S. Stojkovic and S. Larsen (2009b). 'Living in a high CO2 world: Impacts of global climate change on marine phytoplankton'. In: *Plant Ecology and Diversity* 2.2, pp. 191–205. ISSN: 17550874. DOI: 10.1080/17550870903271363.

Beets, D. J. and A. J. van der Spek (2000). 'The Holocene evolution of the barrier and the back-barrier basins of Belgium and the Netherlands as a function of late Weichselian morphology, relative sea-level rise and sediment supply'. In: *Geologie en Mijnbouw/Netherlands Journal of Geosciences* 79, pp. 3–16. ISSN: 00167746. DOI: 10.1017/S0016774600021533.

Behrenfeld, M. J., R. T. O'Malley, E. S. Boss et al. (2016). 'Revaluating ocean warming impacts on global phytoplankton'. In: *Nature Climate Change* 6.3, pp. 323–330. ISSN: 17586798. DOI: 10.1038/nclimate2838.

Behrenfeld, M. J., R. T. O'Malley, D. A. Siegel et al. (2006). 'Climate-driven trends in contemporary ocean productivity'. In: *Nature* 444.7120, pp. 752–755. ISSN: 14764687. DOI: 10.1038/nature05317.

Beisner, B. E., H. P. Grossart and J. M. Gasol (2019). 'A guide to methods for estimating phago-mixotrophy in nanophytoplankton'. In: *Journal of Plankton Research* 41, pp. 77–89. ISSN: 14643774. DOI: 10.1093/plankt/fbz008.

Beninger, P. G. and P. Decottignies (2005). 'What makes diatoms attractive for suspensivores? The organic casing and associated organic molecules of Coscinodiscus perforatus are quality cues for the bivalve Pecten maximus'. In: *Journal of Plankton Research* 27.1, pp. 11–17. ISSN: 01427873. DOI: 10.1093/plankt/fbh156.

Beusekom, J. van and S. Diel-Christiansen (1993). *A synthesis of phyto- and zooplankton dynamics in the North Sea environment*. Tech. rep. WWF - World Wide Fund For Nature.

Beusekom, J. E. E., D. Mengedoht, C. B. Augustin, M. Schilling and M. Boersma (2009). 'Phytoplankton, protozooplankton and nutrient dynamics in the Bornholm Basin (Baltic Sea) in 2002-2003 during the German GLOBEC Project'. In: *International Journal of Earth Sciences* 98.2, pp. 251–260. ISSN: 14373254. DOI: 10.1007/s00531-007-0231-x.

Beusekom, J. E. van and S. Diel-Christiansen (2009). 'Global change and the biogeochemistry of the North Sea: The possible role of phytoplankton and phytoplankton grazing'. In: *International Journal of Earth Sciences* 98, pp. 269–280. ISSN: 14373254. DOI: 10.1007/s00531-007-0233-8.

Bindoff, N., W. Cheung, J. Kairo et al. (2019). 'Changing Ocean, Marine Ecosystems, and Dependent Communities'. In: *IPCC Special Report on the Ocean and Cryosphere in a Changing Climate [H.-O. Pörtner, D.C. Roberts, V. Masson-Delmotte, P. Zhai, M. Tignor, E. Poloczanska, K. Mintenbeck, A. Alegría, M. Nicolai, A. Okem, J. Petzold, B. Rama, N.M. Weyer (eds.)]*., pp. 447–588.

Blauw, A. N., H. F. J. Los, M. Bokhorst and P. L. A. Erftemeijer (2009). 'GEM: A generic ecological model for estuaries and coastal waters'. In: *Hydrobiologia* 618.1, pp. 175–198. ISSN: 00188158. DOI: 10.1007/s10750-008-9575-x.

Bopp, L, C Bowler, L Guidi, E Karsenti and C de Vargas (2015). *The Ocean: a Carbon Pump. See http://www.ocean-climate.org*. Tech. rep. Ocean and Climate Platform.

Bouvier, T., S. Becquevort and C. Lancelot (1997). 'Biomass and feeding activity of phagotrophic mixotrophs in the northwestern Black Sea during the summer 1995'. In: *Hydrobiologia* 363, pp. 289–301. ISSN: 00188158. DOI: 10.1023/A:1003196932229.

Boyer, T. P., J. I. Antonov, O. K. Baranova et al. (2013). *World ccean database 2013*. Tech. rep. NOAA, 209 pp. DOI: 10.7289/V5NZ85MT.

Broch, O. J., I. H. Ellingsen, S. Forbord et al. (2013). 'Modelling the cultivation and bioremediation potential of the kelp Saccharina latissima in close proximity to an exposed salmon farm in Norway'. In: *Aquaculture Environment Interactions* 4.2, pp. 187–206. ISSN: 18697534. DOI: 10.3354/aei00080.

Broch, O. J. and D. Slagstad (2012). 'Modelling seasonal growth and composition of the kelp Saccharina latissima'. In: *Journal of Applied Phycology* 24.4, pp. 759–776. ISSN: 09218971. DOI: 10.1007/s10811-011-9695-y.

Brochard, C., A. van den Oever, R. van Wezel et al. (2013). *Geannoteerde soortenlijst biomonitoring fytoplankton Nederlandse zoete wateren 1990-2012.* Tech. rep. Koeman en Bijkerk bv, Haren.

Brockmann, U., R. Laane and H Postma (1990). 'Cycling of nutrient elements in the North Sea'. In: *Netherlands Journal of Sea Research* 26.2-4.

Brown, M. R., S. W. Jeffrey, J. K. Volkman and G. A. Dunstan (1997). 'Nutritional properties of microalgae for mariculture'. In: *Aquaculture* 151.1-4, pp. 315–331. ISSN: 00448486. DOI: 10.1016/S0044-8486(96)01501-3.

Bruckner, T., I. A. Bashmakov, Y. Mulugetta et al. (2008). 'Energy systems'. In: *Climate Change 2014: Mitigation of Climate Change Contribution from Working Group III to the Fifth Assessment Report of the Intergovernmental Panel on Climate Change*. Cambridge University Press, pp. 5–1–5–30. ISBN: 9781420091878. DOI: 10.2307/j.ctt1hfr0s3.40.

Buck, B. H. and R. Langan (2017). *Aquaculture Perspective of Multi-Use Sites in the Open Ocean*. SpringerOpen. ISBN: 9783319511573. DOI: 10.1007/978-3-319-51159-7.

Burg, S. W. van den, P. Kamermans, M. Blanch et al. (2017). 'Business case for mussel aquaculture in offshore wind farms in the North Sea'. In: *Marine Policy* 85, pp. 1–7. ISSN: 0308597X. DOI: 10.1016/j.marpol.2017.08.007.

Burg, S. van den, M. Stuiver, F. Veenstra et al. (2013). *A Triple P review of the feasibility of sustainable offshore seaweed production in the North Sea*. Tech. rep. Wageningen UR (University and Research centre).

Burkhard, B., S. Opitz, H. Lenhart et al. (2011). 'Ecosystem based modeling and indication of ecological integrity in the German North Sea-case study offshore wind parks'. In: *Ecological Indicators* 11.1, pp. 168–174. ISSN: 1470160X. DOI: 10.1016/j.ecolind.2009.07.004.

Burkholder, J. A. M., P. M. Glibert and H. M. Skelton (2008). 'Mixotrophy, a major mode of nutrition for harmful algal species in eutrophic waters'. In: *Harmful Algae* 8, pp. 77–93. ISSN: 15689883. DOI: 10.1016/j.hal.2008.08.010.

Calbet, A. and M. Alcaraz (2007). 'Microzooplankton, key organisms in the pelagic food web'. In: *Fisheries and Aquaculture*. Ed. by P. Safran. Vol. 5. Encyclopedia of Life Support Systems (EOLSS), pp. 227–242. ISBN: 978-1-84826-562-2.

Calbet, A. and M. R. Landry (2004). 'Phytoplankton growth, microzooplankton grazing, and carbon cycling in marine systems'. In: *Limnology and Oceanography* 49.1, pp. 51–57. ISSN: 00243590. DOI: 10.4319/lo.2004.49.1.0051.

Canfield, D. E. (2005). 'The early history of atmospheric oxygen: Homage to Robert M. Garrels'. In: *Annual Review of Earth and Planetary Sciences* 33, pp. 1–36. ISSN: 00846597. DOI: 10.1146/annurev.earth.33.092203.122711.

Canfield, D. E., A. N. Glazer and P. G. Falkowski (2010). 'The evolution and future of earth's nitrogen cycle'. In: *Science* 330.6001, pp. 192–196. ISSN: 00368075. DOI: 10.1126/science.1186120.

Caron, D. A. (2016). 'Mixotrophy stirs up our understanding of marine food webs'. In: *Proceedings of the National Academy of Sciences* 113, pp. 2806–2808. ISSN: 0027-8424. DOI: 10.1073/pnas.1600718113.

Caron, D. A., A. F. Michaels, N. R. Swanberg and F. A. Howse (1995). 'Primary productivity by symbiont-bearing planktonic sarcodines (Acantharia, Radiolaria, Foraminifera) in surface waters near Bermuda'. In: *Journal of Plankton Research* 17.1, pp. 103–129. ISSN: 01427873. DOI: 10.1093/plankt/17.1.103.

Carpenter, J. R., L. Merckelbach, U. Callies et al. (2016). 'Potential impacts of offshore wind farms on North Sea stratification'. In: *PLoS ONE* 11.8, pp. 1–28. ISSN: 19326203. DOI: 10.1371/journal.pone.0160830.

Cho, B. C., S. C. Na and D. H. Choi (2000). 'Active ingestion of fluorescently labeled bacteria by mesopelagic heterotrophic nanoflagellates in the East Sea, Korea'. In: *Marine Ecology Progress Series* 206, pp. 23–32. ISSN: 01718630. DOI: 10.3354/meps206023.

Chung, I. K., C. F. Sondak and J. Beardall (2017). 'The future of seaweed aquaculture in a rapidly changing world'. In: *European Journal of Phycology* 52.4, pp. 495–505. ISSN: 14694433. DOI: 10.1080/09670262.2017.1359678.

Copernicus Program (2020). *CMEMS. Available at https://resources.marine.copernicus.eu/?option=com_csw&task=results.*

Davey, M., G. A. Tarran, M. M. Mills et al. (2008). 'Nutrient limitation of picophytoplankton photosynthesis and growth in the tropical North Atlantic'. In: *Limnology and Oceanography* 53.5, pp. 1722–1733. ISSN: 00243590. DOI: 10.4319/lo.2008.53.5.1722.

Davidson, K., R. J. Gowen, P. J. Harrison et al. (2014). 'Anthropogenic nutrients and harmful algae in coastal waters'. In: *Journal of Environmental Management* 146, pp. 206–216. ISSN: 00015644. DOI: 10.1016/j.jenvman.2014.07.002.

Decelle, J., I. Probert, L. Bittner et al. (2012). 'An original mode of symbiosis in open ocean plankton'. In: *Proceedings of the National Academy of Sciences of the United States of America* 109.44, pp. 18000–18005. ISSN: 00278424. DOI: 10.1073/pnas.1212303109.

Deltares (2017). *Modelondersteuning MER winning suppletie- en ophoogzand Noordzee 2018 – 2027*. Tech. rep. Deltares.

— (2020). *Delft3D. Available at https://oss.deltares.nl/web/delft3d. Accessed 2020-11-09.*

Delwiche, C. F. (2007). 'The Origin and Evolution of Dinoflagellates'. In: *Evolution of Primary Producers in the Sea*. Elsevier Inc., pp. 191–205. ISBN: 9780123705181. DOI: 10.1016/B978-012370518-1/50011-4.

Domingues, R. B., A. B. Barbosa, U. Sommer and H. M. Galvão (2011). 'Ammonium, nitrate and phytoplankton interactions in a freshwater tidal estuar-

ine zone: Potential effects of cultural eutrophication'. In: *Aquatic Sciences* 73.3, pp. 331–343. ISSN: 10151621. DOI: 10.1007/s00027-011-0180-0.

Doney, S. C., M. Ruckelshaus, J. Emmett Duffy et al. (2012). 'Climate change impacts on marine ecosystems'. In: *Annual Review of Marine Science* 4, pp. 11–37. ISSN: 19411405. DOI: 10.1146/annurev-marine-041911-111611.

Donnelly, C, J. Andersson and B Arheimer (2020). 'Using flow signatures and catchment similarities to evaluate a multi-basin model (E-HYPE) across Europe.' In: *Hydrological Sciences Journal* 61.2. DOI: https://doi.org/10.1080/02626667.2015.1027710.

Droop, M. R. (1974). 'The nutrient status of algal cells in continuous culture'. In: *Journal of the Marine Biological Association of the United Kingdom* 54.4, pp. 825–855. ISSN: 14697769. DOI: 10.1017/S002531540005760X.

Duarte, C. M., J. Wu, X. Xiao, A. Bruhn and D. Krause-Jensen (2017). 'Can seaweed farming play a role in climate change mitigation and adaptation?' In: *Frontiers in Marine Science* 4.APR. ISSN: 22967745. DOI: 10.3389/fmars.2017.00100.

Dugdale, R. C., F. P. Wilkerson, V. E. Hogue and A. Marchi (2007). 'The role of ammonium and nitrate in spring bloom development in San Francisco Bay'. In: *Estuarine, Coastal and Shelf Science* 73.1-2, pp. 17–29. ISSN: 02727714. DOI: 10.1016/j.ecss.2006.12.008.

Duhamel, S., E. Kim, B. Sprung and O. R. Anderson (2019). 'Small pigmented eukaryotes play a major role in carbon cycling in the P-depleted western subtropical North Atlantic, which may be supported by mixotrophy'. In: *Limnology and Oceanography* 64. ISSN: 0024-3590. DOI: 10.1002/lno.11193.

Dundas, I., O. Johannessen, G. Berge and B. Heimdal (2013). 'Toxic Algal Bloom in Scandinavian Waters, May–June 1988'. In: *Oceanography* 2.1, pp. 9–14. ISSN: 10428275. DOI: 10.5670/oceanog.1989.24.

Dyall, S. D., M. T. Brown and P. J. Johnson (2004). 'Ancient Invasions: From Endosymbionts to Organelles'. In: *Science* 304.5668, pp. 253–257. ISSN: 00368075. DOI: 10.1126/science.1094884.

Edwards, K. F. (2019). 'Mixotrophy in nanoflagellates across environmental gradients in the ocean'. In: *Proceedings of the National Academy of Sciences* 116.13, pp. 6211–6220. ISSN: 0027-8424. DOI: 10.1073/pnas.1814860116.

Edwards, K. F., C. A. Klausmeier and E. Litchman (2011). 'Evidence for a three-way trade-off between nitrogen and phosphorus competitive abilities and cell size in phytoplankton'. In: *Ecology* 92.11, pp. 2085–2095. ISSN: 00129658. DOI: 10.1890/11-0395.1.

Elser, J. J., R. W. Sterner, E. Gorokhova et al. (2000). 'Biological stoichiometry from genes to ecosystems'. In: *Ecology Letters* 3.6, pp. 540–550. ISSN: 1461023X. DOI: 10.1046/j.1461-0248.2000.00185.x.

Emeis, K. C., J. van Beusekom, U. Callies et al. (2015). 'The North Sea - A shelf sea in the Anthropocene'. In: *Journal of Marine Systems* 141, pp. 18–33. ISSN: 09247963. DOI: 10.1016/j.jmarsys.2014.03.012.

EMODnet (2020). *EMODnet - European Marine Observation and Data Network. Available at http://www.emodnet-bathymetry.eu.*

EMODnet Biology (2021). *EMODnet Biology map portal. Available via https://www.emodnet-biology.eu/portal/ Accessed 07-09-2021.*

Eppley, R. (1972). 'Temperature and phytoplankton growth in the sea'. In: *Fishery bulletin* 70.4, pp. 1063–85.

Falcón, L. I., S. Magallón and A. Castillo (2010). 'Dating the cyanobacterial ancestor of the chloroplast'. In: *ISME Journal* 4.6, pp. 777–783. ISSN: 17517370. DOI: 10.1038/ismej.2010.2.

Falkowski, P. and A. H. Knoll, eds. (2011). *Evolution of primary producers in the sea.* Academic Press. ISBN: 978-0-12-370518-1.

Falkowski, P. G. (1994). 'The role of phytoplankton photosynthesis in global biogeochemical cycles'. In: *Photosynthesis Research* 39.3, pp. 235–258. ISSN: 01668595. DOI: 10.1007/BF00014586.

Falkowski, P. G., M. E. Katz, A. H. Knoll et al. (2004). 'The evolution of modern eukaryotic phytoplankton'. In: *Science* 305.5682, pp. 354–360. ISSN: 00368075. DOI: 10.1126/science.1095964.

Falkowski, P. G. and M. J. Oliver (2007). 'Mix and match: how climate selects phytoplankton'. In: *Nature Reviews Microbiology* 5, pp. 813–819. DOI: https://doi.org/10.1038/nrmicro1751.

Fasham, M., H. Ducklow and S. McKelvie (1990). 'A nitrogen-based model of plankton dynamics in the oceanic mixed layer'. In: *Journal of Marine Research* 48.

Faure, E., F. Not, A. S. Benoiston et al. (2019). 'Mixotrophic protists display contrasted biogeographies in the global ocean'. In: *ISME Journal* 13, pp. 1072–1083. ISSN: 17517370. DOI: 10.1038/s41396-018-0340-5.

Fei, X. (2004). 'Solving the coastal eutrophication problem by large scale seaweed cultivation'. In: *Hydrobiologia* 512, pp. 145–151. ISSN: 00188158. DOI: 10.1023/B:HYDR.0000020320.68331.ce.

Fernand, F., A. Israel, J. Skjermo et al. (2017). 'Offshore macroalgae biomass for bioenergy production: Environmental aspects, technological achievements and challenges'. In: *Renewable and Sustainable Energy Reviews* 75.January 2016, pp. 35–45. ISSN: 18790690. DOI: 10.1016/j.rser.2016.10.046.

Field, C. B., M. J. Behrenfeld, J. T. Randerson and P. Falkowski (1998). 'Primary production of the biosphere: Integrating terrestrial and oceanic components'. In: *Science* 281.5374, pp. 237–240. ISSN: 00368075. DOI: 10.1126/science.281.5374.237.

Finkel, Z. V. (2007). *Does Phytoplankton Cell Size Matter? The evolution of Modern Marine Food Webs*. Elsevier Inc., pp. 333–350. DOI: 10.1016/B978-0-12-370518-1.50016-3.

Finkel, Z. V., J. Beardall, K. J. Flynn et al. (2010). 'Phytoplankton in a changing world: Cell size and elemental stoichiometry'. In: *Journal of Plankton Research* 32.1, pp. 119–137. ISSN: 01427873. DOI: 10.1093/plankt/fbp098.

Flanders Marine Institute (2019). *Maritime Boundaries Geodatabase: Maritime Boundaries and Exclusive Economic Zones (200NM), version 11. Available online at https://www.marineregions.org/*. DOI: https://doi.org/10.14284/386.

Flynn, K. J. (2001). 'A mechnistic model for describing dynamic multi-nutrient, light, temperature interactions in phytoplankton'. In: *Journal of Plankton Research* 23.9, pp. 977–997. DOI: https://doi.org/10.1093/plankt/23.9.977.

Flynn, K. J. and K. Flynn (1998). 'Release of nitrite by marine dinoflagellates: Development of a mathematical simulation'. In: *Marine Biology* 130.3, pp. 455–470. ISSN: 00253162. DOI: 10.1007/s002270050266.

Flynn, K. J. and P. J. Hansen (2013). 'Cutting the canopy to defeat the "Selfish Gene"; Conflicting selection pressures for the integration of phototrophy in mixotrophic protists'. In: *Protist* 164.6, pp. 1–13. ISSN: 16180941. DOI: 10.1016/j.protis.2013.09.002.

Flynn, K. J. and V. Martin-Jézéquel (2000). 'Modelling Si-N-limited growth of diatoms'. In: *Journal of Plankton Research* 22.3, pp. 447–472. ISSN: 0142-7873. DOI: 10.1093/plankt/22.3.447.

Flynn, K. J. and A. Mitra (2009). 'Building the "perfect beast": modelling mixotrophic plankton'. In: *Journal of Plankton Research* 31, pp. 965–992. ISSN: 0142-7873. DOI: 10.1093/plankt/fbp044.

— (2016). 'Why Plankton Modelers Should Reconsider Using Rectangular Hyperbolic (Michaelis-Menten, Monod) Descriptions of Predator-Prey Interactions'. In: *Frontiers in Marine Science* 3. ISSN: 2296-7745. DOI: 10.3389/fmars.2016.00165.

Flynn, K. J., A. Mitra, P. M. Glibert and J. M. Burkholder (2018). 'Mixotrophy in Harmful Algal Blooms: By Whom, on Whom, When, Why, and What Next'. In: *Global Ecology and Oceanography of Harmful Algal Blooms*. Springer International Publishing AG, pp. 113–132. ISBN: 978-3-319-70068-7 978-3-319-70069-4. DOI: 10.1007/978-3-319-70069-4.

Flynn, K. J., D. K. Stoecker, A. Mitra et al. (2013). 'Misuse of the phytoplankton-zooplankton dichotomy: The need to assign organisms as mixotrophs within plankton functional types'. In: *Journal of Plankton Research* 35, pp. 3–11. ISSN: 01427873. DOI: 10.1093/plankt/fbs062.

Flynn, K. J. (2021). *Enhancing Microalgal Production - constructing decision support tools using system dynamics modelling*. Zenodo. DOI: http://doi.org/10.5281/zenodo.5036605.

Flynn, K. J., A. Mitra, K. Anestis et al. (2019). 'Mixotrophic protists and a new paradigm for marine ecology: where does plankton research go now?' In: *Journal of Plankton Research* 41. DOI: 10.1093/plankt/fbz026.

Foissner, W. and D. L. Hawksworth (2008). *Protist Diversity and Geographical Distribution*. Springer. ISBN: 9789048128006.

Fux, E., S. Gonzalez-Gil, M. Lunven, P. Gentien and P. Hess (2010). 'Production of diarrhetic shellfish poisoning toxins and pectenotoxins at depths within and below the euphotic zone'. In: *Toxicon* 56.8, pp. 1487–1496. ISSN: 0041-0101. DOI: 10.1016/J.TOXICON.2010.09.007.

Geider, J. and T Piatt (1986). 'A mechanistic model of photoadaptation in microalgae'. In: *Marine Ecology Progress Series* 30.Falkowski 1980, pp. 85–92. ISSN: 0171-8630. DOI: 10.3354/meps030085.

Geider, R. J., H. L. MacIntyre and T. M. Kana (1997). 'Dynamic model of phytoplankton growth and acclimation: Responses of the balanced growth rate and the chlorophyll a:carbon ratio to light, nutrient-limitation and temperature'. In: *Marine Ecology Progress Series* 148.1-3, pp. 187–200. ISSN: 01718630. DOI: 10.3354/meps148187.

Geider, R. J. (1993). 'Quantitative phytoplankton physiology: implications for primary production and phytoplankton growth'. In: *ICES Marine Science Symposia* 197, pp. 52–62.

Geider, R. J., H. L. MacIntyre and T. M. Kana (1998). 'A dynamic regulatory model of phytoplanktonic acclimation to light, nutrients, and temperature'. In: *Limnology and Oceanography* 43.4, pp. 679–694. ISSN: 00243590. DOI: 10.4319/lo.1998.43.4.0679.

Geider, R. J. and B. A. Osborne (1989). 'Respiration and microalgal growth: a review of the quantitative relationship between dark respiration and growth'. In: *New Phytologist* 112.3, pp. 327–341. ISSN: 14698137. DOI: 10.1111/j.1469-8137.1989.tb00321.x.

Ghyoot, C., K. J. Flynn, A. Mitra, C. Lancelot and N. Gypens (2017a). 'Modeling Plankton Mixotrophy: A Mechanistic Model Consistent with the Shuter-Type Biochemical Approach'. In: *Frontiers in Ecology and Evolution* 5.August. ISSN: 2296-701X. DOI: 10.3389/fevo.2017.00078.

Ghyoot, C., C. Lancelot, K. J. Flynn, A. Mitra and N. Gypens (2017b). 'Introducing mixotrophy into a biogeochemical model describing an eutrophied coastal ecosystem: The Southern North Sea'. In: *Progress in Oceanography* 157, pp. 1–11. ISSN: 00796611. DOI: 10.1016/j.pocean.2017.08.002.

Glibert, P. M. and J. M. Burkholder (2018). 'Causes of Harmful Algal Blooms'. In: *Harmful algal blooms*. Ed. by S. E. Shumway, J. M. Burkholder and S. L. Morton. John Wiley & Sons Ltd. ISBN: 1042-8275. DOI: 10.1016/0140-6736(93)92085-8.

Glibert, P. M. (2016). 'Margalef revisited: A new phytoplankton mandala incorporating twelve dimensions, including nutritional physiology'. In: *Harmful Algae* 55, pp. 25–30. ISSN: 15689883. DOI: 10.1016/j.hal.2016.01.008.

Goldman, J. C. and P. M. Glibert (1982). 'Comparative rapid ammonium uptake by four species of marine phytoplankton'. In: *Limnology and Oceanography* 27.5, pp. 814–827. ISSN: 19395590. DOI: 10.4319/lo.1982.27.5.0814.

Gray, M. W., G. Burger and B. F. Lang (1999). 'Mitochondrial evolution'. In: *Science* 283.5407, pp. 1476–1481. ISSN: 00368075. DOI: 10.1126/science.283.5407.1476.

Große, F., N. Greenwood, M. Kreus et al. (2016). 'Looking beyond stratification: A model-based analysis of the biological drivers of oxygen deficiency in the North Sea'. In: *Biogeosciences* 13, pp. 2511–2535. ISSN: 17264189. DOI: 10.5194/bg-13-2511-2016.

Grover, J. P. (1991). 'Resource Competition in a Variable Environment: Phytoplankton Growing According to the Variable-Internal-Stores Model'. In: *American Naturalist* 138.4, pp. 811–835. DOI: https://doi.org/10.1086/285254.

Gustafson, D. E., D. K. Stoecker, M. D. Johnson, W. F. Van Heukelem and K. Sneider (2000). 'Cryptophyte algae are robbed of their organelles by the marine ciliate Mesodinium rubrum'. In: *Nature* 405.6790, pp. 1049–1052. ISSN: 00280836. DOI: 10.1038/35016570.

Hallegraeff, G., B. Mooney and K. Evans (2010). *What Triggers Fish-Killing Karlodinium veneficum Dinoflagellate Blooms in the Swan Canning River system?* Tech. rep. Swan Canning Research and Innovation Program.

Hallegraeff, G. M. (2010). 'Ocean climate change, phytoplankton community responses, and harmful algal blooms: A formidable predictive challenge'. In: *Journal of Phycology* 46.2, pp. 220–235. ISSN: 00223646. DOI: 10.1111/j.1529-8817.2010.00815.x.

Hammer, A. C. and J. W. Pitchford (2005). 'The role of mixotrophy in plankton bloom dynamics, and the consequences for productivity'. In: *ICES Journal of Marine Science* 62.5, pp. 833–840. ISSN: 10543139. DOI: 10.1016/j.icesjms.2005.03.001.

Hansen, P. J., R. Anderson, D. K. Stoecker et al. (2019). 'Mixotrophy among freshwater and marine protists'. In: *Encyclopedia of Microbiology*, pp. 199–210. DOI: 10.1016/B978-0-12-809633-8.20685-7.

Hansen, P. J., L. Miranda and R. Azanza (2004). 'Green Noctiluca scintillans: A dinoflagellate with its own greenhouse'. In: *Marine Ecology Progress Series* 275, pp. 79–87. ISSN: 01718630. DOI: 10.3354/meps275079.

Hansson, T. H., H.-P. Grossart, P. A. del Giorgio, N. F. St-Gelais and B. E. Beisner (2019). 'Environmental drivers of mixotrophs in boreal lakes'. In: *Limnology and Oceanography* 64, pp. 1–18. DOI: 10.1002/lno.11144.

Haraguchi, L., H. H. Jakobsen, N. Lundholm and J. Carstensen (2018). 'Phytoplankton Community Dynamic: A Driver for Ciliate Trophic Strategies'. In: *Frontiers in Marine Science* 5. DOI: 10.3389/fmars.2018.00272.

Harrison, P. J., K. Furuya, P. M. Glibert et al. (2011). 'Geographical distribution of red and green Noctiluca scintillans'. In: *Chinese Journal of Oceanology and Limnology* 29, pp. 807–831. ISSN: 02544059. DOI: 10.1007/s00343-011-0510-z.

Hartmann, M., C. Grob, G. A. Tarran et al. (2012). 'Mixotrophic basis of Atlantic oligotrophic ecosystems'. In: *PNAS* 109. DOI: 10.1073/pnas.1118179109/-/DCSupplemental.www.pnas.org/cgi/doi/10.1073/pnas.1118179109.

Hays, G. C., A. J. Richardson and C. Robinson (2005). 'Climate change and marine plankton'. In: *Trends in Ecology and Evolution* 20, pp. 337–344. ISSN: 01695347. DOI: 10.1016/j.tree.2005.03.004. arXiv: arXiv:1011.1669v3.

Heath, M., A. Sabatino, N. Serpetti, C. McCaig and R. O'Hara Murray (2017). 'Modelling the sensitivity of suspended sediment profiles to tidal current and wave conditions'. In: *Ocean and Coastal Management* 147, pp. 49–66. ISSN: 09645691. DOI: 10.1016/j.ocecoaman.2016.10.018.

Heip, C. (1988). 'Biota and abiotic environment in the Westerschelde estuary'. In: *Hydrobiologica Bulletin* 22.1.

HELCOM (2019). *HELCOM phytoplankton biovolumes. Release date: 2019-7-06. URL: http://www.helcom.fi/helcom-at-work/projects/phytoplankton.*

Hinder, S. L., G. C. Hays, M. Edwards et al. (2012). 'Changes in marine dinoflagellate and diatom abundance under climate change'. In: *Nature Climate Change* 2, pp. 271–275. ISSN: 1758678X. DOI: 10.1038/nclimate1388.

Hoeksema, H. (2002). *Grevelingenmeer van kwetsbaar naar weerbaar?* Tech. rep. Rijksinstituut voor Kust en Zee/RIKZ.

Hohmann-Marriott, M. F. and R. E. Blankenship (2011). 'Evolution of photosynthesis'. In: *Annual Review of Plant Biology* 62, pp. 515–548. ISSN: 15435008. DOI: 10.1146/annurev-arplant-042110-103811.

Holland, H. D. (2002). 'Volcanic gases, black smokers, and the great oxidation event'. In: *Geochimica et Cosmochimica Acta* 66.21, pp. 3811–3826. ISSN: 00167037. DOI: 10.1016/S0016-7037(02)00950-X.

Holling, C. (1959). 'Some Characteristics of Simple Types of Predation and Parasitism'. In: *The Canadian Entomologist* 111.7.

IPCC (2014). *Climate Change 2014: Synthesis Report. Contribution of Working Groups I, II and III to the Fifth Assessment Report of the Intergovernmental Panel on Climate Change*. Geneva, Switzerland: [Core Writing Team, R.K. Pachauri and L.A. Meyer (eds.)]. IPCC.

Jansen, H. M., S. Van Den Burg, B. Bolman et al. (2016). 'The feasibility of offshore aquaculture and its potential for multi-use in the North Sea'. In: *Aquaculture International* 24.3, pp. 735–756. ISSN: 1573143X. DOI: 10.1007/s10499-016-9987-y.

Janssen, A. B., G. B. Arhonditsis, A. Beusen et al. (2015). 'Exploring, exploiting and evolving diversity of aquatic ecosystem models: a community perspective'. In: *Aquatic Ecology* 49.4, pp. 513–548. ISSN: 13862588. DOI: 10.1007/s10452-015-9544-1.

Jassby, A. D. and T. Platt (1976). 'Mathematical formulation of the relationship between photosynthesis and light for phytoplankton'. In: *Limnology and Oceanography* 21.4, pp. 540–547. ISSN: 19395590. DOI: 10.4319/lo.1976.21.4.0540.

Jeong, H. J., Y. du Yoo, J. S. Kim et al. (2010). 'Growth, feeding and ecological roles of the mixotrophic and heterotrophic dinoflagellates in marine planktonic food webs'. In: *Ocean Science Journal* 45, pp. 65–91. ISSN: 17385261. DOI: 10.1007/s12601-010-0007-2.

John, U. (2020). *Data of HE513 Pangea. Release date: 2020-7-17. URL: https://doi.pangaea.de/10.1594/PANGAEA.897217*.

Johnson, B. W. and B. A. Wing (2020). 'Limited Archaean continental emergence reflected in an early Archaean 18O-enriched ocean'. In: *Nature Geoscience* 13.3, pp. 243–248. ISSN: 17520908. DOI: 10.1038/s41561-020-0538-9.

Johnson, M. D. (2011). 'The acquisition of phototrophy: adaptive strategies of hosting endosymbionts and organelles'. In: *Photosynthesis Research*.

Joliff, J. K., J. C. Kindle, I. G. Shulman and B. Penta (2009). 'Summary diagrams for coupled hydrodynamic-ecosystem model skill asessment'. In: *Journal of Marine Systems* 98. DOI: https://doi.org/10.1016/j.jmarsys.2008.05.014.

Keeling, P. J. (2010). 'The endosymbiotic origin, diversification and fate of plastids'. In: *Philosophical Transactions of the Royal Society B: Biological Sciences* 365.1541, pp. 729–748. ISSN: 14712970. DOI: 10.1098/rstb.2009.0103.

Kim, J. K., C. Yarish, E. K. Hwang, M. Park and Y. Kim (2017). 'Seaweed aquaculture: Cultivation technologies, challenges and its ecosystem services'. In: *Algae* 32.1, pp. 1–13. ISSN: 20930860. DOI: 10.4490/algae.2017.32.3.3.

Knoll, A. H. and M. A. Nowak (2017). 'The timetable of evolution'. In: *Science Advances* 3.5, pp. 1–14. ISSN: 23752548. DOI: 10.1126/sciadv.1603076.

Kooistra, W. H., R. Gersonde, L. K. Medlin and D. G. Mann (2007). 'The Origin and Evolution of the Diatoms. Their Adaptation to a Planktonic Existence.'

In: *Evolution of Primary Producers in the Sea*. Elsevier Inc., pp. 207–249. ISBN: 9780123705181. DOI: 10.1016/B978-012370518-1/50012-6.

Kwadijk, J., N. W. Arnell, M. Christoph et al. (2016). 'Recent Change - River Flow'. In: *North Sea Region Climate Assessment*. Ed. by M. Quante and F. Colijn. Springer Links. ISBN: 9783319397436. DOI: 10.1007/978-3-319-39745-0.

Lancelot, C., Y. Spitz, N. Gypens et al. (2005). 'Modelling diatom and Phaeocystis blooms and nutrient cycles in the Southern Bight of the North Sea: The MIRO model'. In: *Marine Ecology Progress Series* 289.3, pp. 63–78. ISSN: 01718630. DOI: 10.3354/meps289063.

Lancelot, C. and G. Billen (1984). 'Activity of heterotrophic bacteria and its coupling to primary production during the spring phytoplankton bloom in the southern bight of the North Sea'. In: *Limnology and Oceanography* 29.4, pp. 721–730. ISSN: 19395590. DOI: 10.4319/lo.1984.29.4.0721.

Laval-Peuto, M. and M. Febvre (1986). 'On plastid symbiosis in Tontonia appendiculariformis (Ciliophora, Oligotrichina)'. In: *Biosystems* 19.2.

Lawrence, C. and S. Menden-Deuer (2012). 'Drivers of protistan grazing pressure: Seasonal signals of plankton community composition and environmental conditions'. In: *Marine Ecology Progress Series* 459, pp. 39–52. ISSN: 01718630. DOI: 10.3354/meps09771.

Leles, S. G., A. Mitra, K. J. Flynn et al. (2017). 'Oceanic protists with different forms of acquired phototrophy display contrasting biogeographies and abundance'. In: *Proceedings of The Royal Society B* 284, pp. 1–6. ISSN: 0962-8452. DOI: 10.1098/rspb.2017.0664.

Leles, S. G., G. A. Moser, J. L. Valentin and G. M. Figueiredo (2018a). 'A Lagrangian study of plankton trophodynamics over a diel cycle in a eutrophic estuary under upwelling influence'. In: *Journal of the Marine Biological Association of the United Kingdom* 98.7, pp. 1547–1558. ISSN: 14697769. DOI: 10.1017/S0025315417001333.

Leles, S. G., J. Bruggeman, L. Polimene et al. (2021). 'Differences in physiology explain succession of mixoplankton functional types and affect carbon fluxes in temperate seas'. In: *Progress in Oceanography* 190.August 2020, p. 102481. ISSN: 00796611. DOI: 10.1016/j.pocean.2020.102481.

Leles, S. G., A. Mitra, K. J. Flynn et al. (2018b). 'Sampling bias misrepresents the biogeographical significance of constitutive mixotrophs across global oceans'. In: *Global Ecology and Biogeography* 28.4, pp. 418–428. ISSN: 14668238. DOI: 10.1111/geb.12853.

Leles, S. G., L. Polimene, J. Bruggeman et al. (2018c). 'Modelling mixotrophic functional diversity and implications for ecosystem function'. In: *Journal of*

Plankton Research 40.6, pp. 627–642. ISSN: 14643774. DOI: 10.1093/plankt/fby044.

Leonardos, N. and R. J. Geider (2004). 'Effects of nitrate: Phosphate supply ratio and irradiance on the C:N:P stoichiometry of Chaetoceros muelleri'. In: *European Journal of Phycology* 39.2, pp. 173–180. ISSN: 09670262. DOI: 10.1080/0967026042000201867.

Li, A., D. K. Stoecker and J. E. Adolf (1999). 'Feeding, pigmentation, photosynthesis and growth of the mixotrophic dinoflagelatte Gyrodinium galatheanum'. In: *Aquatic Microbial Ecology* 19, pp. 163–176. DOI: doi:10.3354/ame019163.

Li, A., D. K. Stoecker and D. W. Coats (2000a). 'Mixotrophy in Gyrodinium galatheanum (Dinophyceae): Grazing responses to light intensity and inorganic nutrients'. In: *Journal of Phycology* 36.1, pp. 33–45. ISSN: 00223646. DOI: 10.1046/j.1529-8817.2000.98076.x.

Li, A., D. K. Stoecker and D. W. Coats (2000b). 'Spatial and temporal aspects of Gyrodinium galatheanum in Chesapeake Bay : distribution and mixotrophy'. In: *Journal of Plankton Research* 22.11, pp. 2105–2124. DOI: https://doi.org/10.1093/plankt/22.11.2105.

Liebig, J. (1840). *Die organische Chemie in ihrer Anwendung auf Agricultur und Physiologie.* F. Vieweg und Sohn.

Lin, S., R. W. Litaker and W. G. Sunda (2016). 'Phosphorus physiological ecology and molecular mechanisms in marine phytoplankton'. In: *Journal of Phycology* 52.1, pp. 10–36. ISSN: 15298817. DOI: 10.1111/jpy.12365.

Litchman, E., C. A. Klausmeier, J. R. Miller, O. M. Schofield and P. G. Falkowski (2006). 'Multi-nutrient, multi-group model of present and future oceanic phytoplankton communities'. In: *Biogeosciences* 3.4, pp. 585–606. ISSN: 17264189. DOI: 10.5194/bg-3-585-2006.

Litchman, E. (2007). 'Resource Competition and the Ecological Success of Phytoplankton'. In: *Evolution of Primary Producers in the Sea.* Elsevier Inc., pp. 351–375. DOI: 10.1016/B978-0-12-370518-1.50017-5.

Livanou, E., A. Lagaria, I. Santi et al. (2019). 'Pigmented and heterotrophic nanoflagellates: Abundance and grazing on prokaryotic picoplankton in the ultra-oligotrophic Eastern Mediterranean Sea'. In: *Deep-Sea Research Part II: Topical Studies in Oceanography* 164, pp. 100–111. ISSN: 09670645. DOI: 10.1016/j.dsr2.2019.04.007.

Löder, M. G. J., A. C. Kraberg, N. Aberle, S. Peters and K. H. Wiltshire (2012). 'Dinoflagellates and ciliates at Helgoland Roads, North Sea'. In: *Helgoland Marine Research* 66, pp. 11–23. ISSN: 1438387X. DOI: 10.1007/s10152-010-0242-z.

Los, H. (2009). 'Eco-hydrodynamic modelling of primary production in coastal waters and lakes using BLOMM'. PhD thesis. Wageningen Universiteit.

Maar, M., T. G. Nielsen, K. Bolding, H. Burchard and A. W. Visser (2007). 'Grazing effects of blue mussel Mytilus edulis on the pelagic food web under different turbulence conditions'. In: *Marine Ecology Progress Series* 339, pp. 199–213. ISSN: 01718630. DOI: 10.3354/meps339199.

Mansour, J. S. and K. Anestis (2021). 'Eco-Evolutionary Perspectives on Mixoplankton'. In: *Frontiers in Marine Science* 8.May. DOI: 10.3389/fmars.2021.666160.

Margalef, R. (1963). 'On Certain Unifying Principles in Ecology'. In: *The American Naturalist* 97, pp. 357–374. ISSN: 0003-0147. DOI: 10.1086/282286.

Martin, J. L. (2020). *Belgian coastal zone sampling with RV Simon Stevin.*

Martin-Jézéquel, V., M. Hildebrand and M. A. Brzezinski (2003). 'Silicon metabolism in diatoms: implications for growth'. In: *Journal of Phycology* 36, pp. 821–840. ISSN: 0022-3646. DOI: 10.1046/j.1529-8817.2000.00019.x.

Maselli, M., A. Altenburger, D. K. Stoecker and P. J. Hansen (2020). 'Ecophysiological traits of mixotrophic Strombidium spp'. In: *Journal of Plankton Research* 42.5, pp. 485–496. ISSN: 14643774. DOI: 10.1093/plankt/fbaa041.

Menden-Deuer, S. and E. J. Lessard (2000). 'Carbon to volume relationships for dinoflagellates, diatoms, and other protist plankton'. In: *Limnology and Oceanography* 45.3, pp. 569–579. ISSN: 00243590. DOI: 10.4319/lo.2000.45.3.0569.

MET Norway (2020). *EMEP MSC-W modelled air concentrations and depositions. Available at https://emep.int/mscw/mscw_moddata.html.*

Millette, N. C., J. J. Pierson, A. Aceves and D. K. Stoecker (2017). 'Mixotrophy in Heterocapsa rotundata: A mechanism for dominating the winter phytoplankton'. In: *Limnology and Oceanography* 62, pp. 836–845. ISSN: 19395590. DOI: 10.1002/lno.10470.

Ministry of Infrastructure and the Environment (2014). *North Sea 2050 Spatial Agenda*. Tech. rep. Ministrie van Infrastructuur en Milieu, p. 78.

Mitra, A., K. J. Flynn, J. M. Burkholder et al. (2014a). 'The role of mixotrophic protists in the biological carbon pump'. In: *Biogeosciences* 11, pp. 995–1005. ISSN: 17264170. DOI: 10.5194/bg-11-995-2014. arXiv: 0402594v3 [arXiv:cond-mat].

Mitra, A., K. J. Flynn, U. Tillmann et al. (2016). 'Defining Planktonic Protist Functional Groups on Mechanisms for Energy and Nutrient Acquisition: Incorporation of Diverse Mixotrophic Strategies'. In: *Protist* 167, pp. 106–120. ISSN: 16180941. DOI: 10.1016/j.protis.2016.01.003.

Mitra, A., C. Castellani, W. C. Gentleman et al. (2014b). 'Bridging the gap between marine biogeochemical and fisheries sciences; configuring the zooplankton link'. In: *Progress in Oceanography* 129.PB, pp. 176–199. ISSN: 00796611. DOI: 10.1016/j.pocean.2014.04.025.

Mitra, A. and K. J. Flynn (2005). 'Predator-prey interactions: Is 'ecological stoichiometry' sufficient when good food goes bad?' In: *Journal of Plankton Research* 27.5, pp. 393–399. ISSN: 01427873. DOI: 10.1093/plankt/fbi022.

Moorthi, S. D., R. Ptacnik, R. W. Sanders et al. (2017). 'The functional role of planktonic mixotrophs in altering seston stoichiometry'. In: *Aquatic Microbial Ecology* 79.3, pp. 235–245. ISSN: 09483055. DOI: 10.3354/ame01832.

Moreno, A. R. and A. C. Martiny (2018). 'Ecological Stoichiometry of Ocean Plankton'. In: *Annual Review of Marine Science* 10.1, pp. 43–69. ISSN: 1941-1405. DOI: 10.1146/annurev-marine-121916-063126.

Muis, S., M. Verlaan, H. C. Winsemius, J. C. Aerts and P. J. Ward (2016). 'A global reanalysis of storm surges and extreme sea levels'. In: *Nature Communications* 7.May. ISSN: 20411723. DOI: 10.1038/ncomms11969.

Nielsen, L. T., B. Krock and P. J. Hansen (2012). 'Effects of light and food availability on toxin production, growth and photosynthesis in Dinophysis acuminate'. In: *Marine Ecology Progress Series* 471, pp. 37–50. ISSN: 01718630. DOI: 10.3354/meps10027.

Nielsen, T. G., B. Lokkegaard, K. Richardson, F. B. Pedersen and L. Hansen (1993). 'Structure of plankton communities in the Dogger Bank area (North Sea) during a stratified situation'. In: *Marine Ecology Progress Series* 95, pp. 115–131. ISSN: 01718630. DOI: 10.3354/meps095115.

O'Kelly, C. J. (2007). 'The Origin and Early Evolution of Green Plants'. In: *Evolution of Primary Producers in the Sea*. Elsevier Inc., pp. 287–309. ISBN: 9780123705181. DOI: 10.1016/B978-012370518-1/50014-X.

Olli, K. (1999). 'Diel vertical migration of phytoplankton and heterotrophic flagellates in the Gulf of Riga'. In: *Journal of Marine Systems* 23.1-3, pp. 145–163. ISSN: 0924-7963. DOI: 10.1016/S0924-7963(99)00055-X.

Otto, L., J. T. Zimmerman, G. K. Furnes et al. (1990). 'Review of the physical oceanography of the North Sea'. In: *Netherlands Journal of Sea Research* 26.2-4, p. 161. ISSN: 00777579. DOI: 10.1016/0077-7579(90)90091-T.

Paetsch, J. and H. Lenhart (2004). 'Daily Loads of Nutrients, Total Alkalinity, Dissolved Inorganic Carbon and Dissolved Organic Carbon of the European Continental Rivers'. In: *Berichte aus dem Zentrum für Meeres- und Klimaforschung* 48.

Pahlow, M. and A. Oschlies (2009). 'Chain model of phytoplankton P, N and light colimitation'. In: *Marine Ecology Progress Series* 376.2, pp. 69–83. ISSN: 01718630. DOI: 10.3354/meps07748.

Pahlow, M. and A. E. Prowe (2010). 'Model of optimal current feeding in zooplankton'. In: *Marine Ecology Progress Series* 403, pp. 129–144. ISSN: 01718630. DOI: 10.3354/meps08466.

PBL (2008). *Evaluation of the Water Framework Directive in the Netherlands; costs and benefits. Summary of PBL report 50014001 (in Dutch)*. Tech. rep. Netherlands Environmental Assessment Agency (PBL), pp. 1–40.

Peperzak, L. (2003). 'Climate change and harmful algal blooms in the North Sea'. In: *Acta Oecologica* 24.SUPPL. 1. ISSN: 1146609X. DOI: 10.1016/S1146-609X(03)00009-2.

— (2010). 'An objective procedure to remove observer-bias from phytoplankton time-series'. In: *Journal of Sea Research* 63, pp. 152–156. ISSN: 13851101. DOI: 10.1016/j.seares.2009.11.004.

Pernice, M. C., I. Forn, A. Gomes et al. (2015). 'Global abundance of planktonic heterotrophic protists in the deep ocean'. In: *ISME Journal* 9.3, pp. 782–792. ISSN: 17517370. DOI: 10.1038/ismej.2014.168.

Perry, M. J. (1976). 'Phosphate utilization by an oceanic diatom in phosphorus-limited chemostat culture and in the oligotrophic waters of the central North Pacific'. In: *Limnology and Oceanography* 21.1, pp. 88–107. ISSN: 19395590. DOI: 10.4319/lo.1976.21.1.0088.

Philippart, C. J., J. J. Beukema, G. C. Cadée et al. (2007). 'Impacts of nutrient reduction on coastal communities'. In: *Ecosystems* 10.1, pp. 95–118. ISSN: 14329840. DOI: 10.1007/s10021-006-9006-7.

Pierella Karlusich, J. J., F. M. Ibarbalz and C. Bowler (2020). 'Phytoplankton in the Tara Ocean'. In: *Annual Review of Marine Science* 12, pp. 233–265. ISSN: 19410611. DOI: 10.1146/annurev-marine-010419-010706.

Planktomania (2021). *Available from http://http://planktomania.org/en/ Accessed 2021-06-28*.

Polovina, J. J., E. A. Howell and M. Abecassis (2008). 'Ocean's least productive waters are expanding'. In: *Geophysical Research Letters* 35.3, pp. 2–6. ISSN: 00948276. DOI: 10.1029/2007GL031745.

Price, C., K. D. Black, B. T. Hargrave and J. A. Morris (2014). 'Marine cage culture and the environment: Effects on water quality and primary production'. In: *Aquaculture Environment Interactions* 6.2, pp. 151–174. ISSN: 18697534. DOI: 10.3354/aei00122.

Prins, T. C., X. Desmit and J. G. Baretta-Bekker (2012). 'Phytoplankton composition in Dutch coastal waters responds to changes in riverine nutrient loads'. In: *Journal of Sea Research* 73, pp. 49–62. ISSN: 13851101. DOI: 10.1016/j.seares.2012.06.009.

Rabalais, N. N., R. E. Turner, R. J. Díaz and D. Justić (2009). 'Global change and eutrophication of coastal waters'. In: *ICES Journal of Marine Science* 66.7, pp. 1528–1537. ISSN: 10543139. DOI: 10.1093/icesjms/fsp047.

Reguera, B., L. Velo-Suárez, R. Raine and M. G. Park (2012). 'Harmful Dinophysis species: A review'. In: *Harmful Algae* 14, pp. 87–106. ISSN: 15689883. DOI: 10.1016/j.hal.2011.10.016.

Richardson, A. J. and D. S. Schoeman (2003). 'Climate Impact on Plankton Ecosystems in the Northeast Atlantic'. In: *Science* 305, p. 2. DOI: 10.1126/science.1100958.

RIKZ (2007). *Waterkwaliteit en ecologie Veerse Meer: het tij is gekeerd*. Tech. rep. 008. Rijksinstituut voor Kust en Zee, p. 86.

Roleda, M. Y. and C. L. Hurd (2019). 'Seaweed nutrient physiology: application of concepts to aquaculture and bioremediation'. In: *Phycologia* 58.5, pp. 552–562. ISSN: 23302968. DOI: 10.1080/00318884.2019.1622920.

Rose, J. M. and D. A. Caron (2007). 'Does low temperature constrain the growth rates of heterotrophic protists? Evidence and implications for algal blooms in cold waters'. In: *Limnology and Oceanography* 52.2, pp. 886–895. ISSN: 00243590. DOI: 10.4319/lo.2007.52.2.0886.

Rothschild, B. and T. Osborn (1988). 'Small-scale turbulence and plankton contact rates'. In: *Journal of Plankton Research* 10.3. DOI: https://doi.org/10.1093/plankt/10.3.465.

RWS (2019). *Servicedesk data. Available at www.rws.nl at RWS. Accessed 2019-01-16*.

Safi, K. A. and J. A. Hall (1999). 'Mixotrophic and heterotrophic nanoflagellate grazing in the convergence zone east of New Zealand'. In: *Aquatic Microbial Ecology* 20, pp. 83–93. ISSN: 09483055. DOI: 10.3354/ame020083.

Sanders, R. W. and K. G. Porter (1988). 'Phagotrophic Phytoflagellates'. In: *Advances in Microbial Ecology* 10.

Sanders, R. W., K. G. Porter and D. A. Caron (1990). 'Relationship between phototrophy and phagotrophy in the mixotrophic chrysophyte Poterioochomonas malhamensis'. In: *Microbial Ecology* 19.

Sarthou, G., K. R. Timmermans, S. Blain and P. Treguer (2005). 'Growth physiology and fate of diatoms in the ocean: a review'. In: *Journal of Sea Research* 53.1-2. DOI: https://doi.org/10.1016/j.seares.2004.01.007.

Sato, M., T. Shiozaki and F. Hashihama (2017). 'Distribution of mixotrophic nanoflagellates along the latitudinal transect of the central North Pacific'. In: *Journal of Oceanography* 73, pp. 159–168. ISSN: 1573868X. DOI: 10.1007/s10872-016-0393-x.

Schneider, L. K., K. Anestis, J. Mansour et al. (2020a). 'A dataset on trophic modes of aquatic protists'. In: *Biodiversity Data Journal* 8. DOI: 10.3897/BDJ.8.e56648.

Schneider, L. K., K. Flynn, P. M. Herman, T. A. Troost and W. Stolte (2020b). 'Exploring the trophic spectrum: placing mixoplankton into plankton community

assessments of the Southern North Sea'. In: *Frontiers in Marine Science* 7. DOI: 10.3389/fmars.2020.586915.

Schneider, L. K., N. Gypens, T. A. Troost and W. Stolte (2021). 'Modeling mixoplankton along the biogeochemical gradient of the Southern North Sea'. In: *Ecological Modelling* 459.

Schoener, D. M. and G. B. McManus (2012). 'Plastid retention, use, and replacement in a kleptoplastidic ciliate'. In: *Aquatic Microbial Ecology* 67.3, pp. 177–187. ISSN: 09483055. DOI: 10.3354/ame01601.

Schoener, D. M. and G. B. McManus (2017). 'Growth, grazing, and inorganic C and N uptake in a mixotrophic and a heterotrophic ciliate'. In: *Journal of Plankton Research* 39.3, pp. 379–391. ISSN: 14643774. DOI: 10.1093/plankt/fbx014.

Schueder, R. and L. Van Duren (2019). *First version of IMTA model focused on the North Sea. EU H2020 IMPAQT Deliverable 3.2. Available at https://impaqtproject.eu/knowledge-center/*. Tech. rep. Delft, Deltares, p. 91.

Schuetzenmeister, A. and F. Dufey (2019). *VCA: Variance Component Analysis. R package version 1.4.2. https://CRAN.R-project.org/package=VCA*.

Schuwirth, N., F. Borgwardt, S. Domisch et al. (2019). 'How to make ecological models useful for environmental management'. In: *Ecological Modelling* 411.August, p. 108784. ISSN: 03043800. DOI: 10.1016/j.ecolmodel.2019.108784.

Sellner, K. G. (1997). 'Physiology, ecology, and toxic properties of marine cyanobacteria blooms'. In: *Limnology and Oceanography* 42.5 II, pp. 1089–1104. ISSN: 00243590. DOI: 10.4319/lo.1997.42.5_part_2.1089.

Selosse, M. A., M. Charpin and F. Not (2017). 'Mixotrophy everywhere on land and in water: the grand écart hypothesis'. In: *Ecology Letters* 20, pp. 246–263. ISSN: 14610248. DOI: 10.1111/ele.12714.

Šimek, K., V. Grujčić, J. Nedoma et al. (2019). 'Microbial food webs in hypertrophic fishponds: Omnivorous ciliate taxa are major protistan bacterivores'. In: *Limnology and Oceanography* 64.5, pp. 2295–2309. ISSN: 19395590. DOI: 10.1002/lno.11260.

Simpson, J. H., W. G. Bos, F. Schirmer et al. (1993). 'Periodic stratification in the Rhine ROFI in the North Sea'. In: *Oceanologica Acta* 16, pp. 23–32. ISSN: 03991784.

Skogen, M. D., E. Svendsen, J. Berntsen, D. Aksnes and K. B. Ulvestad (1995). 'Modelling the Primary Production in the North Sea using a Coupled Three-dimensional Physical-Chemical-Biological Ocean Model'. In: *Estuarine, Coastal and Shelf Science* 41. DOI: https://doi.org/10.1016/0272-7714(95)90026-8.

Skovgaard, A. (1996). 'Mixotrophy in Fragilidium subglobosum (Dinophyceae): Growth and grazing responses as functions of light intensity'. In: *Marine Eco-*

logy Progress Series 143.1-3, pp. 247–253. ISSN: 01718630. DOI: 10.3354/meps143247.

Smalley, G. W., D. Wayne Coats and D. K. Stoecker (2012). 'Influence of inorganic nutrients, irradiance, and time of day on food uptake by the mixotrophic dinoflagellate Neoceratium furca'. In: *Aquatic Microbial Ecology* 68.1, pp. 29–41. ISSN: 09483055. DOI: 10.3354/ame01599.

Smayda, T. J. (1997). 'What is a bloom? A commentary'. In: *Limnology and Oceanography* 42.5 II, pp. 1132–1136. ISSN: 00243590. DOI: 10.4319/lo.1997.42.5_part_2.1132.

Smith, E. L. (1936). 'Photosynthesis in Relation to Light and Carbon Dioxide'. In: *Proceedings of the National Academy of Sciences* 22.8, pp. 504–511. ISSN: 0027-8424. DOI: 10.1073/pnas.22.8.504.

Soetaert, K. and P. M. J. Herman (2009). *A Practical Guide to Ecological Modelling: Using R as a Simluation Platform*, p. 364. ISBN: 9781402086236.

Soetaert, K. and P. M. Herman (1995). 'Carbon flows in the Westerschelde estuary (The Netherlands) evaluated by means of an ecosystem model (MOSES)'. In: *Hydrobiologia* 311.1-3, pp. 247–266. ISSN: 00188158. DOI: 10.1007/BF00008584.

Stelfox-Widdicombe, C. E., S. D. Archer, P. H. Burkill and J. Stefels (2004). 'Microzooplankton grazing in Phaeocystis and diatom-dominated waters in the southern North Sea in spring'. In: *Journal of Sea Research* 51.1, pp. 37–51. ISSN: 13851101. DOI: 10.1016/j.seares.2003.04.004.

Stévant, P., C. Rebours and A. Chapman (2017). 'Seaweed aquaculture in Norway: recent industrial developments and future perspectives'. In: *Aquaculture International* 25.4, pp. 1373–1390. ISSN: 1573143X. DOI: 10.1007/s10499-017-0120-7.

Stevens, J. O., F. G. Blanchet, M. Friendly et al. (2019). *vegan: Community Ecology Package. R package version 2.5-5. https://CRAN.R-project.org/package=vegan.*

Stickney, H. L., R. R. Hood and D. K. Stoecker (2000). 'The impact of mixotrophy on planktonic marine ecosystems'. In: *Ecological Modelling* 125.2-3, pp. 203–230. ISSN: 03043800. DOI: 10.1016/S0304-3800(99)00181-7.

Stoecker, D. K., P. J. Hansen, D. A. Caron and A. Mitra (2017). 'Mixotrophy in the Marine Plankton'. In: *Annual Review of Marine Science* 9, pp. 311–335. ISSN: 1941-1405. DOI: 10.1146/annurev-marine-010816-060617.

Stoecker, D. K., M. W. Silver, A. E. Michaels and L. H. Davis (1988). 'Obligate mixotrophy in Laboea strobila, a ciliate which retains chloroplasts'. In: *Marine Biology* 99.3, pp. 415–423. ISSN: 00253162. DOI: 10.1007/BF02112135.

Stoecker, D. K., A. Taniguchi and A. Michaels (1989). 'Abundance of autotrophic, mixotrophic and heterotrophic planktonic ciliates in shelf and slope waters'.

In: *Marine Ecology Progress Series* 50, pp. 241–254. ISSN: 0171-8630. DOI: 10.3354/meps050241.

Stoecker, D. K. (1998). 'Conceptual models of mixotrophy in planktonic protists and some ecological and evolutionary implications'. In: *European Journal of Protistology* 34.3, pp. 281–290. ISSN: 09324739. DOI: 10.1016/S0932-4739(98)80055-2.

Stoecker, D. K., M. D. Johnson, C. De Vargas and F. Not (2009). 'Acquired phototrophy in aquatic protists'. In: *Aquatic Microbial Ecology* 57.3, pp. 279–310. ISSN: 09483055. DOI: 10.3354/ame01340.

Stoecker, D. K. and P. J. Lavrentyev (2018). 'Mixotrophic Plankton in the Polar Seas: A Pan-Arctic Review'. In: *Frontiers in Marine Science* 5. ISSN: 2296-7745. DOI: 10.3389/fmars.2018.00292.

Stolte, W. and R. Riegman (1995). 'Effect of phytoplankton cell size on transient-state nitrate and ammonium uptake kinetics'. In: *Microbiology* 141.5, pp. 1221–1229. ISSN: 13500872. DOI: 10.1099/13500872-141-5-1221.

Sukenik, A., J. Bennett and P. G. Falkowski (1987). 'Light-saturated photosynthesis - limitation by electron transport or carbon fixation?' In: *Biochimica et Biophysica Acta* 891. DOI: https://doi.org/10.1016/0005-2728(87)90216-7.

Tamarin-Brodsky, T. and Y. Kaspi (2017). 'Enhanced poleward propagation of storms under climate change'. In: *Nature Geoscience* 10.12, pp. 908–913. ISSN: 17520908. DOI: 10.1038/s41561-017-0001-8.

Thingstad, T. F., H. Havskum, K. Garde and B. Riemann (1996). 'On the Strategy of "Eating Your Competitor": A Mathematical Analysis of Algal Mixotrophy'. In: *Ecology* 77.7. ISSN: 00129658. DOI: 10.2307/2265705.

Thornton, D. C. (2014). 'Dissolved organic matter (DOM) release by phytoplankton in the contemporary and future ocean'. In: *European Journal of Phycology* 49.1, pp. 20–46. ISSN: 14694433. DOI: 10.1080/09670262.2013.875596.

Tréguer, P. J. and C. L. De La Rocha (2013). 'The world ocean silica cycle'. In: *Annual Review of Marine Science* 5, pp. 477–501. ISSN: 19411405. DOI: 10.1146/annurev-marine-121211-172346.

Troost, T. A., B. W. Kooi and S. A. L. M. Kooijman (2005). 'Ecological Specialization of Mixotrophic Plankton in a Mixed Water Column'. In: *The American Naturalist* 166, pp. 45–61. ISSN: 0003-0147. DOI: 10.1086/432038.

UNEP (2006). *Marine and coastal ecosystems and human well-being: A synthesis report based on the findings of the Millennium Ecosystem Assessment*. Tech. rep. UNEP, p. 76. DOI: 10.1196/annals.1439.003.

Unrein, F., R. Massana, L. Alonso-Sáez and J. M. Gasol (2007). 'Significant year-round effect of small mixotrophic flagellates on bacterioplankton in an oligo-

trophic coastal system'. In: *Limnology and Oceanography* 52, pp. 456–469. DOI: https://doi.org/10.4319/lo.2007.52.1.0456.

Vallina, S. M. and R. Simó (2007). 'Strong relationship between DMS and the solar radiation dose over the global surface ocean'. In: *Science* 315.5811, pp. 506–508. ISSN: 00368075. DOI: 10.1126/science.1133680.

Vandepitte, L., B. Vanhoorne, W. Decock et al. (2015). 'How aphia-the platform behind several online and taxonomically oriented databases-can serve both the taxonomic community and the field of biodiversity informatics'. In: *Journal of Marine Science and Engineering* 3.4, pp. 1448–1473. ISSN: 20771312. DOI: 10.3390/jmse3041448.

Van't Hoff, J. H. (1884). *Etudes de dynamique chimique*. Amsterdam: Muller.

Vargas, C. de, M. P. Aubry, I. Probert and J. Young (2007). *Chapter 12 - Origin and Evolution of Coccolithophores. From Coastal Hunters to Oceanic Farmers*. Elsevier Inc., pp. 251–285. ISBN: 9780123705181. DOI: 10.1016/B978-012370518-1/50013-8.

Vilmin, L. and L. van Duren (2021). *Modelling seaweed cultivation on the Dutch continental shelf. Available at https://www.deltares.nl/en/publications/*. Tech. rep. Deltares.

Ward, B. A. and M. J. Follows (2016). 'Marine mixotrophy increases trophic transfer efficiency, mean organism size, and vertical carbon flux'. In: *Proceedings of the National Academy of Sciences* 113.11, pp. 2958–2963. ISSN: 0027-8424. DOI: 10.1073/pnas.1517118113.

Waterbase Deltares (2019). *Waterbase. Available from http://opendap.deltares.nl at Deltares. Accessed 2020-02-28.*

Wickham, H. (2014). 'Tidy Data'. In: *Journal of Statistical Software* 59.10. DOI: 10.18637/jss.v059.i10.

Wijnhoven, S., V. Escaravage, E. Daemen and H. Hummel (2010). 'The Decline and Restoration of a Coastal Lagoon (Lake Veere) in the Dutch Delta'. In: *Estuaries and Coasts* 33.6, pp. 1261–1278. ISSN: 15592723. DOI: 10.1007/s12237-009-9233-1.

Wilken, S., J. Huisman, S. Naus-Wiezer and E. Van Donk (2013). 'Mixotrophic organisms become more heterotrophic with rising temperature'. In: *Ecology Letters* 16.2, pp. 225–233. ISSN: 1461023X. DOI: 10.1111/ele.12033.

Wilken, S., C. C. Yung, M. Hamilton et al. (2019). 'The need to account for cell biology in characterizing predatory mixotrophs in aquatic environments'. In: *Philosophical Transactions of the Royal Society B: Biological Sciences* 374.1786. ISSN: 14712970. DOI: 10.1098/rstb.2019.0090.

Wind Europe (2021). *Wind Europe. Available from https://windeurope.org/about-wind/reports/our-energy-our-future/. Accessed 2021-06-29.*

Wirtz, K. W. and M. Pahlow (2010). 'Dynamic chlorophyll and nitrogen: Carbon regulation in algae optimizes instantaneous growth rate'. In: *Marine Ecology Progress Series* 402, pp. 81–96. ISSN: 01718630. DOI: 10.3354/meps08333.

Worden, A. Z., M. J. Follows, S. J. Giovannoni et al. (2015). 'Rethinking the marine carbon cycle: Factoring in the multifarious lifestyles of microbes'. In: *Science* 347. ISSN: 10959203. DOI: 10.1126/science.1257594.

WoRMS Editorial Board (2020). *World Register of Marine Species. Available from http://www.marinespecies.org at VLIZ. Accessed 2020-02-28. doi:10.14284/170.*

Xiao, X., S. Agusti, F. Lin et al. (2017). 'Nutrient removal from Chinese coastal waters by large-scale seaweed aquaculture'. In: *Scientific Reports* 7.April, pp. 1–6. ISSN: 20452322. DOI: 10.1038/srep46613.

Yoshiyama, K. and C. A. Klausmeier (2008). 'Optimal cell size for resource uptake in fluids: A new facet of resource competition'. In: *American Naturalist* 171.1, pp. 59–70. ISSN: 00030147. DOI: 10.1086/523950.

Zehr, J. P. and R. M. Kudela (2011). 'Nitrogen cycle of the open ocean: From genes to ecosystems'. In: *Annual Review of Marine Science* 3, pp. 197–225. ISSN: 19411405. DOI: 10.1146/annurev-marine-120709-142819.

Zheng, Y., R. Jin, X. Zhang, Q. Wang and J. Wu (2019). 'The considerable environmental benefits of seaweed aquaculture in China'. In: *Stochastic Environmental Research and Risk Assessment* 33.4-6, pp. 1203–1221. ISSN: 14363259. DOI: 10.1007/s00477-019-01685-z.

Zijl, F., J. Veenstra and J. Groenenboom (2018). 'The 3D Dutch Continental Shelf Model - Flexible Mesh (3D DCSM-FM). Available at https://www.deltares.nl/app/uploads/2020/12/Development-of-a-3D-model-for-the-NW-European-Shelf-3D-DCSM-FM.pdf'. In: *Deltares rapport 1220339-000*, p. 41.

Zimorski, V., C. Ku, W. F. Martin and S. B. Gould (2014). 'Endosymbiotic theory for organelle origins'. In: *Current Opinion in Microbiology* 22, pp. 38–48. ISSN: 18790364. DOI: 10.1016/j.mib.2014.09.008.

Appendix A

Supplementary information for data analysis on trophic spectrum of marine protist communities (Chapter 3)

A.1 Supplementary figure

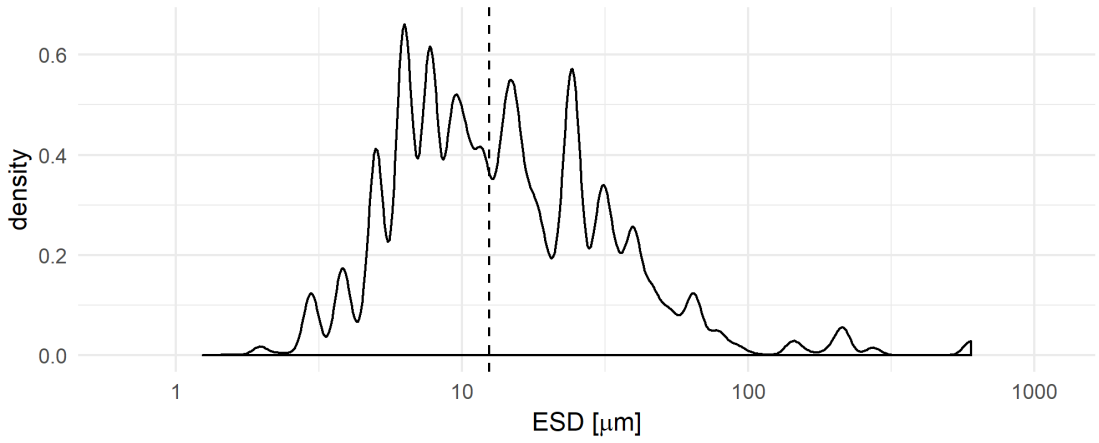

Figure A.1: Size ranges of the plankton data given in Equivalent Spherical Diameter (ESD). The dashed vertical line denotes the median ESD.

A.2 Temporal analysis of the datasets

This study uses a 24 year timeseries for 11 location classes. The timeseries display strong spatial gradients between the location classes and seasonal signals within the location classes. As we analyzed temporal data over strong spatial gradients, we were especially interested in determining whether the year-to-year changes contributed more to the variance than the spatial changes. We determined the mean value per location class, abiotic parameter and trophic mode. We first tested these mean values for autocorrelation and could not determine significant lags. We then conducted an estimation of variation analysis using the R-package VCA (Schuetzenmeister and Dufey, 2019). For all timeseries, the location classes clearly explained more of the variation than the years (tables E1 - E4). We thus conclude that for this study the year-to-year changes in the abiotic parameters and the trophic modes are smaller than the spatial difference between the location classes. The protozooplankton composition did not vary between the three classifications, so the analysis was only completed once (see table E2). The location classes contributed 17.16 % and the years 6.62 % of the variance for the protozooplankton distribution. That is less than for the other trophic modes. However, protozooplankton rely only indirectly on the abiotic environment and season, so much of the factors contributing to the variance in protozooplankton are located in the error term of the VCA.

Table A.1: Estimation of variation components (in %) for abiotic data.

	error	location class	year
DIN limitation	10.87	87.27	1.86
DIP limitation	12.68	84.77	2.54
DISi limitation	10.46	88.46	1.08
maturity index	13.93	83.03	3.04
salinity	16.37	81.96	1.67
suspended sediments	8.11	91.01	0.88

Table A.2: Estimation of variation components (in %) for the three trophic classifications.

		error	location class	year
phytoplankton	A	54.58	36.59	8.83
	B	32.19	57.65	10.17
	C	49.06	39.90	11.04
mixoplankton	A	63.49	27.75	8.75
	B	17.82	71.26	10.92
	C	30.72	64.05	5.23
protozooplankton	A-C	76.12	17.26	6.62

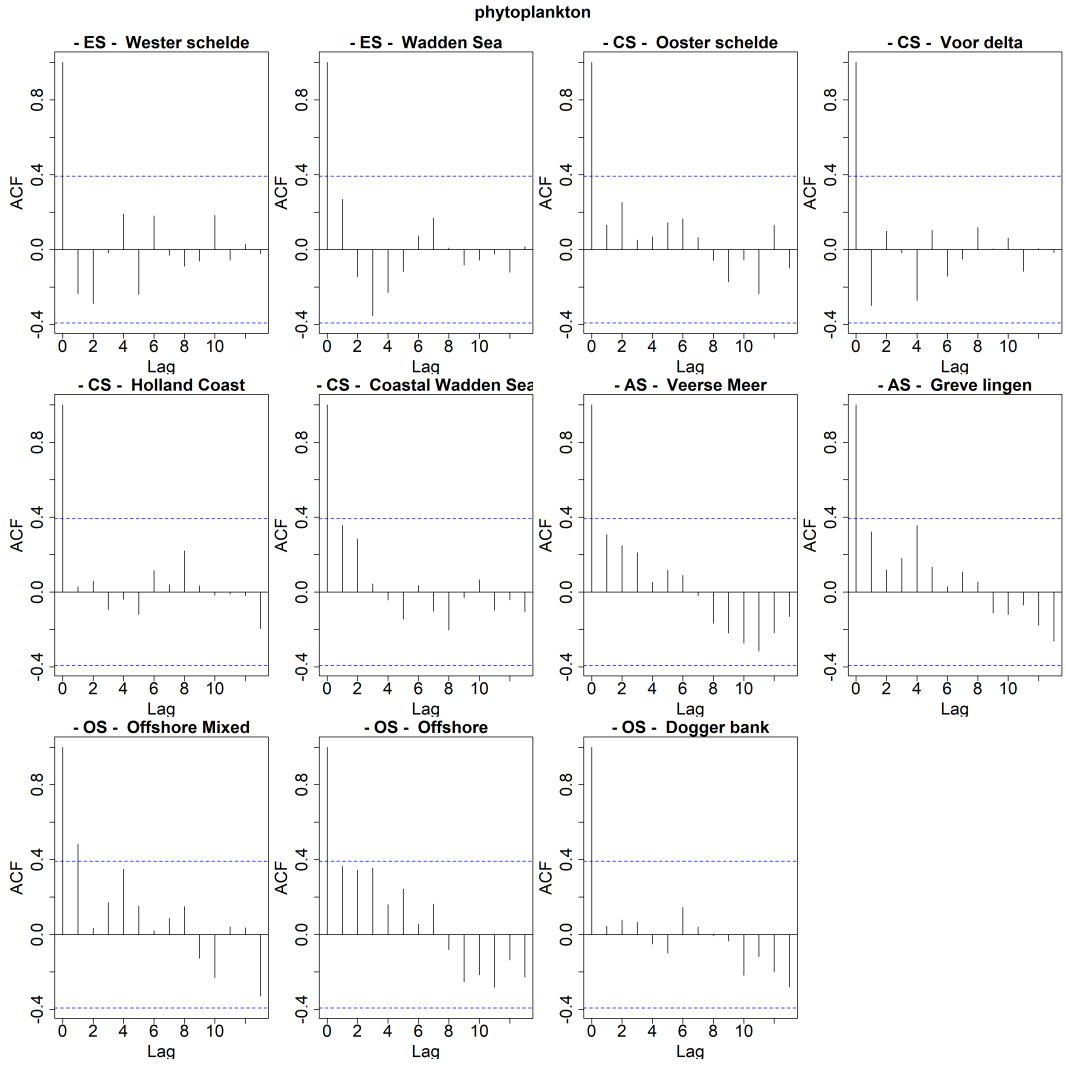

Figure A.2: Autocorrelation plots for phytoplankton of classification A.

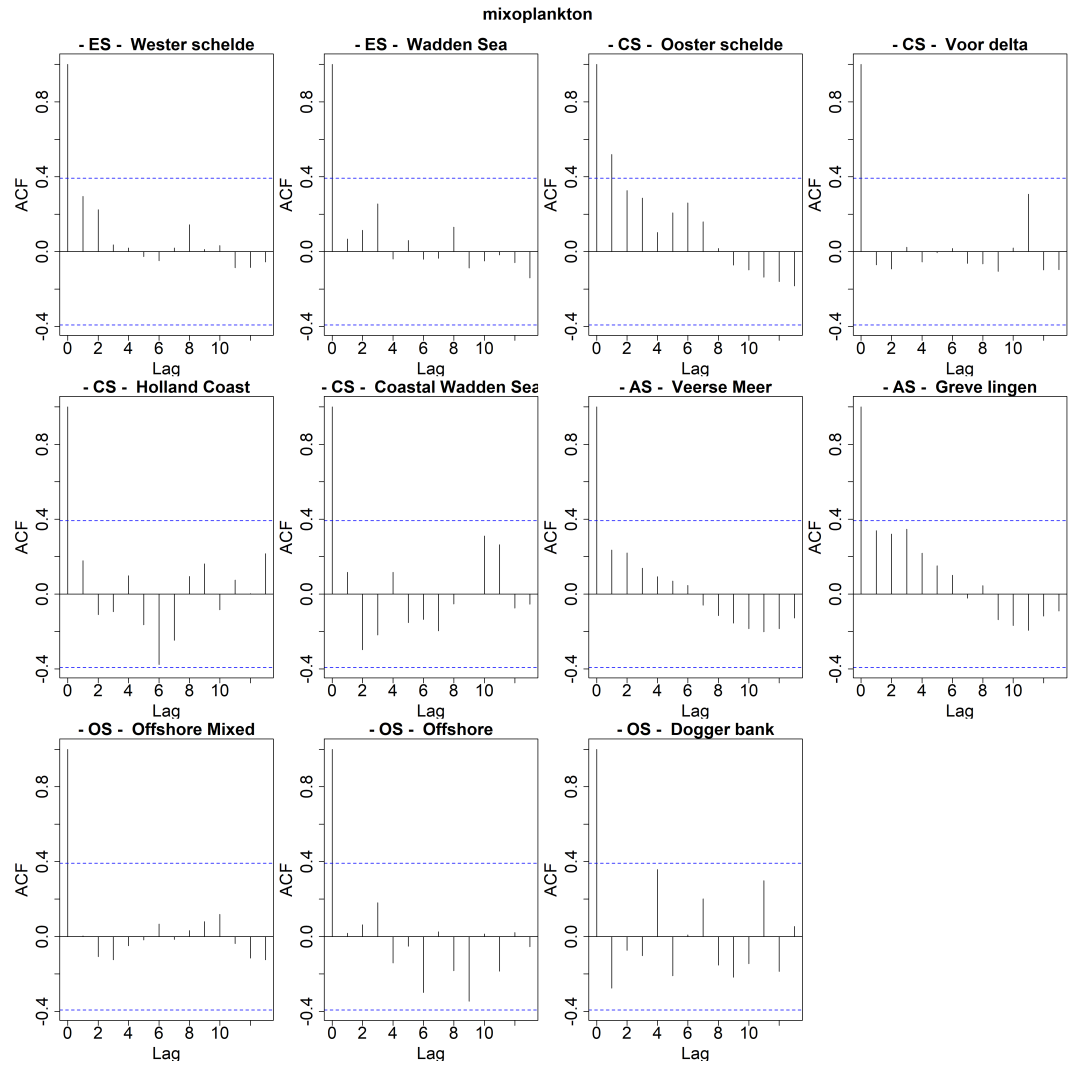

Figure A.3: Autocorrelation plots for mixoplankton of classification A.

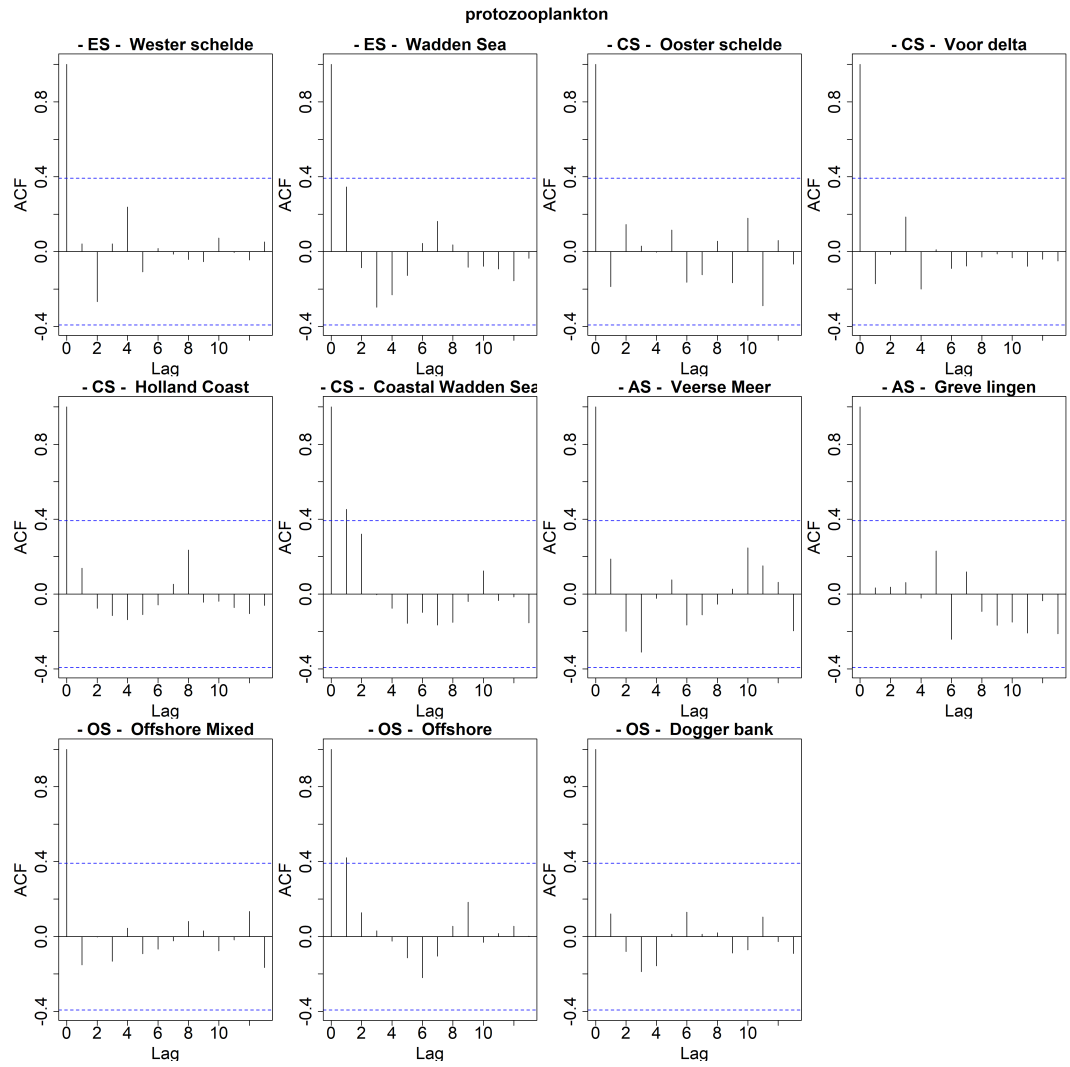

Figure A.4: Autocorrelation plots for protozooplankton of classification A.

A.3 Heatmaps of bottom and pycnocline

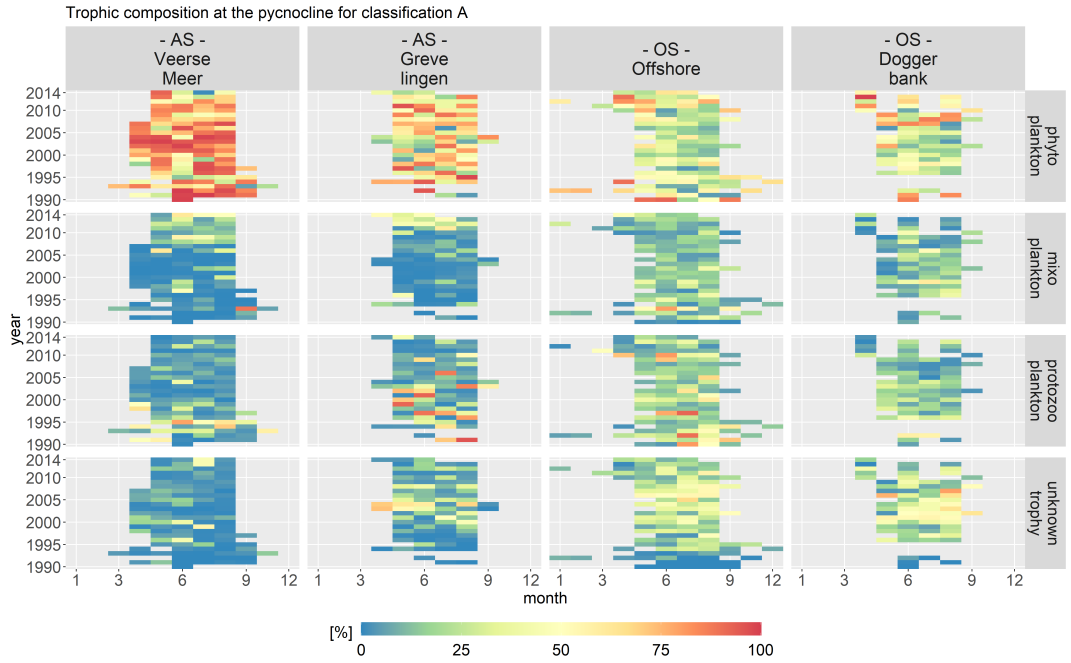

Figure A.5: Monthly fractions of the total biomass per trophic mode for trophic classification A at the pycnocline. The location classes are grouped into estuary (ES), coastal (CS), anthropogenically modified (AS) and offshore systems (OS).

Figure A.6: Monthly fractions of the type of mixoplankton for trophic classification A at the pycnocline. The location classes are grouped into estuary (ES), coastal (CS), anthropogenically modified (AS) and offshore systems (OS).

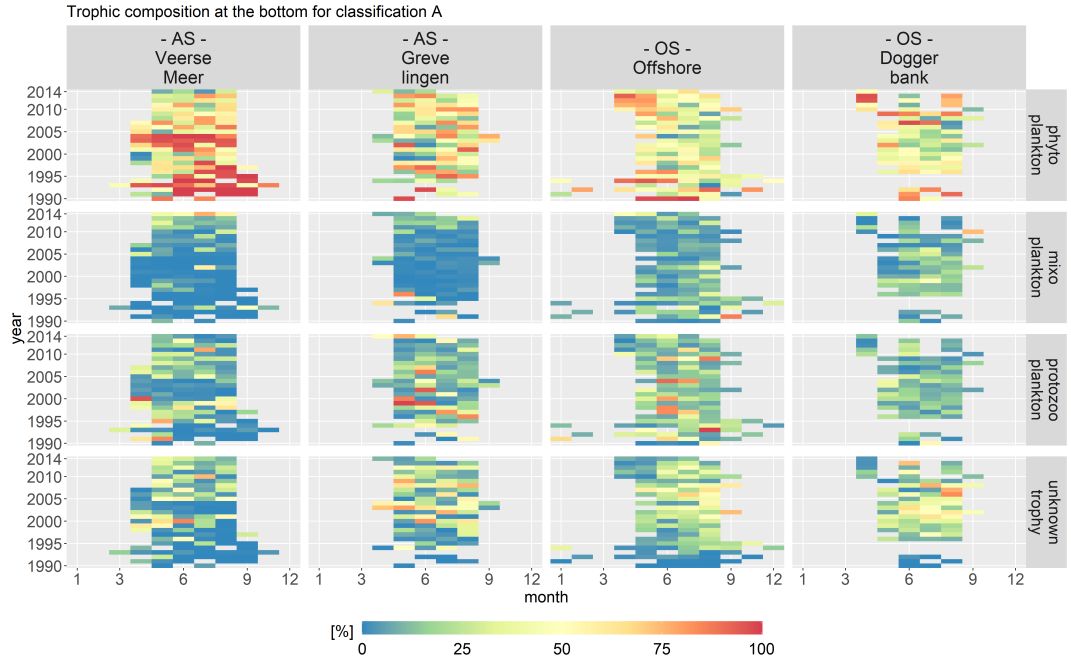

Figure A.7: Monthly fractions of the total biomass per trophic mode for trophic classification A at the pycnocline. The location classes are grouped into estuary (ES), coastal (CS), anthropogenically modified (AS) and offshore systems (OS).

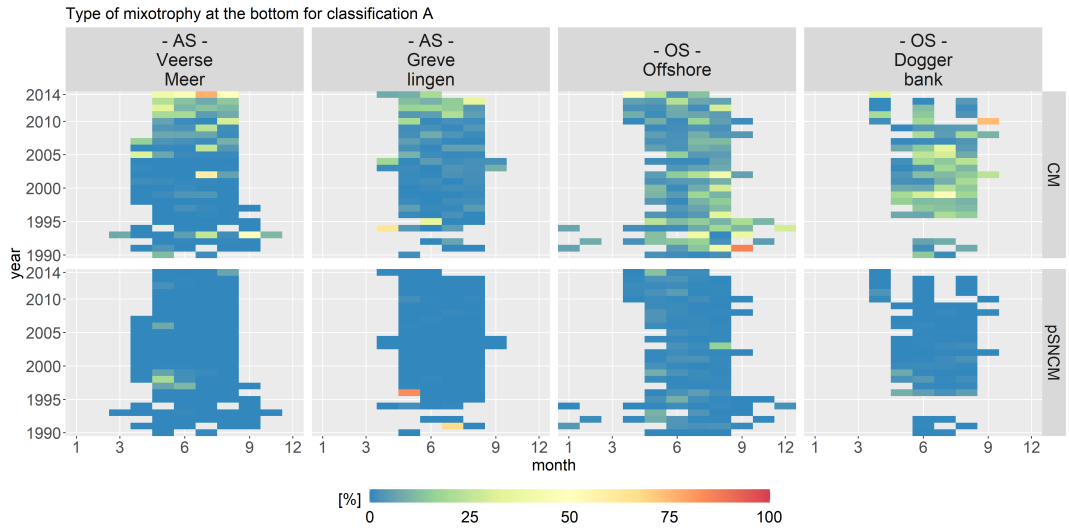

Figure A.8: Monthly fractions of the type of mixoplankton for trophic classification A at the pycnocline. The location classes are grouped into estuary (ES), coastal (CS), anthropogenically modified (AS) and offshore systems (OS).

Appendix B

Supplementary information for PROTIST module (Chapter 5)

B.1 General information

The module PROTIST is based on model equations from Flynn (2001), Flynn and Mitra (2009) and Flynn (2021). Those model equations have recently been summarized in a model called SAPPM (Switchable Acclimative Protist Plankton - Model) that can be used to describe protozooplankton, phytoplankton (as diatoms and non-diatoms) and constitutive mixoplankton (Flynn, 2021).
For the module PROTIST, the SAPPM structure was implemented. The SAPPM equations were adapted to work in a 3D modelling software environment. To separate between the stand-alone version of the model and the 3D implementation, the name PROTIST was applied. The module PROTIST can simultaneously model protozooplankton, phytoplankton (as diatoms and non-diatoms) and constitutive mixoplankton. The code for PROTIST was written in Fortran and can be downloaded at `https://github.com/lkschn/PROTISTcode.git`. The authors recommend to look at the Fortran code as it give the best overview of the PROTIST module structure.
In the following the PROTIST module state variable, parameters, auxiliaries, equations and their origin will be listed.

B.2 Model description

B.2.1 Model SV

Table B.1: List of all model state variables, their description, unit and initial value. Values labeled with a * differ for each location class.

state variable	**state variable description**	**unit**	**value**
PO4	initial DIP	gP m^{-3}	*
NH4	initial NH_4^+	gN m^{-3}	*
NO3	initial NO_3^-	gN m^{-3}	*
Si	initial Si	gSi m^{-3}	*
Opal	Opal-Si	gSi m^{-3}	*
POC1	POC1 (fast decomposing fraction)	gC m^{-3}	0.0
PON1	PON1 (fast decomposing fraction)	gN m^{-3}	0.0
POP1	POP1 (fast decomposing fraction)	gP m^{-3}	0.0
DOClab	labile DOC	gC m^{-3}	0.0
OXY	oxygen	gO2 m^{-3}	0.0
greenC	green C-biomass	gC m^{-3}	0.01
greenChl	green Chl-biomass	gChl m^{-3}	0.0002
greenN	green N-biomass	gN m^{-3}	0.0015
greenP	green P-biomass	gP m^{-3}	0.00024
diatC	diatom C-biomass	gC m^{-3}	0.01
diatChl	diatom Chl-biomass	gChl m^{-3}	0.0002
diatN	diatom N-biomass	gN m^{-3}	0.0015
diatP	diatom P-biomass	gP m^{-3}	0.00024
diatSi	diatom Si-biomass	gSi m^{-3}	0.002
cmC	CM C-biomass	gC m^{-3}	0.01
cmChl	CM Chl-biomass	gChl m^{-3}	0.0002
cmN	CM N-biomass	gN m^{-3}	0.0015
cmP	CM P-biomass	gP m^{-3}	0.00024
zooC	protozooplankton C-biomass	gC m^{-3}	0.01
zooN	protozooplankton N-biomass	gN m^{-3}	0.0015
zooP	protozooplankton P-biomass	gP m^{-3}	0.00024
ncmC	NCM C-biomass	gC m^{-3}	0.01
ncmChl	NCM Chl-biomass	gChl m^{-3}	0.0002
ncmN	NCM N-biomass	gN m^{-3}	0.0015
ncmP	NCM P-biomass	gP m^{-3}	0.00024

B.2.2 Model parameters

Table B.2: List of all model parameters for a generic PFT, their description, unit and default value. Values labeled with a * can be found in table B.3. The abbreviation dl is short for dimensionless.

parameter	parameter description	unit	value
AEm	maximum assimilation efficiency (AE)	dl	0.6
AEo	minimum AE	dl	0.3
alpha	alpha for photosynthesis in protist	gC gChl^{-1} m^2 umol^{-1} photon	*
abcChl	light absorbance coefficient for chlorophyll	m^2 gChl^{-1}	20
Ccell	C content of protist cell	pgC cell^{-1}	*
ChlCm	maximum cellular Chl:C ratio	gChl gC^{-1}	*
ChlCo	minimum cellular Chl:C ratio	gChl gC^{-1}	0.001
CR	catabolic respiration quotient	dl	0.05
degChl	Chl degradation	d^{-1}	0.72
FrAut	fraction of mortality to autolysis	dl	0.3
FrDet	fraction of mortality to detritus	dl	0.7
kAE	control of AE in response to prey quality	dl	1000
KtNH4	Kt for NH_4^+ transport	gN m^{-3}	0.007
KtNO3	Kt for NO_3^- transport	gN m^{-3}	0.007
KtP	Kt for DIP transport	gP m^{-3}	0.031
KtSi	Kt for DiSi transport	gSi m^{-3}	0.028
MrtRT	mortality at reference temperature	dl	*
Mphoto	acclimation rate to light	dl	0.5
NCmax	N:C that totally represses NH_4^+ transport	gN gC^{-1}	*
NCmin	minimum N-quota	gN gC^{-1}	*
NCopt	N:C for growth under optimal conditions	gN gC^{-1}	*
NO3Cmax	N:C that totally represses NO_3^- transport	gN gC^{-1}	*
NO3Copt	N:C for growth on NO_3^- under optimal conditions	gN gC^{-1}	*
optCR	proportion of prey captured by starved Zoo	dl	0.1
PCmax	PC maximum quota	gP gC^{-1}	*
PCmin	PC minimum quota	gP gC^{-1}	*
PCoNCm	maximum NC when PC is minimum (PCu = 0)	gN gC^{-1}	*
PCoNCop	optimum NC when PC is minimum (PCu = 0)	gN gC^{-1}	*
PCopt	PC optimum quota	gP gC^{-1}	*
PSDOC	proportion of current PS being leaked as DOC	dl	0.1
Q10	Q10 for UmRT	dl	*
r	radius of nutrient repleted protist cell	um	*
redco	C respired to support nitrate reduction for NH_4^+	gC gN-1	1.71
relPhag	relative phagotrophy in night:day	dl	*
relPS	relative PSmax:Umax on phototrophy	dl	*
ReUmNH4	max. growth rate supported by NH_4^+:Umax	dl	0.9
ReUmNO3	max. growth rate supported by NO_3^-:Umax	dl	0.8
RT	reference temperature for UmRT	deg C	10

Continued on next page

Table B.2 – *Continued from previous page*

parameter	**parameter description**	**unit**	**value**
SDA	specific dynamic action	dl	0.3
UmRT	maximum growth rate at reference T	d^{-1}	*
SCmax	absolute maximum Si:C (diatom)	gSi gC^{-1}	0.2
SCmin	minimum Si:C (diatom)	gSi gC^{-1}	0.02
SCopt	optimum Si:C for (diatom) growth	gSi gC^{-1}	0.1
AR	anabolic respiration cost in terms of C	gC gN^{-1} d^{-1}	1.5
M	scalar for controlling photoacclimation rate	dl	0.5

Table B.3: Summary of the PFT specific parameters established through literature as stated in text. Note that the protozooplankton mortality (marked with *) uses a quadratic closure function, while the phytoplankton and CM mortality use a linear mortality function.

parameter	units	diatom	green algae	CM	protozoo-plankton	origin
ESD	μm	24.0	10.0	18.0	40.0	Schneider et al., 2020b
Ccell	pgC $cell^{-1}$	909.19	77.20	404.29	3833.51	calculated using Menden-Deuer and Lessard, 2000
ChlCmax	gChl gC^{-1}	0.058	0.033	0.021	-	Geider et al., 1997
α^{Chl}	gC $gChl^{-1}$ m^2 $umol^{-1}$ photon	9.5e-6	7e-6	7e-6	-	Geider et al., 1997
NCmin	gN gC^{-1}	0.11	0.14	0.09	0.05	Leonardos and Geider, 2004
NCopt	gN gC^{-1}	0.15	0.17	0.12	0.15	Leonardos and Geider, 2004
NCmax	gN gC^{-1}	0.2	0.2	0.2	0.2	Leonardos and Geider, 2004
PCminNCopt	gN gC^{-1}	0.12	0.15	0.1	-	calibrated using Flynn, 2021
PCminNCmax	gN gC^{-1}	0.13	0.16	0.11	-	calibrated using Flynn, 2021
NO3Copt	gN gC^{-1}	0.14	0.16	0.11	-	based on Leonardos and Geider, 2004
NO3Cmax	gN gC^{-1}	0.16	0.18	0.13	-	based on Leonardos and Geider, 2004
PCmin	gP gC^{-1}	0.009	0.02	0.006	0.005	Leonardos and Geider, 2004

Continued on next page

Table B.3 – *Continued from previous page*

parameter	units	diatom	green algae	CM	protozoo-plankton	origin
PCopt	gP gC^{-1}	0.014	0.028	0.012	0.024	Leonardos and Geider, 2004
PCmax	gP gC^{-1}	0.029	0.036	0.028	0.05	Leonardos and Geider, 2004
relPS	dl	2	2	2	-	Geider et al., 1998
relPhag	dl	-	-	0.1	1	Skovgaard, 1996; Li et al., 1999; Adolf et al., 2006; Anderson et al., 2018
PR diatom	dl	-	-	-	1	information from Jeong et al., 2010
PR green algae	dl	-	-	1	1	information from Jeong et al., 2010
PR CM	dl	-	-	-	1	information from Jeong et al., 2010
sed	m d^{-1}	0.38	-	-	-	Stokes law
mrt	d^{-1}	0.07	0.07	0.07	0.007 *	Blauw et al., 2009

B.2.3 Model auxiliaries

Table B.4: List of all model auxiliaries for a generic PFT, their description and unit.

auxiliary	**auxiliary description**	**unit**
NC	cellular nitrogen:carbon ratio	gN gC^{-1}
PC	cellular phosphate:carbon ratio	gP gC^{-1}
SC	cellular silica:carbon ratio	gSi gC^{-1}
ChlC	cellular chlorphyll:carbon ratio	gChl gC^{-1}
UmT	temperature dependent maximum growth rate	gC gC^{-1} d^{-1}
BR	temperature dependent basal respiration rate	gC gC^{-1} d^{-1}
NCu	cellular nitrogen status	dl
PCu	cellular phosphate status	dl
SCu	cellular silica status	dl
NPCu	Liebig nutrient limitation	dl
mot	motility of the protist	m s-1
upP	uptake rate of phosphate	gP gC^{-1} d^{-1}
upNH4	uptake rate of ammonium	gN gC^{-1} d^{-1}
upNO3	uptake rate of nitrate	gN gC^{-1} d^{-1}
upSi	uptake rate of silica	gSi gC^{-1} d^{-1}
upChl	uptake rate of chlorphyll	gChl gC^{-1} d^{-1}
PSqm	maximum photosynthetic rate	gC gC^{-1} d^{-1}
PS	gross photosynthetic rate	gC gC^{-1} d^{-1}
Cfix	net photosynthetic rate	gC gC^{-1} d^{-1}
synChl	synthesis rate of chlorophyll-a	gChl gC^{-1} d^{-1}
degChl	degradation rate of chlorphyll	gChl gC^{-1} d^{-1}
sumCP	rate of all potential prey captures	gC gC^{-1} d^{-1}
ingNC	rate of captured nitrogen:carbon	gN gC^{-1} d^{-1}
ingPC	rate of captured phosphate:carbon	gP gC^{-1} d^{-1}
ppNC	ratio of captured prey nitrogen: predator nitrogen	dl
ppPC	ratio of captured prey nitrogen: predator nitrogen	dl
stoichP	limiting nutrient in prey	dl
opAE	assimilation efficiency of predator	dl
maxIng	maximum ingestion rate	gC gC^{-1} d^{-1}
ingSat	satiation ingestion rate	gC gC^{-1} d^{-1}
ingC	ingestion rate of prey carbon	gC gC^{-1} d^{-1}
assC	assimilation rate of prey carbon	gC gC^{-1} d^{-1}
ingN	ingestion rate of prey nitrogen	gN gC^{-1} d^{-1}
ingP	ingestion rate of prey phosphate	gP gC^{-1} d^{-1}
assN	assimilation rate of prey nitrogen	gN gC^{-1} d^{-1}
assP	assimilation rate of prey phosphate	gP gC^{-1} d^{-1}
totR	total respiration rate	gC gC^{-1} d^{-1}
Cu	carbon-specific growth rate	gC gC^{-1} d^{-1}
mrt	mortality rate	gC gC^{-1} d^{-1}
lInh	light inhibition factor	dl
capPrey	potential C-specific capture of prey	gC gC^{-1} d^{-1}

Continued on next page

Table B.4 – *Continued from previous page*

auxiliary	**auxiliary description**	**unit**
exat	extinction by phytoplankton	m^{-1}

B.2.4 Model fluxes

Table B.5: List of all model fluxes for a generic PFT, their description and unit.

flux	**flux description**	**unit**
dNH4up	uptake of NH_4^+ into algal biomass	gN m^{-3} d^{-1}
dNO3up	uptake of NO_3^- into algal biomass	gN m^{-3} d^{-1}
dPup	uptake of PO_4^{3-} into algal biomass	gP m^{-3} d^{-1}
dSiup	uptake of Si into algal biomass	gSi m^{-3} d^{-1}
dCfix	contribution to biomass growth from C-fixation	gC m^{-3} d^{-1}
dChlsyn	synthesis Chl rate of change	gChl m^{-3} d^{-1}
dChldeg	degradation Chl rate of change	gChl m^{-3} d^{-1}
dChlup	acquistion of prey Chl by NCM	gChl m^{-3} d^{-1}
dCresp	total respiration rate	gC m^{-3} d^{-1}
dCleak	release of DOC	gC m^{-3} d^{-1}
dCvoid	voiding of C as DOC if NC falls below NCmin	gC m^{-3} d^{-1}
dNH4out	NH_4^+ release by regeneration	gN $^{-3}$ d^{-1}
dPout	PO_4^{3-} release by regeneration	gP $^{-3}$ d^{-1}
dCeat	assimilation of C from prey	gC m^{-3} d^{-1}
dNeat	assimilation of N from prey	gN m^{-3} d^{-1}
dPeat	assimilation of P from prey	gP m^{-3} d^{-1}
dPOCout	rate of voiding of C as particulates	gC m^{-3} d^{-1}
dPONout	rate of voiding of N as particulates	gN m^{-3} d^{-1}
dPOPout	rate of voiding of P as particulates	gP m^{-3} d^{-1}
dAutC	protist-C mortality through Autolysis	gC m^{-3} d^{-1}
dDetC	protist-C mortality through Detritus	gC m^{-3} d^{-1}
dAutN	protist-N mortality through Autolysis	gN m^{-3} d^{-1}
dDetN	protist-N mortality through Detritus	gN m^{-3} d^{-1}
dAutP	protist-P mortality through Autolysis	gP m^{-3} d^{-1}
dDetP	protist-P mortality through Detritus	gP m^{-3} d^{-1}
dAutSi	protist-Si mortality through Autolysis	gSi m^{-3} d^{-1}
dDetSi	protist-Si mortality through Detritus	gSi m^{-3} d^{-1}
dAutChl	protist-Chl mortality through Autolysis	gChl m^{-3} d^{-1}
dDetChl	protist-Chl mortality through Detritus	gChl m^{-3} d^{-1}
dD1C	mortality of prey i through predator j	gC m^{-3} d^{-1}
dD1Chl	mortality of prey i through predator j	gChl m^{-3} d^{-1}
dD1N	mortality of prey i through predator j	gN m^{-3} d^{-1}
dD1P	mortality of prey i through predator j	gP m^{-3} d^{-1}
dD1Si	mortality of prey i through predator j	gSi m^{-3} d^{-1}

Table B.6: Generic protist state variable names used in the following tables and equations.

generic SV	generic SV description	unit
protC	protist carbon biomass	gC m^{-3}
protN	protist nitrogen biomass	gN m^{-3}
protP	protist phosphorus biomass	gP m^{-3}
protChl	protist chlorophyll biomass	gChl m^{-3}
protSi	protist silica biomass	gSi m^{-3}

$$dNH4up = protC \cdot upNH4 \tag{B.1}$$
$$dNO3up = protC \cdot upNO3 \tag{B.2}$$
$$dPup = protC \cdot upP \tag{B.3}$$
$$dSiup = protC \cdot upSi \tag{B.4}$$
$$dCfix = protC \cdot Cfix \tag{B.5}$$
$$dChlsyn = protC \cdot synChl \tag{B.6}$$
$$dChldeg = protC \cdot degChl \text{ or } protC \cdot degChl_{NCM} \tag{B.7}$$
$$dChlup = protC \cdot (ingC \cdot \frac{capPrey}{sumCP}) \cdot \frac{preyChl}{preyC} \cdot upChl \tag{B.8}$$
$$dCresp = protC \cdot totR \tag{B.9}$$
$$dCleak = protC \cdot (PS - Cfix) \tag{B.10}$$
$$dCvoid = protC - protN/NCmin \tag{B.11}$$
$$dNH4out = max(0.0, protN - protC \cdot NCmax) \tag{B.12}$$
$$dPout = max(0.0, protP - protC \cdot PCmax) \tag{B.13}$$
$$dCeat = protC \cdot assC \tag{B.14}$$
$$dNeat = protC \cdot assN \tag{B.15}$$
$$dPeat = protC \cdot assP \tag{B.16}$$
$$dPOCout = protC \cdot (ingC - assC) \tag{B.17}$$
$$dPONout = protC \cdot (ingN - assN) \tag{B.18}$$
$$dPOPout = protC \cdot (ingP - assP) \tag{B.19}$$
$$dAutC = protC \cdot mrt \cdot FrAut \tag{B.20}$$
$$dDetC = protC \cdot mrt \cdot FrDet \tag{B.21}$$
$$dAutN = protN \cdot mrt \cdot FrAut \tag{B.22}$$
$$dDetN = protN \cdot mrt \cdot FrDet \tag{B.23}$$
$$dAutP = protP \cdot mrt \cdot FrAut \tag{B.24}$$
$$dDetP = protP \cdot mrt \cdot FrDet \tag{B.25}$$
$$dAutSi = protSi \cdot mrt \cdot FrAut \tag{B.26}$$
$$dDetSi = protSi \cdot mrt \cdot FrDet \tag{B.27}$$
$$dAutChl = protChl \cdot mrt \cdot FrAut \tag{B.28}$$
$$dDetChl = protChl \cdot mrt \cdot FrDet \tag{B.29}$$
$$dD1C = protC \cdot (ingC \cdot \frac{capPrey}{sumCP}) \tag{B.30}$$
$$dD1Chl = dD1C \cdot (preyChl/preyC) \tag{B.31}$$
$$dD1N = dD1C \cdot (preyN/preyC) \tag{B.32}$$
$$dD1P = dD1C \cdot (preyP/preyC) \tag{B.33}$$
$$dD1Si = dD1C \cdot (preySi/preyC) \tag{B.34}$$
$$\tag{B.35}$$

APPENDIX B. SUPPLEMENTARY INFORMATION: MODELING MIXOPLANKTON

B.2.5 Conservation equations

Table B.7: Conservation equations for diatom SVs.

conservation equation		unit
$\frac{dDiat_C}{dt} = dCfix - dCleak - dCvoid - dCresp - dAutC - dDetC - \sum Pred$	(B.36)	gC m^{-3} d^{-1}
$\frac{dDiat_N}{dt} = dNH4up + dNO3up - dNH4out - dAutN - dDetN - \sum Pred$	(B.37)	gN m^{-3} d^{-1}
$\frac{dDiat_P}{dt} = dPup - dPout - dAutP - dDetP - \sum Pred$	(B.38)	gP m^{-3} d^{-1}
$\frac{dDiat_{Si}}{dt} = dSiup - dAutSi - dDetSi - \sum Pred$	(B.39)	gSi m^{-3} d^{-1}
$\frac{dDiat_{Chl}}{dt} = dChlsyn - dChldeg - dAutChl - dDetChl - \sum Pred$	(B.40)	gChl m^{-3} d^{-1}

Table B.8: Conservation equations for green algae SVs.

conservation equation		unit
$\frac{dGreen_C}{dt} = dCfix - dCleak - dCvoid - dCresp - dAutC - dDetC - \sum Pred$	(B.41)	gC m^{-3} d^{-1}
$\frac{dGreen_N}{dt} = dNH4up + dNO3up - dNH4out - dAutN - dDetN - \sum Pred$	(B.42)	gN m^{-3} d^{-1}
$\frac{dGreen_P}{dt} = dPup - dPout - dAutP - dDetP - \sum Pred$	(B.43)	gP m^{-3} d^{-1}
$\frac{dGreen_{Chl}}{dt} = dChlsyn - dChldeg - dAutChl - dDetChl - \sum Pred$	(B.44)	gChl m^{-3} d^{-1}

Table B.9: Conservation equations for protozooplankton SVs.

conservation equation		unit
$\frac{dZoo_C}{dt} = dCeat - dPOCout - dCresp - dAutC - dDetC$	(B.45)	gC m^{-3} d^{-1}
$\frac{dZoo_N}{dt} = dNeat - dPONout - dAutN - dDetN$	(B.46)	gN m^{-3} d^{-1}
$\frac{dZoo_P}{dt} = dPeat - dPOPout - dAutP - dDetP$	(B.47)	gP m^{-3} d^{-1}

Table B.10: Conservation equations for CM SVs.

conservation equation		unit
$\frac{dCM_C}{dt} = dCfix + dCeat - dCleak - dCvoid - dPOCout - dCresp - dAutC - dDetC - \sum Pred$	(B.48)	gC m^{-3} d^{-1}
$\frac{dCM_N}{dt} = dNH4up + dNO3up + dNeat - dNH4out - dPONout - dAutN - dDetN - \sum Pred$	(B.49)	gN m^{-3} d^{-1}
$\frac{dCM_P}{dt} = dPup + dPeat - dPout - dPOPout - dAutP - dDetP - \sum Pred$	(B.50)	gP m^{-3} d^{-1}
$\frac{dCM_{Chl}}{dt} = dChlsyn - dChldeg - dAutChl - dDetChl - \sum Pred$	(B.51)	gChl m^{-3} d^{-1}

Table B.11: Conservation equations for NCM SVs.

conservation equation		unit
$\frac{dNCM_C}{dt} = dCfix + dCeat - dCleak - dCvoid - dPOCout - dCresp - dAutC - dDetC - \sum Pred$	(B.52)	gC m^{-3} d^{-1}
$\frac{dNCM_N}{dt} = dNeat - dPONout - dAutN - dDetN - \sum Pred$	(B.53)	gN m^{-3} d^{-1}
$\frac{dNCM_P}{dt} = dPeat - dPOPout - dAutP - dDetP - \sum Pred$	(B.54)	gP m^{-3} d^{-1}
$\frac{dNCM_{Chl}}{dt} = dChlup - dChldeg - dAutChl - dDetChl - \sum Pred$	(B.55)	gChl m^{-3} d^{-1}

APPENDIX B. SUPPLEMENTARY INFORMATION: MODELING MIXOPLANKTON

B.2.6 Model equations

B.2.6.1 Mathematical equations

$$normalize(x, x_{min}, x_{max}) = \frac{x - x_{min}}{x_{max} - x_{min}} \tag{B.56}$$

$$gompertz(L, b, x) = L \cdot exp(-b \cdot exp(-k \cdot x)) \tag{B.57}$$

$$monod(R, kt) = \frac{R}{R + kt} \tag{B.58}$$

Table B.12: List of all parameters for the mathematical functions listed above.

parameter	**parameter description**	**unit**
L	upper asymptote	dl
b	displacement along the x-axis	dl
k	growth rate of gompetz curve	dl
R	resource	dl
kt	hald-saturation constant	dl

B.2.6.2 Module cellular status

Table B.13: Summary of the auxiliaries in the module cellular status.

auxiliary	description	unit	origin	eq. #
Nut_iC	cellular carbon quota for nitrogen, phosphate, silica and chlorophyll-a	gNut gC^{-1}	Flynn, 2001	B.59, B.60, B.61,B.62
UmT	maximum possible growth rate at the current temperature	d^{-1}	Flynn, 2021	B.63
BR	basal respiration at the current temperature	d^{-1}	Flynn, 2001	B.65
$totR$	total respiration taking metabolic, anabolic and foraging costs into account.	gC gC^{-1} d^{-1}	Flynn, 2021	B.70
Cu	net carbon specific growth rate taking phagotrophic and phototrophic carbon sources into account	gC gC^{-1} d^{-1}	Flynn, 2021	B.71
NCu	cellular nitrogen status (1 = saturated; 0 = limited) determined using a linear relationship.	dl	modified from Flynn, 2021	B.67
PCu	cellular phosphate status (1 = saturated; 0 = limited) determined using a Gompertz curve	dl	modified from Flynn, 2021	B.68
SCu	cellular silica status (1 = saturated; 0 = limited)	dl	Flynn, 2021	B.69
$DOCvoid$	voiding of DOC if minimum quota is reached	gC gC^{-1}	Flynn, 2021	B.66
mrt	mortality rate	gC gC^{-1}	Flynn, 2021	B.64

$$NC = \frac{protN}{protC} \tag{B.59}$$

$$PC = \frac{protP}{protC} \tag{B.60}$$

$$SC = \frac{protSi}{protC} \tag{B.61}$$

$$ChlC = \frac{protChl}{protC} \tag{B.62}$$

$$UmT = UmRT \cdot Q10^{\frac{Temp-RT}{10}} \tag{B.63}$$

$$mrt = mrtRT \cdot Q10^{\frac{Temp-RT}{10}} \tag{B.64}$$

$$BR = UmT \cdot CR \tag{B.65}$$

$$DOCvoid = NC < NCmin, protC - \frac{protN}{NCmin}, 0.0 \tag{B.66}$$

$$NCu = min(1.0, max(0.0, normalizeNC, NCmin, NCmax)) \tag{B.67}$$

$$PCu = gompertz(1.0, 6.0, 10.0, normalize(PC, PCmin, PCmax)) \tag{B.68}$$

$$SCu = min((monod(Si, ktSi) \cdot \frac{SCopt}{SCmin}), 1.0) \tag{B.69}$$

$$totR = (redco \cdot upNO3) + AR \cdot (upNH4 + upNO3 + assN \cdot SDA) + (assC \cdot SDA) + BR \tag{B.70}$$

$$Cu = Cfix + assC - totR \tag{B.71}$$

B.2.6.3 Module uptake

Table B.14: Summary of the auxiliaries in the module uptake.

auxiliary	description	unit	origin	eq. #
upP	uptake of phosphate described using the monod function and enhanced or repressed using two logistic sigmoid functions.	gP gC^{-1} d^{-1}	modified from Flynn, 2021	B.72
$upNH4$	uptake of ammonium described using the monod function and enhanced or repressed using two logistic sigmoid functions.	gN gC^{-1} d^{-1}	modified from Flynn, 2021	B.73
$upNO3$	uptake of nitrite described using the monod function and enhanced using a logistic sigmoid functions.	gN gC^{-1} d^{-1}	modified from Flynn, 2021	B.74
$upSi$	uptake of silica described using the monod function and enhanced using a logistic sigmoid functions.	gSi gC^{-1} d^{-1}	modified from Flynn, 2021	B.75

P uptake

$$
\begin{aligned}
APin_P &= logistic(1.0, -16.0, 0.7, normalize(PC, PCmin, PCopt)) \\
APde_P &= logistic(1.0, -40.0, 0.9, normalize(PC, PCmin, PCmax)) \\
upP_{opt} &= monod(P, ktP) \cdot UmT \cdot PCopt \\
upP &= upP_{opt} \cdot APin_P \cdot 10.0 + upP_{opt} \cdot APde_P
\end{aligned} \tag{B.72}
$$

NH_4^+ uptake

$$
\begin{aligned}
NCPopt &= ((PCu < NCu), PCoNCop + PCu \cdot (NC - PCoNCop), NC) \\
APin_{NH4} &= logistic(1.0, -24.0, 0.85, normalize(NC, NCmin, NCPopt)) \\
NCPopt &= ((PCu < NCu), PCoNCm + PCu \cdot (NC - PCoNCm), NC) \\
APde_P &= logistic(1.0, -40.0, 0.85, normalize(NC, NCmin, NCPmax)) \\
upNH4_{opt} &= monod(NH4, ktNH4) \cdot UmT \cdot NCopt \cdot relUm_{NH4} \\
upNH4 &= upNH4_{opt} \cdot APin_{NH4} \cdot 3.0 + upNH4_{opt} \cdot APde_{NH4}
\end{aligned} \tag{B.73}
$$

NO_3^- uptake

$$
\begin{aligned}
NCPm &= ((PCu < NCu), PCoNCm + PCu \cdot (NC - PCoNCm), NC) \\
APde_{NO3} &= logistic(1.0, -55.0, 0.9, normalize(NC, NCmin, NCPm)) \\
upNO3_{opt} &= monod(NO3, ktNO3) \cdot UmT \cdot NCopt \cdot relUm_{NO3} \\
upNO3 &= upNO3_{opt} \cdot APde_{NO3}
\end{aligned} \tag{B.74}
$$

Si uptake

$$APde_{Si} = logistic(1.0, -80.0, 0.95, normalize(SC, SCmin, SCmax))$$
$$upSi_{opt} = monod(Si, ktSi) \cdot UmT \cdot SCopt$$
$$upSi = upSi_{opt} \cdot APde_{Si} \tag{B.75}$$

B.2.6.4 Module phototrophy

Table B.15: Summary of the auxiliaries in the module phototrophy.

auxiliary	description	unit	origin	eq. #
$PSqm$	maximal attainable photosynthetic rate under optimum light (plateau of the PE-curve)	gC gC^{-1} d^{-1}	Flynn, 2001	B.76
PS	carbon fixation through photosynthesis at current light and current cellular status	gC gC^{-1} d^{-1}	Flynn, 2001	B.77
$Cfix$	net carbon fixation taking leakage into account	gC gC^{-1} d^{-1}	Flynn, 2001	B.78
$synChl$	synthesis of chlorophyll-a	gChl gC d^{-1}	modified from Flynn, 2021	B.79
$degChl$	degradation of chlorophyll-a	gChl gC^{-1} d^{-1}	Flynn, 2021	B.80
$degChl_{NCM}$	loss of chlorophyll-a	gChl gC^{-1} d^{-1}	Ghyoot et al., 2017a	B.81
$upChl$	uptake of chlorophyll-a from prey	gChl gC^{-1} d^{-1}	modified from Ghyoot et al., 2017a	B.82

$$PSqm = [UmT \cdot relPS \cdot (1 + PSDOC) + NCm \cdot UmT \cdot (redco + AR)] \cdot NCu + BR \tag{B.76}$$

$$X = \frac{\alpha^{Chl} \cdot ChlC \cdot PFD \cdot 24.0 \cdot 60.0 \cdot 60.0}{PSqm}$$

$$PS = \frac{PSqm \cdot (log(X + sqrt(1.0 + X^2)) - log(X \cdot exat + sqrt(1.0 + (X \cdot exat)^2)))}{atten} \tag{B.77}$$

$$Cfix = PS \cdot (1.0 - PSDOC) \tag{B.78}$$

$$synChl = ChlCmax \cdot UmT \cdot NPSiCu \cdot M \cdot (1.0 - \frac{Cfix}{PSqm}) \cdot$$
$$logistic(0.95, -24.0, 0.85, normalize(ChlC, ChlCmin, ChlCmax)) \tag{B.79}$$

$$degChl = (min(ChlC, ChlCmax) \cdot UmT \cdot (1.0 - NPSiCu)) \tag{B.80}$$

$$degChl_{NCM} = constant \tag{B.81}$$

$$upChl = logistic(1.0, -80, 0.93, normalize(ChlC, 0.0, ChlCmax)) \tag{B.82}$$

B.2.6.5 Module phagotrophy

Table B.16: Summary of the auxiliaries in the module phagotrophy.

auxiliary	description	unit	origin	eq. #
mot	motility of the protists	m s-1	Flynn and Mitra, 2016	B.83
nrPrey	density of prey in segment	nr cells m^{-3}	modified from Flynn, 2021	B.84
enc	encounter rate	prey predator-1 d^{-1}	Rothschild and Osborn, 1988	B.85
capPrey	potential C-specific capture of prey	gC gC^{-1} d^{-1}	Flynn, 2021	B.86
sumCP	captured prey	gC gC^{-1} d-1	Flynn, 2021	B.87
opAE	assimilation efficiency	dl	Flynn, 2021	B.91
maxIng	maximum ingestion rate	gC gC^{-1} d-1	Flynn, 2021	B.92
satIng	saturation ingestion rate	gC gC^{-1} d^{-1}	Flynn, 2021	B.93
ingC	actual carbon ingestion rate	gC gC^{-1} d^{-1}	Flynn, 2021	B.94
$ingNut_i$	nutrient ingestion rate	gNut gC^{-1} d^{-1}	Flynn, 2021	B.95, B.96
assC	carbon assimilation rate	gC gC^{-1} d^{-1}	Flynn, 2021	B.97
$assNut_i$	nutrient assimilation rate	gNut gC^{-1} d^{-1}	Flynn, 2021	B.98, B.99

$$mot = 1e^{-6} \cdot (38.542 \cdot (r \cdot 2)^{0.5424}) \tag{B.83}$$

$$lightInh = sigmoidLogistic((1 - relPhag), 10.0, 1.0, PFD) + (1.0 - (1 - relPhag))$$

$$nrPrey = lightInh \cdot 1e12 \cdot \frac{preyC}{CcellPrey} \tag{B.84}$$

$$encPrey = (24.0 \cdot 60.0 \cdot 60.0) \cdot \pi \cdot (\frac{rPrey}{1E6} + \frac{rProt}{1E6})^2 \cdot nrPrey$$
$$\cdot ((vel^2_{prey} + 3 \cdot vel^2_{pred} + 4 \cdot wTurb^2) \cdot ((vel^2_{pred} + wTurb^2)^{-0.5})) \cdot 3.0^{-1.0} \tag{B.85}$$

$$capPrey = encPrey \cdot PR \cdot optCR \cdot \frac{CcellPrey}{CcellPred} \tag{B.86}$$

$$sumCP = sum(capPrey) \tag{B.87}$$

$$ingNC = \frac{capPrey}{sumCP} \cdot \frac{preyN}{preyC} \tag{B.88}$$

$$ingPC = \frac{capPrey}{sumCP} \cdot \frac{preyP}{preyC} \tag{B.89}$$

$$stoichP = min(\frac{ingNC}{NCopt}, \frac{ingPC}{PCopt}, 1.0) \tag{B.90}$$

$$opAE = (AEo + (AEm - AEo) \cdot monod(stoichP, kAE) \cdot (1.0 + kAE)) \cdot stoichP \tag{B.91}$$

$$maxIng = \frac{UmT + BR}{1.0 - SDA} \cdot \frac{1}{opAE} opAE \tag{B.92}$$

$$satIng = maxIng \cdot monod(sumCP, \frac{maxIng}{4}) \tag{B.93}$$

$$ingC = min(ingSat, sumCP) \tag{B.94}$$

$$ingN = ingC \cdot ingNC \tag{B.95}$$

$$ingP = ingC \cdot ingPC \tag{B.96}$$

$$assC = ingC \cdot opAE \tag{B.97}$$

$$assN = assC \cdot NCopt \tag{B.98}$$

$$assP = assC \cdot PCopt \tag{B.99}$$

B.3 Boundary forcings

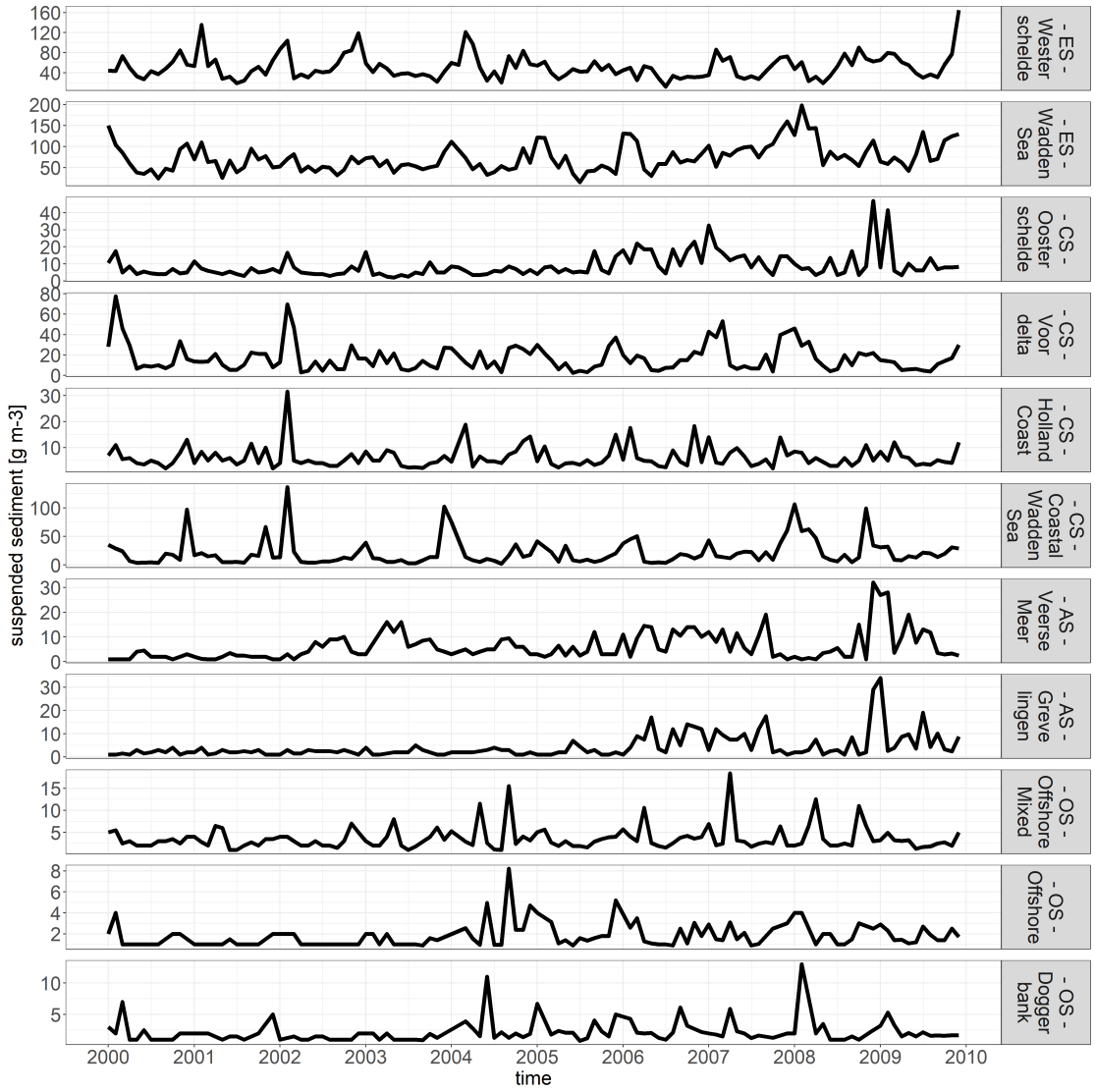

Figure B.1: Boundary transport of suspended sediment.

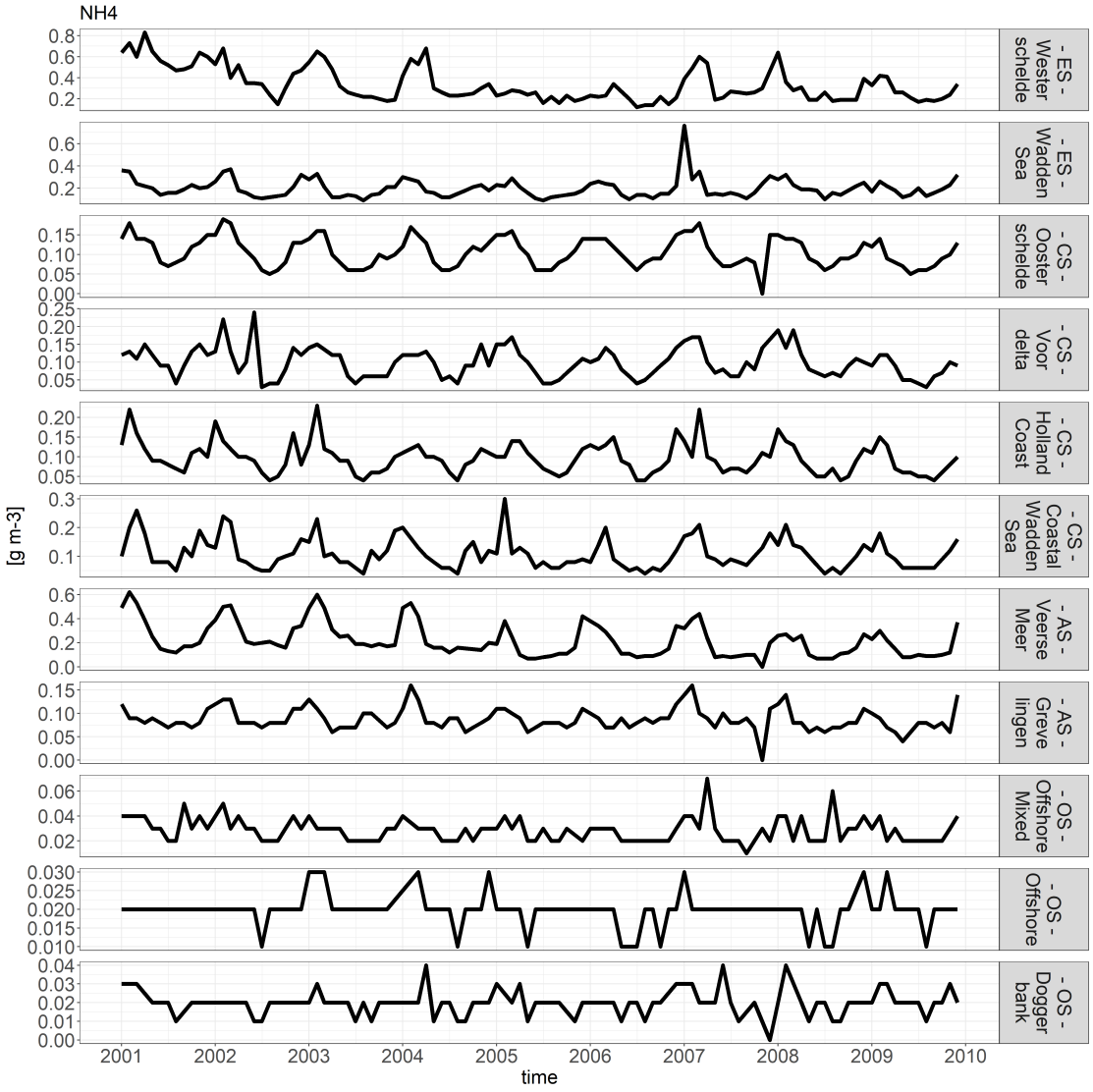

Figure B.2: Boundary transport of ammonium.

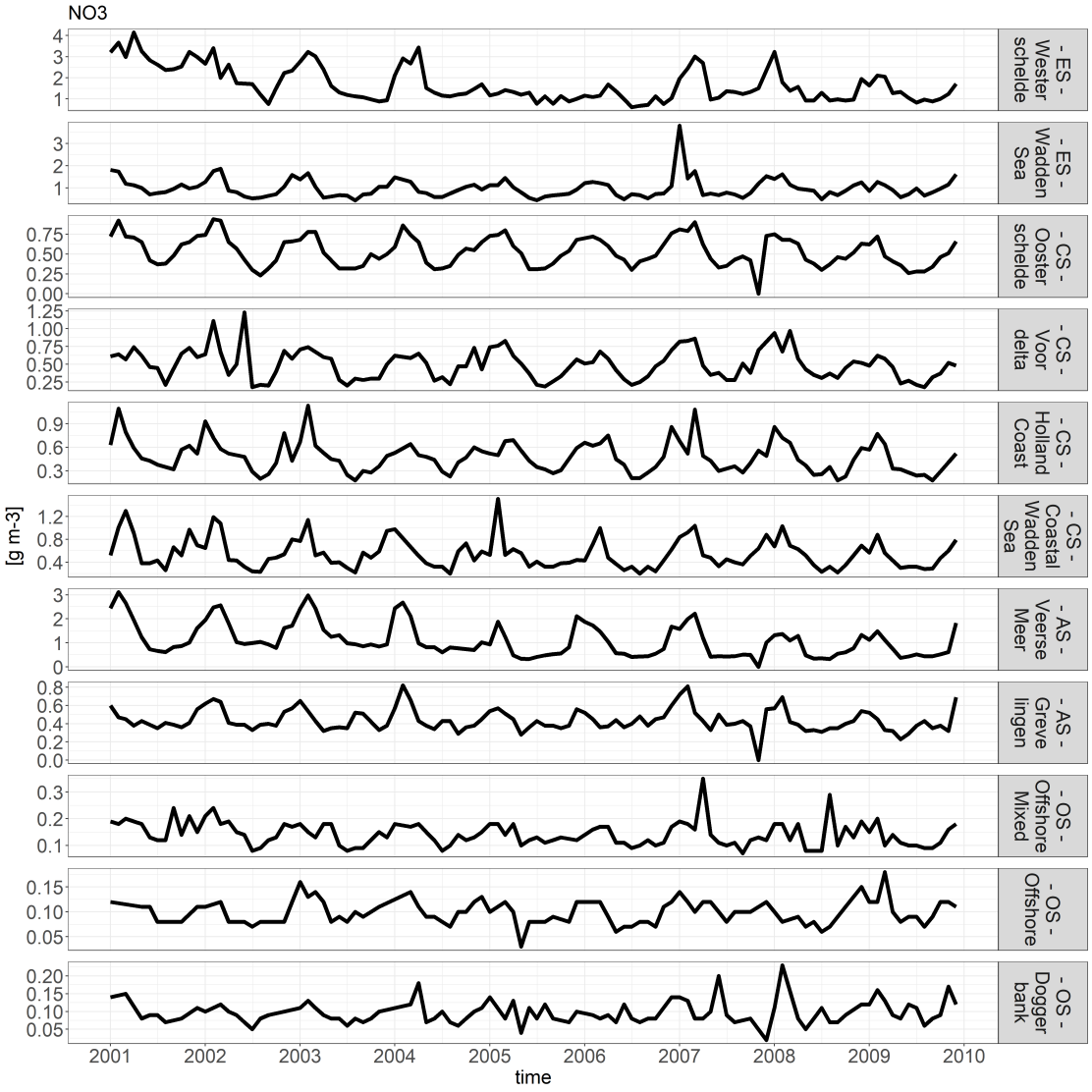

Figure B.3: Boundary transport of nitrate.

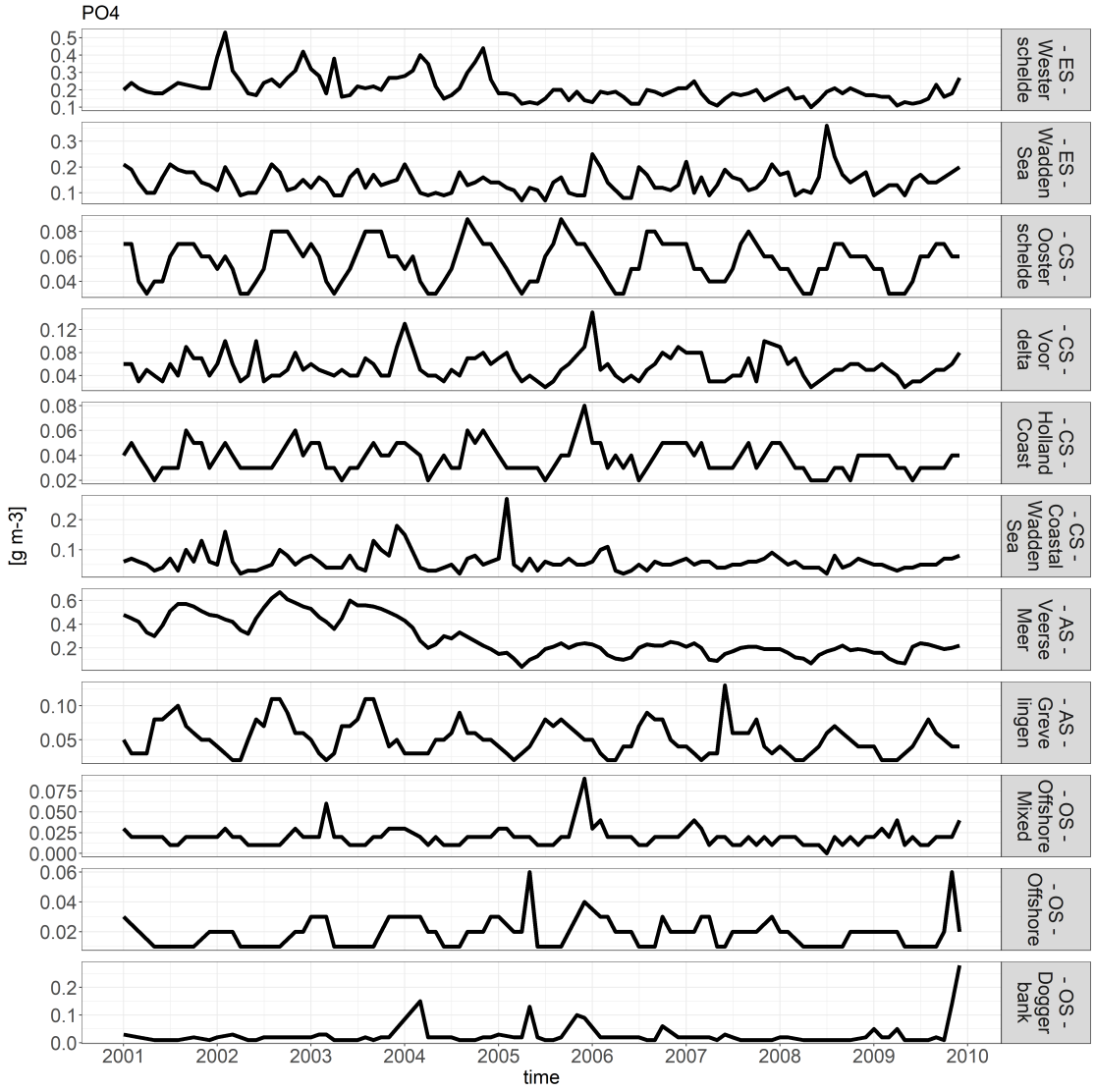

Figure B.4: Boundary transport of phosphorus.

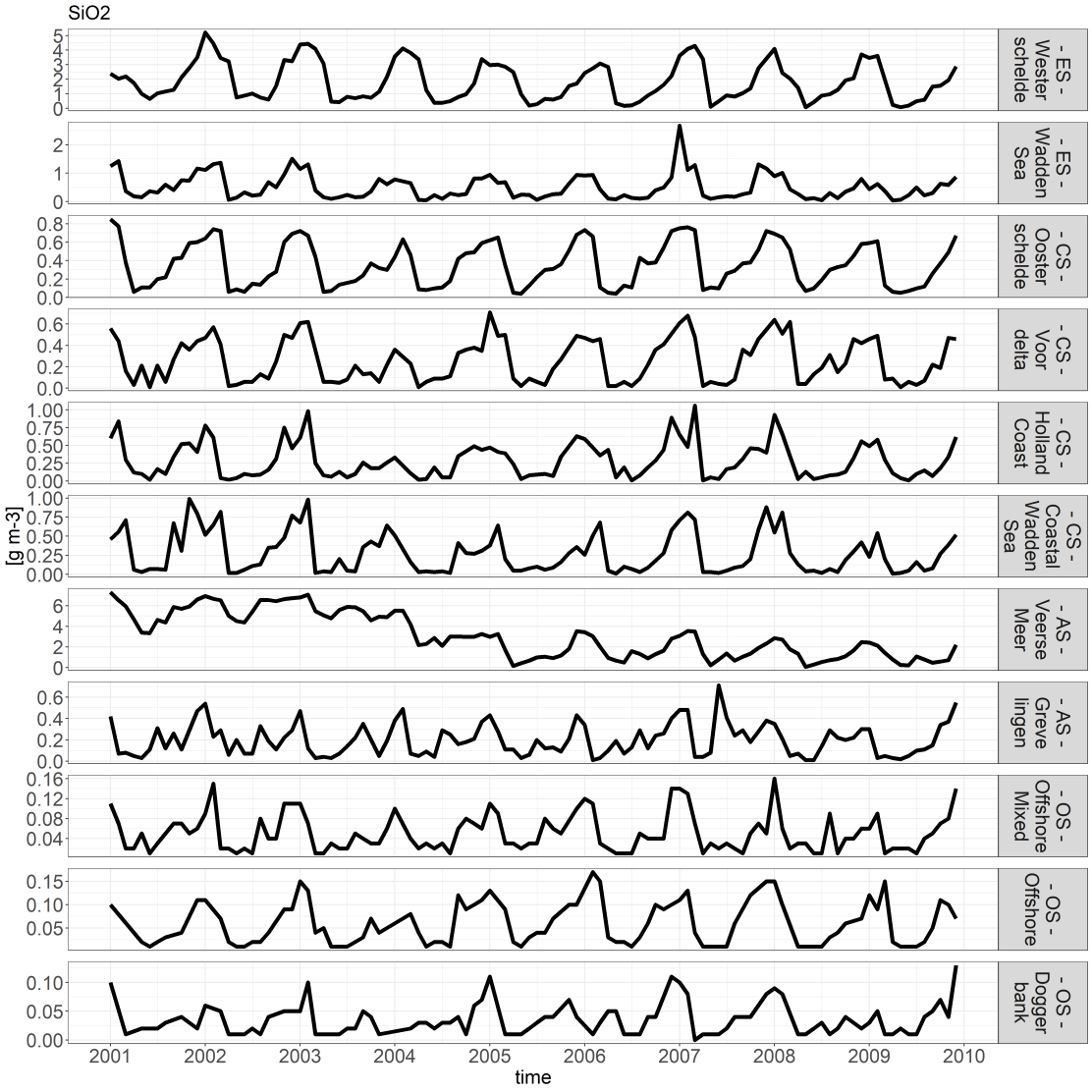

Figure B.5: Boundary transport of silica.

B.4 Model forcings

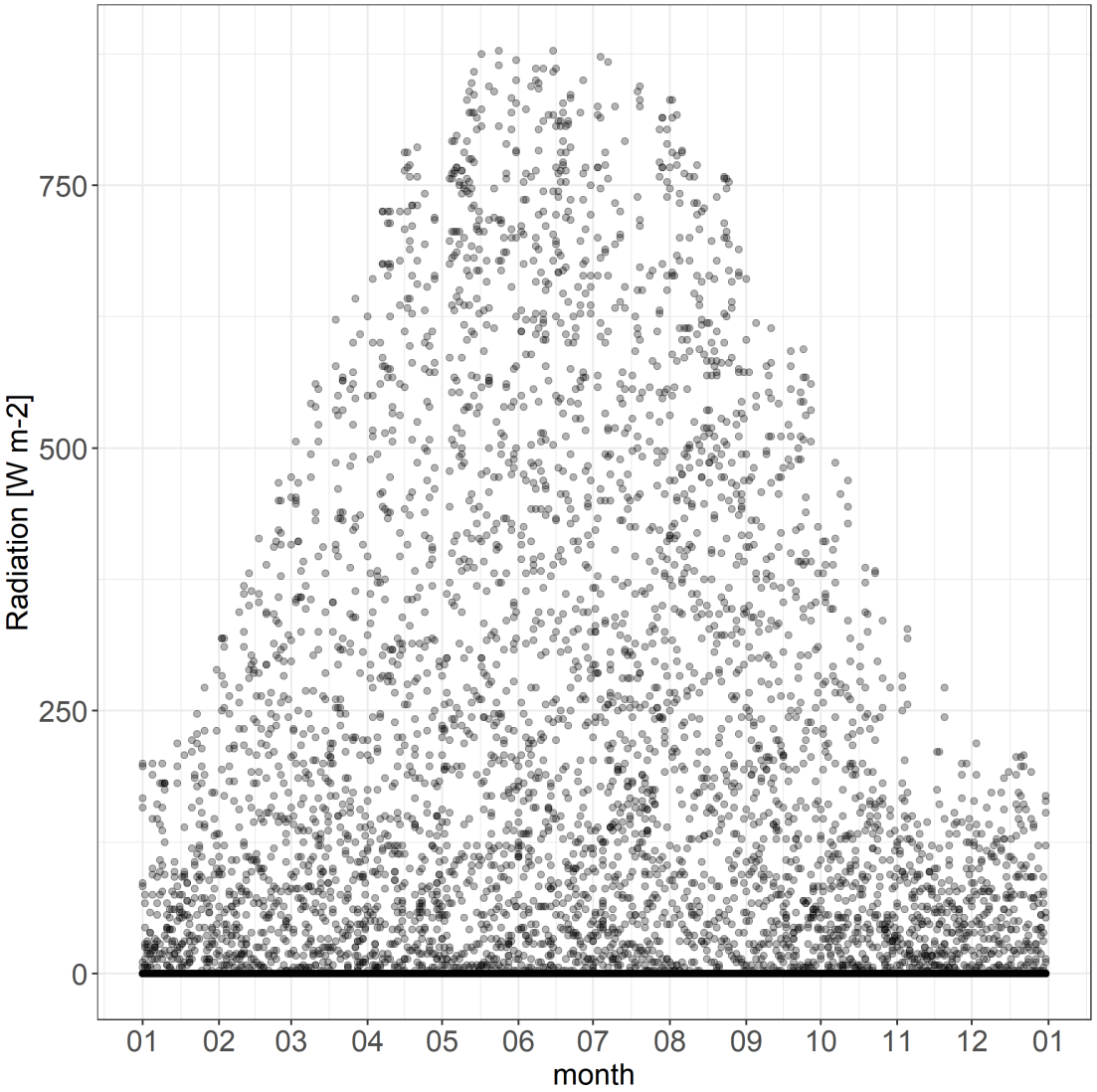

Figure B.6: Forced hourly radiation. Data was retrieved from the Royal Netherlands Meterorological Institute (KNMI) for the year 2019 for the sampling station de Kooy.

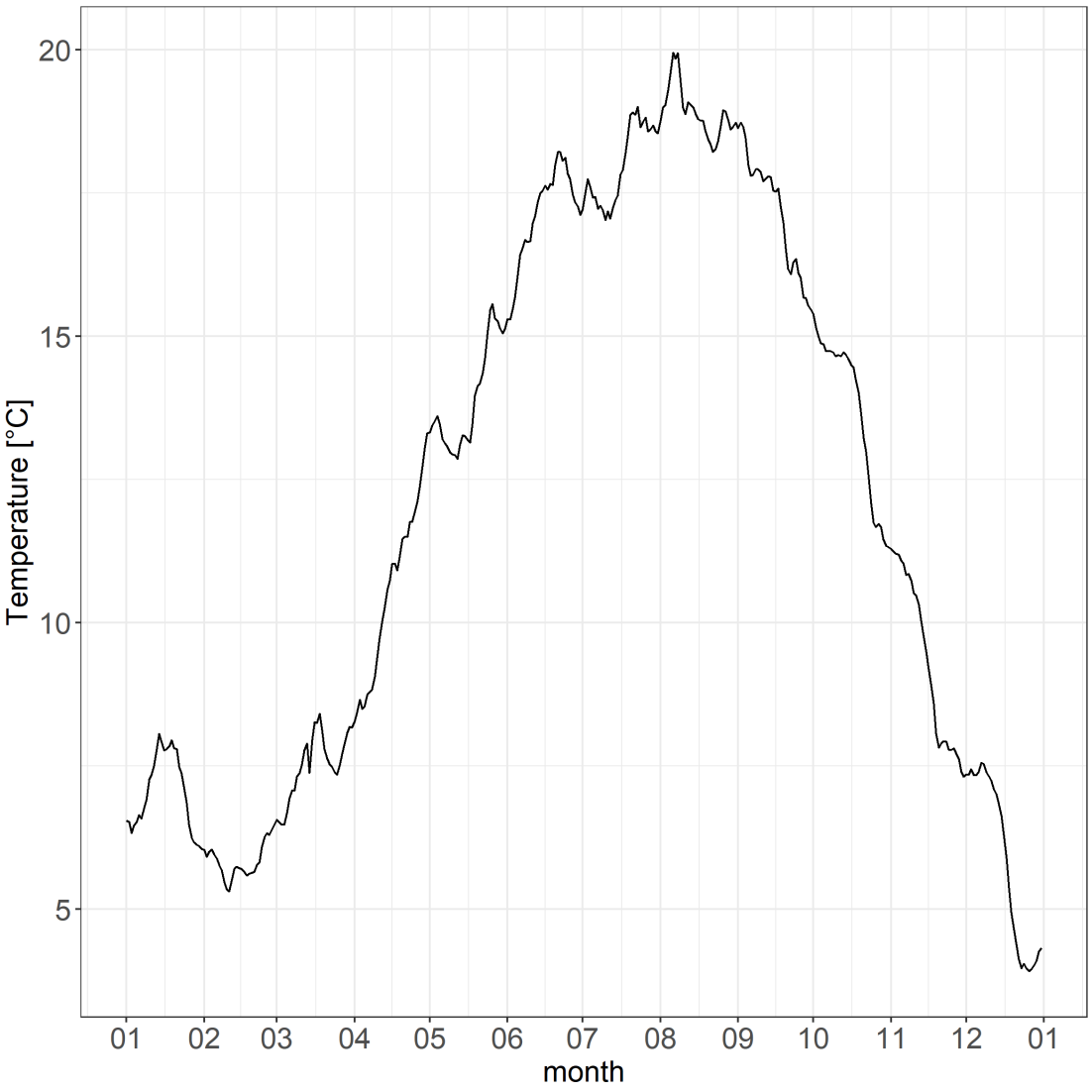

Figure B.7: Forced daily temperature. Data was retrieved from the 3D model Merzandwinning for the year 2014.

B.5 Box model

B.5.1 Box model set-up

The box model is used to demonstrate growth and competition between the five PFTs, diatoms, green algae, protozooplankton, CMs and NCMs. Only the PROTIST module was activated for the box model. It was run for 60 days with a timestep of 3 min and an output timestep of 2 h. The box model set-up mimics a batch culture with an initial nutrient supply, a day-night cycle of 12:8 h, no remineralization of particulate organics and no additional mortality apart from grazing.
All PFTs had a growth rate of 0.81 d^{-1}. Mortality was deactivated. The dimensionless parameter $relPS$ (the ratio of photosynthesis rate to maximum growth rate) was set to 2 for the primarily phototrophic organisms and to 0.5 for NCMs. Stoecker et al., 1988 showed that NCMs ingest less prey in the dark, so the ingestion of prey by NCMs is slightly light dependent (0.7). As there were no NCMs present in that dataset, the size for NCMs was set to 40 μm ESD to mimic an average *Strombidium*. The parameters for the other PFTs were set according to the table in B.2.

B.5.2 Box model results

Figure B.8 displays a 60 days run of the box model mimicking a batch culture. It displays the carbon biomass SVs (fig. B.8a), the nutrient SVs (figs. B.8b, B.8d, B.8f) as well as the assimilation rates (fig. B.8c) and carbon fixation rates (fig. B.8e). These plots demonstrate that PROTIST responds as would be expected.
The primarily phototrophic organisms bloom first with diatoms displaying the highest biomass peak (see fig. B.8a). All primarily phototrophic organisms initially display high rates of carbon fixation, which respond to the day-night cycle (see fig. B.8e), but those carbon fixation rates decline as the macro nutrients become limiting. Macronutrients become limiting after approximately 15 days (see figs. B.8b, B.8d, B.8f) leading to a decline of the diatoms and green algae. As the diatoms remain silica limited (see fig. B.8f), their biomass as well as carbon fixation rates remain low compared to green algae and CMs which display an increase of biomass as ammonium and phosphate become available again through voiding.
Fig. B.8c shows that all organisms capable of phagotrophy are prey limited as their assimilation rates closely follow their preys' biomass curves. The assimilation of prey by NCMs is also reflected in their carbon fixation rates, which are initially very low but increase as the NCM assimilated prey and retains their chloroplasts (see fig. B.8e).

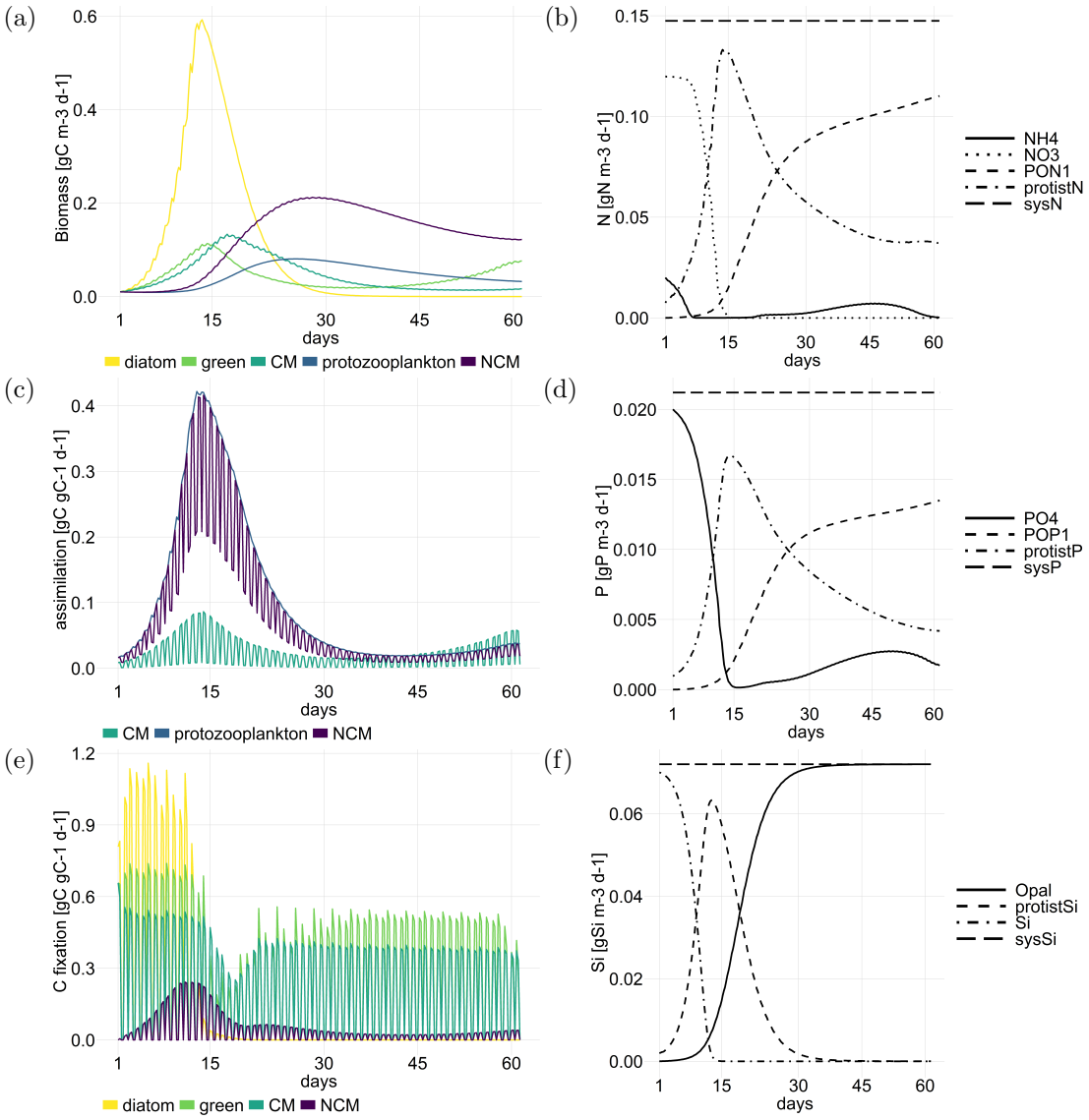

Figure B.8: Graphs displaying a) the carbon biomass per PFT, b) all SV related to nitrogen, c) assimilation of prey, d) all SV related to phosphate, e) carbon fixation and f) all SV related to silica.

B.6 Normalized standard deviation

Table B.17: Normalized standard deviations of the abiotic factor included in the sensitivity analysis.

	$\overline{sd_x}$
NH_4^+	0.95
NO_3^-	0.95
PO_4^{3-}	1.24
SiO_2	1.78
suspended sediment	1.46

Appendix C

Supplementary information for aquatic ecosystem model researching seaweed - protist interactions (chapter 6)

C.1 Absolute difference maps

C.1.1 Dissolved inorganic nutrients

(a)

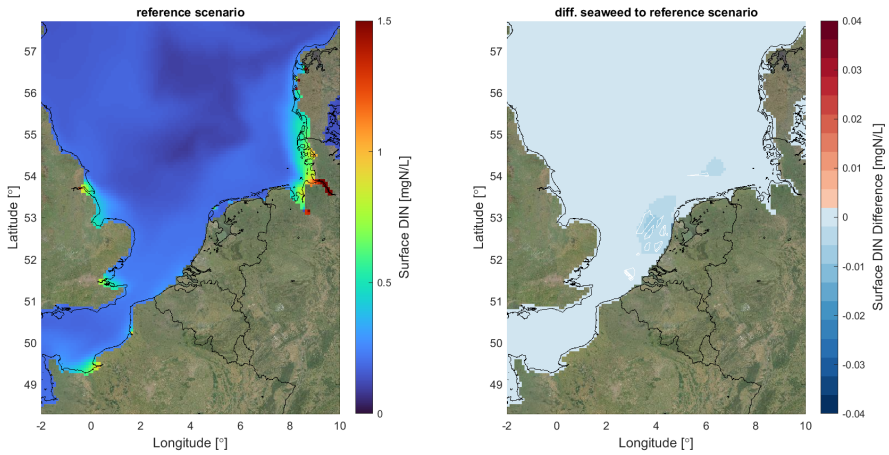

(b)

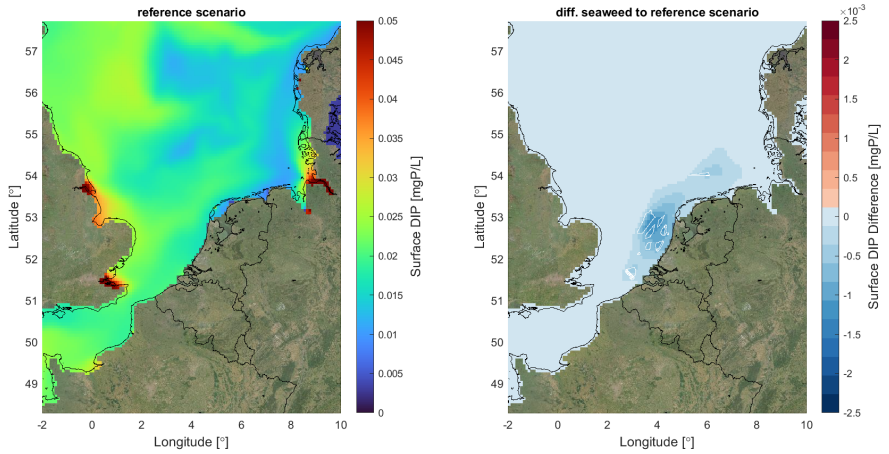

Figure C.1: Visualization of averaged dissolved inorganic nitrogen (a) and phosphate (b) concentrations for the months December 2016, January and February 2017. The left maps visualizes the absolute values for the reference scenario and the right maps the absolute difference between the reference and seaweed scenario.

(a)

(b)

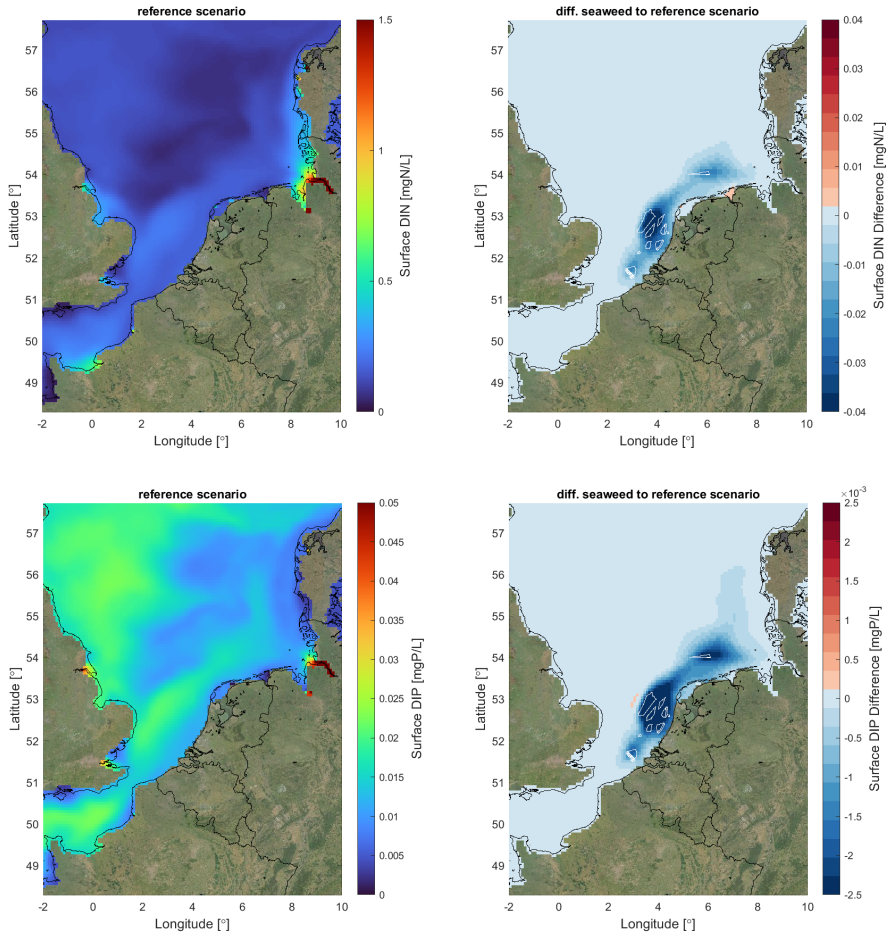

Figure C.2: Visualization of averaged dissolved inorganic nitrogen (a) and phosphate (b) concentrations for the months March, April and May 2017. The left maps visualizes the absolute values for the reference scenario and the right maps the absolute difference between the reference and seaweed scenario.

(a)

(b)

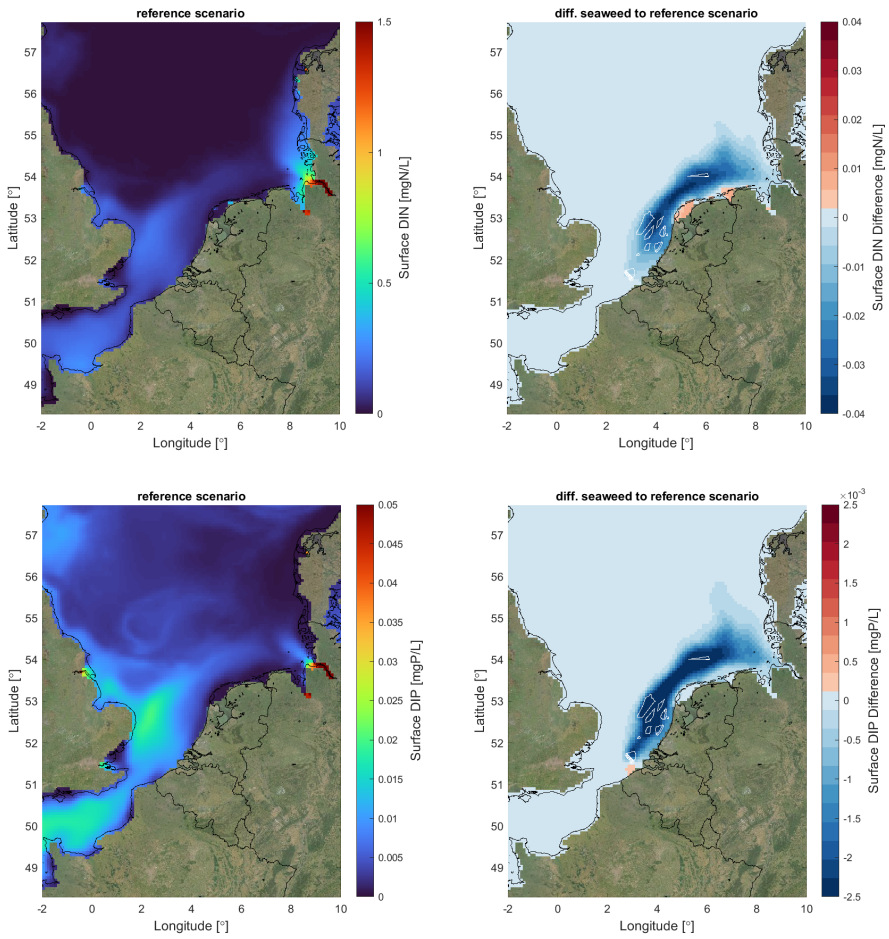

Figure C.3: Visualization of averaged dissolved inorganic nitrogen (a) and phosphate (b) concentrations for the months June, July and August 2017. The left maps visualizes the absolute values for the reference scenario and the right maps the absolute difference between the reference and seaweed scenario.

C.1.2 Protist functional types

(a)

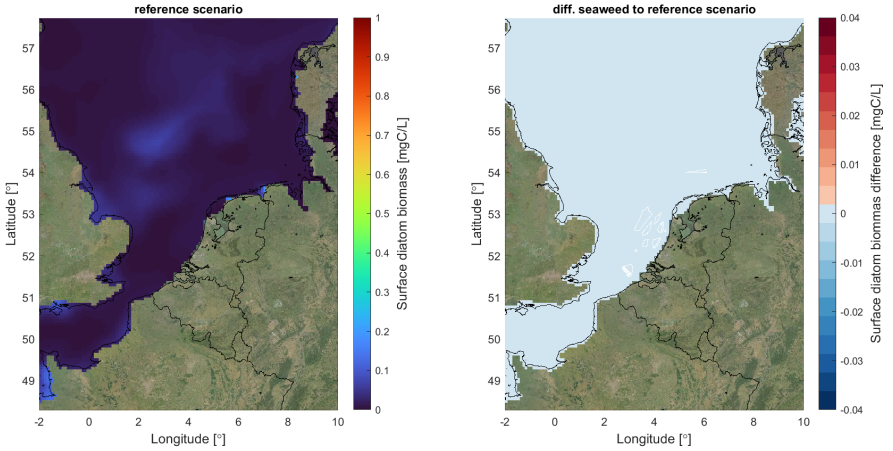

(b)

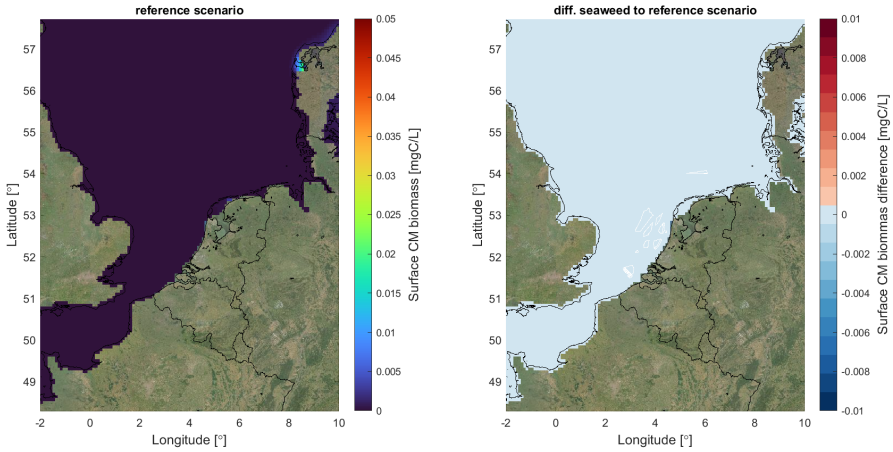

Figure C.4: Visualization of averaged phyoplankton (a) and constitutive mixoplankton (b) biomass for the months December 2016, January and February 2017. The left maps visualizes the absolute values for the reference scenario and the right maps the absolute difference between the reference and seaweed scenario.

(a)

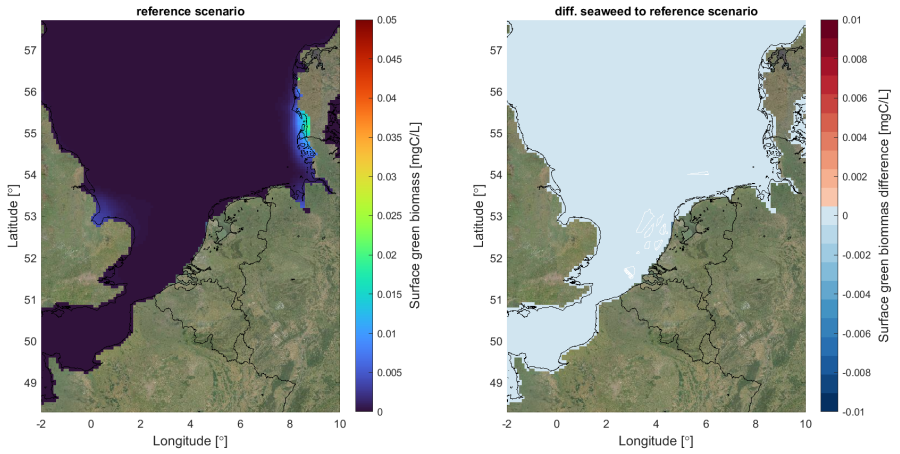

(b)

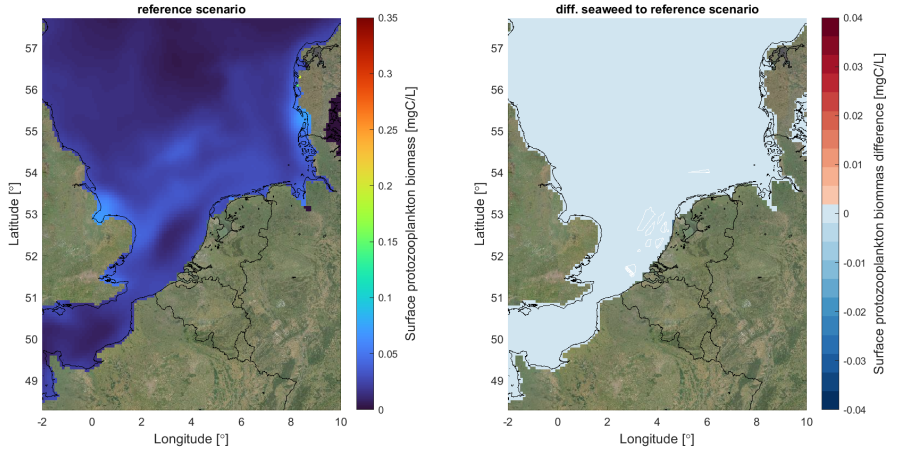

Figure C.5: Visualization of averaged green algae (a) and protozooplankton (b) biomass for the months December 2016, January and February 2017. The left maps visualizes the absolute values for the reference scenario and the right maps the absolute difference between the reference and seaweed scenario.

(a)

(b)

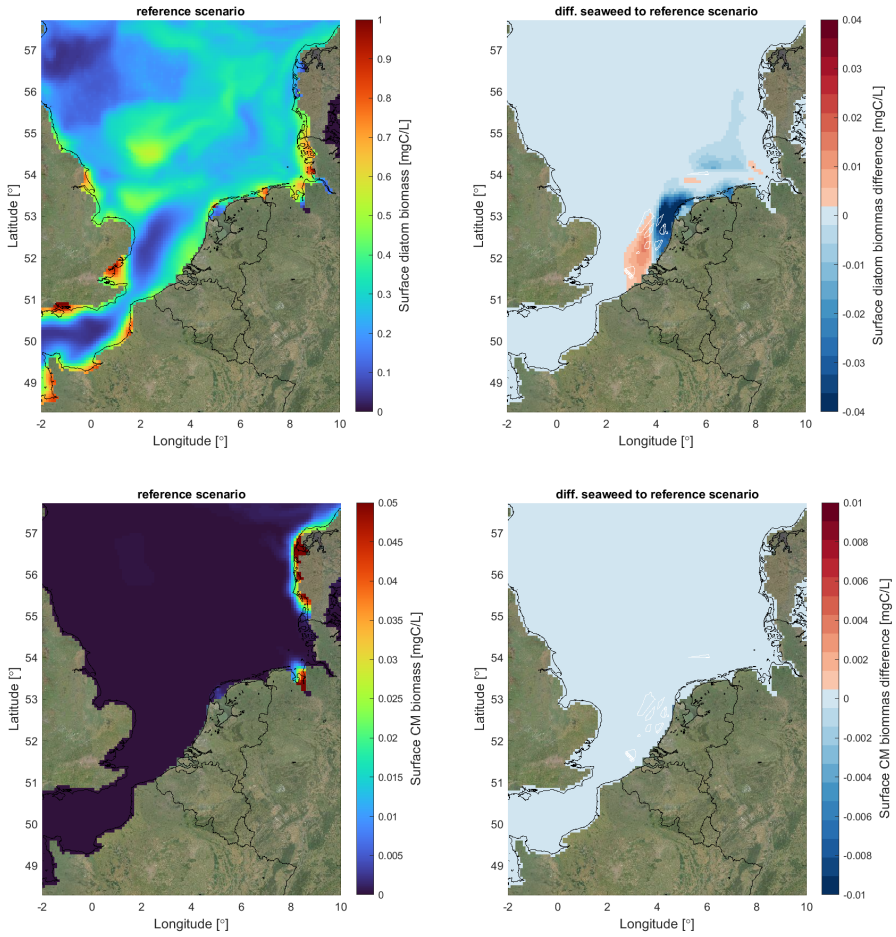

Figure C.6: Visualization of averaged phyoplankton (a) and constitutive mixoplankton (b) biomass for the months March, April and May 2017. The left maps visualizes the absolute values for the reference scenario and the right maps the absolute difference between the reference and seaweed scenario.

(a)

(b)

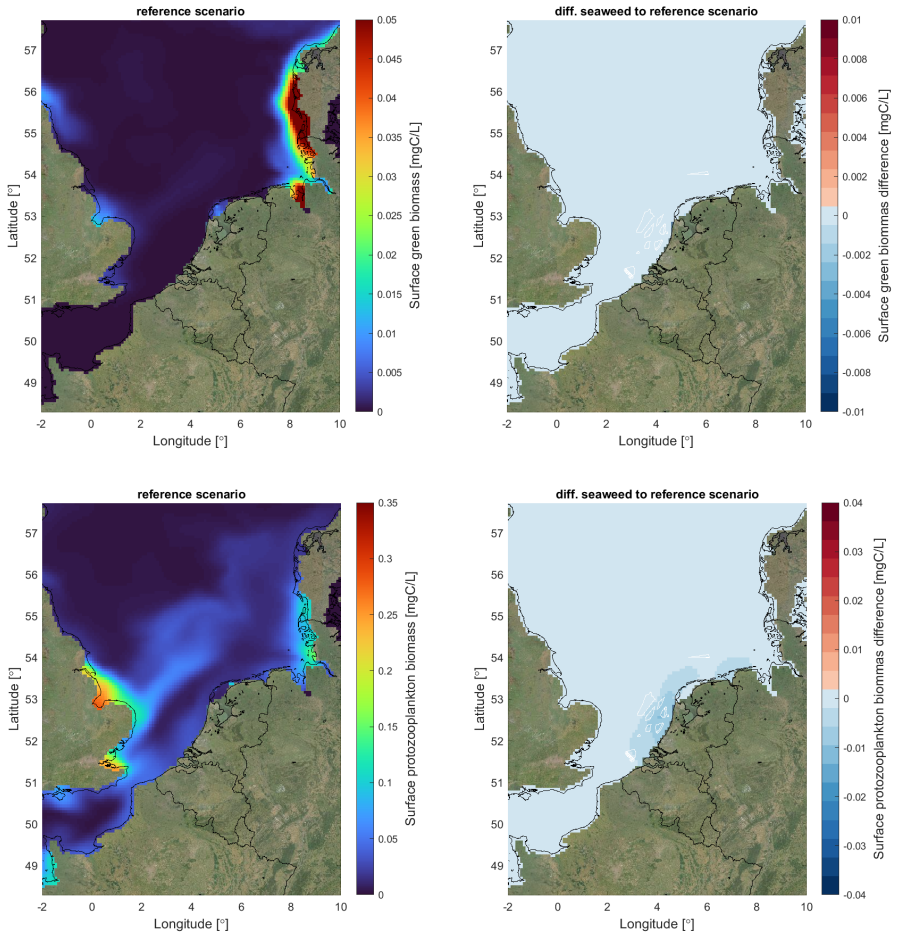

Figure C.7: Visualization of averaged green algae (a) and protozooplankton (b) biomass for the months March, April and May 2017. The left maps visualizes the absolute values for the reference scenario and the right maps the absolute difference between the reference and seaweed scenario.

(a)

(b)

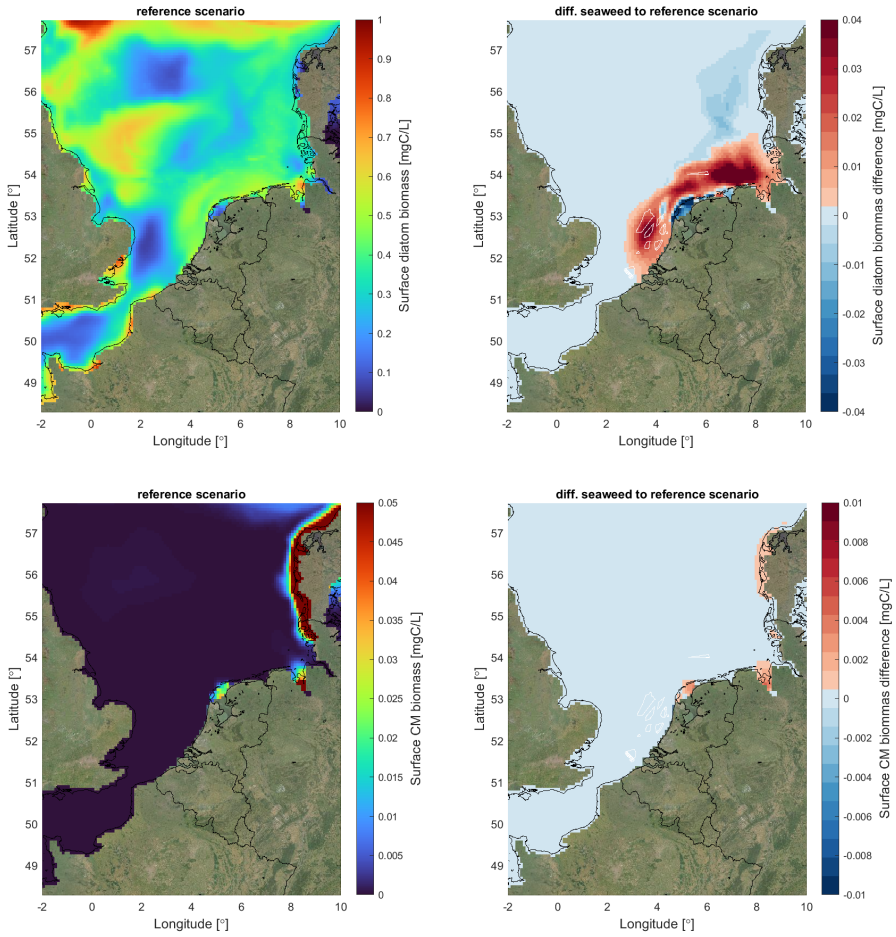

Figure C.8: Visualization of averaged phyoplankton (a) and constitutive mixoplankton (b) biomass for the months June, July and August 2017. The left maps visualizes the absolute values for the reference scenario and the right maps the absolute difference between the reference and seaweed scenario.

(a)

(b)

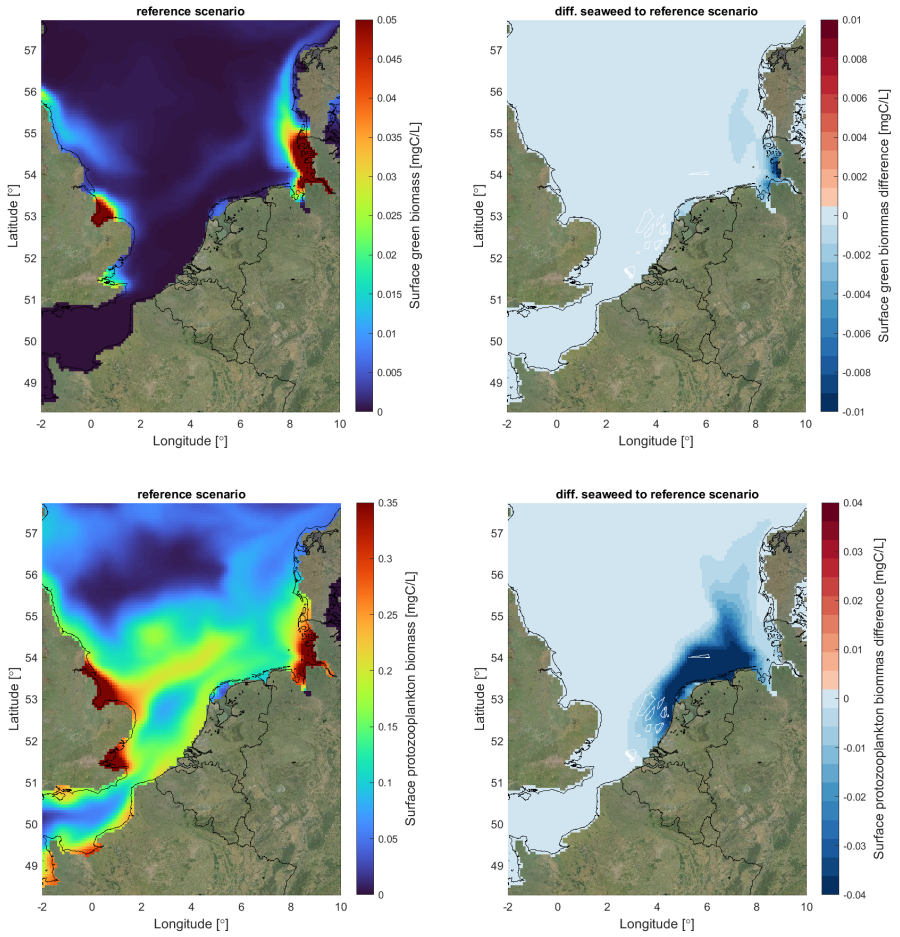

Figure C.9: Visualization of averaged green algae (a) and protozooplankton (b) biomass for the months June, July and August 2017. The left maps visualizes the absolute values for the reference scenario and the right maps the absolute difference between the reference and seaweed scenario.

C.2 Relative difference maps

C.2.1 Dissolved inorganic nutrients

(a)

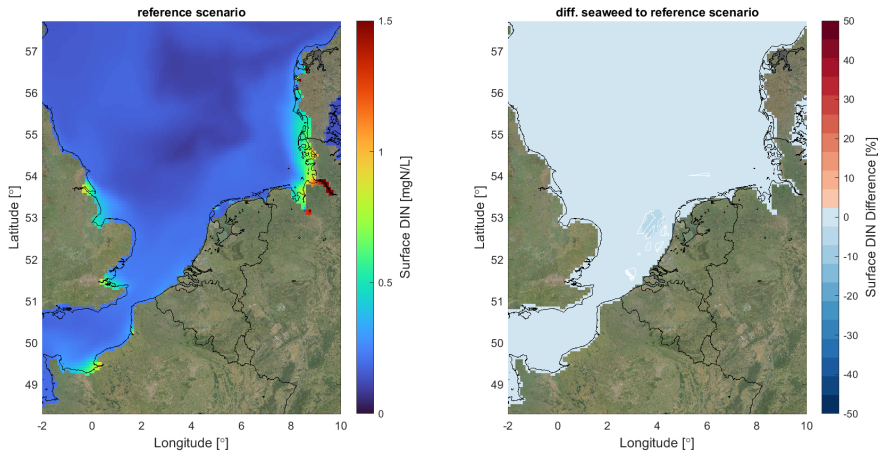

(b)

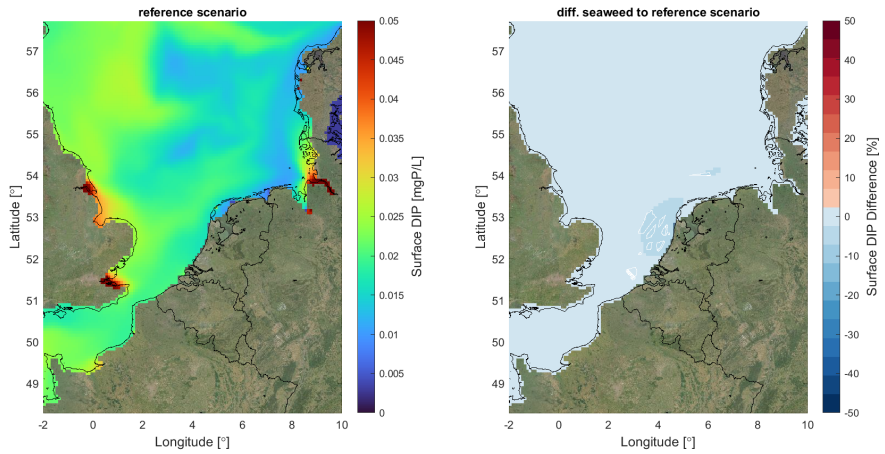

Figure C.10: Visualization of averaged dissolved inorganic nitrogen (a) and phosphate (b) concentrations for the months December 2016, January and February 2017. The left maps visualizes the absolute values for the reference scenario and the right maps the relative difference between the reference and seaweed scenario.

(a)

(b)

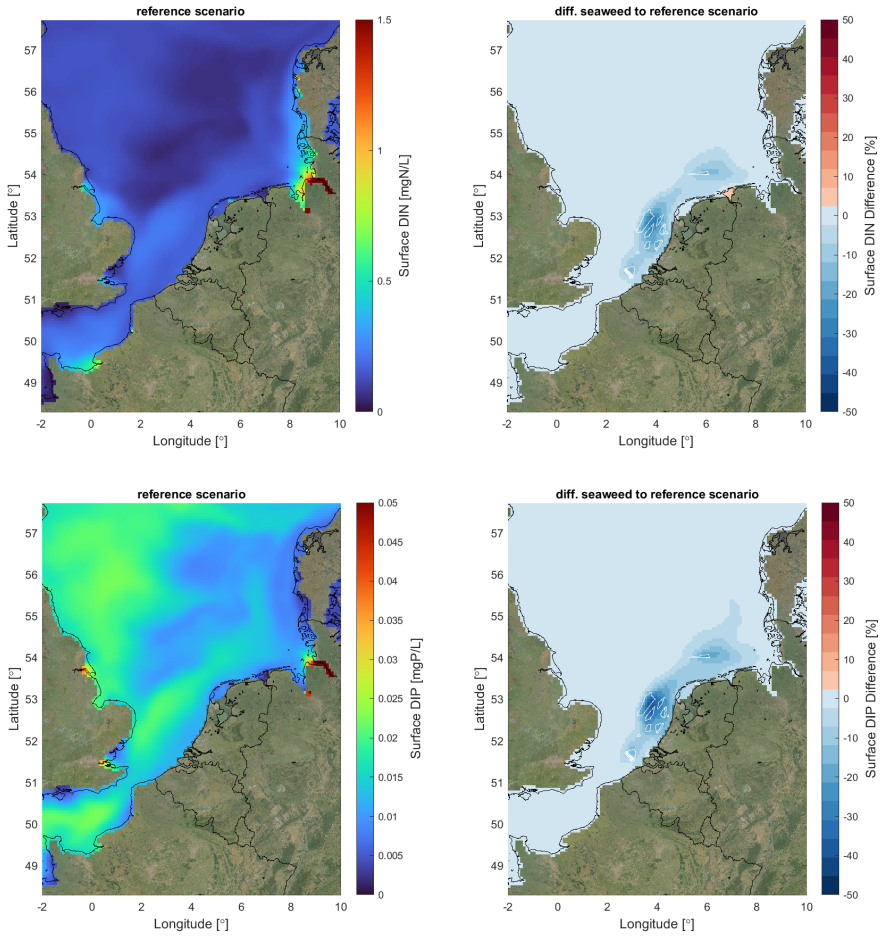

Figure C.11: Visualization of averaged dissolved inorganic nitrogen (a) and phosphate (b) concentrations for the months March, April and May 2017. The left maps visualizes the absolute values for the reference scenario and the right maps the relative difference between the reference and seaweed scenario.

C.2.2 Protist functional types

(a)

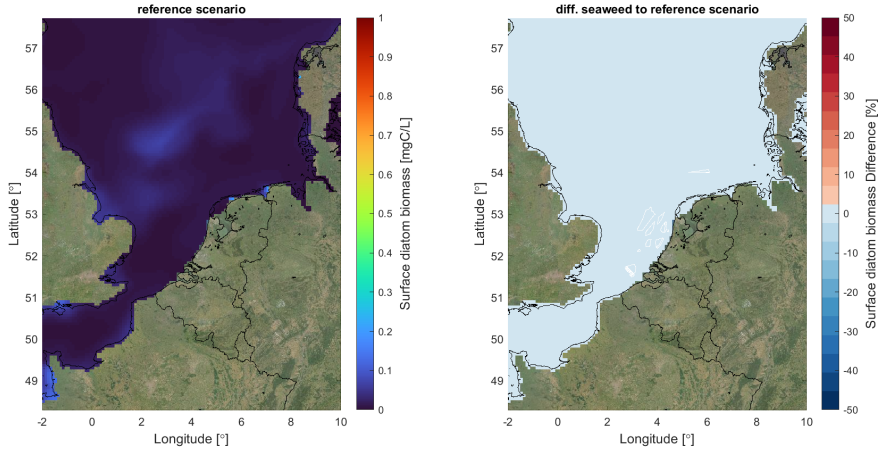

(b)

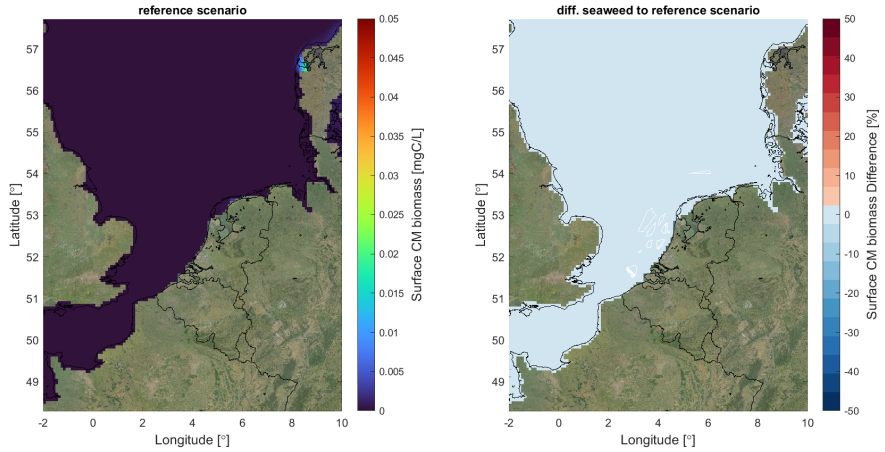

Figure C.12: Visualization of averaged phyoplankton (a) and constitutive mixoplankton (b) biomass for the months December 2016, January and February 2017. The left maps visualizes the absolute values for the reference scenario and the right maps the relative difference between the reference and seaweed scenario.

(a)

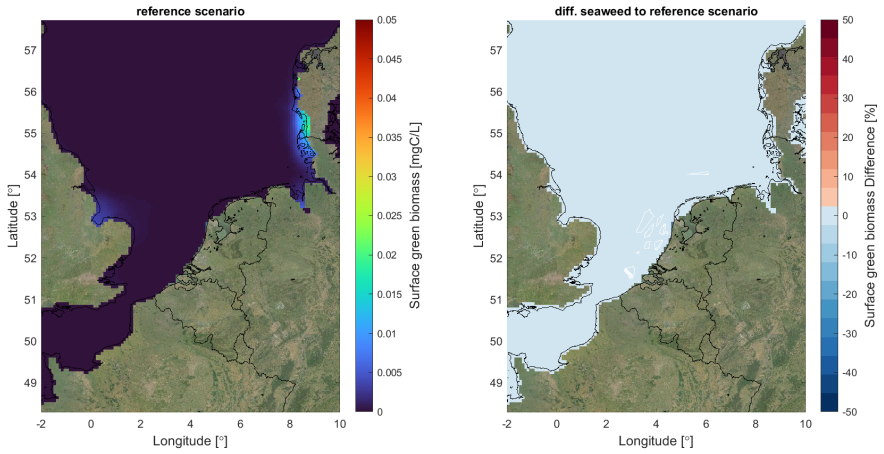

(b)

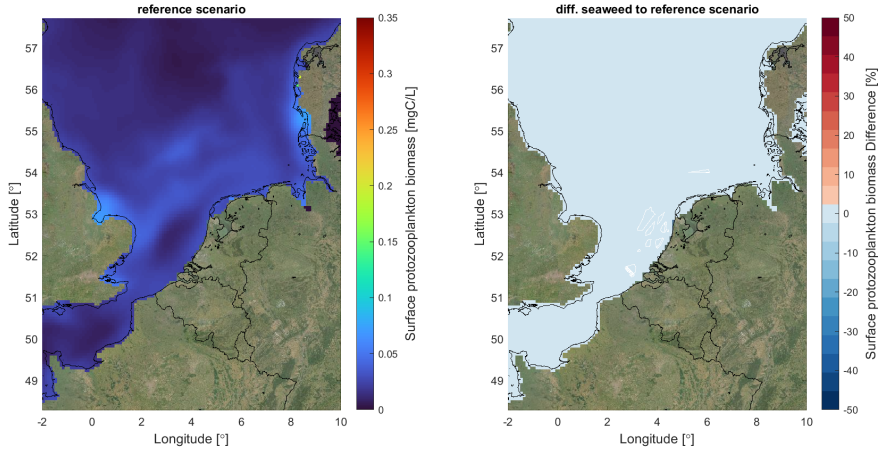

Figure C.13: Visualization of averaged green algae (a) and protozooplankton (b) biomass for the months December 2016, January and February 2017. The left maps visualizes the absolute values for the reference scenario and the right maps the relative difference between the reference and seaweed scenario.

(a)

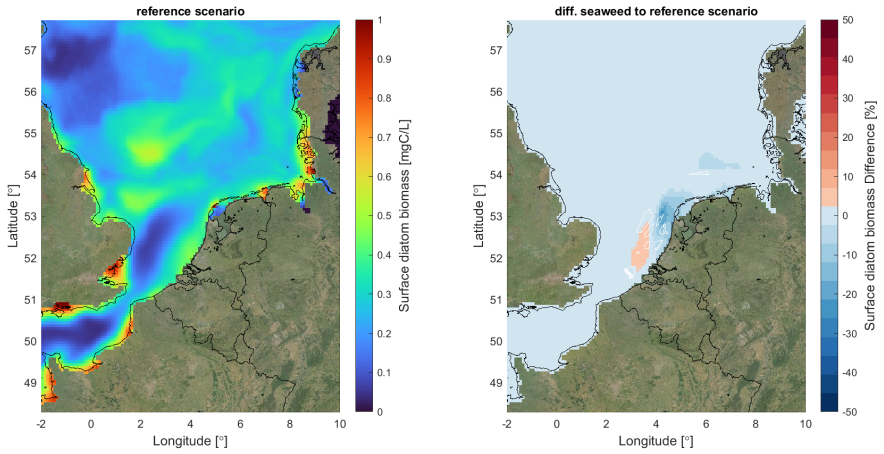

(b)

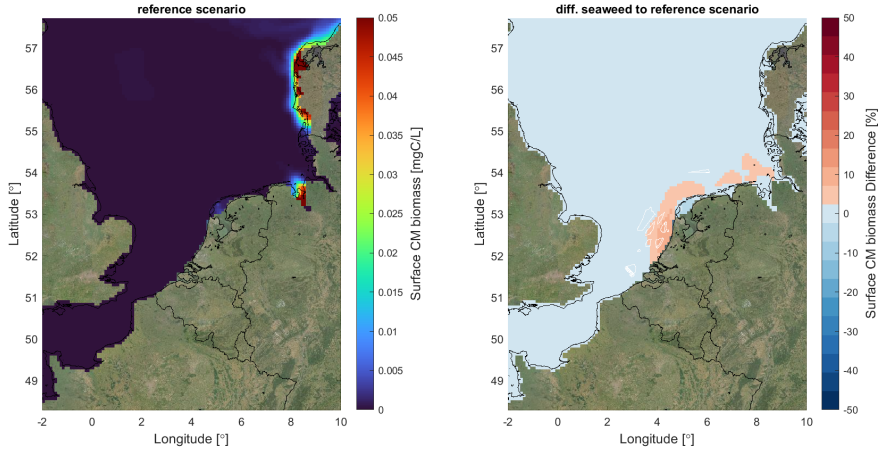

Figure C.14: Visualization of averaged phyoplankton (a) and constitutive mixoplankton (b) biomass for the months March, April and May 2017. The left maps visualizes the absolute values for the reference scenario and the right maps the relative difference between the reference and seaweed scenario.

(a)

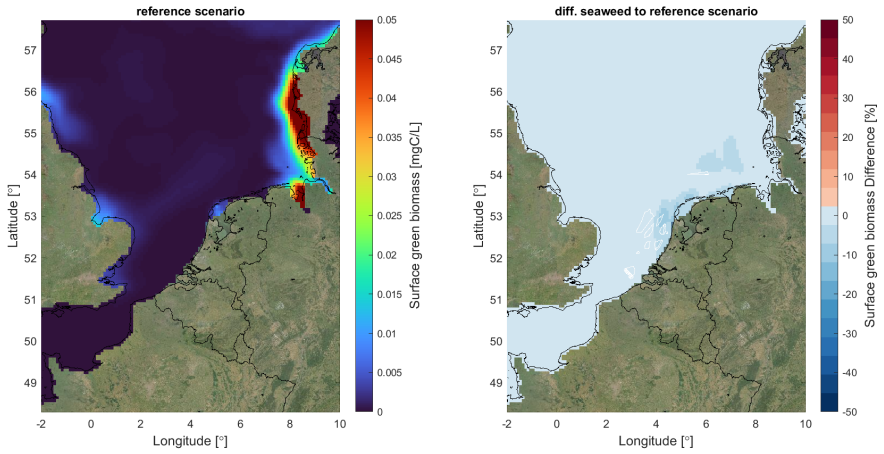

(b)

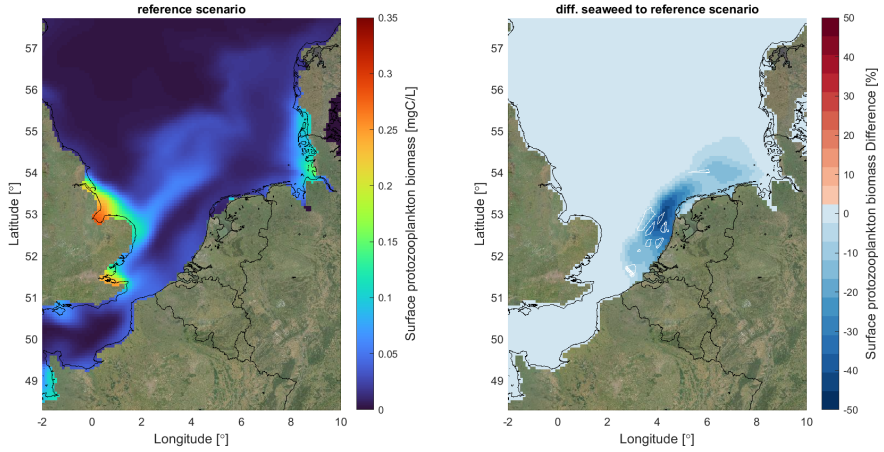

Figure C.15: Visualization of averaged green algae (a) and protozooplankton (b) biomass for the months March, April and May 2017. The left maps visualizes the absolute values for the reference scenario and the right maps the relative difference between the reference and seaweed scenario.